

DYNAMIC TESTS OF A REINFORCED CONCRETE BUILDING

by

T. V. Galambos and R. L. Mayes

Final Report to the National Science Foundation

on NSF Grant ENV 76-08244

Any opinions, findings, conclusions
or recommendations expressed in this
publication are those of the author(s)
and do not necessarily reflect the views
of the National Science Foundation.

REPORT DOCUMENTATION PAGE	1. REPORT NO. NSF/RA-780215	2.	3. Recipient's Accession No. PB297835
4. Title and Subtitle Dynamic Tests of a Reinforced Concrete Building		5. Report Date June 1978	
7. Author(s) T.V. Galambos, R.L. Mayes		6.	
9. Performing Organization Name and Address Washington University School of Engineering and Applied Science St. Louis, Missouri		8. Performing Organization Rept. No. Research Report No. 51	
12. Sponsoring Organization Name and Address Engineering and Applied Science (EAS) National Science Foundation 1800 G Street, N.W. Washington, D.C. 20550		10. Project/Task/Work Unit No.	
15. Supplementary Notes		11. Contract(C) or Grant(G) No. (C) ENV7608244 (G)	
		13. Type of Report & Period Covered	
		14.	

15. Abstract (Limit: 200 words)

An eleven-story reinforced concrete building was subjected to many cycles of sinusoidal lateral loads, which significantly altered the dynamic and structural properties of the building, and induced extensive damage to the structural frame components and the non-structured wall and stair elements. The structure and the equipment used for the tests are described. The tests ran for 138 days, and were divided into four phases: 1) measurement of the dimensional and structured properties of the building; 2) small amplitude shaking on the top floor to determine the original dynamic properties of the structure; 3) large amplitude shaking on the top floor and acquisition of the resulting data; and 4) analysis of the results. The tests demonstrated that it is feasible to mechanically cause major damage to a massive structure, and provided data that can be used to check advanced conceptual models of structural behavior under repetitive cyclic forces.

17. Document Analysis a. Descriptors

Earthquake resistant structures
Earthquakes
Dynamic loads

Concrete construction
Dynamic properties
Dynamic tests

b. Identifiers/Open-Ended Terms

c. COSATI Field/Group

Availability Statement

NTIS

19. Security Class (This Report)

21. No. of Pages

245

20. Security Class (This Page)

22. Price

A11-A01

11

11/11/11

TABLE OF CONTENTS

Abstract	1
1. Introduction	2
1.1 The Pruitt-Igoe Housing Complex of St. Louis	2
1.2 History of the Pruitt-Igoe Shaking Tests	5
2. Description of the Test Structure and Test Equipment	15
2.1 Test Structure	15
2.2 Small Amplitude Shaking Tests	21
2.3 Large Amplitude Shaking Tests	23
2.4 Discussion	32
3. Discussion of Damage	34
3.1 General Comments	34
3.2 Status before Large Amplitude Tests	34
3.3 Damage after Moderate E-W Shaking	35
3.4 Damage after Completion of E-W Tests	36
3.5 Damage During the N-S Tests	38
4. Description of Tests Performed	42
4.1 Introduction	42
4.2 Small Amplitude Tests	42
4.3 Large Amplitude Tests	44
4.4 Performance of the Vibration Generator During the Tests	49
4.5 Data Collected, Stored and Digitized	51
5. Methods of Data Analysis	53
5.1 Mode Shapes	53
5.2 Damping and Resonant Frequencies	53

5.3	Uniform Building Code Equivalent of the Base Shear Force Induced During Testing	64
6.	Discussion of Test Results	66
6.1	Period	66
6.2	Mode Shapes	68
6.3	Damping	69
6.4	Uniform Building Code Equivalent of the Base Shear Force Induced During Testing	72
6.5	Comparison of Large and Small Amplitude Tests	73
6.6	Summary	75
7.	Correlation of Analytical Models and Experimental Results	76
7.1	General	76
7.2	Computer Program ETABS	76
7.3	Structural Models	77
7.4	Results of Analysis	79
7.5	Comparison of Experimental and Analytical Results	79
7.6	Summary of Results	81
8.	Summary and Conclusions	83
8.1	Summary of Research	83
8.2	Large Amplitude Shaking Device	84
8.3	Test Results	85
8.4	State-of-Art Analyses	86
8.5	Conclusions and Recommendations	87
9.	Acknowledgements	91
10.	References	92
	Tables 1 through 23	93
	Tables 1 through 127	113

Appendix A.	Organizations and Individuals Involved in the Pruitt-Igoe Testing Project	A-1
Appendix B.	Log of Activities	B-1
Appendix C.	Summary of Tests of "FORCID" Computer Program Using Simulated Data	C-1

/.

DYNAMIC TESTS OF A REINFORCED CONCRETE BUILDING

Theodore V. Galambos¹, Fellow, ASCE, Ronald L. Mayes², A.M., ASCE

An eleven-story reinforced concrete building was subjected to a variety of dynamic tests during the period July through November 1976. This report presents the description of these tests, it sums up the data, and it evaluates the results. The research was conducted under the management of Washington University in St. Louis, and it was sponsored by the National Science Foundation (NSF Grant ENV 76-08244).

1 Professor of Civil Engineering, Washington University, St. Louis, Mo.

2 President, COMPUTECH CO., Berkeley, California.

1. INTRODUCTION

1.1 THE PRUITT-IGOE HOUSING COMPLEX OF ST. LOUIS

The building structure which was subjected to the dynamic tests described in this report was part of a building from the St. Louis Housing Authority's Pruitt-Igoe Complex which was demolished in the period between February and December of 1976.

The reason for the demolition of this series of apartments, and thus the availability of this building for testing, is a long, complex and sad story of urban decay. The history of the rise and fall of this experiment to house the poor, the expectations, the disappointments, the attempts at complete or partial remedy, and the final decisions to raze the area is beyond the scope of this report, and its description is well beyond the competence of the authors. Contemporary newspaper and magazine articles (1950-1976), the Congressional record, as well as numerous general and specific studies can be consulted for details. It is the opinion of the authors that the ultimate causes of failure are not fully understood, that they are complex, and that a good explanation will have to await the cooler perspective of time.

This report will thus restrict itself to a few factual statements of the background necessary to understand this research report.

The Pruitt-Igoe apartments were located about two miles NW from the Arch in St. Louis. The housing complex was one of several low-rent projects in St. Louis, and it was opened for occupancy in 1955-1956. The owner of the project was the St. Louis Housing Authority. The overall and architectural design was performed by the St. Louis firm Hellmuth, Yamasaki and Leinweber, Architects; the structural design was made by the

firm W. C. E. Becker, Consulting Engineers, and the buildings were constructed by the I. E. Millstone Construction Company*.

The apartment complex had 2800 units in 33 eleven-story buildings on a 57 acre (23,100m²) tract bounded by Jefferson Avenue in the West, Cass Avenue in the North, 20th Street in the East and Carr Street in the South (Fig. 1). This area also contains a library, a community center and several churches and elementary schools. Upwards of 10,000 residents occupied these apartments at one time, but the project's high vacancy rate, vandalism and other problems created a constant drain on the St. Louis Housing Authority's finances. The last families moved out in August 1973, and the buildings stood empty until demolition in 1976. Various plans were examined to rehabilitate the buildings, but by January 1975 it was decided to raze the area completely. What happened was that these buildings were effectively occupied from 15 to 18 years, after which they were abandoned and subsequently demolished. From a structural engineering viewpoint these buildings were relatively modern, built and designed according to contemporary standards. Structurally, then, these buildings were relatively new and undamaged prior to demolition.

Prior to the final razing of the buildings in 1976 two structures were subjected to experimental demolition by explosives: one complete A-type building, and the central narrow 360 ft x 29 ft (110m x 8.8m) section of Building C-3 (Fig. 2). The wider 45 ft x 40 ft (13.7m x 12.2m) end portions of this building were left undamaged by the explosions, the connecting beams and slabs having been separated by pneumatic hammer and

*These organizations are still active in St. Louis, and excellent cooperation was rendered by each during the dynamic test project. The firm names are the ones in effect when the project was built, and some of the organizations have since changed their names.

torch before the explosion. One of the remaining "towers" from Building C-3 was the building used for the dynamic tests. The explosive demolition method received wide publicity in the news media when it was performed in 1972, but this method was not used when the remaining buildings were demolished during 1976. These structures were razed instead by conventional methods, using a "headache ball" of lead. This method of demolition permitted the eventual recovery of the reinforcing steel for sale as scrap, and the remaining rubble, consisting of bricks, concrete block and chunks of concrete, was easily loaded and hauled away.

The demolition of the Pruitt-Igoe buildings was planned and supervised by the Sverdrup and Parcel consulting firm of St. Louis, and the actual work was performed under contract by the Cleveland Wrecking Company of Cincinnati, Ohio, and the AALCO Wrecking Company of St. Louis.

The buildings in this project were all of similar construction: they were all eleven stories tall from the ground up, and they had a short sub-basement used as pipe galleries. Columns had each a spread footing, and the structure consisted of square columns, beams and slabs. Three types of buildings were constructed, Types A, B and C (Fig. 2), the only difference being the length of the central narrow portion. All buildings had their longest dimensions in the East-West direction.

The outside faces of the buildings were brick facade, backed up between the structural frame with concrete blocks. Concrete block walls existed also around the stair-wells and elevator shafts. All other interior partitions were plasterboard walls with metal lath. The structural elements, such as the beams, slabs and columns, were clear concrete on the surface except for some interior columns which were faced with plaster.

The structure was designed according to the 1953 ACI Code for gravity load only. The frame was of continuous construction.

The situation, then, in 1974 and 1975 was that there existed a great number of structurally sound contemporary buildings which were slated for demolition. This presented a unique opportunity to perform tests on one or more of these buildings without regard to possible damage from the experiments in an area of the city remote from inhabitants. The photographs of Figs. 3 through 10 depict various details of construction and of the demolition operation. Structural details of the test-building are presented in later parts of this report.

1.2 HISTORY OF THE FRUITT-IGOE SHAKING TESTS

Background

Attention was drawn in a very dramatic way to the social problems of the Pruitt-Igoe Housing Project in St. Louis when one entire building and a part of another building was demolished by explosives in 1972. The explosive experiments were conducted to demonstrate the feasibility of this method of removing abandoned buildings from an urban area, but they went far beyond that in their significance. They forcefully illustrated to the city, the nation, and the world that Pruitt-Igoe as originally planned had failed as a social experiment and that something had to be done about it. Whatever was to be done in terms of social and physical renovation would take a great deal of time and money, and it appeared

at that time that if some or all of these structurally sound buildings were to stand empty for a long time then they might just as well be used for some structural engineering experiments.

The desirability of different types of tests was discussed during 1973 and 1974 with various professional friends who were interested in the full scale performance of structures, most notably with members of

the Research Council on Performance of Structures (RCPS) of the American Society of Civil Engineers (ASCE). The object of RCPS, as stated in its Rules of Procedures is "to advance engineering knowledge and practice on the subject of actual performance of full scale structures". A variety of possible test schemes were explored such as static tests under gravity and lateral loads, survey of actual physical properties and their comparison with design properties, progressive collapse tests by explosive to damage parts of a structure, small-scale and large scale dynamic tests, the study of the propagation of fire from one building to another, etc. It appeared that one could have transformed the whole complex into a laboratory for building research in which valuable experimental studies could have been performed for a decade or more.

The realities of politics and finance do not generally consider the desires of the researcher of the art and science of building engineering, and by 1974 it became apparent from newspaper articles that serious consideration was being given to the complete demolition of the project. Thus it seemed that if there was to be any testing at all, it would have to be of limited scope and it would have to be done quickly. The professional opinion of the members of RCPS was that the greatest need existed for information of the behavior of structures which were subjected to large amplitude dynamic motion which produced damage to some structural components. Such information was thought to be valuable as input to the dynamic analysis of non-linear structures.

The principal investigator, in connection with an NSF site visit in September 1974 at Berkeley, met Dr. Ronald Mayes, who subsequently became the co-principal investigator of the project, and explored the feasibility of large-amplitude tests on large concrete buildings. Dr. Mayes seemed to

feel that such tests were within the realm of technological possibility. The outcome of the discussion was that the principal investigator contacted the National Science Foundation, and this agency indicated that they might be interested in funding a feasibility study of performing large amplitude tests on one of the Pruitt-Igoe buildings.

Consequently a proposal was prepared and submitted to NSF on February 24, 1975, and this proposal was funded on April 4, 1975 for the period April 1, 1975 through December 31, 1975. The amount of the contract was \$20,000. The proposed work had two objectives:

- 1) It was desired to find out if large-amplitude dynamic tests were technically feasible for such buildings.

- 2) In case that it was judged possible to perform the tests, then these experiments were to be planned and a new proposal was to be prepared to perform this work.

During the initial phases of this feasibility study, which was performed with the aid of Dr. Mayes and Dr. Hatcher (of Washington University) it seemed that it was indeed possible to generate enough force to excite part of a building but that it would take several large shakers to produce significant motion in a whole building. Since only one large dynamic shaker was available, and since the coordination of the motion of several shakers was believed to represent formidable control problems, it was decided that tests should be performed only on an isolated part of a building. Isolation of the end or the center of a building was considered, using jack-hammer and torch, but the cost of this separation was found to be very high. Attention was drawn at this time to the two remaining end towers of building C-3 which were left standing after the center part of this building was blown out. One of the towers, the one at the West end

of the building, is shown in Fig. 10. The central portion of C-3, 270 ft long by 29 ft wide (82.3m x 8.84m) was blasted away in 1972, and the rubble was removed, leaving two 40 ft x 45 ft (12.19m x 13.72m) towers separated by a 270 ft (82.3m) space. Prior to blasting the connecting beams and slabs were completely separated by jack-hammer and torch between the part to be blasted and the part which was to remain intact. Furthermore, the blasting operation was carefully planned not to damage the separated end parts of this building. This was a successful operation, and a careful inspection of the two end towers of Building C-3 in the summer of 1975 revealed that visually these structures were whole and completely intact. This was further borne out in the subsequently performed dynamic tests on this building.

It appeared then that two ready-made structurally sound test-buildings existed which could actually be tested such that significant deformations could be induced with equipment then available. Furthermore, it was probably possible to perform these tests at a reasonable cost.

During the performance of the feasibility study in the summer months of 1975 the St. Louis Housing Authority completed plans for the total demolition of all the remaining buildings in the Pruitt-Igoe complex. The demolition operation was probably to commence early in 1976, and it was to move quickly, with a planned completion in a period of about 18 months. This placed several obstacles into the research plan: We would be pressed for time, since the contractor would want to finish with the job as quickly as possible, and we would have to test while demolition work, rubble removal, and possibly also blasting, was taking place. We felt that if the contractor was cooperative and if the test site was separated by a fenced-off region, then the testing work could proceed

independently of the other operations on the site.

Considerable thought was given during the feasibility study to perform tests on both of the end towers of Building C-3. Unfortunately this would have cost a great deal more money (about one-and-a-half to one-and-two-thirds of the expense for testing only one tower) and time. As it turned out, there was barely enough time to test one building without causing delays to the demolition contractor.

Another subject under consideration was the selection of the equipment for the large amplitude tests. Dr. Mayes examined in detail all the available systems of dynamic shakers. It was felt that we wanted to use an available system rather than to plan, design and build a new system from the ground up. Perhaps with more time and considerably more money it would have been advantageous to build such a system for this and future uses. Maybe this would have been a good thing to do. Subsequent experience in the actual testing has shown, however, that it was possible to assemble a system from available components for this particular site. Other sites would most likely be considerably different, and future tests could again be designed on the basis of the particular site conditions. The final selection of the Boeing Company's system was an easy choice for this project because their equipment was the only one judged to be able to produce the required forces and it was the only one available in the final time schedule.

It turned out that the feasibility study examined most of the relevant aspects of the work, and finally, a proposal was completed and submitted to the National Science Foundation. This proposal was subsequently funded in full.

The Proposal for the Project

Upon completion of the feasibility study a proposal entitled "Full Scale Tests on Eleven Story Building in the Pruitt-Igoe Housing Project of St. Louis" was submitted to NSF on October 23, 1975. The planned starting date was January 1, 1976, and the period of the project was for one year. The budget called for an expenditure of \$365,101. However, due to changes in the rates charged by the sub-contractors a request for an increase was submitted on January 30, 1976, and the final proposed budget was \$370,459.

Approval of the proposal did not proceed as rapidly as expected. Several review comments were received on February 25, 1976. The replies to the comments were sent to NSF on March 16, 1976. By late May it was apparent that NSF would fund the project, and final approval was received on June 11, 1976, permitting to start the work. Initial funding was for the amount of \$219,000, and the remaining \$151,500 was transmitted by NSF to Washington University on December 13, 1976, giving a total \$370,500. As it turned out, this money was just sufficient to perform all of the work planned in the proposal.

The period of the project is from June 1, 1976 through November 30, 1977, a period of 18 months, including an unfunded six-month flexibility period. The project termination was extended in October 1977 to May 31, 1978.*

During the period between the end of October 1975, when the proposal was submitted, and the beginning of June, 1976, several things happened which were of significance to the project. After several failed attempts by a North St. Louis citizens' group to rehabilitate at least some of the buildings for occupancy, a contract was let to demolish the entire project.

*The termination date was extended to August 30, 1978.

This contract was awarded to the Cleveland Wrecking Company of Cincinnati, Ohio, and to the AALCO Wrecking Company of St. Louis.

The whole area was fenced in and demolition work proceeded in January 1976. In February of 1976, assurance was obtained from Mr. Crane, the supervising engineer for the Cleveland Wrecking Company, that the remaining West tower of building C-3 would not be demolished or damaged unless word was received that the proposal was turned down. Mr. Crane also promised that the adjacent building (Bldg. A-2, Fig. 1) would be removed sooner so that our testing operations would not be hampered. These promises were kept, and when we were finally ready to start, only the test building stood in the area, clear of all obstruction and separated from all the demolition operations.

We did experience some anxious moments in the period between the submittal and the approval of the proposal. Because of security, safety, and insurance requirements, it was not possible to visit the test-building to make preliminary measurements and to study the site. This was a handicap because a lot of time was spent later which should have been spent on other matters. Another cause for anxiety was that the legal, security and insurance obstacles would be so severe that we might not, after all, be able to get on the site. A great deal of this anxiety was removed when Mr. Marvin Rose, Chairman of the Board of the Cleveland Wrecking Company, reviewed the proposal and pledged his full support and cooperation. This pledge was crucial to the subsequent success of the project, and it marked a turning point in the prospects of the undertaking.

The proposal to NSF-RANN outlined the following work to be done:

- 1) Survey of dimensional and material properties
- 2) Small amplitude shaking tests
- 3) Large amplitude shaking tests.

Phase 1. Survey of dimensional and material properties.

The rationale for this survey was two-fold: (1) to provide the necessary data for interpreting the results from the dynamic tests and (2) to determine the correlation between properties and dimensions in the original plans and specifications with the actual structure as it existed 20 years later. This latter purpose would shed some light on the more general question in structural design methodology of the correlation between the plans and the executed construction.

The proposed work was planned to involve the measurement of the relevant structural dimensions (story heights, plan dimensions, beam and column cross-sectional dimensions, slab thicknesses), the determination of the location, size and the yield strength of the reinforcing bars, and the evaluation of the strength and the modulus of elasticity of the concrete by direct (coring) and indirect (sonic) means at enough positions in the building so as to obtain statistically significant results.

Phase 2. Small amplitude shaking tests.

The reason for these tests was

- a) To determine the dynamic characteristics of the structure by methods that have been extensively used over the past decade.
- b) To compare the results obtained in a) with those obtained from the large amplitude forced vibration tests.
- c) To use the information obtained in a) to plan the large amplitude forced vibration tests.

Phase 3. Large amplitude shaking tests.

The proposed large amplitude shaking tests represented something beyond anything which had been previously attempted as far as the intended shaking device and the size of the structure was concerned.

The testing was planned

- a) To determine changes in mode shapes, frequencies, and damping values as the force level of excitation increased.
- b) To determine the resistance capability of the non-seismically designed building as the force level of excitation increased.

Performance of the planned research.

Actual work on the project site started on June 25, 1976, and the final day of our presence on the Pruitt-Igoe Housing Complex was November 10, 1976, a total of 138 days. During this period many people and organizations helped to make the research work possible. A list of these, as well as their functions and contributions, are presented in Appendix A.

The major dates and events are as follows:

1. Proposal for Feasibility Study:

 Submittal to NSF, February 24, 1975

 Funding: April 4, 1975

2. Proposal for Testing Program:

 Submittal to NSF*, October 23, 1975

 Comments from reviewers, February 25, 1976

 Reply to reviewer's comments, March 16, 1976

 Funding approved and start of project: June 11, 1976

3. Contract dates with subcontractors:

 Night-Hawk Security Agency, June 22, 1976

 Applied Nucleonics Co., July 7, 1976

 McDonnell-Douglas, July 20, 1976, September 13, 1976

 Sachs Electric Co., June 18, 1976, August 13, 1976

*This proposal was also the final report for the feasibility study.

The Wightman Agency, Insurance, June 23, 1976

Boeing Engineering and Construction, September 29, 1976,

October 19, 1976.

4. Site work:

Clean-up of test building, June 25 - June 30:

Measuring dimensional and material properties; planning

large amplitude tests, July 1 - September 3:

Small amplitude shaking tests, July 9 - July 12:

Installation and trial of large amplitude shaking

equipment, September 6 - October 2:

Large amplitude tests in E-W direction, October 4 -

October 15:

Removal of walls and realignment and repair of shaking

equipment, October 16 - October 26:

Large amplitude tests in N-S direction, October 27 -

November 4:

Removal of equipment from the site, November 5 - November 7:

Demolition of the building and removal of debris, November 8 -

November 10:

The various activities which took place are given in greater detail
in Appendix B.

2. DESCRIPTION OF TEST STRUCTURE AND TEST EQUIPMENT

2.1 TEST STRUCTURE

2.1.1 General Description of Test Site

The test structure is located in a now (1978) empty tract of land, located in the area bounded by Cass Avenue on the North, Twentieth Street on the East, Carr Street on the South, and Jefferson Avenue on the West. The general area is situated about 20 blocks West and 10 blocks North of the Gateway Arch on the Mississippi Riverfront in St. Louis.

The test structure is part of a building originally designated as Building C-3; its North face is located about 300 ft (91 m) South of Cass Avenue, and its West face is about 800 ft (244 m) East of Jefferson Avenue. (Fig. 29).

Building C-3, like every other apartment building in the Pruitt-Igoe Housing Complex, was eleven stories tall above the ground level and its long dimension was in the EW direction. This building had an overall length of 360 ft (109.7 m), with a narrower 29 ft (8.8 m) wide and 270 ft (82.3 m) long center portion flanked at the East and West ends by a 45 ft x 41 ft (13.7 x 12.5 m) "end tower" (see Fig. 29). Adjacent to Building C3 were Buildings A2 and A4, offset to the South but touching at the SW and the SE corner (Fig. 29).

Building C3 was constructed in the period March 1, 1954 through March 29, 1955.

The sequence of demolition of the group of buildings near C3 is shown in Fig. 30. The original cluster of structures, i.e., A2, C3, A4, is shown in Fig. 30a. During 1972 the narrower center portion of C3 was removed to the ground level by blasting (Fig. 30b), leaving the two end-

towers standing by themselves. Great care was taken to properly separate the portions of C3 which were to remain by cutting the connecting beams and slabs with jack-hammer and torch. The East face of the remaining W-tower of C3 (the test structure) is seen in Fig. 16 with the severed beams and slabs. Subsequent inspection showed that the blast did not result in structural damage. Only the connecting block wall was damaged (Fig. 16). During the Spring of 1976, prior to May, the E-tower of C3, as well as all of Buildings A2 and A4, were removed by conventional demolition techniques, using a lead ball suspended from a crane boom, leaving the test structure completely isolated (Fig. 30c). The demolition operations in the adjacent A2 building were performed carefully, resulting in slight damage to the wall of C3, but no structural damage.

2.1.2 The Test Structure

The test building was the W-tower of Building C3, left completely isolated, structurally essentially undamaged and with superficial damage to the outside walls only. Clearly, the test structure was not new, and it had sustained a) a nearby blast strong enough to demolish a separated part of the building and b) several accidental impacts with a heavy lead sphere. Careful visual inspection, as well as the record of elastic dynamic performance, indicated that overall the structure was not damaged to any noticeable degree prior to the sequence of tests performed as part of this project.

The plan of the test structure was identical on every floor above ground level. A plan view showing the column and beam locations (square symbols are the columns and the solid lines are the beams) is given in Fig. 31. The cross-section is rectangular, with nine peripheral columns and four interior ones. The columns are mainly square in cross-section,

although some are rectangular. The column dimensions are listed in Table 1. The upper columns are tied columns and the lower columns are spirally reinforced. The spiral reinforcement terminated above and below a joint, leaving each beam-column joint without confining reinforcement. The joint details are illustrated in Fig. 32. Typical column cross-sections and spiral reinforcement data are presented in Fig. 33. Footing, pier and basement column details are given in Fig. 34*. A clear view of a joint is shown in the photograph of Fig. 35, taken on another building during demolition.

Two sets of identifying numbers are given in Fig. 31 for the columns: one set corresponds to the identification in the original plans, and the other set was used during the testing to identify photographs**.

The locations of the column centers are dimensioned in Fig. 36. Beams are identified in Fig. 37, and beam dimensions and beam reinforcements are listed in Table 2. Slab designations and dimensions are given in Fig. 38 and Table 3, respectively.

The building elevation in Fig. 39 shows eleven floors of 8.5 ft (2.59 m) height each above ground level, a crawl-space (basement), the piers (i.e., the columns below the crawl-space floor) and the footings. The pier lengths, and thus the footing elevations, are variable, ranging from 1 ft to 7 ft (0.3 to 2.1 m). The footings are individual spread footings for each column, except that columns 45 and 46, and 47 and 48 have a shared pedestal (Fig. 40 and Table 4). Each footing is a two-level pedestal of reinforced concrete.

* Figs. 32, 33 and 34 were reproduced from the construction drawings.

** Care will be taken in the following portions of this report to precisely define a particular column using both sets of identification.

In summary, the test-structure is a rectangular building, approximately 40 ft x 45 ft (12.2 x 13.7 m) in plan and approximately 94 ft (29 m) in height above the ground. The height-to-width ratio is thus about 2:1. The structure has eleven stories of equal height above the ground, and a low crawl-space below the ground. The structure consists of columns, beams, slabs, piers and footings. In addition, the crawl-space periphery consists of a 12 in. (0.30 m) thick reinforced wall which is monolithic with the columns. The slabs are 5 in. (0.127 m) thick except in the West end of the floor (Fig. 38) where there is a 4 in. (0.102 m) slab. The slabs were designed as one-way slabs. The structure was designed according to the 1953 ACI Code for a concrete strength of 3000 psi (20.5 MPa).

Several features of the structure are of relevance to the subsequently observed behavior under shaking:

- 1) A substantial portion of the mass of the concrete was below ground level (see Table 5 for the concrete volume at each level). The volume of the concrete above the ground level is about 13,700 cu. ft (389 m³) out of a total of 19,100 cu. ft (540 m³); thus about 30% of the mass was below the ground, concentrated mainly in the massive footings and the basement walls. This explains the lack of any significant response to the dynamic excitation in the bottom of the crawl-space and in the ground near the building. In addition, the sensitive seismographs at St. Louis University, about 2 km from the test site, did not pick up any vibrations from the test. It must then be concluded that for all practical purposes the dynamic forces did not penetrate into the soil around the test-structure and that the test frame was essentially fixed at the ground level.

- 2) The beam-to-column joints were without any confining reinforcement, and this permitted the occurrence of the characteristic joint failure

observed especially in the NS shaking where the concrete eventually spalled out completely, leaving only the exposed main reinforcement.

3) The bottom reinforcing bars at the beam ends were generally not anchored into the joint, thus permitting an easy pull-out of the bottom bar under positive joint moment. This resulted in the characteristic hinging observed especially during the EW shaking.

The nominal design strength of the concrete used was 3000 psi (20.7 MPa). The cylinder strengths of the concrete, taken during construction, ranged from 2830 psi (19.5 MPa) to 5130 psi (35.4 MPa) with an average of 3800 psi (26.2 MPa). Core samples taken as part of this research project gave an average of 5,600 psi (38.6 MPa), and results of a Schmidt hammer investigation showed an average of 8020 psi (55.3 MPa). The steel reinforcing had a nominal yield stress of 50 ksi (345 MPa). The actual yield stress of the in-situ reinforcing bars was determined by laboratory samples taken from demolished adjacent buildings, giving a range of yield stress values of 55 to 62.5 ksi (379 to 431 MPa).

The slabs, while designed as one-way slabs, were reinforced enough transversely* so that they acted essentially as two-way slabs. During the erection of the large amplitude shaker on the eleventh floor portions of the slab in the SE corner were inadvertently loaded to 700 or so psf (34 kPa), i.e., to an order of magnitude larger than the design live load of 70 psf (3.35 kPa) and no undue distress was observed.

The dimensions of the beams and columns were essentially the design values.

The structure was thus for all practical purposes built according to the plans, except that the concrete strength was considerably higher than

* Further details of the in-situ material strengths and dimensions is presented in a separate report.

the design value.

The footings sat on silty brown clay which extended some 10 to 20 ft (3 to 6 m) below the footings to broken limestone.

The original structural design considered only gravity loads. Beams were designed with moment coefficients and columns were designed for axial load only.

2.1.3 The Cladding

Prior to testing the whole building was clad in walls from the second story up, leaving the space between the ground (level 1 in Fig. 39) and the second floor (level 2) free of any walls. This fact of an open first floor may have contributed to the experimentally observed spread of the structural damage from level 2 upward. The first structural distress, in the form of cracks at the beam ends, was observed in the EW beams of level 2.

Above level 2 the whole building was encased in a wall extending around the whole periphery. In the NE portion of the E wall, where the test-building joined the previously demolished central portion of C3, the wall consisted of one thickness of 8 in (0.203 m) thick concrete block (Fig. 41). This wall was interrupted by a door between the two central columns, and it was loose on the top on each floor. There were also some holes in the wall (Fig. 16). This wall was damaged from the blast. The remaining portion of the E wall (SE corner) was in excellent condition and it was not interrupted by windows. This wall, as well as the remaining walls on the S, W and N periphery, consisted of one thickness of 8 in (0.203 m) concrete block between the columns and one thickness 4 in (0.102 m) brick extending beyond the column faces. The brick was supported by a steel angle at every second floor level, and, in addition, every second brick in every sixth course was turned at right angles to dovetail into the block

wall behind it. The quality of workmanship of the wall construction was of a high grade. The N and S walls were interrupted in each floor by three windows, one extending almost from column-to-column (Fig. 41), and there were four smaller windows in the W wall. There were almost no window panes left but the window frames were in place.

The stair-well (landings and stairs) was enclosed by concrete block walls which were interrupted by one door on the N and the S wall (Fig. 41). The walls were 8 in. (0.203 m) blocks on the N and S side, and 12 in. (0.305 m) blocks on the W side.

The inside of the space was subdivided into rooms by means of plaster-board partitions. Most of these were damaged prior to the dynamic tests, and during the shaking they produced an eerie scraping, groaning noise. These partitions were easily removed manually, first in the top floor to make room for the test equipment, and then later on the other floors.

The structural components and walls were not plastered and there was no insulation. Therefore, it was easy to gain access to the structure in order to make observations and to take measurements.

The stair-system (Figs. 39, 41 and 42) consisted of reinforced concrete stairs between landings. These stairs provided the only access to the top floor where the test equipment was located.

2.2 SMALL AMPLITUDE SHAKING TESTS

The first experiments on the test-structure were a series of small-amplitude shaking tests to determine the dynamic properties of the undamaged structure as it existed at the beginning of the project. These tests were performed under a subcontract by a team from the Applied Nucleonics Company of Los Angeles, California.

The small-amplitude shaking tests were made in the three days from July 10 to July 12, 1976. The details of the test equipment, the test

data and the test results are described in the report "Moderate Level Vibration Tests on an Eleven Story Reinforced Concrete Building" prepared by the technical staff of the Applied Nucleonics Company (dated September 1976). Only a brief description of the test apparatus will be given here, and the results are further discussed in a later portion of this report.

Two types of eccentric mass vibrators were used in the experiments: one type, a rotating eccentric arm shaker (Fig. 18, Applied Nucleonics designation MK-14) and a shaker with two rotating baskets (Fig. 19, ANC designation MK-13). The vibrator was attached by bolts to the floor of level 11, near the S.W. corner of the building (Fig. 43). The rotating eccentric arm shaker (MK-14) supplied an omnidirectional horizontal force and the other shaker (MK-13) gave a unidirectional (EW and NS) horizontal force. The vibrators were driven by a motor-control system (2 hp motor), with the control capable of maintaining the vibrator frequency within 0.1% of the desired value.

Data were taken over the range of 0 to 18 Hz to determine structural response, to estimate modal damping ratios, and to determine the response shape at resonance. Data were taken and recorded by coupling eight accelerometers (six strain-gage type and two force-balance types) to a Hewlett-Packard Model 7418A 8-channel strip-chart recorder and a Spectral Dynamics Model SD-330 real time analyzer. The ANC MK-14 omnidirectional eccentric mass shaker was used over the frequency ranges of 0-2 Hz and 0-4 Hz at eccentricities of 140 Kg-m (12,110 lb-in) and 51.0 Kg-m (4,440 lb-in), respectively. The ANC MK-13 unidirectional shaker was used over the frequency ranges of 0-6 Hz, 0-13.5 Hz and 0-18.5 Hz at eccentricities of 27.8 Kg-m (2415 lb-in), 5.81 Kg-m (505 lb-in) and

2.86 Kg-m (249 lb-in), respectively, with both NS and EW forcing applied. Two triaxial arrays of accelerometers (NS, EW, vertical) were located in the NW and the SE corner of the 11th level, and one biaxial accelerometer (NS, EW) was located near the stairwell on the 5th level for the sweep and damping runs. The biaxial array was kept permanently in the NE corner of the 11th level, while the two triaxial accelerometers were moved about the building during the response mapping operation while the building was kept in resonance. Five points (the four corners and the center of the floor) were mapped on each the 1st, 3rd, 5th, 7th, 9th and 11th level, and three points were mapped on the ground outside the building.

A total of 17 frequency sweep tests were recorded and mode shape surveys were made at 8 resonant frequencies. A total of 9 resonant frequencies (EW, NS and torsional first, second and third modes) were identified.

The results of the small-amplitude shaking tests were extremely valuable for the planning of the large amplitude tests. The results and their significance is further discussed in a later portion of this report. While this was not intentional, the small amplitude shaking did induce some non-structural and perhaps slight structural damage, as described later. The testing operation was very efficient, and the shaking and data-taking was performed without delays or difficulties.

2.3 LARGE AMPLITUDE SHAKING TESTS

2.3.1 General Considerations

The large amplitude shaking tests were the novel feature of this project: never before had a relatively new structure of such a size been subjected to so many cycles of large damage-producing cycles of lateral load. The eventual deflections (approximately ± 16 in, or ± 0.41 m, or

1. 4% of the height of the building above ground level), the dramatic sway, and the spectacular damage, far exceeded the initial expectations of the researchers and the experts^{*}. In some respects this initial innocence of the eventual behavior was good, because it was difficult enough to persuade the city and the insurance authorities to permit the tests in the first place. As it turned out, fortunately, no one was hurt and complete collapse and loss of equipment was avoided.

The shaking equipment used to produce such dramatic effects was a relatively simple system: a moving mass on rollers was pushed back and forth on the top floor, and the inertial forces from this mass, reacting against the building at resonance, provided the forces which produced the response.

The idea for the unidirectional horizontal moving mass exciter came from a similar but smaller system employed by John A. Blume and Associates in a test on a 4-story full scale concrete frame in Nevada (Refs. 1, 2, 3). A system of this type was preferred over the more frequently used rotating mass shaker because of the high force and power requirements. Based on preliminary calculations during the proposal development phase, and on more solid estimates based on the results of the small amplitude tests, it was specified that the large amplitude shaker should have the following capabilities: maximum force level of 30 Kip (133.5 KN) over the range of 0.5 to 10 Hz and a maximum piston displacement of ± 20 in (0.28 m). A careful search of available equipment revealed that the Boeing Company alone had equipment which a) was able to fulfill the requirements, b) was portable, c) was available on short notice and d) was able to be accompanied by experienced engineers and technicians.

* Quoting one reviewer of the proposal "... the equipment ... will not be capable to damage the building."

The heart of the system was a pump-motor assembly, able to deliver 140 gpm hydraulic power, run by two electric motors (200 HP and 125 HP), weighing about 10,000 lbs (4500 Kg) and taking up a volume of about 12 x 12 ft in area x 6 ft in height (4 x 4 x 2 m). Adequate power having been assured by this system, the rest of the shaking machine could be designed around it.

Other fortuitous facets of the project were that 1) the building was isolated by at least 400 ft (120 m) from the nearest buildings which were, anyway, almost in ruins and which appeared to be only intermittently occupied, and 2) there was adequate room and strength in the structure to accommodate the equipment.

2.3.2 Site Preparation

During July and August 1976, after the Applied Nucleonics small amplitude tests and prior to the installation of the large amplitude shaker in September, the following activities took place: 1) Dr. R. L. Mayes planned the details of the large amplitude tests on the basis of the dynamic properties obtained from the small-amplitude tests; 2) the teams at Boeing and at McDonnell-Douglas designed, purchased, manufactured, assembled and tested out the shaking system (Boeing) and the data taking system (McDonnell-Douglas), respectively; 3) on the site work continued on the survey of the dimensional and material properties*. Site and building preparation during this period consisted of further clean-up of the building near areas where accelerometers were to be located. Power, water, telephone and toilet service was arranged for and installed. The area was fenced and guard service was instituted (nights and weekends).

* While the results of the survey have some bearing on the dynamic test interpretation, the work is of sufficient independence to be presented in a separate report.

Finally a portion of the roof slab was removed in the SE corner of the building to facilitate installation of the shaking equipment (Fig. 44). Electric power supply was required for the pump-motor assembly (440V 3-phase), for the water pump needed to lift cooling water from a city hydrant to the 11th floor (220V 3-phase), and for the instrumentation (110V). The switch boxes were located on the ground about 20 ft (6 m) S of the building (Fig. 45). The high-voltage cable ran diagonally from the switch-box to the opening in the S wall of the 11th floor external to the building. The water hose and the cables for the control, communication and low-voltage electricity were run up through the stairwell.

In retrospect it is evident that the pole for the power terminal, the switch boxes, the instrumentation and the fence should all have been further away from the test-building. Power cables and water hoses were severed several times by flying debris, thus causing delay.

2.3.3 The Shaker

The moving mass shaker consisted of a compartmentalized steel box, 8 x 8 ft square and 1'-4" high (2.44 x 2.44 x 0.41 m) with 16 2 x 2 ft (0.61 x 0.61 m) compartments. These compartments could be empty or they could fully or partially be filled with lead ingots. The box was completely filled up with 72 700 or 350 lb lead ingots (320 Kg or 160 Kg), totaling about 58,000 lb (26,300 Kg) of lead. When fully loaded the total mass of steel box and lead was 60,000 lb (27,200 Kg). In the beginning of testing the lead in the box was varied to achieve the desired horizontal force, but as testing continued it was found more convenient to keep the total amount of lead in the box and to vary the force solely through the stroke of the hydraulic piston.

The moving mass box was positioned on a stiffened steel plate, 12 x 12 ft (3.66 x 3.66 m) square which was fastened to the floor-slab of the 11th floor by bolts. This stiffened plate was located in the center of the space between columns 43-44-45-46 (Fig. 31) in the middle of the building (Fig. 46). Hardened 1 in. (25.4 mm) diameter balls, held in place by a perforated 1/4 in. (6.4 mm) thick aluminum plate on a 6 x 6 in (152 x 152 mm) grid were placed between the stiffened steel plate and the bottom of the moving mass box. This provided a relatively frictionless surface. The side of the moving mass was attached to the horizontal piston of the hydraulic activator. The non-moving housing of the actuator was bolted to the floor. The end of the actuator situated away from the moving mass was attached to the building (Fig. 46). The inertia force reaction to the building was made through a steel wide-flange column spanning from the roof slab to the slab of the 11th floor, and attached to the concrete slabs by bolts bearing on steel plates on both sides of the slab. The base of the steel column was pinned but the top was welded fixed. Approximately 12 in (305 mm) from the floor a steel stub beam was welded to the column to provide the reaction attachment to the actuator. The actuator was driven by the pump-motor assembly which was also bolted to the floor. A large oil accumulator was also fixed to the floor (Fig. 46).

The initial testing was in an EW direction, and the set-up is as shown in Fig. 46. The final shaking was in the NS direction, and the reaction column and the actuator was rotated 90° to bear against the S edge of the slab.

The shaker was a closed-loop servo-controlled inertial force generator. It consisted of a 42-inch hydraulic actuator connected to a steel

box filled with lead. The box was supported on a steel plate by several hundred 1-inch steel ball bearings. This allowed the box and weight to be freely accelerated and input the resultant force into the building back through the actuator which was attached to the building.

The hydraulic supply was a dual motor pump of 325 HP capacity at 3000 PSI and 150 gallons per minute flow. The 10 square inch actuator area allowed a 30,000 pound force to be generated. Hydraulic fluid to the actuator was controlled with a Moog series 79 3-stage servo valve. Figure (47) shows a block diagram of the servo control system.

A sinusoidal signal from a variable frequency function generator was used as a command signal to the controller. The position of the mass was controlled and a force transducer interposed between the actuator rod and the mass was used to determine the required test levels.

The force, position, and command signals were displayed on a strip chart recorder for use in adjusting and monitoring the test parameters.

Force, position, and control error were put into a detector device to shut down the hydraulic pump in the event that any of the signals went over predetermined safe levels.

The test levels were obtained by manually adjusting the signal generator and visually observing the force level displayed on the recorder. Increased amplitude or increased frequency caused increased force.

The empty steel box, the steel balls and the stiffened panel are shown in the photo taken during a mock-up exercise in Boeing's laboratory in Seattle (Fig. 48). The whole set-up, including the box, the plate, the actuator, the reaction column, the accumulator and the pump motor assembly are shown in Fig. 49 (mock-up photo). The details of the connection between the reaction column and the actuator are seen in Fig. 50.

The fully loaded box is shown in Fig. 51, and the piston, with its connection to the moving box, is seen in Fig. 52. Coupled to the piston is the force transducer, and above the piston is the LVDT controlling piston displacement. The control panel in the instrument van is seen in Fig. 53, while Figs. 54 and 55 show, respectively, the cribbing on the 10th floor and an overall view of the test site.

2.3.4 Instrumentation and Data Acquisition

The instrumentation and data acquisition system was provided under subcontract by the McDonnell-Douglas Company of St. Louis. The system was designed to measure and record accelerations in various parts of the building during the shaking tests. Details of the tests are described later in this report, but they will be also discussed here in sufficient detail to explain the functioning of the data system.

Two types of tests were performed: (1) damping tests to determine resonant frequencies and damping values of modes of interest at various input force levels, and (2) mode-shape tests to determine the mode shapes at various resonant frequencies.

During the damping tests the approximate resonant frequency at a required force level was determined by a slow continuous sweep beginning at approximately one Hz above the estimated resonant frequency, and sweeping down to below the actual resonant frequency.

During this sweep, two recordings were made: First, the signal of the reference accelerometer on the eleventh floor (Fig. 56 and Table 6) was analyzed by a spectrum analyzer. The peak of the resulting curve was used to identify the resonant frequency. Second, the force signal from the moving-mass vibrator was plotted against the signal from the reference accelerometer on a two-channel oscilloscope. Theoretically for an elastic

system at resonance the two signals are 90° out-of-phase and the resulting plot traces a perfect circle on the oscilloscope screen. Both the spectrum analyzer and the oscilloscope were used to identify the resonant frequency during the sweep.

Once the resonant frequency was analyzed, a stepped sweep was performed at appropriate frequency intervals to determine the damping and resonant frequency at that particular force input level. At each frequency step the structure was vibrated until steady-state was achieved and the data was recorded.

Mode shape tests at resonance were made to record the detailed response of the building. Acceleration data were obtained from each of 25 locations in turn (see Fig. 56) from levels 12, 10, 8, 6, 4 and 2. After it was discovered that the response of the basement floor was below the sensitivity of the available accelerometers, no mode-shape measurements were made on level 1. Mode shape data were taken on level 3 during some of the NS mode shape tests (See Fig. 57 for the identification of the story levels in the structure).

The primary source of data from the instrumentation was produced by the accelerometers. Three accelerometers each were assembled into a tri-axial mount (Fig. 58). All of the accelerometers used on the test structure were strain-gage type accelerometers. Servo-accelerometers were used on the ground stations outside of the building. The accelerations on the ground were, however, too weak to give meaningful data within the sensitivity range of these instruments and thus few recordings of ground acceleration were made. The strain-gage type accelerometers on the test-structure were sensitized in the range of ± 1.0 g. These instruments were calibrated using a 30/60 degree fixture in a static calibration at the

start of testing and at intervals during the tests.

The accelerometers were used to drive constant band-width voltage controlled oscillators (VCO's). Six of these VCO's each were combined into one multiplex which thus served six accelerometers, i.e., two floors (Fig. 59). The signals from the multiplexes were transmitted by wires to the instrumentation trailer where they were recorded on a standard 14 track instrumentation recorder. The four multiplexes were placed on the following locations: levels 11 (serving the two accelerometers on levels 12 and 10), 7 (serving 8 and 6), 3 (serving 4 and 2) and 1 (serving the ground stations and level 1). The 14 tracks on the recorder were assigned as follows: 4 tracks for the acceleration from the four multiplexes, 1 track for the reference accelerometer, 1 track for the force level, 1 track for the IRIG (Inter-Range Instrumentation Group) time code, 1 track for location identification, 1 track for frequency identification, 1 track for voice and 2 tracks for control.

On-site data collection consisted of the following items:

- 1) The accelerations from the multiplexes recorded on tape (as described above);
- 2) twelve channels of discriminators to permit real time observation of any two multiplex data (six accelerations), the load and the reference acceleration on an 8 channel strip chart recorder.
- 3) frequency of the moving mass actuator and real time strip chart records of the displacement and the force produced by the moving mass (Fig. 60)
- 4) two-axis oscilloscope display
- 5) spectrum analyzer display (Fig. 61).

2.4 DISCUSSION

At this place in the report it is instructive to provide a brief critique of the activities performed in this project. In retrospect it must be clearly stated that, given the constraints that existed on the site, the operation was very successful. Furthermore, the delays were minimal, the weather was mostly favorable and we were spared accidents which could have harmed people. The testing project was not without dangers from the political side (insurance, legal, crime, and labor problems), from injuries due to flying debris and the possibility of people falling off the building, and from the total collapse of the structure which could have resulted in the loss of some or all of the equipment. For all the experience which any of the participants had previously, the whole large-amplitude shaking could well have not worked at all.

The main constraint was lack of time on the site during the preliminary planning. A one-month lead-time prior to the small amplitude tests, and a period of three months between the completion of these tests and the start of installation of the large amplitude shaking equipment would have been very desirable. The various components of the large amplitude shaking system could then have been more thoroughly tested out in the laboratory and the delays due to the inappropriate packing of the hydraulic actuator could have been avoided. As it turned out, the problems with the shaking equipment were expeditiously solved in the field.

A more serious problem was with the data taken in the field. We should have installed an array of accelerometers on the ground near the building. This was not done because McDonnell-Douglas could not furnish enough accelerometers of sufficient sensitivity to do the job. However,

this is only one side of the story. For a proper pick-up of the ground accelerations it would have been necessary to prepare each position beforehand, excavating the overlaying debris to undisturbed soil, and rendering the point waterproof. For this there was neither time or space available. Due to inadequate time, planning, space and equipment then valuable data was not recovered.

Visual and photographic data taking was not nearly as complete as it should have been, and so the sequence of damage at critical locations was not systematically recorded. The reasons for this were lack of prior experience regarding what should be expected, lack of time, and the danger to an observer in the building. Particularly valuable would have been close-up moving pictures of critical joints as they deteriorated under large amplitude shaking. Perhaps one or two remotely operated cameras should have been installed.

Whatever the reasons, the visual recording of the damage should have received a great deal of attention during the planning stage, and during critical stages of the testing remote photographic recording close up to several key locations should have been made.

All of this, however, is hind-sight, useful for planning the next tests. In further parts of this report we will concentrate on presenting the data and the results we did manage to obtain.

3. DISCUSSION OF DAMAGE

3.1 GENERAL COMMENTS

The novel feature of this project is in the fact that an actual full-scale, relatively new and originally structurally sound reinforced concrete frame building, which was designed and built according to the current state of the art in the 1950's, was subjected to many repetitive damage-producing cycles of lateral load. The significant data from the tests are the accelerations and displacements measured in various parts of the structure and the dynamic properties which were computed from them. These results are treated in a later portion of this report. This part of the report will present a qualitative description of the observed damage during the progress of the test program.

Damage observation was made continuously, as far as that was possible, during the whole testing period. Unfortunately the observations were not made as thoroughly as they should have been made because (1) we did not know, prior to the tests, just what to expect, (2) we did not know for sure until the tests commenced whether or not the equipment could indeed induce large amplitude deformations, (3) time for proper prior preparations was inadequate, and (4) it was not safe to be in the building to make close observations during crucial points of the testing program. The following discussion is based on observed damage after the completion of major phases of the testing.

3.2 STATUS BEFORE LARGE AMPLITUDE TESTS

At the beginning of October, prior to the commencement of the large amplitude shaking the building was essentially undamaged from the structural point of view (Fig. 15). There were a few hairline cracks in the

beams and the columns of the top floor (at level 12)* which were induced by the small amplitude shaking performed in July by the Applied Nucleonics Company (Fig. 62), and there were some diagonal cracks in the EW filler walls around the stairwell (Fig. 63) on the 4th, 5th and 11th story. The outside E-wall (Fig. 16) was already damaged by the blast when the center portion of the building was removed in 1972, and the small amplitude shaking loosened some of the blocks on the top layers further. The stairs were completely whole, and the outside brick facade was essentially intact except for a small part of the SW corner (Fig. 12) which was inadvertently hit by a headache ball when the adjacent building was demolished. The only modification to the structure consisted in removing a portion of the roof slab at the end of August to facilitate placing the equipment (Fig. 64).

3.3 DAMAGE AFTER MODERATE E-W SHAKING

After the fully clad structure was subjected to a series of test-runs (October 8, Test Run 12E-D) with 5 and 10 Kip force levels damage to the slab and structural frame was slight, consisting mainly of hairline cracks at the column tops (notably in Col. 33,* 1st story) and at the ends of some EW beams (notably in Beams B4 at levels 2 and 3). Some blocks fell off the E block wall in the 2nd story, and cracks developed all across the joints between the stairs and the stairway landing at the 1st story and the 1 level landings. Those cracks became quite large later and subsequent photos will show them in a more developed stage. The most interesting feature of these moderate level shake tests was the behavior of the EW block infill wall around the stairway. These wall panels moved with the

* See Fig. 57 for the convention used to define vertical locations in the building.

** See Fig. 31 for column locations. Column 33 is No. 48 in the original plans.

frame above level 4, but in stories 2 and 3 the panels remained essentially stationary while the frame moved back and forth, leaving a gap of up to 1/8 inch between wall and column at maximum amplitude, and knocking against the wall on the opposite side (Fig. 65). There was noise due to friction as the beams rubbed against the top face of these walls.

3.4 DAMAGE AFTER COMPLETION OF E-W TESTS

The major amount of testing in the EW direction on the fully clad structure was performed during the period October 9 through October 13. Some 10K force-level tests were performed on October 15, and finally the most severe EW shaking (cca 25 kip force level; \pm 8 inch sway on top, Test No. 24E-D) took place in the evening of October 15 just before this phase of testing was discontinued.

All of the damage to the structure above level 9 was restricted to hairline cracks at some column tops and beam ends, and no new cracks were discovered between levels 6 and 9. It can be stated that no substantial structural damage was discernible above level 6. Major structural damage occurred at level 2, with damage diminishing with height. All of the EW beams on levels 2 and 3 had cracks at their ends, and most of the beams on levels 4 and 5 had hairline cracks at their ends. Typically the most severe cracking and spalling took place on level 2, and the following photos illustrate this:

Typical interior joint X-cracks are seen in Fig. 66, which show the joint of Col. 36* at the top of story 1. The top of Col. 11** (SW corner) in story 2 is shown in Fig. 67. This same column, at one level below, exhibits a crack through the beam and into part of the column (Fig. 68). A typical level 2 beam end (SE corner) shown in Fig. 69 illustrates the

* Col. 45 in original plans. (Fig. 31)

** Col. 1 in original plans. (Fig. 31)

crack at the column face. This crack opened and closed during the motion of the building. The most severe column damage occurred at the top of column 37* in the 2nd story (Fig. 70). The most severe beam cracking occurred at the E end of beams B4 in level 2, and Figs. 71 through 73 illustrate the progression of damage, including the fracture of the reinforcing steel. During the final severe EW cycling it appeared from the observed motion of the structure that the EW beams connected to the exterior columns on levels 2 and 3 acted essentially as hinges when the bottom beam steel was in tension (Fig. 74). The slab on levels 2 and 3 cracked through from N to S across the building.

The stairway up to the fourth level was severely cracked at each joint between the stairs and the landing. This joint heaved up and down during each cycle of loading. The lowest joint (between levels 1 and 2) is shown during the early tests (cca Oct. 9) and after the EW tests in Figs 75 through 77, respectively. Top and bottom stairway joints are shown in Figs. 78 and 79.

A considerable portion of the E block wall fell out during the tests (Fig. 80; compare with Fig. 16 to see the extent of wall damage), and some of the outside brick walls fell off also (Figs. 81 and 82; compare with Fig. 15 to see the damage on the N brick wall). A portion of the lower part of the S wall, shown in Fig. 83, demonstrates the horizontal fracture lines at the top of the window. The adjacent parts of the wall rubbed against each other during load cycling.

On levels 2 and 3 at the end of the EW tests the EW beam ends were cracked through, some columns were cracked and one was moderately damaged, the slab was cracked across the building, the stairway was behaving as a

* Col. 44 in original plans (Fig. 31).

mechanism with hinges at the stair-landing joints, the E block wall had fallen out, the EW brick faces were severely damaged or had fallen out, and the EW block infill walls next to the stairway had lost their capacity to act as infill walls. The NS beams and the N wall were essentially undamaged. Damage to columns, beams, stairs and walls diminished progressively from the third to the fifth story, with the structure-stair-wall system intact and acting as a unit above level 6. Below that level the walls and the stairway system were broken up and the beams were hinging. As testing continued damage seemed to be confined to the lower three to four floors, the top riding along as the softening and damaged lower floors swayed back and forth. Little damage was observed on the eleventh floor where the heavy moving machinery subjected the frame and the slab to continued severe impacts. It appears that once softening started on level 2 the damage became isolated on the lower part of the building.

3.5 DAMAGE DURING THE N-S TESTS

During the period between October 15 and October 27 the cladding was removed from all but the upper two floors of the building (Fig. 28) and the shaking apparatus on the 11th floor was rotated 90 degrees to produce forces in the NS direction. The removal of all of the brick and block cladding did not result in any additional damage to the structure.

The NS testing commenced on October 27 and continued through November 4 when the experiment was terminated. During October 27, 28, 29 and 30 the tests were performed at mainly low force levels (5 to 10 Kips, Tests up to 16N-D) and only one 15 Kip level test of the second mode was performed. The new damage due to this shaking was slight, consisting of the development of flexural cracks between the column faces and the NS beam ends. The motion of the building during the first mode NS tests consisted of

NS translation of the whole building and of torsion centered toward the E of the building. This torsional motion at the first translational mode tended to wrack the W face considerably more than the E face, and damage was mainly confined to the beams and columns on the W face.

The shaking tests on November 1 through November 4 consisted of the larger input-force level tests (Tests 17N-D to 41N-D), and severe damage was inflicted on the W portion of the structure. This damage occurred in essentially two ways: (1) with continued shaking more and more joints in the NW (Col. 9)^{*} and SW (Col. 11)^{**} column failed, and (2) columns 37 and 38^{***} crushed in compression. There was also damage in the joints of the center columns on the W-face (Col. 13)⁺. A typical damaged joint of this center column tier (Col. 13, level 5) is shown in Figs. 84 and 85, where the damage prior to Test No. 25N-D (Fig. 84) consists of spalling and after Test No. 31N-D part of the lower beam reinforcing bar is exposed. The extent of damage to this joint did not increase with later tests. The other joints of this column experienced similar damage, with all joints losing some concrete from level 2 through level 9. The corner columns (Cols. 9 and 11) were damaged rather more severely, all joints from level 2 through level 9 losing almost all the concrete from the joints, leaving the beam flexural reinforcing fully exposed.

The photo in Fig. 86 shows a portion of the NW corner, illustrating the severe damage at the end of the tests at the joint. All columns appeared to be a series of hinged elements between stories, with the reinforcing holding them in place. Progression of damage from Test No. 21N-D

* Col. 41 in original plans (Fig. 31)
 ** Col. 1 in original plans (Fig. 31)
 *** Col's. 44 and 43 in original plans (Fig. 31)
 + Col. 42 in original plans (Fig. 31)

through Test No. 41N-D for one typical joint (Col. 9, level 4) is shown in the sequence of pictures given in Figs. 87 through 95. All but one of these figures show the outside of this joint, and Fig. 94 shows the inside of the corner, from below.

The deterioration of the interior column (Col. 38^{*}, 4th story) is seen in Figs. 96 (after Test No. 28N-D) and 97 after all the tests, and a close-up of the crushing failure is seen in Fig. 98.

During the last test on the evening of November 4 (Test 41N-D) the following damage was evident: All the joints below the 10th level in the two W corner columns (C 9 and C 11) had lost almost all of the concrete from the joints (see Fig. 99), and the column in the NW corner of the 6th story was visibly pushed out (Fig. 100). The joints in the center columns of the W-face (Col. 10) were also damaged up to level 9, but not as severely. Interior columns 37^{**} and 38 were severely crushed on the 2nd, 3rd and 4th floor, with Col. 38 completely crushed in the 4th floor. The other columns showed little additional damage, except that during the last run X cracks began to develop in the joints of level 6 in the two E central columns (Cols. 33 and 34)^{***}.

During the last test there was very large deformation of the top of the W-face (+ 15 inch), the W-face appeared to be just flopping back and forth, there was a lot of noise (groaning, cracking) and damage progressed apparently toward the columns which appeared to be holding up the structure. For the sake of safety and equipment recovery it was decided to stop the testing. When all motion stopped the structure was to all appearances

* Col. 43 in the original plans (Fig. 31)

** Col. 44 in the original plans (Fig. 31)

*** Col's. 48 and 47 in the original plans (Fig. 31)

straight. No additional structural or cladding damage occurred in the enclosed top two stories.

4. DESCRIPTION OF TESTS PERFORMED

4.1 INTRODUCTION

The dynamic testing of the building consisted of both small and large amplitude tests. The small amplitude tests performed by ANC with the equipment described in Chapter 2 had the following objectives:

- a) To determine the dynamic characteristics of the structure by methods that have been extensively used over the past decade.
- b) To compare the results obtained in a) with those obtained from the large amplitude forced vibration tests.
- c) To use the information obtained in a) to plan the large amplitude forced vibration tests.

The large amplitude tests performed with the equipment described in Chapter 2 had two main objectives:

- a) To determine changes in mode shapes, frequencies, and damping values as the force level of excitation increased.
- b) To determine the resistance capability of the non-seismically designed building as the force level of excitation increased.

4.2 SMALL AMPLITUDE TESTS

4.2.1 Description of the Tests

The eccentric mass vibrators used in these tests were located in the SW corner of the 11th floor (Fig. 43). All tests were performed with the cladding in place. Two different types of tests were performed: The first, a frequency sweep test, was performed to determine resonant frequencies and damping values. The second, a response shape test was

performed to determine the response of the building at various resonant frequencies.

For the frequency sweep tests two triaxial arrays and one biaxial array of accelerometers were located within the building (as shown in Table 7). Locations for these arrays were chosen so that anticipated structural response would be adequate to identify resonant frequencies and to identify the type of building response, that is translation vs. torsion.

For a given test number and run number, with the shaker set to a fixed eccentricity, identification of resonant frequencies and damping values took place in two phases over the frequency range of interest. Phase one consisted of a slow frequency sweep up to the maximum established by safe operating procedures during which system gains were adjusted and the frequency content of the response was observed using a spectrum analyzer. The principal purpose of this slow sweep was to determine the frequency ranges over which detailed data would be taken.

Phase two of a given test number and run number consisted of an extremely slow frequency sweep to establish an upper bound during which bursts of data were taken at small enough incremental increases in frequency to allow the sufficient resolution of resonant peaks and to adequately define modal damping ratios and phase relationships. This detailed data was then returned to Los Angeles, digitized, and digital methods applied to define resonant frequencies and damping values in finer detail than available using the techniques of phase one.

Response of the building in each of the first eight modes was mapped. Two triaxial arrays and one biaxial array of accelerometers were assembled and system gains adjusted so that each instrument indicated the same signal amplitude in a 1.0 g field. The biaxial set was then permanently

located at node four (refer to Fig. 101) to serve as reference. The structure was then brought to resonance using either the MK-13 or MK-14 vibrator and held at constant frequency while bursts of data were taken at each of the 33 nodes indicated on Fig. 101. In this way each of the records from the roving triaxial accelerometer sets could be compared with the reference set to determine phase relationship. Magnitude of the signal was fixed by instrument calibration.

4.2.2 Tests Performed

A summary of all frequency sweep tests performed and their respective results is presented in Table 8. Results of some of the frequency sweep tests are presented in Figures 102-104. The remainder of the plots at the frequency sweep tests can be found in reference 4.

As seen shown in Table 8 frequency sweeps were performed at four different force levels in the lowest two translational modes. It should be noted that these force levels were considerably lower than those used in the large amplitude tests. Response shape tests were performed for eight of the nine resonant frequencies given in Table 8. A response shape was not determined for the third torsional mode. Details of the response shapes are presented in Ref. 4. The EW first and second modes are presented in Figs. 105 and 106, respectively, and a comparison with those obtained in the large amplitude tests is presented in Figs. 107 and 108.

4.3 LARGE AMPLITUDE TESTS

4.3.1 Description of the Tests

The large amplitude tests were performed with the moving mass vibrator described in Ch. 2 and mounted on the eleventh floor.

Large amplitude testing was performed in the E-W direction with the external cladding (infill walls) in place and in the N-S direction with the external cladding removed. Two different types of tests were performed. Damping tests were performed to determine resonant frequencies and damping values of modes of interest at various input force levels. Mode shape tests were performed to determine the mode shapes at various resonant frequencies.

a) Damping Tests

The damping tests were performed such that the force level during a given test varied approximately as a function of the frequency squared. The theoretical force level generated by the moving mass vibrator is given by:

$$F(t) = M \omega^2 X \sin \omega t$$

where M is the mass of the bucket weight, ω is the frequency of excitation, and X is the single amplitude of motion of the moving mass. The purpose of using this forcing function was to enable the data, whenever possible, to be analyzed by techniques normally used for eccentric mass forced vibration tests. The required input force level, F_r , from the moving mass vibrator was determined from the relationship

$$F_r = M \omega_r^2 X$$

where ω_r is the resonant frequency of interest.

The approximate resonant frequency at a required force level was determined by a slow continuous sweep beginning at approximately 1.0 cps. above the estimated resonant frequency and sweeping down below the actual resonant frequency.

During this sweep, two recordings were made. First, the signal of the reference accelerometer on the eleventh floor was analyzed by a

spectrum analyzer. The peak of the resulting curve was used to identify the resonant frequency. Second, the force signal from the moving mass vibrator was plotted against the signal from the reference accelerometer on a two channel oscilloscope. Theoretically for an elastic system at resonance the two signals are 90° out of phase and the resulting plot traces a circle on the oscilloscope. Both methods were used to identify the resonant frequency during the sweep.

In addition to identifying the resonant frequency, the continuous sweep enabled the structure in most cases to achieve a stable structural condition at a particular force level. This was helpful, because as the input force level increased in increments of 5,000 lbs. the structural system changed. An example of this was hinging that occurred in the beams and stairwell of the lower levels. At higher force levels in the first modes, the continuous sweep was not performed because the structural changes were more significant and consequently, data was required as these changes occurred.

Once the resonant frequency was identified, a step-wise sweep was performed at appropriate frequency intervals to determine the damping and resonant frequency at the particular input force level. At each frequency step the structure was vibrated until steady state was achieved and the data was recorded. In all except two tests, the step-wise sweep was performed by sweeping from a frequency above the resonant frequency and sweeping down below the resonant frequency.

At various stages throughout the large amplitude test program a standard damping test was performed. The standard damping test consisted of the damping test described above at a nominal input force level of 5,000 lbs. The objective of the standard damping test was twofold.

First, it provided the means of comparing changes that occurred in the damping and resonant frequencies of the building during various stages of the test sequence. Second, it provided the means of determining whether or not changes that occurred in the damping and resonant frequencies at larger input force levels remained the same at lower force levels.

The location of accelerometers during the damping tests is given in Table 6. During all EW tests and up to and including Test No. 4N-SD a triaxial set of accelerometers was located at the 12th, 10th, 8th, 6th, 4th and 2nd floor levels. For tests 9N-SD to 41N-D a set of biaxial accelerometers in the NS and EW direction were located at the 12th, 10th, 8th, 6th, 4th and 2nd levels. Uniaxial accelerometers in the NS direction were located at the same levels. During all tests a reference accelerometer was located on the 10th floor level in the NE corner. During the EW tests it was oriented in the EW direction and during the NS tests it was oriented in the NS direction.

b) Mode Shape Tests

Mode shape tests were performed at various phases of the test program to determine in detail the response of the building at resonance. Prior to each mode shape test a continuous frequency sweep, described above, was performed to determine the resonant frequency. The building was then vibrated at the resonant frequency and data was recorded. The response of the structure was measured at the 12th, 10th, 8th, 6th, 4th, 2nd and basement levels. At each level the response at 25 grid points shown in Fig. 56 was recorded. At each point a triaxial accelerometer was used enabling the three-dimensional response to be obtained.

4.3.2 TESTS PERFORMED

The sequence of tests performed in the EW direction with the cladding in place is listed in Table 9. Standard damping tests were performed throughout the test sequence to provide a method of comparing changes that occurred in the building and to determine whether or not the changes that occurred at larger input force levels remained the same at lower force levels. The damping tests in both the NS and EW directions were planned so that the nominal force level at resonance increased in increments at 5,000 lbf. Mode shape tests were performed in both the EW and NS directions both before and after the large amplitude tests.

After the first series of standard damping tests in the EW direction (Test Nos. 1E-SD to 3E-SD) the mass of the bucket of the moving mass vibrator was increased from 5,800 lbs. to 19,000 lbs. to improve the performance of the vibrator. Following this increase in bucket weight, a first mode frequency sweep was performed at a force level of 10,000 lbs. No damping data was recorded during this sweep although it was observed from the oscilloscope that the resonant frequency dropped from 1.36 cps. to approximately 1.15 cps. Following this 10,000 lb. sweep test, two standard damping tests were repeated (Test Nos. 5E and 6E-SD). After these two tests, the bucket weight was increased to 57,700 lbs. again to increase the performance at the moving mass vibrator. From this point on the bucket weight remained at 57,700 lbs.

The sequence of tests performed in the N-S direction with the cladding removed is listed in Table 10. Also listed in the table are the resonant frequencies and damping values obtained from the frequency response curves. Damping values from the time domain analysis will be obtained in the next phase of analysis of test results.

In addition to the tabulated values of resonant frequencies and damping values mode shapes measured during the tests are presented in Figures 109 to 114 and a comparison of the EW mode shapes with those obtained from the small amplitude tests are presented in Figures 107 and 108. Force levels generated in the larger amplitude first mode tests in both the EW and NS directions are obtained by the method described in Chapter 5 and presented in Table 11.

4.4 PERFORMANCE OF THE VIBRATION GENERATOR DURING THE TESTS.

A detailed description of the specifications of the vibration generator are given in Section 2.3.3. The purpose of this section is to describe our experience on the performance of the vibration generator during the tests. The experience and hind-sight that follows will be useful for any future tests of this kind.

During the initial design of the vibration generator the objective was to design a machine capable of providing a sinusoidal forcing function with force magnitudes varying between 2,500 lbf (11,120N) and 30,000 lbf (133,500N) over a frequency range at 0.4 Hz to 5 Hz. The theoretical force generated by the moving mass vibrator is given by

$$F = M \omega^2 X \sin \omega t$$

where M is the mass of the bucket and weights, ω is the excitation frequency and X is the amplitude of motion of the moving mass or the stroke of the actuator. The initial design was such that the mass could vary between 5,000 lb (2300 Kg) and 58,000 lb (26,000 Kg) and the stroke of the actuator was ± 20 in. (± 500 mm). With these ranges of the two variables it was possible to obtain the desired force levels over the required frequency range with the minimum stroke of the actuator being 1 in. (25 mm). The 1 in. minimum was assumed in the design to be a

reasonable value in view of the unforeseen effects of friction forces. Control of the actuator was governed by a ± 20 in. Linear Voltage Displacement Transducer (LVDT) and the provision of adequate stiffness for this proved to be difficult. This caused problems with respect to the shape of the forcing function when larger strokes of the actuator were required. We had assumed that the performance of the vibration generator would have been at its best when a reasonable stroke (greater than 1 in.) of the actuator was used to obtain the desired force level. This assumption proved to be incorrect. The first three tests 1E-SD to 3E-SD were performed with a bucket mass of 5,800 lbs. (2600 Kg) and the shape of the forcing function is shown in Fig. 115(a). In test 4E-S the moving mass was increased to 19,000 lbs. (8600 Kg) and the shape of the forcing function improved as seen in Fig. 115(b). In the next test 5E-SD the moving mass was increased to its maximum value of 57,700 lbs (26,200 Kg). and the shape of the forcing function dramatically improved as seen in Fig. 115(c). This series of tests indicated that the vibration generator was capable of providing the desired force level at small actuator strokes and as a result the moving mass remained at its maximum value of 57,700 lbs. throughout the remainder of the tests. The shape of the forcing function for higher frequency tests (2nd mode) was very close to a sinusoid as seen in Fig. 116 a and b.

For the higher force level tests at the lower frequencies the stroke of the actuator had to increase above 2 in. (76 mm) to obtain the required force levels. During these tests the inadequate lateral stiffness of the LVDT caused a very slight flat peak on the displacement trace of the LVDT. This in turn resulted in a very sharp drop in the force causing a deviation from the desired sinusoidal forcing function. This is graphically

illustrated in Fig. 117 a, b and c where the force of the actuator and the acceleration measured at the 10th floor are given for three tests. The three tests show the effect at increasing actuator stroke on the forcing function. Figure 117a is for a single amplitude stroke of approximately 6 in. (152 mm), while Figs. 117 b and c are for single amplitude strokes of 15 in. (380 mm) and 17 in. (430 mm) respectively.

Two other problems, unrelated to the mechanical performance of the vibration generator, caused delays in the test program. The first was the connection between the actuator and the bucket carrying the weights. This suffered a fatigue failure in the bolts twice during the test program. It is suggested that in future tests this be well overdesigned to avoid the problem. The second problem was one of sloshing. During the large amplitude low frequency tests sloshing of the stored oil that drove the hydraulic actuator caused a drop in hydraulic pressure. This shut the system down. The problem was overcome by topping up the storage tank and could have been avoided if a good baffle system had been used.

Adknowledging the problems discussed above we believe that the overall performance of the vibration generator was good especially in view of the fact that this was the first time a test of this order and magnitude had been performed.

4.5 DATA COLLECTED, STORED AND DIGITIZED

During all stages of testing a considerable amount of data was collected and stored with the instrumentation described in Sec. 2.3.4. Storing and analyzing the data proved to be a major effort of data management and without the use of the computer this task would have been almost unmanageable.

For all first mode damping and mode shape tests approximately 10-12 seconds of data was collected at each frequency step and grid point of

interest. For second mode tests approximately 6 seconds of data was collected.

Strip chart recordings of accelerometers taken during the tests showed varying amounts of noise on the accelerometer traces (Fig. 117). Consequently before the data was analyzed each record was passed through a low-band analog filter before it was digitized. The filter used was approximately 1.5 to 2.0 cps above the frequency of interest. Following this filtering all the data was digitized and then analyzed. It should be noted that both the filtered and unfiltered data is available to other investigators who wish to use it.

Methods of analyzing the data are described in Chapter 5. For the frequency response curves and the mode shapes described therein McDonnell-Douglas provided a computer program that was capable of computing the maximum and minimum points of a digitized record and then averaged these values. This provided the unscaled data for all the frequency response curves and mode shapes. This computerized method of analyzing the data for these tests was expensive but essential.

5. METHODS OF DATA ANALYSIS

The analysis of the structural response data recorded and digitized by the instruments and methods described in Sections 2.3.4 and 4.5 is the subject of this chapter. The structural parameters of interest are the mode shapes, resonant frequencies and damping values at the first and second modes of the structure in both the EW and NS directions. Also the base shears generated in the first mode tests are calculated. The mode shapes were easily determined from the data recorded. The damping values were more difficult to obtain and two different methods were used. The first was the commonly used frequency response curve (half-power point) method and the second is based on a curve fitting method in the time domain. Because of budget constraints the second method was only applied to the data recorded in the EW direction.

5.1 MODE SHAPES

Data typical of that obtained from McDonnell-Douglas on the mode shapes is shown in Table 12. The data consists of the three-dimensional response at each grid point given in Fig. 56 at the 12th, 10th, 8th, 6th, 4th and 2nd floor levels. Because the excitation force level varied slightly throughout the tests the data at each grid point was scaled. The scale factor was based on the acceleration obtained from the reference accelerometer which was recorded each time the data of a particular grid point was recorded. Mode shapes shown in Figs. 109 to 114 were plotted from the scaled tabulated values.

5.2 DAMPING AND RESONANT FREQUENCIES

The resonant frequencies and damping values in the EW direction were calculated by two different methods. These were the frequency response

curve (half-power point) method and a curve-fitting method in the time domain. For the NS direction only the frequency response curve method was used, and as a consequence data from the large amplitude first mode tests have not yet been reduced. Both methods will be described but before this is done some general comments on the two methods follows.

Both methods are based on the assumption that the structure is elastic; however the curve-fitting method is capable of analyzing a reasonably short record of data, say 10 cycles, at a particular frequency of excitation. The values of interest are determined from this recorded information, assuming the structure is elastic. For the frequency response curve method the structure is assumed to be elastic over the complete sweep of frequencies.

Figure 118 shows the accelerations measured on the strip chart recorder for two of the larger amplitude tests (Test 24 E-D and 41 N-D) on the 10th floor. It can be observed that as the frequency of excitation changes 0.01 cps in test 24 E-D and 0.005 cps in Test 41 N-D the response of the building builds up and then settles into a new steady state condition. This build-up in response causes structural changes to occur such as beam and stairwell hinging and joint shear cracking. Associated with these structural changes is a change in the resonant frequency and the damping. Although in most cases the change is small from one frequency step to another, the change over a range of frequencies is significant. Consequently the frequency response curve method is not valid for these larger amplitude tests. However the curve-fitting method is, because the data recorded at each frequency step can be analyzed to give the resonant frequency and damping for that recorded set of information.

5.2.1 Frequency Response Curve Method

The approach used to determine the resonant frequencies and damping values by this method are developed in terms of the dynamic response of a single-degree-of-freedom system. The method is easily extended to multidegree-of-freedom systems.

The differential equation which defines the response of the single-degree-of-freedom system (Figure 119) is

$$M\ddot{x}(t) + C\dot{x}(t) + Kx(t) = F(t) \quad (5.1)$$

where $x(t)$ is the displacement of the system from its equilibrium position,

M is the mass of the system,

C is the coefficient of viscous damping,

K is the spring constant or stiffness,

and $F(t)$ is the exciting force, as a function of time, t , seconds.

An alternative form of this equation is:

$$\ddot{x}(t) + 2\beta\omega_n\dot{x}(t) + \omega_n^2 x(t) = F(t)/M \quad (5.2)$$

where $\beta = C/C_c$ is the damping ratio, dimensionless;

$C_c = 2M\omega_n$ is the critical value of damping,

$\omega_n = \sqrt{K/M}$ is the natural frequency of the system,
radians/sec.

In theoretical calculations of the response of a system one assumes that the mass M , the coefficient of damping C , the spring constant K , and the exciting force $F(t)$ are known. The response $x(t)$, can then be calculated. In a steady-state test, however, we know the exciting force $F(t)$ and we measure the response in terms of acceleration or displacement.

The problem is then to determine the mass, damping coefficient (or damping ratio), and the stiffness coefficient (or natural frequency). This information can be obtained from the test results if we can fit a theoretical curve to the experimental data. If the damping is sufficiently low (so that $1 - \beta^2 \approx 1.0$), we may make use of certain simple relationships in performing the fitting process. These relationships are indicated below.

Consider the response of the system if the exciting force is given by

$$F(t) = Mx \omega^2 \sin \omega t \quad (5.3)$$

where M is the mass of a vibration generator

x is the single amplitude displacement of this mass.

Equation 5.3 describes the exciting force created by the vibration generator. The normalized response of the system in terms of the amplitude of the displacement is given by

$$\left| G_o(\omega) \right| = \left| x \right| / \left| x_o \right| = (\omega/\omega_n)^2 / \sqrt{[1 - (\omega/\omega_n)^2]^2 + 4\beta^2 (\omega/\omega_n)^2} \quad (5.4)$$

where x_o is a reference displacement. Figure 120 corresponds to the displacement transfer function when the exciting force is proportional to ω^2 .

The response of the system to a force described by Equation 5.3 may also be expressed in terms of the acceleration of the system. In this case, the transfer function is given by

$$\left| G_1(\omega) \right| = \left| \ddot{x} \right| / \left| \ddot{x}_1 \right| = (\omega/\omega_n)^4 / \sqrt{[1 - (\omega/\omega_n)^2]^2 + 4\beta^2 (\omega/\omega_n)^2} \quad (5.5)$$

where \ddot{x}_1 is a reference acceleration. This transfer function has been plotted in Figure 121; note that it corresponds to the response which is measured in steady-state vibration tests where accelerometers are used to

measure the response.

In both of the theoretical response curves, increasing amounts of damping decrease the maximum response and cause a shift of the frequency at which the maximum response occurs. For low values of damping, the frequency at which the maximum response occurs coincides with the natural frequency of the system. In Figure 121, when the damping ratio is equal to 0.20, there is no maximum in the acceleration response curve near the resonant frequency. Experimental data in the form of acceleration response curves can be converted to displacement curves to accentuate the peaks. For sinusoidal excitation and response, displacements can be computed from acceleration data by dividing by ω^2 .

For single-degree-of-freedom systems with small values of damping, the damping ratio may be determined from the width of the peak in the response curve. The usual procedure is to determine the width of the transfer function at the "half-power" points (i.e., where the response is equal to 0.707 of the peak value), and to use the following approximate relationship

$$\beta = \Delta\omega / 2 \omega_n \quad (5.6)$$

where $\Delta\omega$ is the "bandwidth" or the width of the transfer function curve when the magnitude of the response is equal to 0.707 of the peak response. This relationship may be applied to either of the transfer function curves shown in Fig. 120 or 121 provided that $\Delta\omega < 0.2 \omega_n$. Furthermore, it may be noted that the range of applicability of Equation 5.6 is greater for the first type of transfer function (Fig. 120) than it is for the second (Fig. 121).

If the damping of the system is large, more elaborate procedures are required in order to determine both the natural frequency of the

system and the damping.

Until now, we have considered only the dynamic response of a single-degree-of-freedom system. This effort is not wasted because the dynamic behavior of a multiple-degree-of-freedom system can be analyzed as the combined response of several single-degree-of-freedom systems. Thus, for an n-degree-of-freedom system, there will be n characteristic ways in which this system can vibrate. We refer to these characteristic ways as the eigenmodes of the system, or for convenience, simply the "modes" of the system. It is the eigenmodes of vibration and associated parameters which we are most interested in identifying during vibration tests.

As for a single-degree-of-freedom system, each mode is characterized by a resonant frequency, a damping value, and an effective mass. In addition, a mode shape or eigenvector is required to specify how each point throughout the system would vibrate when responding only in each mode under question. Eigenvectors must be defined for each point in the structure for each mode of vibration.

During testing of a multidegree-of-freedom system the results most readily obtained from the frequency response curves measured at various points in the building are the resonant frequencies and damping values. This assumes that the conditions mentioned previously with regard to the single-degree-of-freedom system are satisfied.

For all damping tests performed frequency sweeps of the type required to define frequency response curves were performed. As stated previously not all these sweeps were capable of defining the resonant frequency and damping for the mode of interest, however wherever possible this method was used.

Typical tabulated data provided by McDonnell Douglas for each frequency sweep is shown in Table 13. The data consists of the steady state

amplitude for each accelerometer located in the building. As with the mode shape data, the excitation force varied slightly from the frequency squared variation (ω^2) required. Consequently the data of each channel was scaled. The scale factor was based on the force at resonance and all other channels were scaled so that their force level satisfied the frequency squared variation required.

5.2.2 Time Domain Analysis

The recorded acceleration time histories for all EW damping tests were analyzed using a time domain least squares curve fitting procedure. As stated earlier this is the only appropriate method to analyze recorded data from a structural system that is constantly changing. A similar method developed by Raggett (5) was used to analyze the data obtained from Blume's tests (Ref. 1,2) in a 4-story building.

The method assumes that for the duration of the record being analyzed the building is elastic. Further the method does not require the forcing function to be sinusoidal. Although the method as developed by Beck (6) is capable of determining mode shapes and participation factors it was only used to determine resonant frequencies and damping values. The participation factors and mode shapes measured during the test series were used in the identification process.

5.2.2.1 Theory of Least Integral Squares Identification

a) Brief Derivation of Modal Equations

The equation of motion of an N degree of freedom linear system is

$$M \ddot{\underline{x}} + C \dot{\underline{x}} + K \underline{x} = \underline{e}_i f(t) \quad (5.7)$$

where $f(t)$ is the force history produced by the shaker at the i -th coordinate and \underline{e}_i is the unit vector, $(\underline{e}_i)_j = \delta_{ij}$.

Let Φ denote the modeshape matrix consisting of ϕ_{ir} , the modal value at the i -th floor for the r -th mode, and define $\underline{\xi}$ by

$$\underline{x}(t) = \Phi \underline{\xi}(t) \quad (5.8)$$

Then

$$\Phi^t M \Phi \ddot{\underline{\xi}} + \Phi^t C \Phi \dot{\underline{\xi}} + \Phi^t K \Phi \underline{\xi} = \Phi^t \underline{e}_i f(t) \quad (5.9)$$

In the modal equivalent viscous damping approach it is assumed that the damper is viscous (i.e., it is proportional to the velocity only) and that uncoupled modes exist. Thus $\Phi^t M \Phi$, $\Phi^t C \Phi$ and $\Phi^t K \Phi$ are all diagonal matrices, and so

$$\ddot{\xi}_r + 2 \omega_r \beta_r \dot{\xi}_r + \omega_r^2 \xi_r = \frac{\phi_{ir}}{M_r} f(t) \quad (5.10)$$

But

$$x_j(t) = \sum_{r=1}^N \phi_{jr} \xi_r(t) = \sum_{r=1}^N x_j^{(r)}(t) \quad (5.11)$$

where

$$x_j^{(r)}(t) = \phi_{jr} \xi_r(t) \quad \text{by definition}$$

Thus

$$\ddot{x}_j^{(r)} + 2 \omega_r \beta_r \dot{x}_j^{(r)} + \omega_r^2 x_j^{(r)} = p_j^{(r)} f(t) \quad (5.12)$$

where ω_r is the natural frequency and β_r is the equivalent viscous damping;

$$p_j^{(r)} = \phi_{jr} \frac{\phi_{ir}}{M_r} \quad (5.13)$$

is the v -th mode participation factor at coordinate j , and

$$M_r = \sum_{i=1}^N m_i \phi_{ir}^2 \quad (5.14)$$

the r -th modal mass, expressed in terms of the lumped mass m_i .

If the system is lightly damped and the natural frequencies are sufficiently well separated, then $\ddot{x}_j \approx \ddot{x}_j^{(r)}$ when the exciting frequency is $\omega \approx \omega_r$. An attempt is thus made to use the time history $\ddot{x}_j(t)$ in this resonant case to estimate the parameters ω_r , β_r and $p_j^{(r)}$.

b) Time-domain Identification vs Frequency-domain

The main advantage of time-domain identification for forced vibrations is when the structural properties are changing, because the identification is done at a particular amplitude. A frequency-domain identification, using frequency response curves, uses data at successively different amplitudes, and at each such amplitude the equivalent linear parameters have changed. Thus, the theory based on linear, time-invariant systems may not produce meaningful results.

Another advantage of the time-domain is that it does not assume that the motion is steady-state and it can handle arbitrary time-histories. Thus, the input (shaker force) does not have to be sinusoidal, as the frequency-response approach assumes.

A difficulty with the time-domain approach using the time-histories of shaker force and response for one frequency of excitation at, or near, the r -th modal frequency is that not all the parameters ω_r , β_r and $p_k^{(r)}$, $k \in K$, can be uniquely determined. (Here K is the set of locations of which the response was measured and which are used in the identification). The reason for this is the narrow-band, essentially monochromatic, frequency content of the excitation. Thus, in contrast to the case where earthquake records are used in the identification, the frequency content of the response gives no information about the system. The information about the system must come from the phase and amplitude of the response relative to those of the shaker force, and this information is not

sufficient to distinguish between the effects of damping and the effects of the modeshape quantities $p_k^{(r)}$. Increasing the number of locations at which the response is measured does not help because for each such location one new parameter $p_k^{(r)}$ is introduced but only the amplitude at the new location leads to additional information. The phase is essentially constant throughout the building because the response is dominated by one mode. To overcome this nonuniqueness, the $p_k^{(r)}$ can be assigned a priori.

The use of more than one response record is recommended, however, because it helps to overcome the difficulties in identification arising from modal interference. This is because the contributions of the other modes are different at different locations and hence the identification process is better able to sort out the dominant mode if several response records are used.

c) Minimization of Integral Square Measure of fit.

In time-domain identification, we need to determine the initial displacement and velocity in order to be able to determine the theoretical response, which is generated for the equations of motion. We therefore define the vector of parameters:

$$\underline{a} = [T_r, \beta_r, x_1(0), \dots, x_k(0), \dot{x}_1(0), \dots, \dot{x}_k(0)] \quad (5.15)$$

and the integral-square measure-of-fit between the recorded acceleration response and the theoretical acceleration response:

$$J(g) = \left[\frac{1}{T_f - T_i} \right] \sum_{k=1}^K \int_{T_i}^{T_f} \left[a_k(t) - \ddot{x}_k(t; a) \right]^2 dt \quad (5.16)$$

where

$$\ddot{x}_k + c_r \dot{x}_k + b_r x_k = p_k^{(r)} f_r(t); \quad k = 1, \dots, K; \quad (5.17)$$

(from the modal equation given earlier)

where

- a_r = recorded acceleration at location k
- b_r = ω_r^2 ($\omega_r = 2\pi/T_r$)
- c_r = $2 \beta_r \omega_r$
- $f_r(t)$ = shaker force history when the excitation frequency $\omega \approx \omega_r$, the natural frequency of mode r
- K = number of response records used
- $p_k^{(r)}$ = r -th mode participation factor at coordinate k
- T_i, T_f = the time interval over which the response matching is to occur
- x_k = theoretical displacement response at location k for a single-mode model of the system.

Note that if only one record was used (i.e., $K = 1$), J would be the mean-square error between the recorded and theoretical response.

The parameters \underline{a} are estimated by minimizing J with respect to these parameters. The technique used to perform this minimization is described in Ref. 6.

5.2.2.2 Analysis of Test Results Using Time-Domain Method

Using the theory described in the preceding sections, a computer program FORCID was developed to analyze the recorded data. The computer program was a modification of the work performed by Beck (Ref. 6) on recorded earthquake data. The modifications were done by Beck. Testing the applicability of the FORCID was performed using simulated data on a 10 story shear building. The simulated tests performed are presented in

Appendix C.

It is clear from the test runs that reasonably accurate results are obtained only when three conditions are met. These are,

- 1) The response of more than one different floor level is used simultaneously in the identification process.
- 2) The participation factors required in the identification procedure are specified from measured values.
- 3) Recorded response close to the resonant frequency is used.

In analyzing the EW data all three of the above conditions were met in obtaining the damping values presented in Table 9. The records used in the identification program were the filtered records obtained from McDonnell-Douglas. The response at the 12th and 10th floors was used in the identification program. The participation factors of Eq. 5.13 at these two levels for the first and second EW translational modes are given in Tables 14 and 15. The tabulated results are presented for the mode shapes measured experimentally before and after the large amplitude tests, i.e., Tests 14E-M and 28E-M for the first mode and 11E-M and 27E-M for the second mode. The actual value used in FORCID was the average of the two results. Test runs were made using both sets of values and as the variation in the damping was less than 10%, the use of the average value was considered to be reasonable. A more extensive analysis of the results using different combinations at floor levels and participation factors, etc., will be performed in the next phase of the analysis of test results.

5.3 UNIFORM BUILDING CODE EQUIVALENT OF THE BASE SHEAR FORCE INDUCED DURING TESTING

In order to provide a frame of reference for the magnitude of forces induced during the large amplitude shaking, the base shear force generated

in the tests was compared with design base shear forces of the Uniform Building Code (UBC). The base shear force, V_T , generated in the structure during testing was calculated as:

$$V_T = \sum_{i=1}^{11} m_i \ddot{x}_i$$

where m_i is the mass at the i^{th} level and \ddot{x}_i is the maximum acceleration at the center of mass of the i^{th} level. The UBC design base shear is calculated from

$$V_c = ZKCW \quad 1974 \text{ UBC}$$

$$V_c = ZKICSW \quad 1976 \text{ UBC}$$

where W is the total weight of the structure, Z is a zone factor and varies from 1 to 1/4 for the 1974 UBC and 1 to 3/8 for the 1976 UBC. K is a factor dependent upon the framing system and for this example was taken as 1.0. I is an importance factor and is taken as 1.0. S is a factor dependent on the soil conditions and was taken at its maximum value of 1.5. C is a function of the period of the building and differs for the 1974 and 1976 codes. In the 1974 UBC,

$$C = \frac{0.05}{\sqrt[3]{T}}$$

and in the 1976 UBC,

$$C = \frac{1}{15\sqrt{T}}$$

where $T = 0.1N$ in both and N is the number of stories.

The base shear force comparison V_T/V_c , presented in Table 11 is made for both the code calculated period and for the period of the structure measured during the test.

6. DISCUSSION OF TEST RESULTS

The experimental values of the natural periods and percent of critical damping are presented in Tables 16 through 21 for each of the modes tested. The experimentally determined mode shapes are depicted in Figs. 109 through 114. The base shear forces generated in the first translational modes in both the EW and NS directions are listed in Table 11. Following is the discussion of these previously presented results.

6.1 PERIOD

There were progressive increases in the period of the building in all of the modes excited during the testing, and the largest changes occurred in the first translational modes. Changes in period which occurred during the lower force levels of excitation (5000 lbf, or 22 KN, nominal) were not associated with significant visual changes in the structural system, although it is obvious that internal structural changes were taking place. During the larger force-level tests (10000 lbf, or 44.5 KN, or larger nominal force) changes were visible and these are described in detail in Chapter 3. The resulting structural changes consisted of beam-end and stair-corner hinging, shear-cracking in the beam-column joints, and decreasing interaction of the infill panels with the structural frame. All of these events occurred gradually because during each sweep there was a slow build-up in the amplitude of the forcing function as the resonant frequency was approached. This is illustrated in Fig. 118 and discussed in Sec. 5.2.

It should be noted that the changes in period associated with the larger amplitude tests were permanent. All lower force-level tests

performed subsequently had essentially the same period as the last large input-force level test. This indicates that permanent changes had occurred in the lateral force resisting system.

From Table 16 it can be seen that for EW shaking with the external cladding in place the period of the first translational mode increased by a factor of 2.6 during the large amplitude tests from 0.74 secs. to 1.92 secs. as the input force increased from 4760 lbf (21.17 KN) to 29,000 lbf (129 KN), respectively. During the small amplitude tests the period measured at the force level of 1050 lbf (4.67 KN) was 0.65 secs. These changes in period were associated with visually significant changes in the structural system (see Chap. 3). The change in the period of the first translational mode before and after an interval of large amplitude second mode tests was small, 0.89 secs. before and 0.93 secs. after, respectively. This indicates that only slight structural damage occurred during the large amplitude second mode tests, and this is consistent with the visual observations.

The data in Table 17 indicates that for the EW direction shaking with the external cladding in place the period of the second translational mode increased approximately 50 percent from 0.21 secs. to 0.31 secs. as the input force level increased from 5,400 lbf (24 KN) to 29,900 lbf (133 KN). As noted above, this increase in period was not associated with any visually significant changes in the structure. Before and after an interlude of large amplitude first mode tests the period of the second mode did increase from 0.31 to 0.39 secs. This change is attributed to the structural damage during the first mode tests.

Data from the first translational mode tests in the NS direction without the cladding are given in Table 18. The period doubled from 1.23 to

2.50 secs. as the force level increased from 3610 lbf (16.1 KN) to 17,000 lbf (75.6 KN). As for the EW tests, the change in the first translational mode period before and after an interval of large amplitude second mode tests was small (1.25 vs 1.32 secs., respectively), indicating but slight changes in the lateral force resisting frame during these second mode tests.

The period of the first torsional mode increased approximately 50% from 1.04 sec. to 1.47 sec. as the force level increased from 5170 lbf (23.0 KN) to 15,000 lbf (66.7 KN), respectively (Table 19). Only a slight change occurred during an interlude of second mode tests (1.08 to 1.09 secs.

Data from the second translational mode in the NS direction tests without cladding are presented in Table 20. The period increased by 35 percent from 0.31 secs. to 0.42 secs. as the force level at resonance changed from 3530 lbf (15.7 KN) to 22,840 lbf (101.6 KN), respectively. As with the tests in the EW direction, this increase in period was not associated with any significant structural changes. The period of the second translational mode before and after the first mode large amplitude tests was 0.37 secs. and 0.53 secs., respectively. This was associated with visually observed structural damage during the first mode tests.

For the second torsional mode from NS shaking the increase in periods was much less (Table 21), changing from 0.28 to 0.32 secs. as the force level increased from 4500 lbf (20.0 KN) to 26,940 lbf (119.8 KN). The period before and after the first mode large amplitude tests was 0.30 before and 0.36 secs. after.

6.2 MODE SHAPES

The mode shapes measured during the shaking tests are presented in Figs. 109 through 114. In the EW direction the first and second translational modes were predominantly translational although after the large

amplitude tests the rotational component in the NS direction increased to approximately 10 percent of the EW translational component. Because the rotational component was small, Figs. 109 and 110 only compare the EW translational components of the first and second modes. As seen in these figures, the changes in both the first and second measured mode shapes, before and after the large amplitude tests, are minor even though the period increased by 110 percent for the first translational mode and 78 percent for the second translational mode. Significant structural damage did not appreciably affect the mode shapes, even though it greatly changed the periods.

In the NS tests without cladding there was a significant rotational component in each of the four measured modes (see Figs. 111 through 117), both before and after the damaging large amplitude tests. This damage was more severe in the NS tests than in the EW tests (Chap. 3). As a consequence the difference in the mode shapes before and after the large amplitude tests was greater than for the EW shaking. A comparison of the first torsional and the second translational mode shapes (Figs. 112 and 113, respectively) shows smaller changes before and after the large amplitude tests than the first translational and second torsional modes (Figs. 111 and 114, respectively).

6.3 DAMPING

It is clear from the damping data in Tables 16 and 17 that there are significant differences in the damping values obtained by the two methods used to determine them. The time-domain method (Sec. 5.2) was not used for the data from the NS shaking tests.

It appears that for the half-power-point method (frequency response curves) the damping varies according to the direction of the sweep (see

Tests 17N-D and 20N-D, Table 21). In the time domain method the damping was dependent on the number of accelerometer signals used in the analysis (see Appendix C). Table 22 shows a comparison of the results of four analyses at different frequencies in which two and three EW response signals were used (10-th and 12-th floor accelerometers in the first instance, and an additional reference accelerometer in the other one). The damping values in Tables 16 and 17 were all obtained using the three signals. Future studies on the data will be performed with a greater number of accelerometer signals.

Until a greater confidence can be placed in the damping results obtained by either of the two methods, the discussion of the damping values will restrict itself here to the ranges in which the results for the various tests fall. For this purpose the ranges will be: 1-2 percent, 2-3 percent, 3-4 percent, 4-6 percent, 6-8 percent and 8-10 percent.

The damping obtained for the lower force level tests (less than 10,000 lbf, or 44.5 KN force), of the EW first translational mode, i.e., tests 10E-SD to 22E-D in Table 16, was 1 to 2 percent by the time domain method and 3 to 4 percent by the half-power-point method (except for Test 1E-SD in which the direction of sweep was up and opposite to all the other tests). For the two large amplitude tests (23E-D and 24E-D in Table 16) only the time domain method of analysis was used, and the damping results for all but the 0.56 cps test were in the 2 to 3 percent range. The damping for the 0.56 cps test was 3.9 percent. In summary it appears that for the first EW translational mode with the cladding in place the damping does not exceed 4 percent. For the lower force level tests the deflection of the roof of the building was less than 0.5 inches (13 mm). Damping values are dependent on the method used to obtain them.

For the second EW translational mode there is a considerable difference in the damping results obtained by the two methods of analysis for the higher force level tests (Table 17). Furthermore, the trends are different: 1) For the half-power-point method the damping increased with force level up to a maximum of 8 percent; it dropped subsequently to approximately 6 percent during a low force level test performed after a high force level test (21E-SD, Table 17) and this value did not change appreciably after an interval of first mode tests (25E-SD). 2) For the time domain method of analysis the damping for all the large amplitude tests is in the 2-4 percent range. For the lower force level test performed after the larger amplitude tests (21E-SD) the damping increased to approximately 5 percent, and after the first mode tests it dropped to 3.4 percent (25E-SD in Table 17).

For the NS shaking tests damping results have only been obtained by the half-power-point method, and as a consequence results for the larger amplitude first mode tests are not available. Because of the discrepancies in the results obtained from the two methods of analysis in the EW direction tests, caution is suggested in drawing definitive conclusions from the NS damping data.

For the first NS translational mode (Table 18) the damping of the lower force level tests performed prior to the large amplitude tests is in the 3-to-4 percent range. These are similar to the EW tests in which the cladding was still in place. Following the large amplitude NS tests the damping increased to 5.8 percent.

For both the NS first and second torsional modes (Tables 19 and 21 respectively) damping did not increase as the force level increased. In fact, for both torsional modes damping was in the 2-to-3 percent range,

except for test 20N-D in which the direction of the sweep was in the opposite direction to all the other tests and damping was close to half that of the equivalent force level tests with the sweep in the opposing direction.

Damping was in the 3-to-4 percent range for the second NS translational mode (Table 20). The two exceptions were for the largest force level test (23N-D) in which damping was 5.6 percent, and for test 19N-D in which the direction of the sweep was in the opposite direction to all other tests. Here damping was about half of the value obtained for test 18N-D which had approximately the same force level but sweep was in the other direction.

6.4 UNIFORM BUILDING CODE EQUIVALENT OF THE BASE SHEAR FORCE INDUCED DURING TESTING.

The base shear force comparison V_T/V_C presented in Table 11 for several of the first mode tests in both the EW and the NS directions is made for both the code calculated period and for the period of the building measured during the particular test. For the code calculated period the maximum base shear force generated during the EW tests was 3.2 times the 1974 UBC design value, 2.4 times the 1976 UBC design value with the $S(\text{soil})$ factor of 1.0 and 1.6 times the code design value with $S = 1.5$, the maximum S -factor. The corresponding base shear ratios were 2.8, 2.1 and 1.4, respectively, for the NS tests. If the measured periods are used for calculating the design base shear force, then the ratio V_T/V_C increases for all tests where the period of the test is greater than the code period of 1.1 secs. As seen from Table 11, this increase is greater for the larger amplitude NS tests than for the EW tests.

In evaluating these results it is of interest to note that the duration of shaking for the tests in which large base shear forces were

generated varied between 20 and 60 minutes. In the EW direction test 23E-D, with cladding in place, it is estimated that the ratio of V_T/V_C for the 1974 UBC exceeded unity for about 45 minutes, and it exceeded 2 for approximately 20 minutes. In the final test (41N-D), when the building was close to collapse, it is estimated that the ratio V_T/V_C exceeded unity for 10 minutes.

In addition to the above described durations of the large amplitude excitations the total time for each of the tests varied between 40 and 90 minutes. As a result it is estimated that the building was subjected to varying amounts of excitation for at least 60 hrs. It is estimated that the ratio V_T/V_C for the 1974 UBC exceeded unity for at least 100 minutes in the EW direction tests and 70 minutes in the NS tests.

Although the code design base shear force values are not equal to the values that would be expected in a large earthquake, they do represent values that would be expected from a moderate earthquake. Furthermore, the building resisted these base shear forces over a much longer duration than the $1\frac{1}{2}$ minutes of an earthquake. It is clear, therefore, that this non-seismically designed building, both with and without external cladding, was able to withstand base shear forces greater than those demanded by recent UBC requirements when subjected to the sinusoidal type of motion induced by the moving mass shaker. Until further analysis of the results it cannot be inferred, however, that this structure would have resisted an earthquake which would have induced a base shear force of the same magnitude.

6.5 COMPARISON OF LARGE AND SMALL AMPLITUDE TESTS.

The small amplitude tests performed with the eccentric mass vibrator (described in Chapter 2) excited the building in both the EW and the NS

direction with the cladding in place. The fully clad building was tested with the moving mass vibrator only in the EW direction. Comparisons between the two series can thus be made only for the EW tests.

From Table 8 it can be seen that the resonant frequency of the first EW translational mode decreased from 1.53 Hz ($T = 0.65$ secs.) to 1.43 Hz ($T = 0.7$ secs.) as the force level increased from 1050 lbf (4.68 KN) to 4260 lbf (18.91 KN) in the small amplitude tests. For the same sequence of tests the damping varied between 1.5 percent and 0.9 percent, with the lower value associated with the larger force level. The first large amplitude test (i.e., resonance induced by the moving mass shaker), test 1E-SD, had a resonant frequency of 1.36 Hz ($T = 0.74$ secs.) and a damping value of 1.4 percent, using the half-power-point method, and 2.2 percent from the time domain method (Table 16). This slight drop in the resonant frequency between the two sets of results is attributable to the shaking that was performed in testing and adjusting the moving mass vibrator prior to the performance of Test 1E-SD.

For the second EW translational mode the resonant frequencies of the two sets of tests were 4.68 Hz for the eccentric mass vibrator and 4.60 Hz for the moving mass vibrator. The corresponding damping values were 1.9 and 2.6 percent, respectively.

A comparison of the mode shapes for the first and second modes is presented in Figs. 107 and 108. The agreement in the first translational mode is reasonable, however, there are significant discrepancies in the lower stories for the second mode results (Fig. 107). As the eccentric mass vibrator test was performed at approximately one third of the force level of the moving mass test the difference in the measured mode shapes is attributed to the decreased interaction of the infill panels in the

lower force level tests.

6.6 SUMMARY

This chapter reviewed the dynamic data obtained in the shaking tests: period, mode-shapes, damping and base shear force, and it presented comparisons and discussions on the effects of cladding, force level, damage, type of excitation and duration of shaking on the dynamic behavior of the test structure. Conclusions from this chapter will be reviewed in detail in Chapter 8 of this report.

7 CORRELATION OF ANALYTICAL MODELS AND EXPERIMENTAL RESULTS

7.1 GENERAL

A mathematical model of the structure, using a state-of-the-art elastic building analysis computer program, was formulated to compare its computed dynamic characteristics with the experimental test results. The model was progressively modified within the limits of the computer program to represent the different stages of stiffness degradation which were visually apparent in the building during testing. This chapter presents a description of (1) the computer program employed in the dynamic analysis, (2) the different models, (3) the results for each analysis and (4) the comparison with experimental results.

Since an elaboration of this project will in the future involve a detailed and more accurate comparison of the analytical and the experimental results, the objective of the limited study presented here is to determine only what differences exist between analytical predictions and experimental performance as obtained from a commonly used building analysis computer program.

7.2 COMPUTER PROGRAM ETABS

The computer program ETABS, developed by the Division of Structural Engineering and Structural Mechanics of the University of California, Berkeley, was used to calculate the mode-shapes and frequencies of each structural model. A detailed description of the program may be found in Ref. 7. The program ETABS is a descendant of the widely used program TABS (Ref. 8). These programs were specifically developed for the analysis of building-type structures; they significantly simplify the

description of the structure. The floors are considered to be rigid in their own plane and they are assumed to possess no transverse stiffness (i.e., any contribution of the floor slab to the out-of-plane bending stiffness must be included in the floor beams). Using these assumptions the structure may be then assembled from several (or a single) frames which are connected by a rigid floor diaphragm. For the program ETABS the frames must be composed of vertical columns and horizontal beam elements, however, the column locations may be arbitrary in plan (as contrasted to TABS where the frames must also be planar). The in-plane floor displacements for each frame are transformed, using the above assumptions, into three degrees of freedom at the center of mass for each floor level (i.e., two translations and one rotation). Coupling between intersecting frames is limited to the floor in-plane degrees of freedom, and is not enforced for local deformations (i.e., two rotations and one vertical displacement at each node).

The story masses and rotational inertias are obtained from the dead loads per floor and lumped at the center-of-mass.

The following analyses were performed on the CDC/6400 computer.

7.3 STRUCTURAL MODELS

The basic model of the building was formulated as a simple frame to allow for full coupling between interconnected column lines. Points where beams intersected without supporting columns required the specification of zero-property dummy columns. The effective size of all rigid joints was included by specifying column widths and beam depths. Shear areas were nominally set to 80% of the axial area for all columns.

Moments of inertia for all beams included the contribution of the

floor slab flanges, the width of which was determined using ACI-368-71. The stiffness properties were based on the uncracked gross section (not including the steel reinforcement). The mass of the infill walls was included in the rotational inertias of the floors where appropriate; however, the in-plane stiffness of the walls was not modeled. Furthermore, the contribution of the stiffness of the stairwell was also excluded.

Three variations of the basic model were formulated to represent, within the limits of the computer program, the visually apparent changes that occurred in the actual structure during the large amplitude testing. Each of these is denoted by a sequential model number in order of increasing stiffness degradation.

- i) Model 1: This is the basic model described above. The mass, including infill walls, is shown in Col. 2 of Table 23. This model is to represent the state of the building at the beginning of the tests. It does not include the stiffness contribution of the infill panels nor that of the stairwell.
- ii) Model 2: This is the same as the basic model except that hinges are inserted at the ends of each EW beam level 2 to level 5 (Fig. 57). This model is to represent the state of the building at the ends of the EW tests, within the limits of the computer program. The model includes the beam hinging which was visually apparent during these tests (see Fig. 72), but it does not include the effect of the shear cracks which were visually apparent at the joints (see Fig. 66).
- iii) Model 3: This is the same as model 2, but with the reduced masses given in Col. 4 of Table 23, reflecting the absence of infill walls except for the top two floors (see Fig. 28). This model was formulated to represent the state of the building at the beginning of the NS tests.

7.4 RESULTS OF ANALYSES

The modal results from ETABS list two translational and one rotational component. The notation for the direction of the mode-shapes is characterized by the predominant component, i.e., an EW mode is a general three-dimensional mode-shape in which the predominant movement is in the EW direction.

Pertinent periods and mode-shapes of the analytical models are shown in Figs. 122 to 127. The EW modes show little if any rotational components. The NS modes show varying amounts of rotation with a general trend that increased from Model 1 through Model 3.

7.5 COMPARISON OF EXPERIMENTAL AND ANALYTICAL RESULTS

Experimental and predicted mode-shapes and periods for the first and second translational EW modes are shown in Figs. 122 and 123. Neither contained significant rotational components. The comparisons shown are for analytical Models 1 and 2 and Tests 11E-M, 14E-M, 27E-M, and 28E-M. Data for Tests 11E-M and 14E-M were obtained before the building was subjected to any large deformations, while mode-shape Tests 27E-M and 28E-M were performed after the building was subjected to large amplitude shaking.

The first translational mode data shown in Fig. 122 indicates, as expected, that Model 1 ($T=1.0$ sec) is more flexible than Test No. 14E-M ($T=0.88$ sec). This difference is attributable to the exclusion of the infill walls and the stairwell in Model 1. Furthermore, the mode-shapes of the two results are significantly different.

Model 2, which includes the hinges at the beam ends up to level 5 and excludes joint shear cracking, is more rigid than Test No. 28E-M

($T=1.38$ sec versus $T=1.85$ sec). In this case the mode-shapes of the two results are in better agreement, although a significant difference exists at the lower levels where joint shear cracking was more prevalent. It should be noted that the infill panels did not appear to interact with the structural frame when the amplitudes of shaking were large, as discussed in Chap. 3 (see also Fig. 65). This effect, and the inability to include the joint shear cracks in the model are postulated as reasons for Model 2 being more rigid than the actual building.

Similar results were obtained for the second translational mode, as shown in Fig. 123. Model 1 ($T=0.34$ sec) is considerably more flexible than Test No. 11E-M ($T=0.33$ sec), and there is a significant difference in the mode-shapes. The reasons for the discrepancy are discussed above. Similarly, Model 2 ($T=0.39$ sec) is more rigid than Test No. 2E-M ($T=0.41$ sec), although there is a better agreement between mode-shapes.

Experimental and analytical mode-shapes and periods for the first and second translational and torsional NS modes are shown in Figs. 124 through 127. Part a) of each figure gives the floor components and Part b) gives the NS translational components of nodes 5, 12, and 21 (Fig. 56). These nodes lie in an EW plane through the center of the building. The comparisons are shown for Model 3 and Tests 5N-M to 8N-M. These mode-shape tests were all performed before any large amplitude shakes in the NS direction were made. For comparative purposes all modes were normalized so that the NS translational component of Node 5 on level 12 was unity.

Model 3, which is the same as Model 2 except for the mass of the walls, is more rigid in all four modes than the actual building, as seen by comparing the periods (Figs. 124 to 127). The experimental periods are: 1.22 sec for the first translational mode, 0.94 sec for the first

torsional mode, 0.32 sec for the second translational mode and 0.29 sec for the second torsional mode. The corresponding periods from Mode 3 are, respectively, 0.93 sec, 0.68 sec, 0.29 sec, and 0.21 sec.

All four mode-shapes, including the two translational modes, contain significant rotational components. Although the agreement between experiment and prediction is not good for all four mode-shapes, it is better for the translational modes (Figs. 124 and 126) than for the torsional ones (Figs. 125 and 127). Furthermore, the comparison of the NS translational components for all modes at Node 5 (at the center of the building) is better than at Nodes 12 and 21 (at the E and W faces of the center of the building, respectively). This indicates that a greater discrepancy occurs in the analytical model for the torsional component of the mode-shape than for the translational one.

In the NS direction the effect of the stairwell as a stiffening element is less significant than in the EW direction and, except for the top two floors, infill panels are not included either in the analytical model nor in the experimental building. Consequently, the difference in behavior is attributed to the effect of joint shear cracking, which was not included in Model 3. Another reason might be the significant damage to Col. 37 at level 2 (see Fig. 70).

7.6 SUMMARY OF RESULTS

The objective of the foregoing comparison between the three analytical models and the test-performance was not so much to determine what degree of correlation exists, but to examine the limitations of both the models and the computer program ETABS. It is clear that better models with some non-linear capabilities are needed in further studies of the

data from these tests in order to improve correlation. The following factors should be included in such studies: 1) the stiffness contribution of the infill panels with and without openings, 2) the stiffness contribution of the stair system and 3) the effect of joint shear cracking.

8. SUMMARY AND CONCLUSIONS

8.1 SUMMARY OF RESEARCH

This report summarizes an experimental research project in which a relatively new and, from the standpoint of structural testing, a rather large structure was subjected to many cycles of sinusoidal lateral loads. These cyclic loads were large enough to significantly alter the dynamic and static structural properties of the building and to induce extensive damage to the structural frame components and to the non-structural in-fill wall and stair elements.

The structure was a nearly rectangular, roughly 40 x 45 ft in plan, eleven story portion of an originally much larger reinforced concrete apartment building, one of many which were demolished in St. Louis during 1976. The structure consisted of columns (tied and spirally reinforced), beams and slabs. It also contained a stair-well and in-fill brick and/or block walls on the periphery and around the stair-wells except for the ground floor which was completely open. The structure was not designed for lateral force, in accordance with the usual design practice for such buildings in the 1950's, and the beam-to-column joints had little capacity to resist positive moment.

The walls, except for a portion of the East face, were in excellent condition before testing, as was the whole structure. Measurements made on the dimensions of the structure and on the location of the reinforcing prior to testing indicated that the structure was, within the usual tolerances, built as designed. Various measurements of the strength of the concrete showed that this strength twenty years after construction was roughly twice the original strength.

The research consisted of the following phases:

- 1) Measurement of the dimensional and structural properties of the building;
- 2) Small amplitude shaking on the top floor to determine the original dynamic properties of the structure;
- 3) Large amplitude shaking on the top floor and acquisition of the resulting dynamic data;
- 4) State-of-the-art analysis of the results.

The details of the methods and the results of the dimensional and material property survey are presented elsewhere (Ref. 9), as are the results of the small amplitude shaking (Ref. 4). This report is mainly concerned with the large amplitude tests.

8.2 LARGE AMPLITUDE SHAKING DEVICE

Sinusoidal forces on the eleventh floor level were induced by moving a mass of lead weighing approximately 60,000 lbs horizontally over a more-or-less frictionless surface first in the EW and then in the NS direction by a hydraulic actuator, one end of which was attached to the mass and the other to the building frame. The power for the actuator was provided by a large motor-and-pump assembly which was also located on the eleventh floor. The piston displacement was ± 20 in, with a frequency capacity of approximately 5Hz, and the maximum horizontal force range was $\pm 30,000$ lbf. The shaking device was used for damping tests (frequency sweeps) and for low-force level mode-shape tests. Data taken during these tests consisted of accelerations in enough locations to determine the resonant frequencies of the lower two modes and the corresponding damping values, and the spatial definition of the mode shapes.

The large amplitude shaking of this building constituted a novel

effort, and the device used worked fairly well, discounting the expected usual initial start-up problems and breakdowns. Time for thorough pre-test planning and shake-down exercises was not available, and so the gaining of experience, taking data, and testing the structure and the equipment proceeded simultaneously.

8.3 TEST RESULTS

The small amplitude shaking tests provided resonant frequencies and damping values (using the frequency response curve method) for the first, second and third EW, NS and torsional modes (Table 8), and mode shapes for the corresponding first and second mode resonant frequencies for the original building prior to any damage. Damping values obtained from the small amplitude shaking tests were approximately 1.5, 2 and 4% for the first, second and third modes, respectively.

The large amplitude shaking tests were performed first in the EW direction with the cladding in place and then in the NS direction with the cladding removed. The runs consisted of sweeps near resonance in the first and second modes at increasingly higher force levels alternating with low force level sweeps over the whole range of frequencies and low force level mode-shape surveys at resonance. The high force level tests damaged the structure, and the standard damping and mode-shape tests measured the resulting changes in its dynamic properties. The pertinent data on the test runs are detailed in Table 9 for the EW tests and in Table 10 for the NS tests. Damping values were determined by the frequency response curve method for most tests (it was not possible to do so for all tests because of the rapid change of the resonant frequency during some of the high force level tests), and for some of the EW tests

damping was also calculated by a curve fitting method in the time domain. The data from the various dynamic tests are presented in Tables 16 through 22 and Figs. 107 through 127, and the results are discussed in Chapter 6. The following brief conclusions are repeated here:

- 1) Major structural damage occurred during the first-mode large force level tests, resulting in major changes in the period (from approximately 0.7 sec to 1.9 sec).
- 2) Structural damage and period changes were relatively small during the second mode tests.
- 3) Mode-shapes remained relatively unaffected by major structural damage.
- 4) Damping values obtained by the two methods of analysis for the same test run, and damping values for different test runs, are not consistent nor do they exhibit strong tendencies. Damping, with some notable exceptions, tends to increase with damage for the same mode, and it tends to be somewhat higher for the second mode than for the first mode. However, the results are erratic, and damping is mostly less than 4%. No strong conclusions can be drawn from these results as regards damping values in a highly damaged structure until more extensive (and expensive) time-domain analyses are performed on the data.

8.4 STATE-OF-THE-ART ANALYSES

Experimental and predicted mode shapes and periods are presented in Figs. 122 through 127, and the comparisons are discussed in Chap. 7. Three models were used in the analyses, representing extreme idealizations of the mass and the structure. These idealizations give but qualitative descriptions of behavior, and future studies should be made with analyses which can account for the stiffness contributions of the

in-fill panels and the non-linearities of the damaged structure. Basically, the state-of-the-art dynamic programs are at best crude approximations.

8.5 CONCLUSIONS AND RECOMMENDATIONS

The tests performed in this project have demonstrated that it is feasible to take a relatively massive structure and to excite this structure by mechanical means to large enough displacements such that major structural damage occurs. Roughly one fourth of the joints were so severely damaged that the rotational stiffness became almost zero. Some of the columns were several inches out of alignment at the termination of the tests, and one column was completely crushed. From on-site experience during the final large force-level test runs it may be postulated that it would have been possible to drive the structure to the extent that total collapse could have been achieved. This was not done because of safety requirements and in order not to lose part or all of the equipment.

While the structure was not designed for reversing lateral loads and thus was not particularly suited to resist earthquakes, it was interesting to visualize in the progressing damage patterns the transfer of the forces from the members which were no longer capable of resisting them to the relatively undamaged members. Thus the structure did essentially what is expected of proper structures: through the multiple redundancies present force redistribution took place such that the frame finally did not collapse although it had conceptually failed. It would have been very instructive of the forces and end-rotations of the beams and columns of at least the first through the fourth level could have been measured. However, this was prohibitive in cost and time, and so only qualitative observations were possible.

From these qualitative observations it is evident that the joints

in the bottom three levels transformed into hinges in the EW direction during the EW tests, with relatively little or no damage above the fifth level. During the NS tests almost all of the joints on the NS face became hinges. That many joints in the structure transformed into hinges is, of course, an extreme idealization, as the analytical studies showed (Chapt. 6). There was certainly some moment capacity due to the interaction with the slab, and partially cracked joints still could absorb considerable moment. Given the structural and dimensional details, as well as the many force and response histories available from this project, future work should concentrate on more accurate modeling, including non-linear behavior of the elements, especially the joints with shear cracks. Such future research could also develop the history of the progression of damage, based on more realistic models of behavior, and comparisons could be made with the qualitative progression of damage recorded in Chap. 3.

The role played by the in-fill walls and the stair-well could not, by the idealized analytical tools used, be clearly isolated. During the initial small amplitude shaking the stiffness of these non-structural elements definitely played a role. However, with larger amplitude shaking these elements sustained the first damage; the stairs buckled, and the walls first cracked and then were battered to pieces by the repetitive lateral deflections of the columns. These elements contributed mass but little lateral stiffness.

The dynamic data provided ample proof of the changes in period with increased damage. Furthermore, these changes were permanent, as evidenced by subsequent small amplitude tests. Major changes in period, and also major damage which caused these changes, occurred during the first mode

resonance, with small effects noted from even the high force level second mode tests. Future analytical work should be performed to predict the structural and dynamic changes by refined analytical models. This need for future more sophisticated studies is especially true for the determination of damping. The damping was relatively small according to the methods used to determine it, even for the damage-producing high level first-mode loading cycles.

In addition to many qualitative results and observations, this project produced a wealth of data (force level, period, duration) on the lateral force applied to the structure and the resulting accelerations in numerous locations of the building. This data, as well as the data on the geometry and material, are available for further research and analysis to permit the checking of advanced conceptual models of structural behavior under repetitive cyclic forces. The verification of such models will provide researchers then with more confidence to use them in earthquake and/or blast analyses of structures of this type.

A final word about earthquakes. The testing did not intend to simulate earthquake loading at all, and any direct conclusions from this work are not valid. One cannot help, however, to contemplate at least some qualitative conclusions. Table 11 provides ratios of the computed base-shear from the test data to the code-specified base-shears in the 1974 and 1976 Uniform Building Code. From this table it is evident that the structure under the most severe shaking did support base shear forces in excess of the required base shear for the highest seismic areas. One could argue, on the one hand, that structures of this type, though not designed for earthquakes, have a very good chance of surviving base shear

forces of this magnitude. On the other hand, one could argue that intense short duration excitations from an earthquake have really nothing in common with the long sequences of regular sinusoidal forces applied in these tests, and that any conclusion as regards earthquakes is meaningless. The actual performance of the damaged test-structure would have to be examined by analyzing the structure, having the experimentally recorded dynamic properties for a basis, under an earthquake record. This was not done, and much future work is left.

However, it might well be that a severe earthquake in St. Louis, such as the New Madrid earthquakes of Dec. 1812 through Feb. 1813, could have relatively regular periods. What is evident is that the New Madrid shakes were repetitive, reoccurring many times during a two month period, and so the excitation and the response of the test building could be representative of local situations. The exploration of this idea, too, is left for future research. It appears, nevertheless, that the very pronounced load sharing and force distribution from damaged to undamaged parts of the building can have but beneficial effects on the resistance of a New Madrid type earthquake. While the structure may possibly survive without collapse, this cannot be said for the cladding. The walls would probably disintegrate rapidly since there is not much beyond gravity to hold them in place.

In conclusion, the most significant results of this research are the data gathered and available for future analytical modeling.

9. ACKNOWLEDGEMENTS

Many people have made this project possible, and these are acknowledged in Appendix A. We wish to express our most sincere thanks again to all of them. This project was a great experience to us, and we are especially grateful to the National Science Foundation for the financial support which made it possible.

10. REFERENCES

1. Chen, C. K., Czarnecki, R. M., Scholl, R. E. "Destructive Vibration Test of a Concrete Structure" in "Advances in Civil Engineering Through Engineering Mechanics," Proceedings of ASCE Specialty Conference, May 23-25, 1977, Raleigh, N. C.
2. Chen, C. K., Czarnecki, R. M., Scholl, R. E. "Vibration Tests of a 4-Story Reinforced Concrete Test Structure," JAB-99-119, URS/John A. Blume Assoc., San Francisco, Calif., Jan. 1976.
3. Smallwood, D. O., Hunter, N. F. "A Transportable 56-KN, 200 mm Displacement Hydraulic Shaker for Seismic Simulation," Proceedings, Environmental Science, 1975.
4. Applied Nucleonics Company "Moderate Level Vibration Tests on an Eleven Story Reinforced Concrete Building", Report No. 1158-1, Sept. 1976.
5. Beck, J. L. "Structural Identification Using Earthquake Records," Earthquake Engineering Research Laboratory (EERL) Report to be published, 1978, California Institute of Technology.
6. Raggett, J. D., "Time Domain Analysis of Structure Motions," JAB-99-103, John A. Blume & Associates Research Division, April, 1973.
7. Wilson, E. L., Hollings, J. P., Dovey, H. H., "Three Dimensional Analysis of Building Systems (Extended Version)," Earthquake Engineering Research Center, Report No. EERC 75-B, 1975.
8. Wilson, E. L., Dovey, H. H., "Static and Earthquake Analysis of Three Dimensional Frame and Shear Wall Buildings," Earthquake Engineering Research Center, Report No. EERC 72-1, May 1972.
9. Gardiner, R. A. "Material and Dimensional Properties of an Eleven Story Reinforced Concrete Building." M.S. Thesis, Washington University, Aug. 1978.

ROOF	1,41	42	40	39	47	48	45, 46	43, 44	2	3
11th FLOOR	12" x 12" 4 #5 TIES	- " -	- " -	- " -	12" x 16" 4 #6 TIES	Same as 47	14" x 12" 4 #5 TIES	12" x 12" 4 #5 TIES	12" x 12" 4 #5 TIES	12" x 12" 4 #5 TIES
10th	12" x 12" 4 #6 TIES	12" x 12" 4 #6 TIES	14" x 14" 4 #7 TIES	14" x 14" 4 #7 TIES	- " -	- " -	- " -	- " -	14" x 14" 4 #7 TIES	12" x 12" 4 #6 TIES
9th	12" x 12" 4 #7 TIES	14" x 14" 4 #6 TIES	14" x 14" 4 #9 TIES	14" x 14" 6 #7 SPIRAL	12" x 16" 4 #7 TIES	Same as 47	14" x 12" 4 #7 TIES	- " -	14" x 14" 4 #10 TIES	14" x 14" 4 #7 TIES
8th	14" x 14" 4 #9 TIES	14" x 14" 4 #8 TIES	14" x 14" 6 #7 SPIRAL	16" x 16" 6 #8 SPIRAL	14" x 16" 4 #9 TIES	Same as 47	14" x 14" 4 #9 TIES	12" x 12" 4 #6 TIES	14" x 14" 6 #7 SPIRAL	14" x 14" 4 #8 TIES
7th	14" x 14" 4 #10 TIES	14" x 14" 4 #10 TIES	16" x 16" 6 #7 SPIRAL	16" x 16" 6 #9 SPIRAL	14" x 16" 6 #7 SPIRAL	Same as 47	14" x 14" 6 #7 SPIRAL	12" x 12" 4 #8 TIES	16" x 16" 6 #8 SPIRAL	14" x 14" 4 #9 TIES
6th	14" x 14" 6 #7 SPIRAL	14" x 14" 6 #7 SPIRAL	16" x 16" 6 #8 SPIRAL	16" x 16" 6 #10 SPIRAL	16" x 16" 6 #8 SPIRAL	Same as 47	14" x 14" 6 #8 SPIRAL	14" x 14" 4 #8 TIES	16" x 16" 6 #9 SPIRAL	14" x 14" 4 #10 TIES
5th	16" x 16" 6 #7 SPIRAL	16" x 16" 6 #8 SPIRAL	16" x 16" 6 #9 SPIRAL	16" x 16" 6 #11 SPIRAL	16" x 16" 6 #9 SPIRAL	Same as 47	16" x 16" 6 #8 SPIRAL	14" x 14" 4 #9 TIES	16" x 16" 6 #10 SPIRAL	14" x 14" 6 #7 SPIRAL
4th	16" x 16" 6 #8 SPIRAL	16" x 16" 6 #9 SPIRAL	16" x 16" 6 #10 SPIRAL	16" x 16" 7 #11 SPIRAL	16" x 16" 6 #10 SPIRAL	Same as 47	16" x 16" 6 #9 SPIRAL	14" x 14" 4 #10 TIES	16" x 16" 6 #11 SPIRAL	16" x 16" 6 #8 SPIRAL
3rd	16" x 16" 6 #9 SPIRAL	16" x 16" 6 #10 SPIRAL	16" x 16" 6 #11 SPIRAL	16" x 18" 7 #11 SPIRAL	16" x 16" 6 #11 SPIRAL	Same as 47	16" x 16" 6 #10 SPIRAL	14" x 14" 6 #7 SPIRAL	16" x 16" 7 #11 SPIRAL	16" x 16" 6 #9 SPIRAL
2nd	16" x 16" 6 #10 SPIRAL	16" x 16" 6 #11 SPIRAL	16" x 16" 7 #11 SPIRAL	16" x 20" SPECIAL DETAIL	18" x 16" 7 #11 SPIRAL	Same as 47	16" x 16" 6 #11 SPIRAL	14" x 14" 6 #8 SPIRAL	16" x 18" 7 #11 SPIRAL	- " -
1st	16" x 16" 6 #11 SPIRAL	16" x 16" 6 #11 SPIRAL	18" x 18" 7 #11 SPIRAL	20" x 20" 8 #11 SPIRAL	20" x 16" SPECIAL DETAIL	Same as 47	16" x 18" 7 #11 SPIRAL	16" x 16" 6 #8 SPIRAL	18" x 18" 8 #11 SPIRAL	16" x 16" 6 #10 SPIRAL
BASEMENT PIERS	22 1/2" x 22 1/2" 8 #7	22 1/2" x 20" 8 #9	22" x 24 1/2" 8 #10	24" x 26 1/2" 8 #10	24" x 20" 8 #11	Same as 47	22" x 22" 8 #10	20" x 20" 4 #9	22" x 24 1/2" 8 #10	22 1/2" x 22 1/2" 8 #7

First Dimension in Column Size is EW Direction

Table 1 Column Properties

BEAM DESIGNATION	SIZE	BEAM CENTER		BEAM ENDS	
		TOP STEEL	BOTTOM STEEL	TOP STEEL	BOTTOM STEEL
S1	12"x18 3/8"	2#10	3#9	2#10*	3#9
S2	12"x18 3/8"	2#6	2#8, 2#9	2#6*, 1#9*	2#8, 1#9*
S3	12"x18 3/8"	2#6	2#6, 1#7 1#8	2#6*, 1#8*	1#7*, 2#6
S6	12"x18 3/8"	-	4#7	2#7	2#7
B2	8"x18 3/8"	2#6	2#6	2#6*	2#6
B3	11"x18 3/8"	-	2#6, 1#9	1#9*	2#6
B4	8 3/4"x18 3/8"	-	2#6, 1#9	1#9*	2#6
B6	12 1/2"x18 3/8"	2#5	3#5	2#5*	3#5
B8	12"x18 3/8"	-	3#7	-	3#7

* Anchored

Table 2 Beam Dimensions and Reinforcement

SLAB DESIGNATION	THICKNESS	BENT BARS	STRAIGHT BARS	SPACING
SL 2	5"	#4	#5	ALT 6"
SL 3	5"	-	#3	8"
SL 4	5"	#5	#5	ALT 6"
SL 5	4"	#4	#4	ALT 6"

Table 3 Slab Details

COLUMN	BOTTOM PART	TOP PART
39	11'-6" x 11'-6" x 1'-4"	8'-6" x 8'-6" x 1'-3"
40	10'-9" x 10'-9" x 1'-3"	8'-0" x 8'-0" x 1'-2"
41	9'-6" x 9'-6" x 1'-3"	7'-0" x 7'-0" x 0'-11"
42	9'-9" x 9'-9" x 1'-3"	7'-3" x 7'-3" x 1'-0"
1	13'-3" x 13'-3" x 1'-6"	10'-0" x 10'-0" x 1'-5"
2	11'-0" x 11'-0" x 1'-3"	8'-3" x 8'-3" x 1'-2"
3	9'-0" x 9'-0" x 1'-3"	6'-9" x 6'-9" x 0'-10"
43, 44	8'-0" x 8'-0" x 1'-3"	6'-0" x 6'-0" x 0'-7"
45, 46	10'-3" x 20'-6" x 1'-5"	4'-0" x 20'-6" x 1'-5"
47, 48	11'-0" x 21'-9" x 1'-6"	4'-3" x 21'-9" x 1'-6"

Table 4 Footing Dimensions

Level	Concrete Volume (cu.ft)			
	Slabs	Beams	Column	Total
Roof	711	370	-	1081
11	"	"	121	1202
10	"	"	121	1202
9	"	"	128	1209
8	"	"	134	1215
7	"	"	151	1232
6	"	"	159	1240
5	"	"	169	1250
4	"	"	186	1267
3	"	"	189	1270
2	"	"	191	1272
1	750	"	199	1280
Basement	750	-	115	865
Piers	-	-	140	<u>140</u>
				15,725 cu.ft (445 m ³)
Basement Walls				770
Footings				<u>2,573</u>
				19,068 cu.ft (540 m ³)

Table 5 Concrete Volume

Level [*]	Locations on Floor ^{**}
12	14, 24
11	No accelerometers
10	14 ^{***} , 1
9	No accelerometers
8	11, 14, 21
7	No accelerometers
6	5, 14, 21
5	No accelerometers
4	5, 12, 24
3	No accelerometers
2	5, 11, 21
1	On ground outside of building
-1	11, 14

* See Fig. 57 for identification on the vertical coordinates.

** See Fig. 56 for identification on the planar coordinates.

*** Reference accelerometer

Table 6 Accelerometer Locations During Damping Tests

<u>Chanel</u>	<u>Elevation (Floor)</u>	<u>Location</u>	<u>Orientation</u>
1	11	North-West Corner	North
2	11	North-West Corner	East
3	11	South-East Corner	North
4	11	South-East Corner	East
5	5	Near Stairwell	North
6	5	Near Stairwell	East
7	11	North-West Corner	Up
8	11	South-East Corner	Down

Table 7 Accelerometer Locations and Orientations Used in Small Amplitude Tests.

Test	Run	Channel	Eccentricity Kg-m (lb-in)	Force N (lbf)	Peak Acc. cm/sec ²	Resonant Frequency Hz	Dominant Response	Damping Ratio (%)
7	2	4	236.6 (20,473)	18,906 (4,258)	62.22	1.43	E-W First Mode	0.88
7	1	4	140.0 (12,110)	11,434 (2,575)	37.59	1.44	E-W First Mode	1.52
1	1	4	140.0 (12,110)	11,964 (2,676)	40.92	1.47	E-W First Mode	1.34
1	2	4	51.0 (4,440)	4,678 (1,053)	9.42	1.53	E-W First Mode	1.45
7	2	3	236.6 (20,473)	22,709 (5,115)	70.37	1.56	N-S First Mode	0.98
7	1	3	140.0 (12,110)	13,836 (3,136)	59.77	1.58	N-S First Mode	1.40
1	1	3	140.0 (12,110)	14,332 (3,206)	47.01	1.61	N-S First Mode	1.28
1	2	3	51.0 (4,440)	5,423 (1,221)	13.94	1.64	N-S First Mode	1.52
1	2	1	51.0 (4,440)	9,886 (2,226)	40.92	2.22	First Torsional	1.70
2	1	1	27.8 (2,415)	5,674 (1,278)	23.55	2.28	First Torsional	1.26
3	1	4	27.8 (2,415)	23,963 (5,397)	60.75	4.68	E-W Second Mode	1.87
2	1	3	27.8 (2,415)	26,735 (6,021)	55.84	4.94	N-S Second Mode	1.77
3	2	1	5.81 (505)	11,714 (2,638)	21.30	7.15	Second Torsional	1.74
2	3	1	2.86 (249)	6,094 (1,372)	13.44	7.35	Second Torsional	2.04
3	2	4	5.81 (505)	36,959 (8,326)	25.52	12.70	E-W Third Mode	3.94
2	3	3	2.86 (249)	22,266 (5,015)	10.89	14.05	N-S Third Mode	
2	3	1	2.86 (249)	36,546 (8,231)		17.4-18.5	Third Torsional	

Table 8 Summary of Results of Frequency Sweep Tests (Small Amplitude Shaking).

TEST NO.	TYPE OF TEST	NOMINAL FORCE LEVEL (LBF)	FORCE LEVEL AT RESONANCE (LBF)	RESONANCE FREQUENCY (CPS)	DAMPING (%)**
1E-SD	Standard Damping	5,000*	4,760	1.36	1.4(2.2)
2E-SD	Standard Damping	5,000	5,050	2.32	---
3E-SD	Standard Damping	5,000	4,310	4.60	2.6(3.3)
4E-S	Sweep	10,000	---	1.15	---
5E-SD	Standard Damping	5,000	5,190	1.23	3.6
6E-SD	Standard Damping	5,000	4,620	4.55	3.3
7E-SD	Standard Damping	5,000	2,770	1.28	3.0
8E-SD	Standard Damping	5,000	6,400	4.50	2.9
9E-D	Damping	10,000	8,940	4.34	2.5(2.3)
10E-D	Damping	10,000	7,800	1.19	3.4(1.8)
11E-M	Mode Shape	10,000	8,900	4.32	---
12E-D	Damping	10,000	10,430	2.32	---
13E-M	Mode Shape	10,000	10,500	2.32	---
14E-M	Mode Shape	10,000	10,500	1.14	---
15E-SD	Standard Damping	5,000	3,960	1.12	---
16E-SD	Standard Damping	5,000	4,920	4.32	---
17E-D	Damping	15,000	15,880	3.94	3.7(2.5)
18E-D	Damping	20,000	18,090	3.63	5.2(2.5)
19E-D	Damping	25,000	29,920	3.23	8.2(3.9)
20E-SD	Standard Damping	5,000	4,590	1.08	4.0(1.8)
21E-SD	Standard Damping	5,000	4,860	3.45	6.3(5.2)
22E-D	Damping	15,000	10,740	0.85	4.5(1.9)
23E-D	Damping	20,000	18,800	0.60	(2.2-3.1)
24E-D	Damping	25,000	----	0.52	(3.0-3.9)
25E-SD	Standard Damping	5,000	4,990	2.59	5.6(3.4)
26E-D	Damping	10,000	11,250	0.52	3.6
27E-M	Mode Shape	10,000	9,200	2.46	---
28E-M	Mode Shape	10,000	10,800	0.54	---

*The direction of sweep for this sweep was up, i.e., from a lower to higher frequency.

**The first damping value was obtained from the frequency response curve. The value in parentheses was determined by the time domain method.

Table 9. Tests Performed in the East-West Direction With External Cladding

TEST NO.	TYPE OF TEST	NOMINAL FORCE LEVEL (LBF)	FORCE LEVEL AT RESONANCE (LBF)	RESONANCE FREQUENCY (CPS)	DAMPING (%)
1N-SD	Standard Damping	5,000	5,170	0.96	3.1
2N-SD	Standard Damping	4,000	3,610	0.81	3.5
3N-SD	Standard Damping	5,000	4,500	3.52	2.6
4N-SD	Standard Damping	4,000	3,530	3.23	3.7
5N-M	Mode Shape	5,000	3,800	0.82	---
6N-M	Mode Shape	5,000	4,600	0.94	---
7N-M	Mode Shape	5,000	4,300	3.14	---
8N-M	Mode Shape	5,000	4,100	3.47	---
9N-SD	Standard Damping	5,000	4,680	0.93	2.5
10N-SD	Standard Damping	4,000	2,920	0.80	3.5
11N-SD	Standard Damping	5,000	5,000	3.51	2.1
12N-SD	Standard Damping	4,000	3,670	3.16	2.8
13N-D	Damping	10,000	9,910	3.41	2.5
14N-D	Damping	7,500	7,640	2.97	3.0
15N-D	Damping	15,000	15,140	3.31	3.2
16N-D	Damping	10,000	10,570	2.84	3.4
17N-D	Damping	20,000	20,160	3.25	2.8
18N-D	Damping	13,000	12,930	2.72	3.7
19N-D	Damping	13,000*	13,180	2.70	2.0
20N-D	Damping	20,000*	19,410	3.21	1.6
21N-D	Damping	25,000	26,960	3.15	2.8
22N-D	Damping	15,000	15,260	2.51	3.2
23N-D	Damping	20,000	22,840	2.36	5.6
24N-SD	Standard Damping	5,000	5,190	3.30	2.5
25N-SD	Standard Damping	4,000	3,290	2.69	3.4
26N-SD	Standard Damping	5,000	5,320	0.92	3.0
27N-SD	Standard Damping	4,000	3,430	0.76	3.0
28N-D	Damping	10,000	8,480	0.81	3.1
29N-D	Damping	10,000	9,610	0.53	---
30N-D	Damping	15,000	---	0.68	---
31N-D	Damping	15,000	---	0.41	---
32N-M	Mode Shape	5,000	5,100	0.40	---
33N-M	Mode Shape	5,000	5,800	0.75	---
34N-M	Mode Shape	5,000	5,600	2.93	---
35N-M	Mode Shape	5,000	5,800	1.91	---
36N-SD	Standard Damping	5,000	5,470	2.91	2.8
37N-SD	Standard Damping	5,000	5,050	1.90	3.9
38N-SD	Standard Damping	5,000	4,720	0.72	3.1
39N-SD	Standard Damping	5,000	5,900	0.40	6.8
40N-D	Damping	10,000	8,130	0.69	2.3
41N-D	Damping	15,000	---	---	---

*The direction of the stepwise sweep was up, i.e., from a lower to higher frequency. For all other tests the direction of the sweep was down, i.e., from a higher to lower frequency.

Reproduced from
best available copy.



Table 10. Tests Performed in the N-S Direction With External Cladding Removed

Test No.	Period of Test (sec)	V_T Base Shear Generated(Kip)	$V_{T/W}^*$	V_T/V_c for Code Period			V_T/V_c for Measured Period		
				74 UBC Zone 3	76 UBC Zone 4, S=1	76 UBC Zone 4, S=1.5	74 UBC Zone 3	76 UBC Zone 4, S=1	76 UBC Zone 4, S=1.5
1E-SD	0.74	115	0.038	0.78	0.60	0.40	0.68	0.49	0.33
10E-SD	0.84	168	0.056	1.16	0.88	0.59	1.06	0.78	0.52
22E-D	1.18	238	0.080	1.65	1.26	0.84	1.69	1.30	0.87
23E-D	1.30	460	0.154	3.18	2.42	1.61	3.36	2.63	1.75
23E-D	1.60	320	0.107	2.21	1.68	1.12	2.50	2.03	1.35
24E-D	1.71	460	0.154	3.18	2.42	1.61	3.68	3.02	2.01
<hr/>									
10N-SD	1.25	60	0.027	0.56	0.42	0.28	0.58	0.45	0.30
29N-D	1.75	160	0.072	1.49	1.13	0.75	1.74	1.43	0.95
31N-D	2.38	300	0.135	2.79	2.12	1.41	3.60	3.12	2.08
41N-D	2.38	210	0.094	1.94	1.45	0.97	2.51	2.18	1.45

* The weight of the building with cladding in place was 2990 Kip (1.36×10^6 Kg).

Table 11. Uniform Building Code Equivalent of Base Shear Forces Induced During Testing.

RUN NO. 001
 T.F. NO. WF 021300
 RECORDED 00/29/70

WASHINGTON UNIVERSITY VIBRATION TEST-PASS 1

TEST NO. 029
 TEST SITE NO. 00
 REFL NO. 0001
 TABULATED 01/10/70

TIME	LOCATION 000	FREOREF 000	REFX1000 001	SCFAC100 050	FORCE-LB 002	10MX1000 003	10EX1000 004	10VA1000 005	12MX1000 006	14EX1000 007
9.20	1.000	0.820	12.611	1.071	4455.298	77.339	-27.267	4.994	-62.175	-63.145
19.71	2.000	0.820	12.934	1.041	3963.931	76.881	-18.733	-3.359	-60.275	-17.316
29.46	3.000	0.820	13.220	1.022	3974.113	58.201	-20.972	3.520	-49.105	-11.475
39.96	4.000	0.820	13.200	1.023	4047.084	57.516	-30.215	5.733	-51.144	-20.372
46.03	5.000	0.820	11.775	1.147	4431.272	42.753	40.730	-2.025	-36.270	-7.759
60.21	6.000	0.820	13.463	1.003	3856.283	40.149	-34.494	-2.246	-35.216	-17.166
68.87	7.000	0.820	12.183	1.109	4100.006	39.639	-54.425	3.501	-34.850	-26.007
91.21	8.000	0.820	12.281	1.100	3954.324	24.638	-42.310	2.729	-167.819	31.205
99.12	9.000	0.820	13.568	0.996	3314.064	30.626	-8.745	1.693	-10.989	120.702
109.71	10.000	0.820	12.936	1.044	3933.158	12.545	-16.901	2.671	-11.475	-13.916
110.46	11.000	0.820	12.940	1.044	4114.924	13.603	-32.628	3.496	-10.970	-25.466
120.96	12.000	0.820	11.452	1.180	4484.650	11.039	30.210	1.438	-10.576	-3.915
129.62	13.000	0.820	12.865	1.050	4023.333	12.460	44.275	-2.677	-11.562	16.914
141.96	14.000	0.820	12.967	1.042	4309.489	15.646	32.376	-2.658	-10.661	29.721
152.46	15.000	0.820	12.092	1.117	4466.258	25.418	32.921	-2.521	-22.149	30.661
162.96	16.000	0.820	12.874	1.049	3697.606	25.640	19.608	-4.261	-21.209	18.918
173.46	17.000	0.820	12.917	1.046	4094.721	24.934	11.070	-2.009	-21.952	11.342
182.12	18.000	0.820	12.775	1.057	3883.973	41.775	21.165	3.534	-36.212	15.301
194.46	19.000	0.820	11.970	1.129	4257.517	45.373	32.336	-2.310	-39.341	29.931
201.28	20.000	0.820	12.321	1.096	4198.694	62.362	5.202	-2.350	-49.043	10.762
215.46	21.000	0.820	12.340	1.095	4198.014	77.331	5.290	-3.038	-61.304	-2.540
225.21	22.000	0.820	12.513	1.082	4118.462	61.822	22.399	-1.788	-50.824	18.447
235.71	23.000	0.820	12.047	1.121	4411.192	62.731	32.129	-3.427	-49.740	32.171
246.21	24.000	0.820	10.677	1.265	5234.825	77.799	27.856	-3.467	-58.441	34.223
256.71	25.000	0.820	13.515	1.000	3587.850	74.820	23.775	2.844	-61.770	21.512

Table 12. Typical Tabulated Data for Mode
 Shape Tests (Test 5N-M)



RUN NO. 002
 T.R. NO. WR 021300
 RECORDED 00/09/70

WASHINGTON UNIVERSITY VIBRATION TEST- PASS 2

Table 13. Typical Tabulated Data for
 Frequency Response Sweeps
 (Test 10E-D)

TEST NO. 004
 TEST SITE NO. 01
 REEL NO. 0000
 TABULATED 00/22/77

TIME	FREQSTEP 000	FREQREF 000	FORCE-LB 002	FORCE-SC 050	SCFACTOR 051	FREQ(IN) 952	REFX1000 001	DEX1000 003	DE-INCH 023	DEX1000 004
5.05	1.500	1.500	15152.499	13176.412	0.869	1.180	21.371	22.858	99.289	17.038
11.21	1.450	1.450	14018.824	12312.625	0.878	1.180	23.157	22.212	103.250	16.049
17.41	1.400	1.400	13775.499	11473.119	0.833	1.180	25.753	23.880	119.074	19.712
23.51	1.380	1.380	13789.537	1152.515	0.808	1.180	26.135	24.001	123.164	23.314
29.56	1.360	1.360	13150.633	10831.595	0.823	1.180	28.329	25.598	135.257	22.050
35.66	1.340	1.340	12733.024	10515.362	0.825	1.180	29.829	25.713	139.950	23.928
40.61	1.320	1.320	12079.583	10203.813	0.844	1.180	33.216	29.323	164.471	26.542
45.45	1.300	1.300	12309.233	9896.949	0.804	1.180	35.837	30.596	176.932	27.037
51.46	1.290	1.290	11949.362	9745.274	0.815	1.180	36.726	32.029	188.105	27.998
57.51	1.280	1.280	11747.287	9594.770	0.815	1.180	37.619	31.801	189.696	28.209
63.56	1.270	1.270	11253.987	9445.438	0.839	1.180	40.884	34.661	210.021	31.594
69.41	1.260	1.260	10919.649	9297.276	0.851	1.180	42.962	36.929	227.331	33.253
74.45	1.250	1.250	10563.683	9150.286	0.866	1.180	47.085	39.890	249.503	35.008
80.49	1.240	1.240	10393.316	9004.467	0.866	1.180	45.594	39.235	249.374	35.053
86.53	1.230	1.230	10042.399	8859.819	0.882	1.180	44.693	42.535	274.771	37.498
91.33	1.220	1.220	8924.024	8716.343	0.976	1.180	54.035	45.536	297.683	40.305
97.41	1.210	1.210	7932.715	8574.038	1.080	1.180	64.064	57.973	386.677	50.372
103.41	1.205	1.205	8109.733	8503.324	1.048	1.180	65.177	54.776	368.677	50.166
109.45	1.200	1.200	8187.299	8432.904	1.030	1.180	64.353	57.290	388.822	51.209
115.49	1.195	1.195	8184.199	8362.776	1.021	1.180	68.914	57.348	392.474	51.082
121.49	1.190	1.190	7802.483	8292.941	1.062	1.180	73.482	61.294	423.015	56.063
127.53	1.185	1.185	8070.733	8223.398	1.018	1.180	64.532	57.675	401.404	52.572
133.53	1.180	1.180	8154.149	8154.149	1.000	1.180	64.859	57.540	403.865	52.441
139.57	1.175	1.175	8408.365	8085.193	0.961	1.180	63.482	53.999	378.704	44.053
145.57	1.170	1.170	8433.715	8016.529	0.950	1.180	63.481	51.794	369.774	44.062
151.61	1.160	1.160	8739.783	7880.080	0.901	1.180	58.759	47.829	347.380	43.228
156.34	1.150	1.150	5433.424	7744.802	0.821	1.180	50.623	42.825	316.474	39.060
161.20	1.140	1.140	5925.224	7610.695	0.799	1.180	48.384	39.597	300.704	34.050
167.37	1.130	1.130	10537.549	7477.760	0.709	1.180	41.829	34.943	267.447	34.222
172.06	1.120	1.120	10084.924	7345.996	0.728	1.180	36.576	29.776	231.990	32.027
176.89	1.110	1.110	10056.274	7215.403	0.717	1.180	33.937	26.787	212.480	29.707
189.09	1.100	1.100	8705.499	7085.981	0.813	1.180	21.966	18.066	145.924	19.046
195.21	1.080	1.080	8521.065	6830.652	0.801	1.180	17.822	14.974	125.464	15.379
199.93	1.050	1.050	7200.499	6456.442	0.806	1.180	8.953	7.677	68.054	7.023
204.94	1.000	1.000	6734.974	5856.183	0.869	1.180	5.534	4.808	46.984	5.330

Reproduced from
 best available copy.

Table 13. Continued

TIME	9E-INCH 024	10EX1000 005	10E-INCH 025	12EX1000 006	12E-INCH 026	NFACTOR 027	SCAN CTR 028
5:05	66.625	30.340	131.783	22.047	95.765	0.000	505.000
11:21	77.389	34.902	162.234	23.043	107.112	0.000	520.000
17:41	98.291	33.713	168.100	25.807	128.680	0.000	540.000
23:51	119.643	33.762	173.261	26.630	136.662	0.000	550.000
29:56	116.510	36.020	190.327	28.335	149.717	0.000	555.000
35:66	128.060	36.713	199.624	29.954	163.034	0.000	565.000
40:61	148.377	42.431	237.993	33.454	187.641	0.000	460.000
45:45	156.353	46.834	270.633	35.993	208.145	0.000	464.000
51:46	160.906	45.976	270.610	37.089	217.820	0.000	585.000
57:51	174.591	48.587	289.824	37.807	225.521	0.000	590.000
63:56	191.441	49.751	301.456	41.188	249.569	0.000	595.000
68:41	204.703	55.304	340.447	43.119	265.439	0.000	480.000
74:45	218.967	59.005	369.066	47.570	297.539	0.000	484.000
80:49	222.798	59.331	377.115	45.971	292.193	0.000	488.000
86:53	242.235	64.056	413.788	50.386	325.488	0.000	492.000
91:33	268.592	67.766	444.960	54.590	358.449	0.000	372.000
97:41	340.242	83.726	558.881	69.692	465.202	0.000	500.000
103:41	337.653	79.853	537.463	66.010	444.293	0.000	500.000
109:45	347.547	84.403	572.827	69.363	470.758	0.000	504.000
115:49	355.068	85.137	582.654	70.086	479.651	0.000	508.000
121:49	391.056	91.348	630.429	74.726	515.715	0.000	508.000
127:53	365.886	85.033	591.807	70.534	490.898	0.000	512.000
133:53	368.080	85.162	597.740	70.739	495.505	0.000	512.000
139:57	344.403	80.372	568.031	65.963	466.931	0.000	516.000
145:57	348.844	76.700	547.586	64.663	461.652	0.000	516.000
151:61	328.491	70.158	509.555	59.989	435.701	0.000	520.000
156:34	294.413	62.467	461.621	51.590	381.242	0.000	393.000
161:20	290.648	59.988	451.112	49.470	372.020	0.000	399.000
167:37	261.931	50.771	388.588	42.762	327.289	0.000	536.000
172:06	254.202	42.713	332.778	37.604	294.972	0.000	405.000
176:89	235.638	40.292	319.597	35.085	278.298	0.000	408.000
189:09	153.849	26.514	214.155	22.704	183.379	0.000	548.000
195:21	130.539	22.730	190.450	18.468	154.741	0.000	560.000
199:93	57.581	13.673	121.209	9.460	83.865	0.000	432.000
204:94	54.048	9.933	97.081	5.781	56.506	0.000	453.000

Reproduced from
best available copy.

	Test 14E-M	Test 28E-M	
Floor	$W_m = 1.14 \text{ Hz}$	$W_m = 0.54 \text{ Hz}$	Average
12	211×10^{-6}	195×10^{-6}	203×10^{-6}
10	205×10^{-6}	170.5×10^{-6}	187×10^{-6}

Table 14. EW First Mode Experimental Participation Factors, Calculated by Eq. 5.13

	Test 11E-M	Test 27E-M	
Floor	$W_m = 4.32 \text{ Hz}$	$W_m = 2.46 \text{ Hz}$	Average
12	266×10^{-6}	249.4×10^{-6}	256×10^{-6}
10	133×10^{-6}	138.3×10^{-6}	135×10^{-6}

Table 15. EW Second Mode Experimental Participation Factors, Calculated by Eq. 5.13

Test No.	Frequency Response Curves			Time Domain Analysis				Base Shear (Kip)	Deflection of 12-th Floor (in.)
	Force Level at Resonance (Lbf)	Period (sec)	Damping (%)	Frequency of Data Analysed (Hz)	Force Level of Data Analysed (Lbf)	Period (sec)	Damping (%)		
Ecc.Vib.	1050	0.65	1.5	--	--	--	--	22	0.04
Ecc.Vib.	4260	0.70	0.9	--	--	--	--	145	0.30
1E-SD	4760	0.74	1.4	1.36	4760	0.72	2.2	115	0.25
4E-S	10000	0.87	--	--	--	--	--	--	--
5E-SD	5190	0.81	3.6	--	--	--	--	111	0.23
7E-SD	2770	0.78	3.0	--	--	--	--	94	0.24
10E-D	7800	0.84	3.4	1.19	7800	0.83	1.8	168	0.51
15E-SD	3960	0.89	--	--	--	--	--	70	0.23
SECOND MODE DAMPING TESTS									
20E-SD	4590	0.93	4.0	1.08	4590	0.91	1.8	115	0.48
22E-D	10740	1.18	4.5	0.85	10740	1.15	1.9	238	1.4
23E-D	--	--	--	0.77	26000	--	--	460	3.4
"	--	--	--	0.72	27800	1.35	2.6	--	--
"	--	--	--	0.72	27800	1.38	3.1	430	3.6
"	18800	1.67	--	0.61	19500	1.60	2.2	320	3.7
24E-D	--	--	--	0.58	29000	1.71	3.0	460	5.8
"	--	--	--	0.56	27000	1.83	3.9	415	5.7
26E-D	11250	1.92	3.6	--	--	--	--	192	3.1

Table 16. First Translational Mode Damping Tests With External Cladding -- EW Tests

Test No.	Force Level at Resonance (Lbf)	Period (sec)	Damping from Frequency Resp. Curves (%)	Damping from Time Domain Anal. (%)	Deflection of 12-th Floor (in).
Ecc. Vibr. Test	5400	0.21	1.9	-	-
3E-SD	4310	0.22	2.6	3.3	0.02
6E-SD	4620	0.22	3.3	-	0.025
8E-SD	6400	0.22	2.9	-	0.033
9E-D	8940	0.23	2.5	2.3	0.058
16E-SD	4920	0.23	-	-	-
17E-D	15,880	0.25	3.7	2.5	0.115
18E-D	18,090	0.28	5.2	2.5	0.161
19E-D	29,920	0.31	8.2	3.9	0.320
21E-SD	4,860	0.29	6.3	5.2	0.032
FIRST MODE DAMPING TESTS					
25E-SD	4,990	0.39	5.6	3.4	0.061

Table 17. Second Translational Mode Damping Tests With External Cladding, EW-Tests

Test No.	Force Level at Resonance (Lbf)	Period (sec)	Damping (%)	Force Level of Test (Lbf)	Period of Test (sec)	Base Shear (Kip)	Deflection* of 12-th Floor (in.)
2N-SD	3710	1.23	3.5	-	-	-	-
10N-SD	2920	1.25	3.5	2920	1.25	60	0.85
SECOND MODE TESTS							
27N-SD	3430	1.32	3.0	3430	1.32	85	1.3
29N-D	-	-	-	13,500	1.75	160	4.4
29N-D	-	-	-	12,800	1.78	145	4.1
29N-D	-	-	-	11,000	1.83	140	4.1
31N-D	-	-	-	17,000	2.38	300	15.5
31N-D	-	-	-	16,500	2.47	290	15.6
39N-SD	5900	2.50	5.8	5,900	2.50	55	2.9
41N-D	-	-	-	17,000	2.38	210	11.0

* NS Translational Component, West Face of Building, Nodes 1, 21 and 24

Table 18. First Translational Mode Damping Tests Without External Cladding, NS Tests

TEST NO.	FORCE LEVEL AT RESONANCE (LBF)	PERIOD (SECONDS)	DAMPING (PERCENT)
1N-SD	5,170	1.04	3.1
9N-SD	4,680	1.08	2.5
SECOND MODE TESTS			
26N-SD	5,320	1.09	3.0
28N-D	8,480	1.24	3.1
30N-D	15,000	1.47	---
38N-SD	4,720	1.39	3.1
40N-D	8,130	1.45	2.3

Table 19. First Torsional Mode Damping Tests
Without External Cladding, NS Tests

TEST NO.	FORCE LEVEL AT RESONANCE (LBF)	PERIOD (SECONDS)	DAMPING (PERCENT)
4N-SD	3,530	0.31	3.7
MODE SHAPE TESTS			
12N-SD	3,670	0.32	2.8
14N-D	7,640	0.34	3.0
16N-D	10,570	0.35	3.4
18N-D	12,930	0.37	3.7
19N-D	13,180*	0.37	2.0
22N-D	15,260	0.40	3.2
23N-D	22,840	0.42	5.6
25N-SD	3,290	0.37	3.4
FIRST MODE TESTS			
37N-SD	5,050	0.53	3.9

*In all tests except 19N-D the direction of sweep was down, i.e., from a higher to lower frequency. In 19N-D the direction of the sweep was the reverse.

Table 20. Second Translational Damping Tests
Without External Cladding, NS Tests

TEST NO.	FORCE LEVEL AT RESONANCE (LBF)	PERIOD (SECONDS)	DAMPING (PERCENT)
3N-SD	4,500	0.28	2.6
11N-SD	5,000	0.28	2.1
13N-D	9,910	0.29	2.5
15N-D	15,140	0.30	3.2
17N-D	20,160	0.31	2.8
20N-D	19,140*	0.31	1.6
21N-D	26,940	0.32	2.8
24N-SD	5,190	0.30	2.5
	FIRST MODE TESTS		
36N-SD	5,470	0.34	2.8

*In all tests except 20N-D the direction of sweep was down, i.e., from a higher to lower frequency. In 20N-D the direction of the sweep was the reverse.

Table 21. Second Torsional Mode Damping Tests
Without External Cladding, NS Tests

Test No.	Frequency of Data Analyzed (Hz)	Damping 10-th & 12-th Floor Response	Damping 10-th, 12-th & Reference Response
10E-D	1.19	1.17	1.75
24E-D	0.56	3.87	3.87
3E-SD	4.6	2.58	3.27
21E-SD	3.46	3.98	5.21

Table 22. Comparison of Two and Three Channel Damping Results
Using Time Domain Analysis

Floor	Walls in Place		Without Walls	
	Trans. (Kip)	Rotat. (Kip-Sec)	Trans. (Kip)	Rotat. (Kip-Sec)
12	0.55	28,800	0.55	28,800
11	0.93	44,900	0.93	44,900
10	0.70	37,140	0.58	28,800
9	0.71	"	0.45	20,460
8	"	"	0.46	"
7	"	"	"	"
6	"	"	"	"
5	0.72	"	0.47	"
4	"	"	"	"
3	"	"	"	"
2	0.60	28,800	0.48	"
1	0	0	0	0

Table 23. Floor Masses for Analytical Model

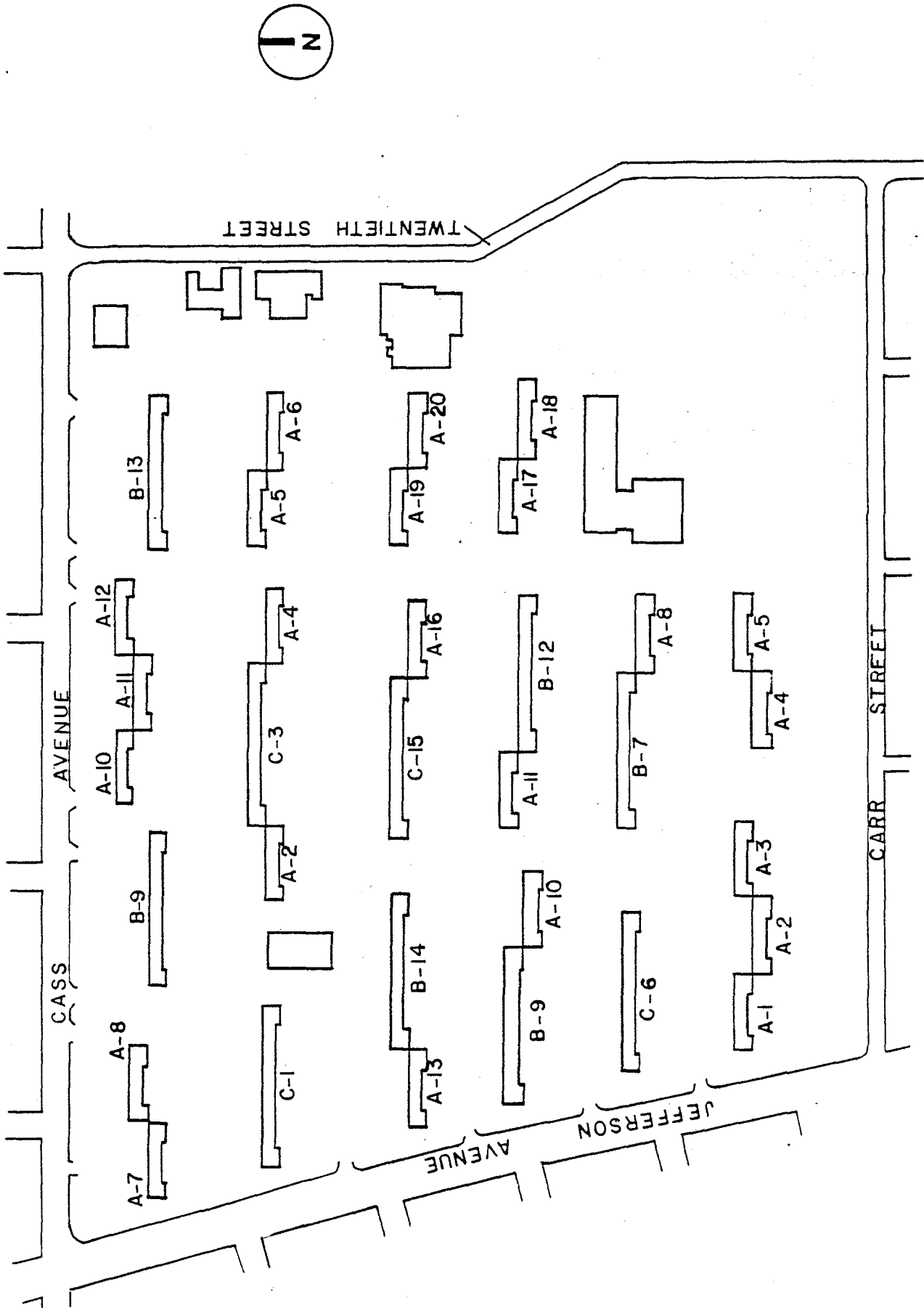
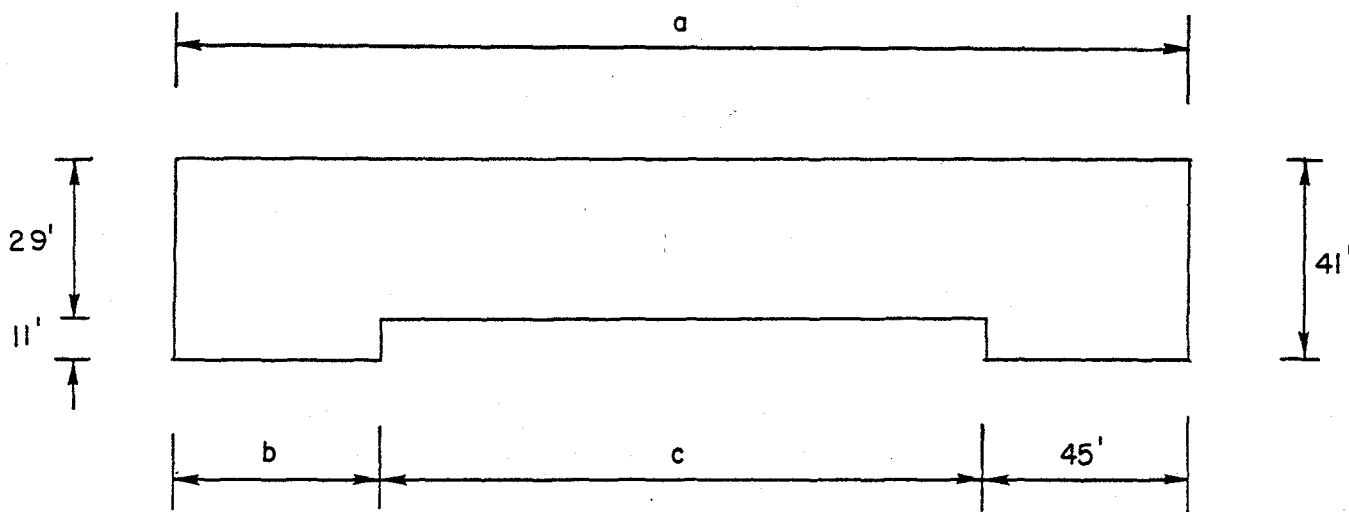


Fig. 1 Plan of Housing Project



Building	a	b	c
A	170'	36''	89'
B	349'	45'	259'
C	360'	45'	270'

Fig. 2 Overall Plan Dimensions

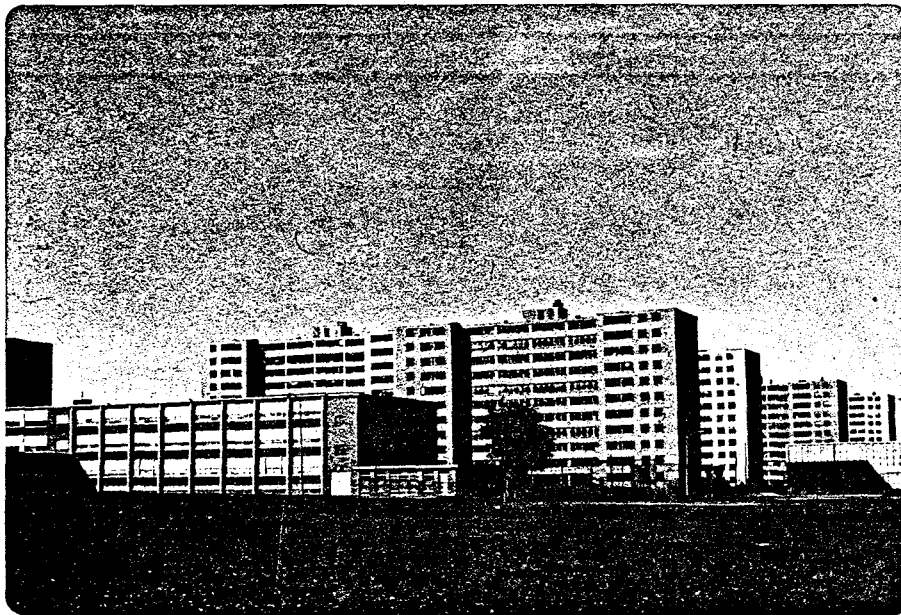


Fig. 3 Pruitt-Igoe, 1974

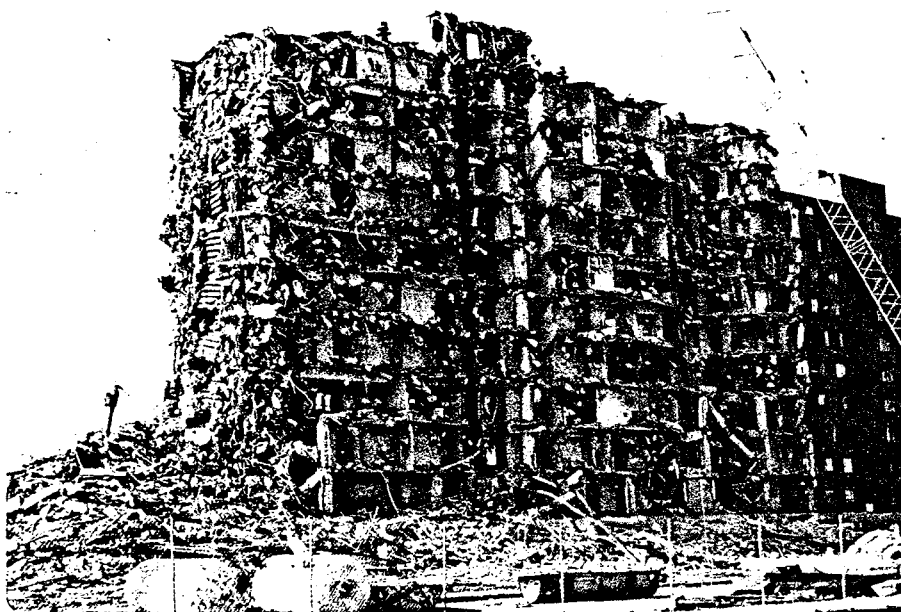


Fig. 4 Pruitt-Igoe, 1976



Fig. 5 Pruitt-Igoe Buildings Before Demolition



Fig. 6 Pruitt-Igoe Buildings During Demolition



Fig. 7 St. Louis and Pruitt-Igoe

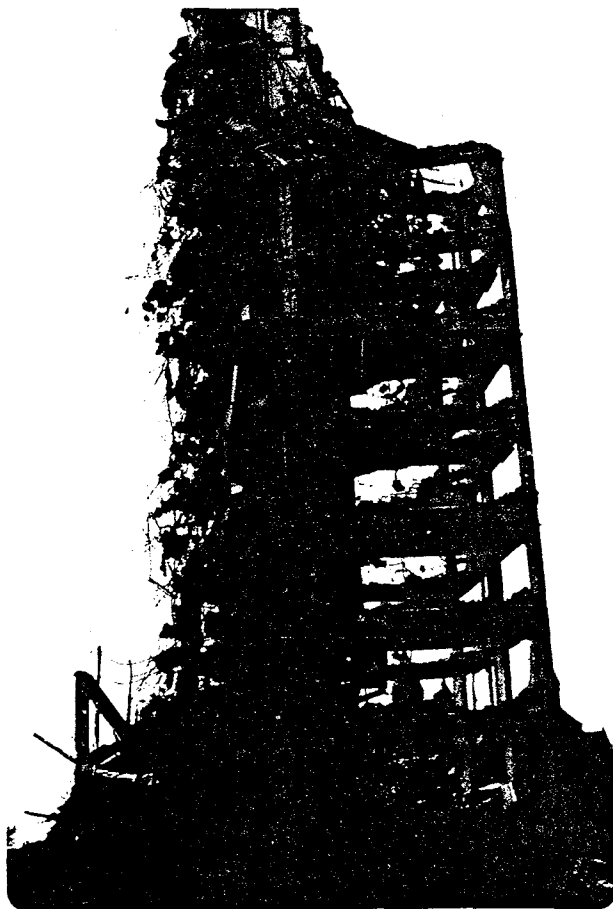


Fig. 8 Demolition of a Building



Fig. 9 A Former Corner Column During Demolition

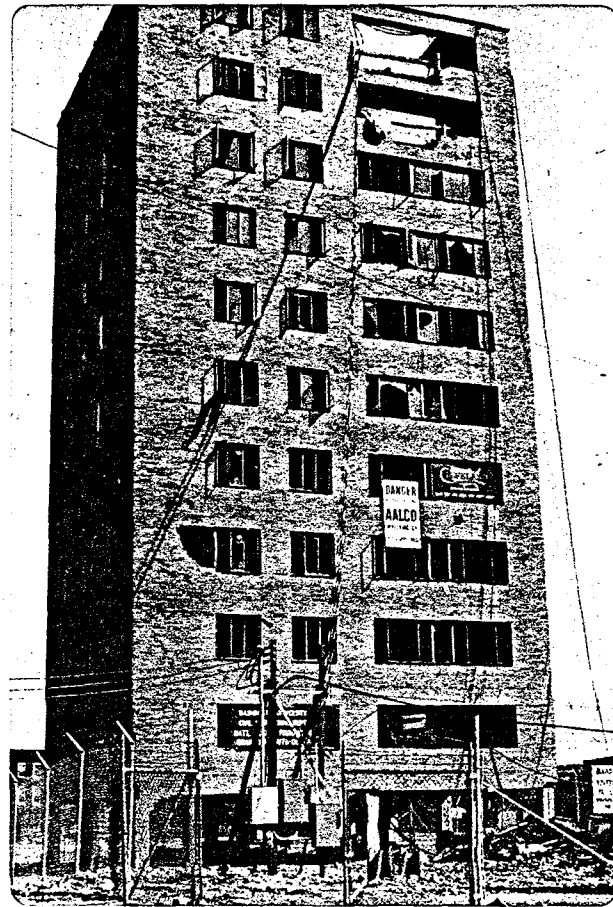


Fig. 10 Main Power Cable to 11th Floor

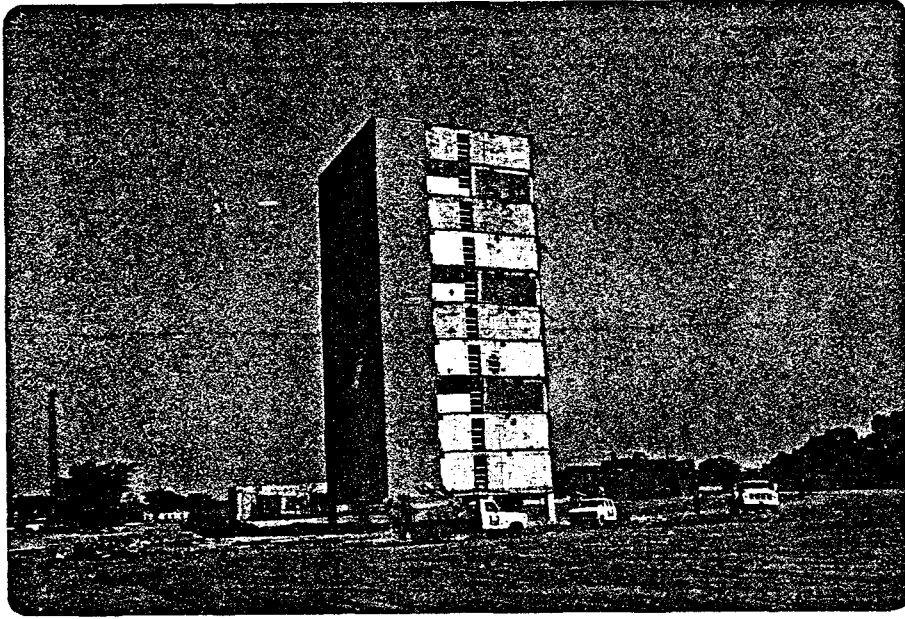


Fig. 11 Overall View of Test Building

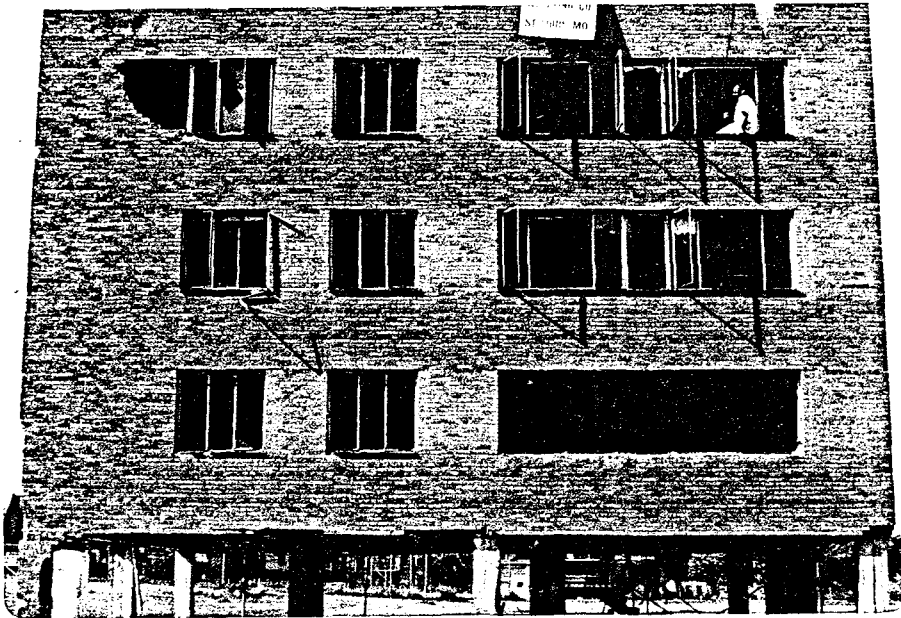


Fig. 12 Wall Damage Prior to Testing,
S. Face

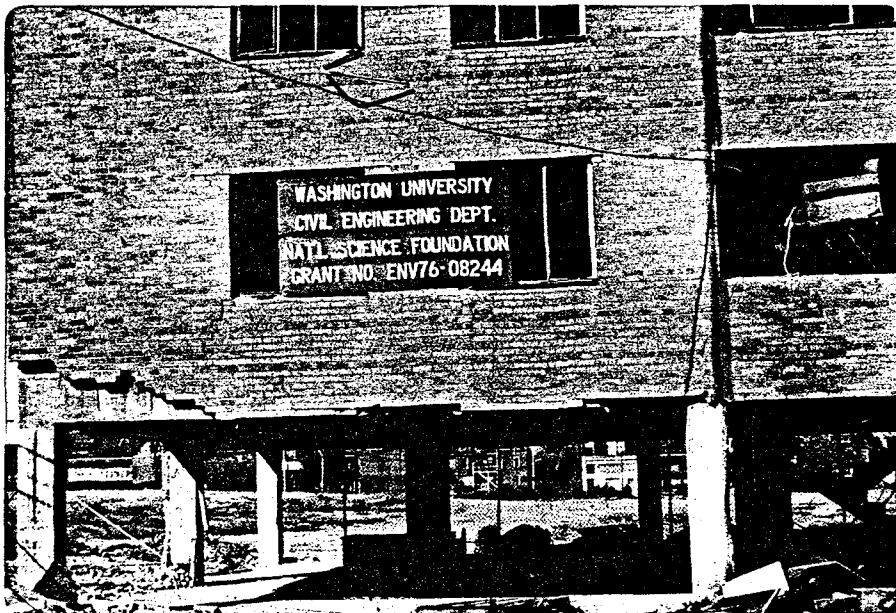


Fig. 13 Open First Floor

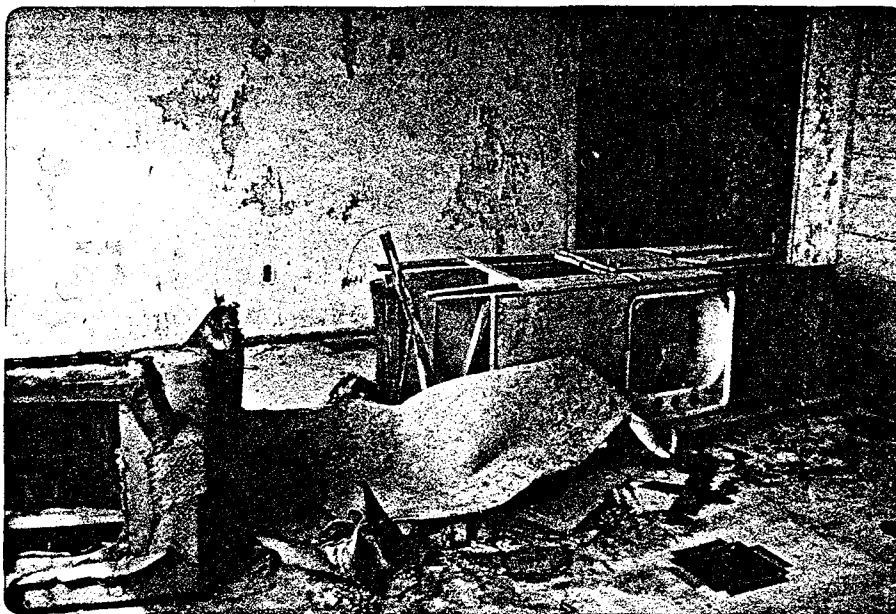


Fig. 14 Debris in Rooms

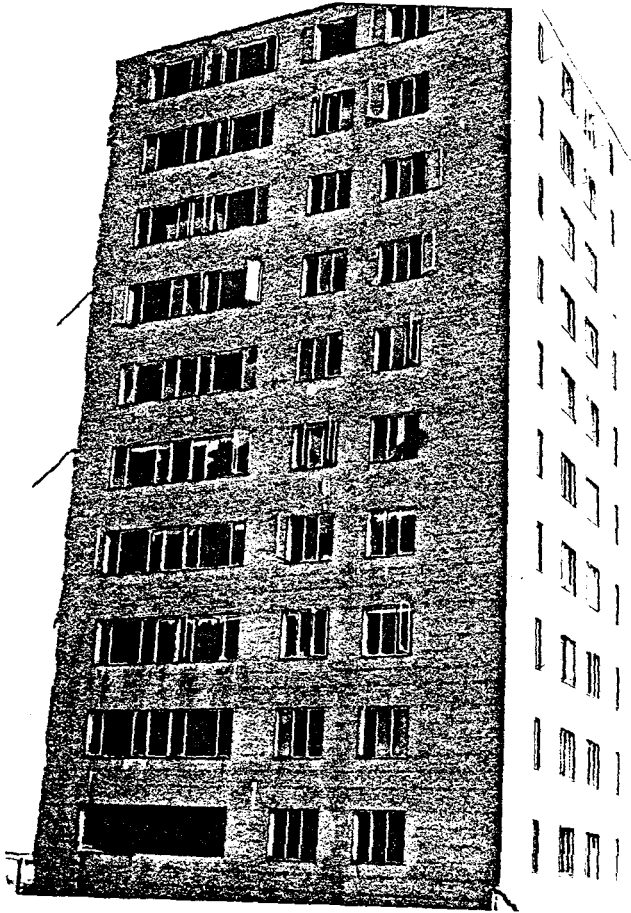


Fig. 15 N. Face Prior
to Testing



Fig. 16 E. Face Prior
to Testing



Fig. 17 View of Test Site

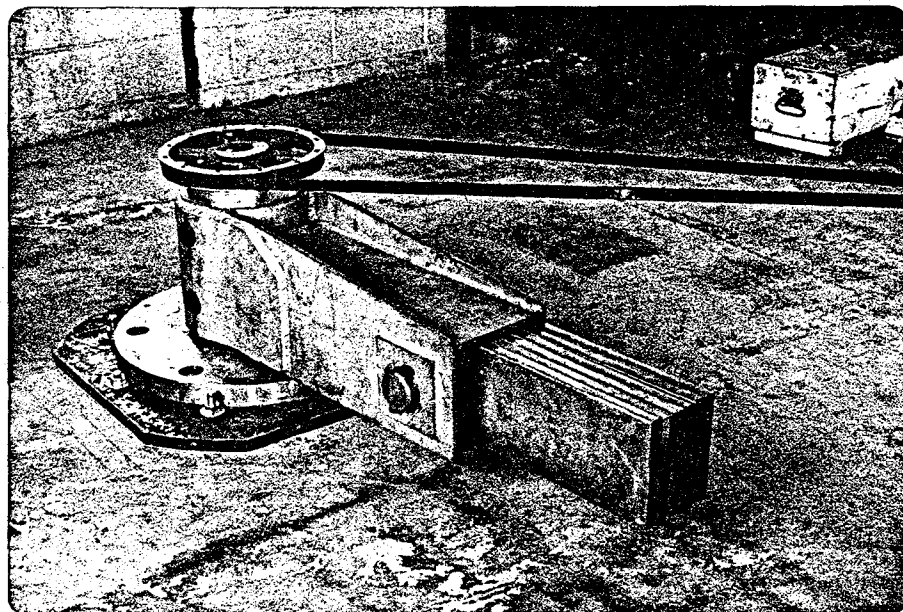


Fig. 18 Applied Nucleonics Shaker

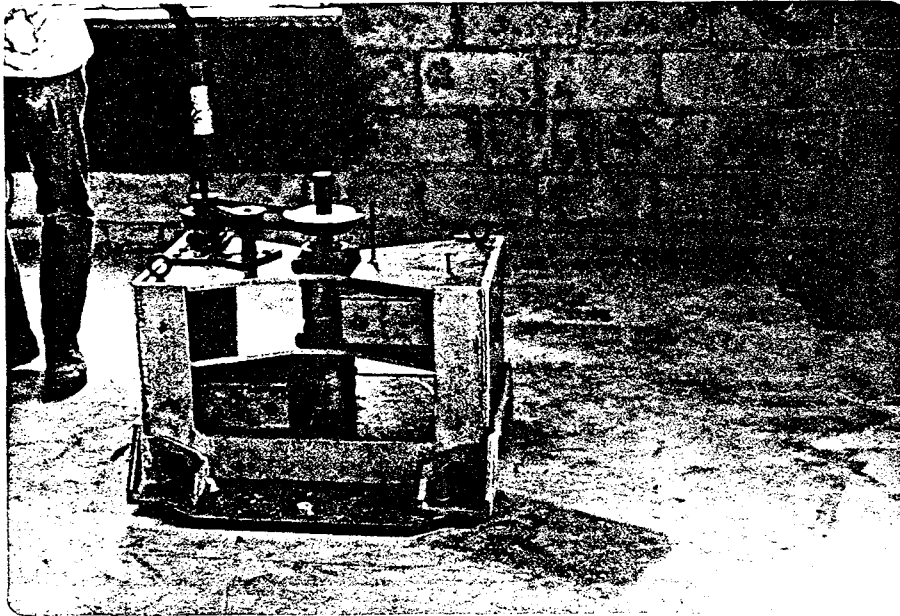


Fig. 19 Applied Nucleonics Shaker
With Rotating Baskets



Fig. 20 Power Distribution Panel



Fig. 21 Opening in Roof



Fig. 22 View of Instruments
Trailer and Lead Ingots

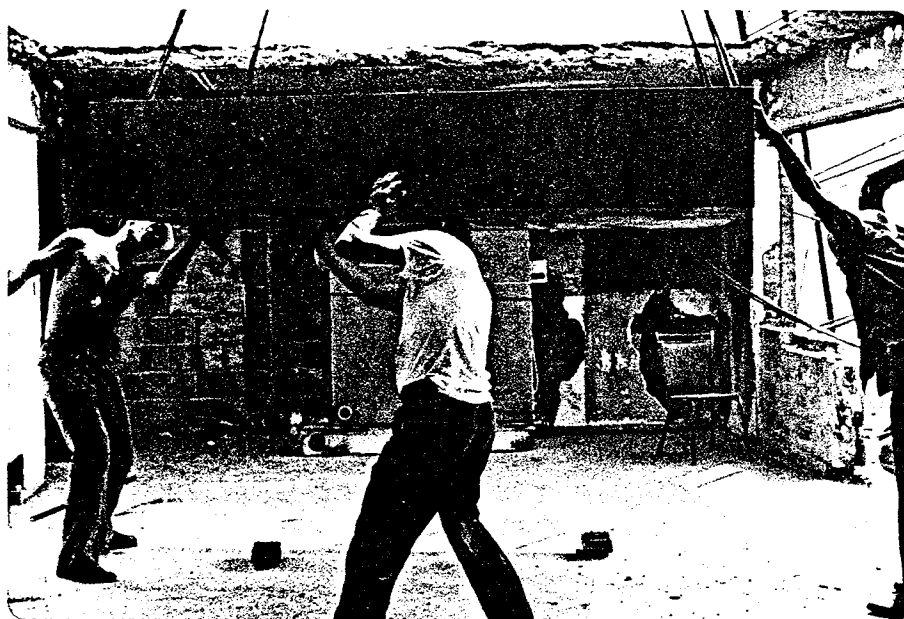


Fig. 23 Lowering of Moving
Box Through Roof

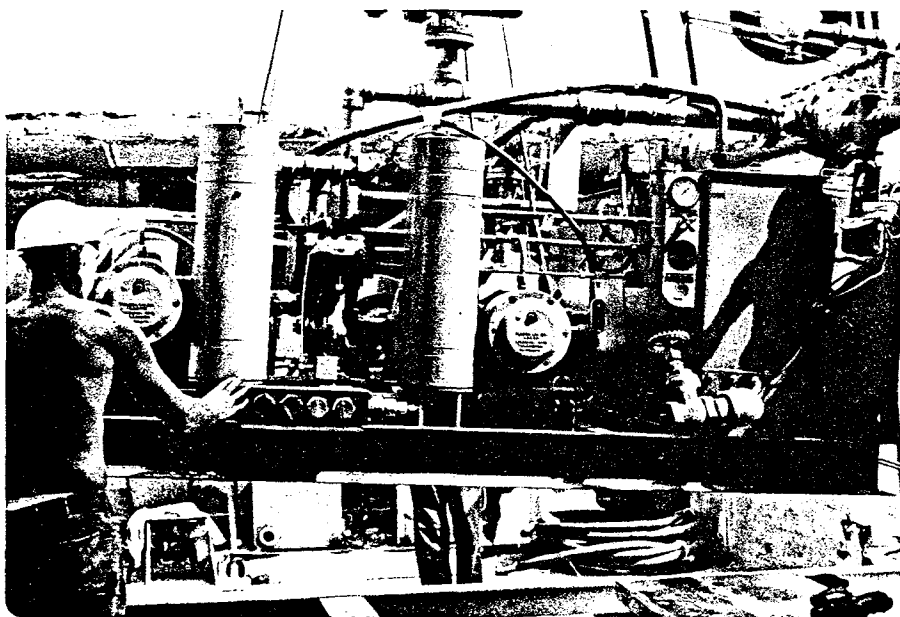


Fig. 24 Lowering of Pump-Motor
Assembly Through Roof

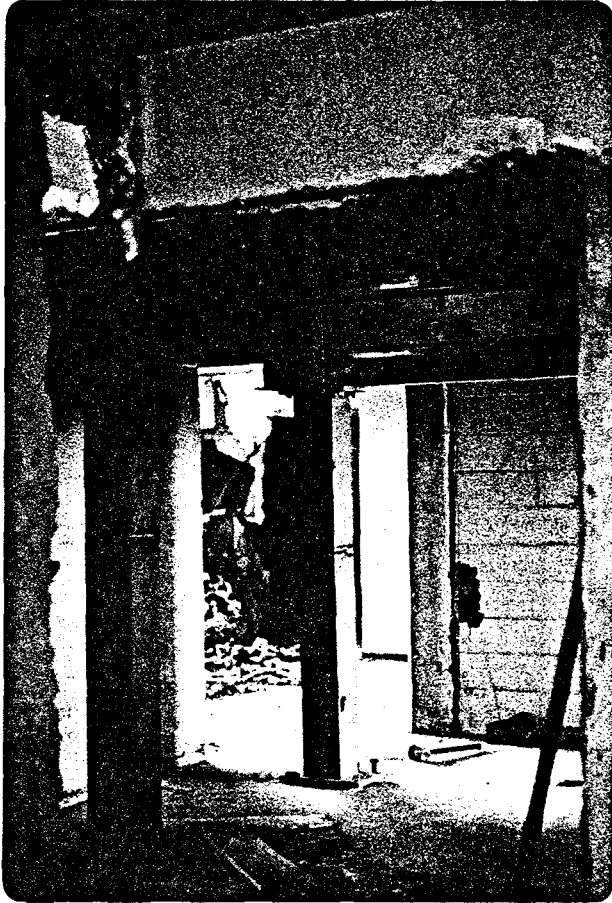


Fig. 25 Cribbing on
10th Floor

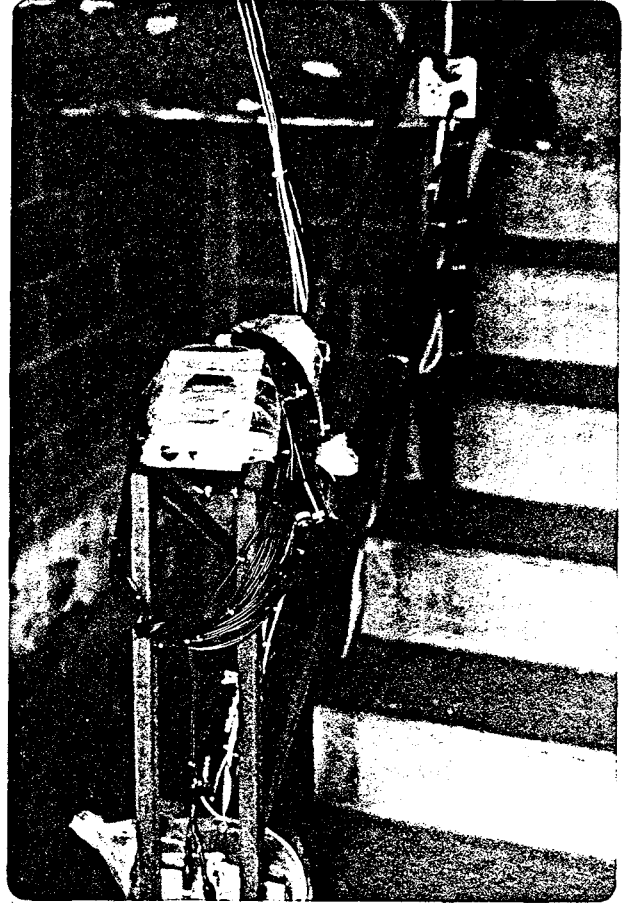


Fig. 26 Communications
Box



Fig. 27 Removal of Walls
after E.W. Shaking

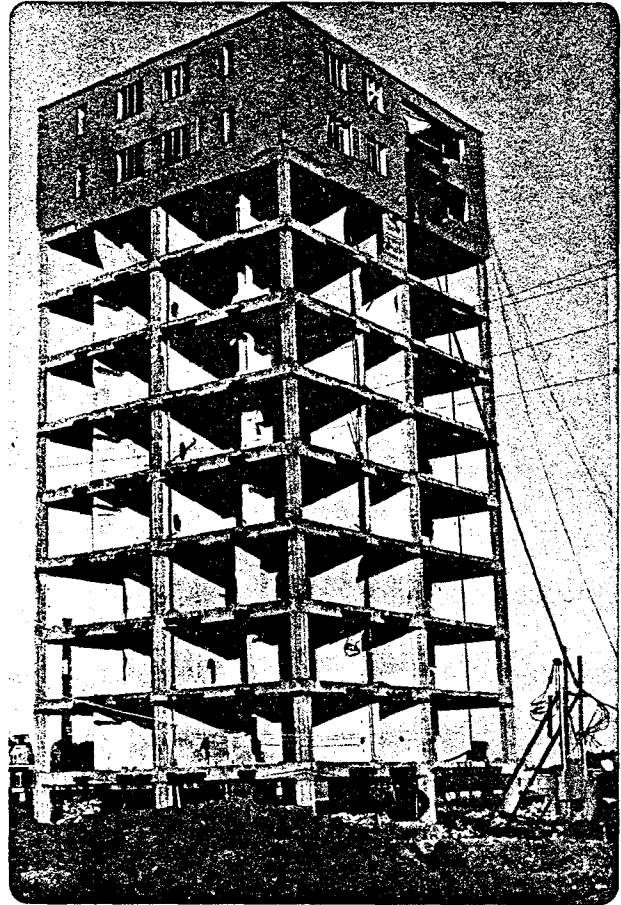


Fig. 28 Structure Prior
to N.S. Shaking

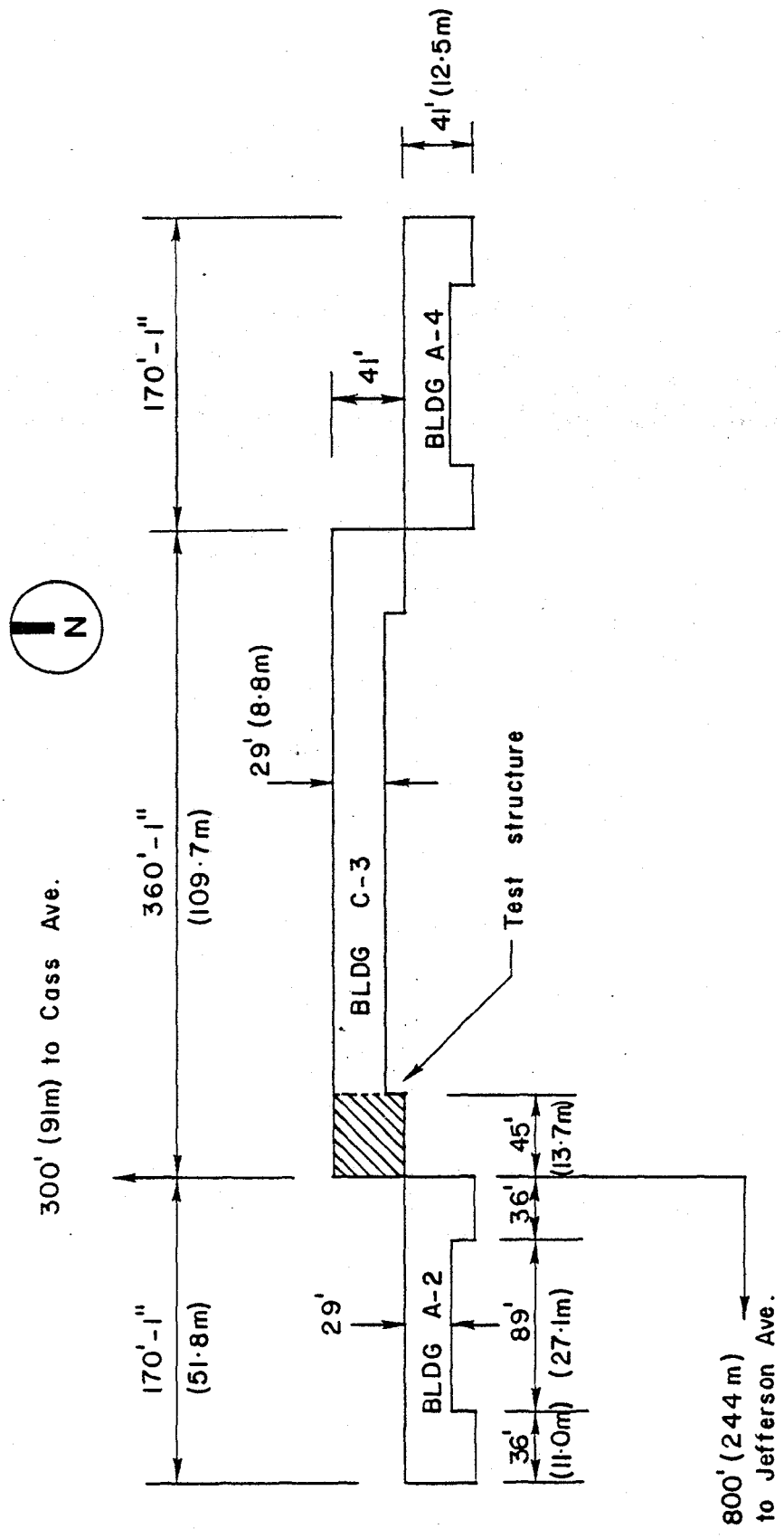


Fig. 29 Overall Plan Dimensions

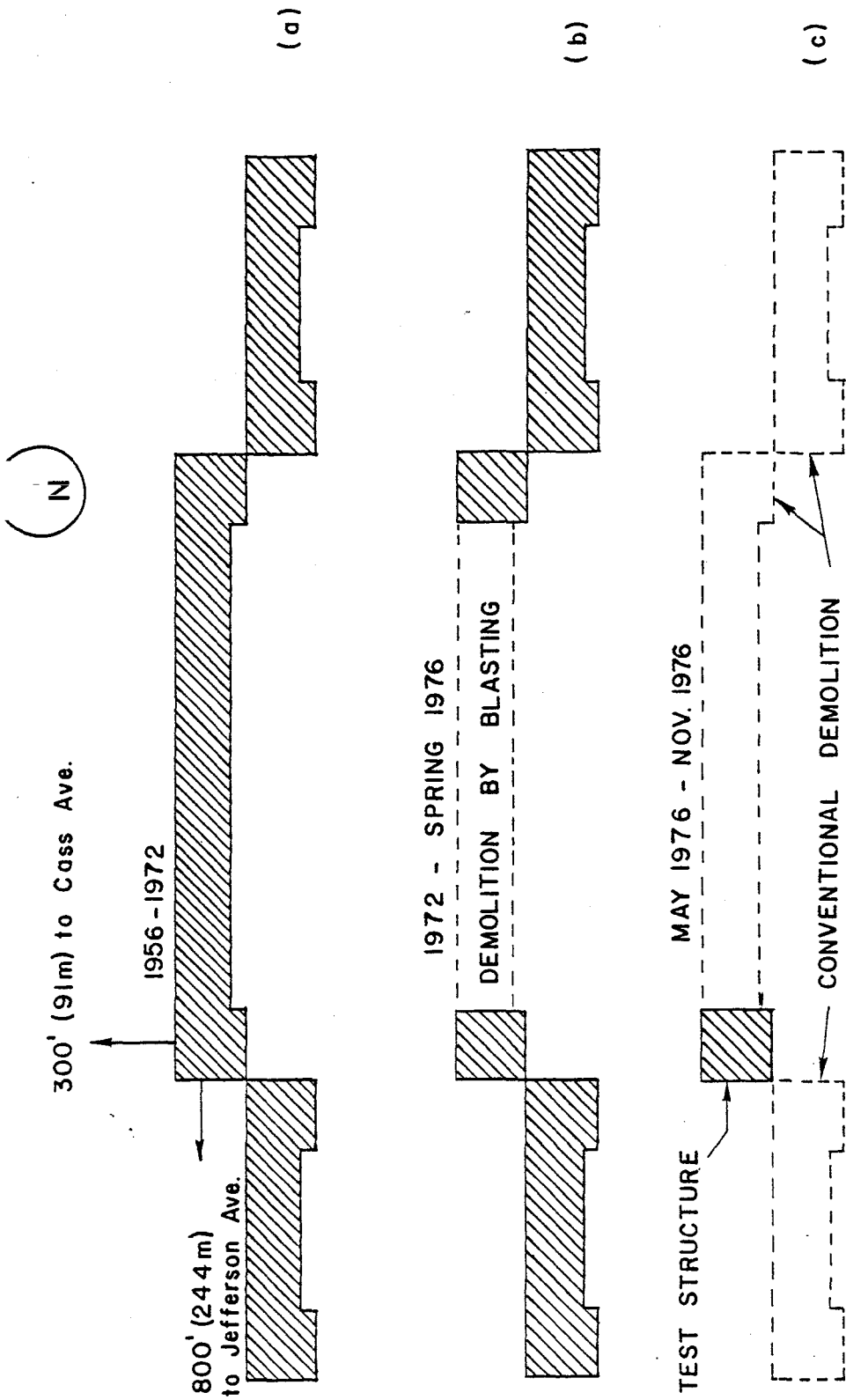


Fig. 30 Demolition Scheme

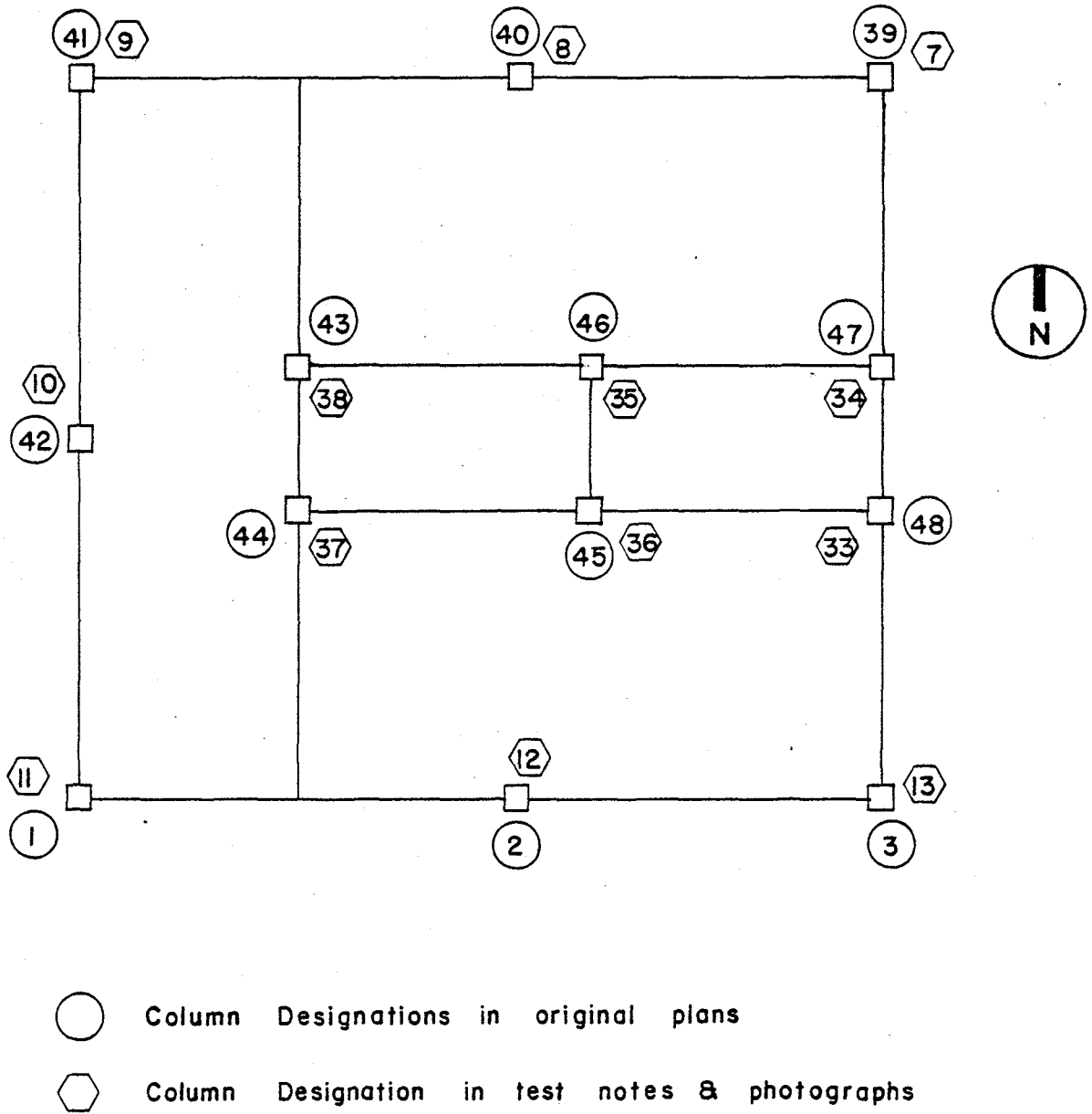


Fig. 31 Column Designations

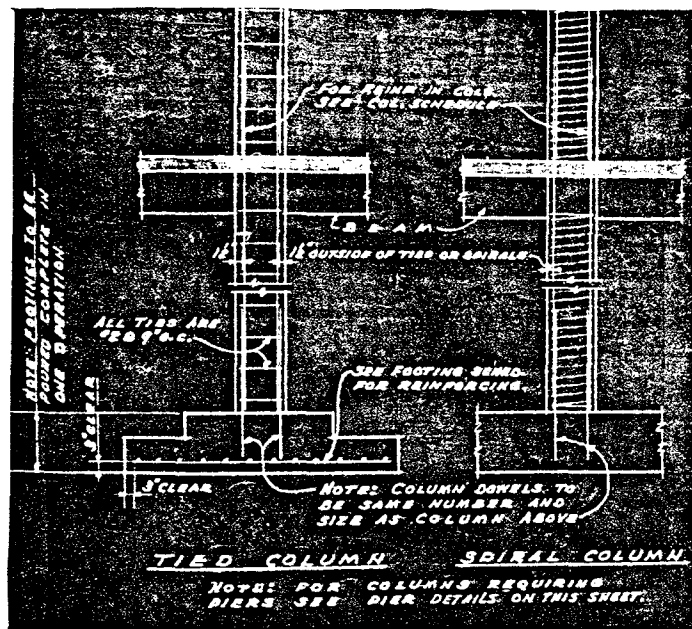


Fig. 32 Column and Footing Details (from original plans)

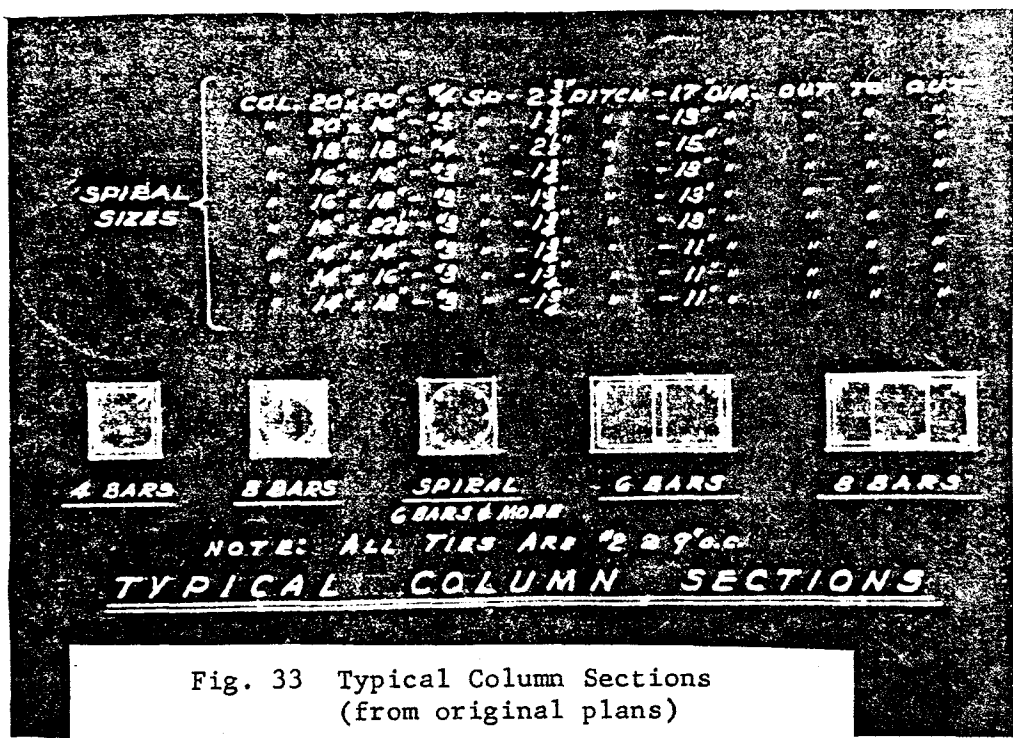


Fig. 33 Typical Column Sections (from original plans)

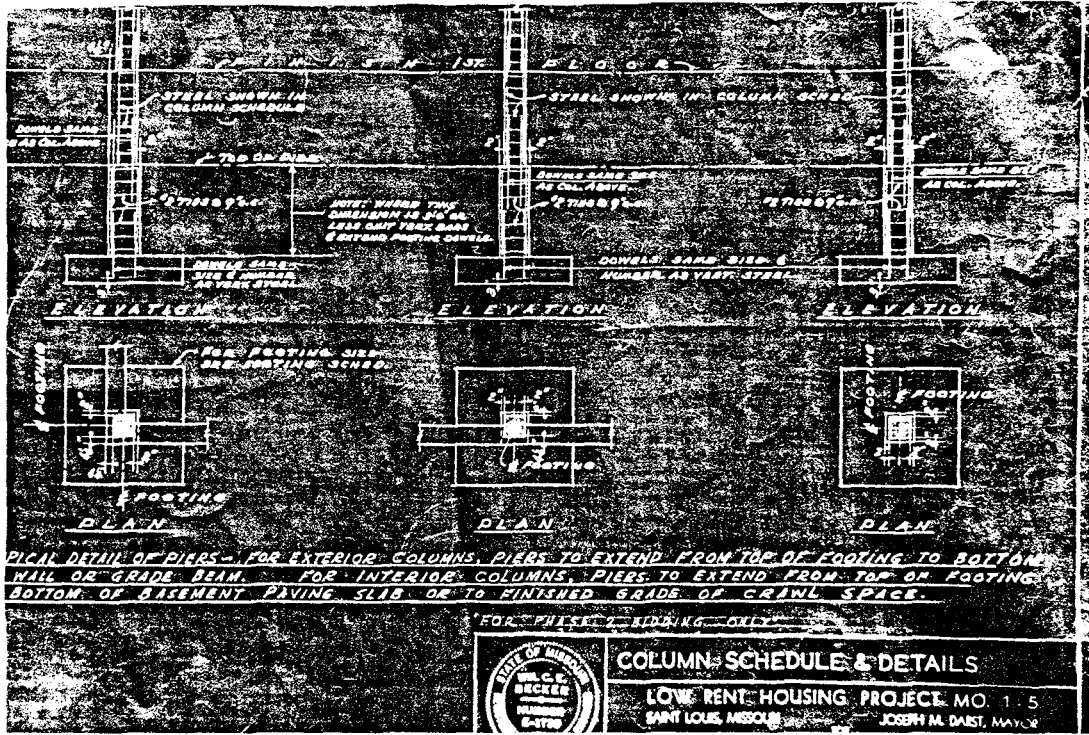


Fig. 34 Column Details
(from original plans)

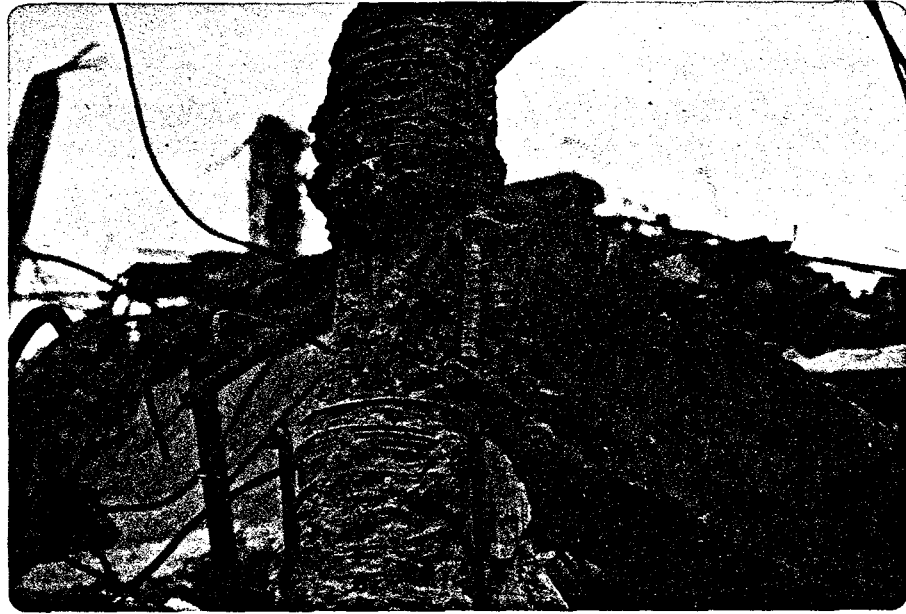


Fig. 35 Reinforcement in Typical
Corner Joint

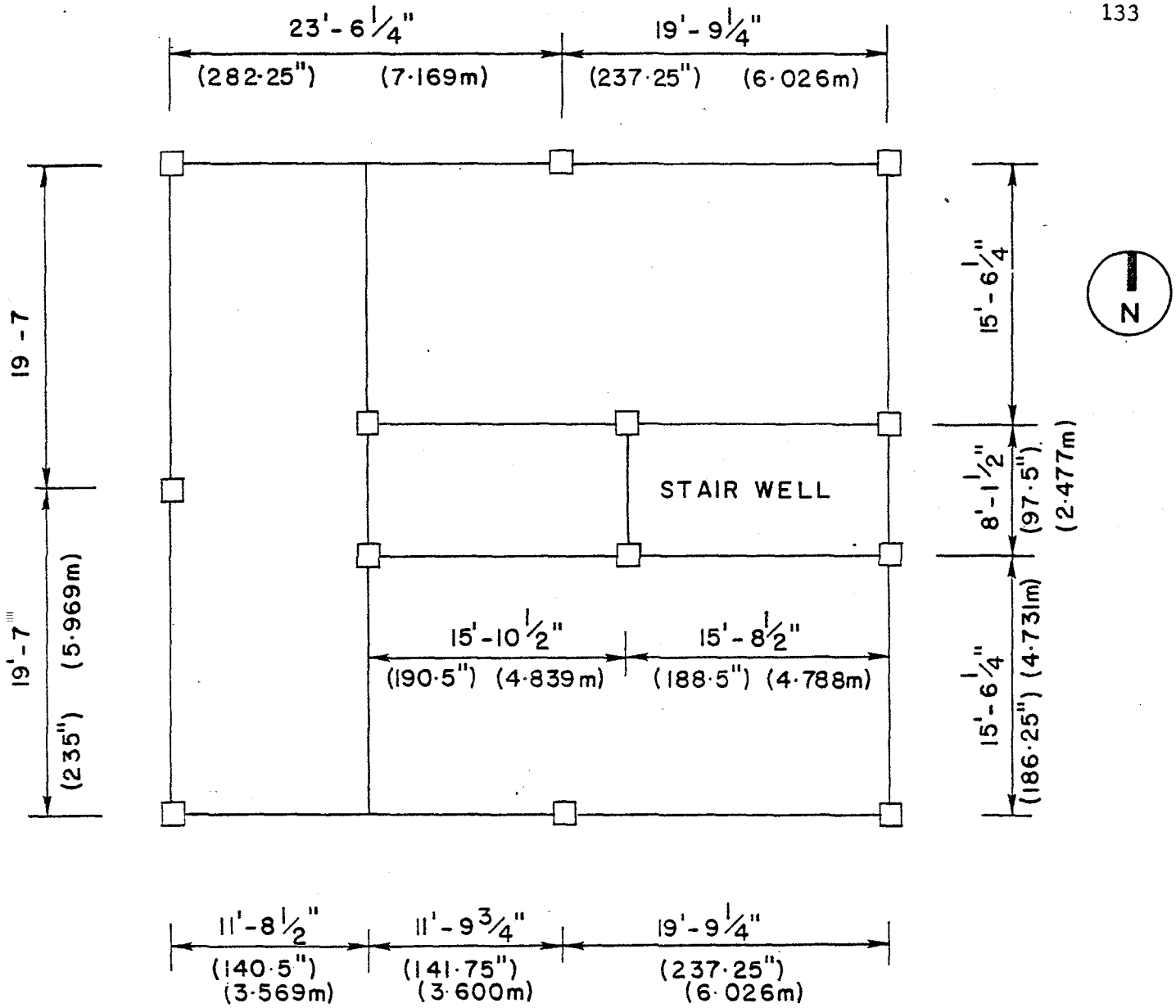


Fig. 36 Theoretical Floor Plan Dimensions Between Column Centers

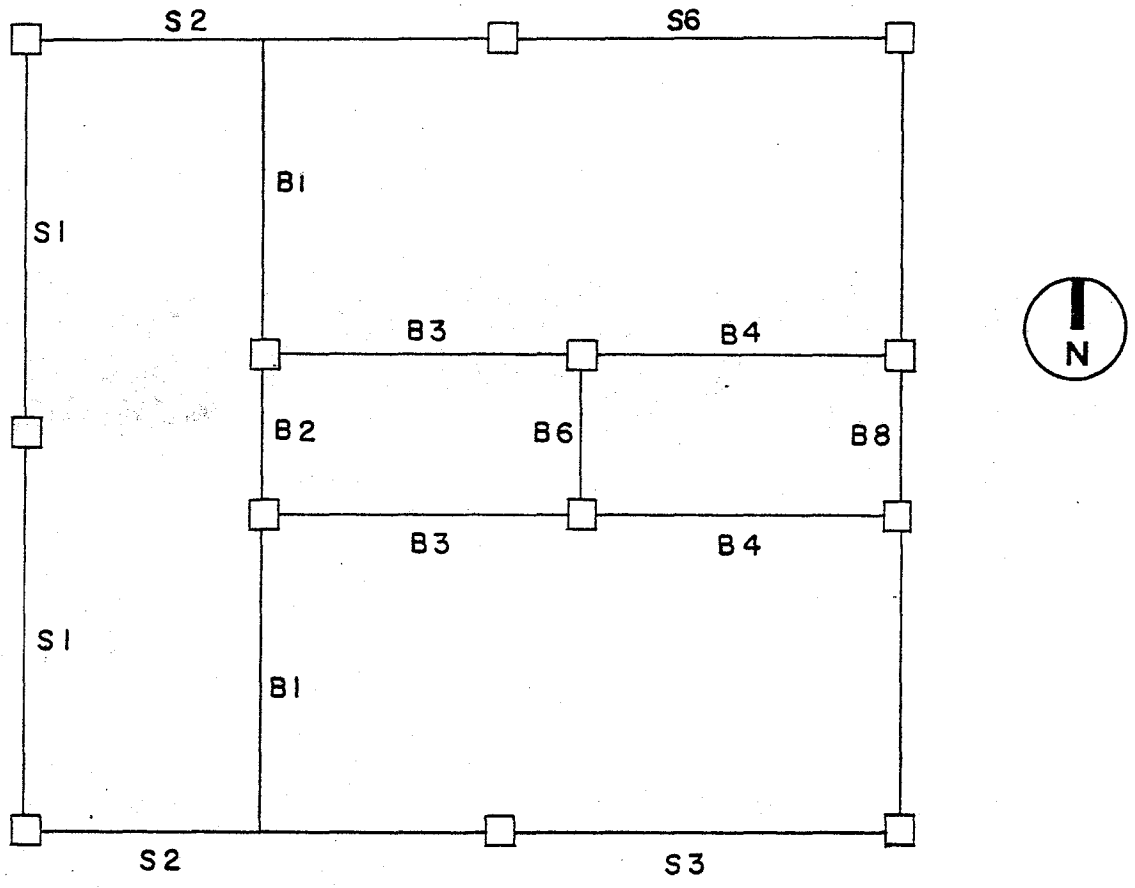


Fig. 37 Beam Designations

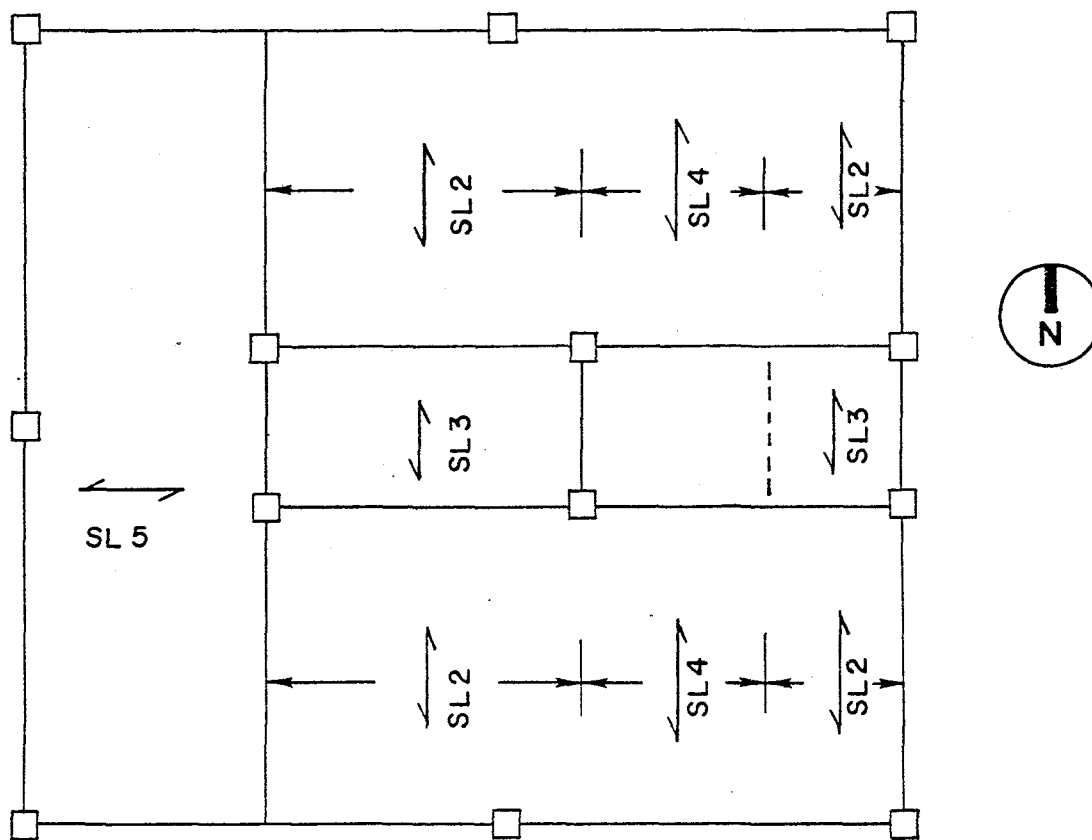


Fig. 38 Slab Designations on All Floors Above Ground Level

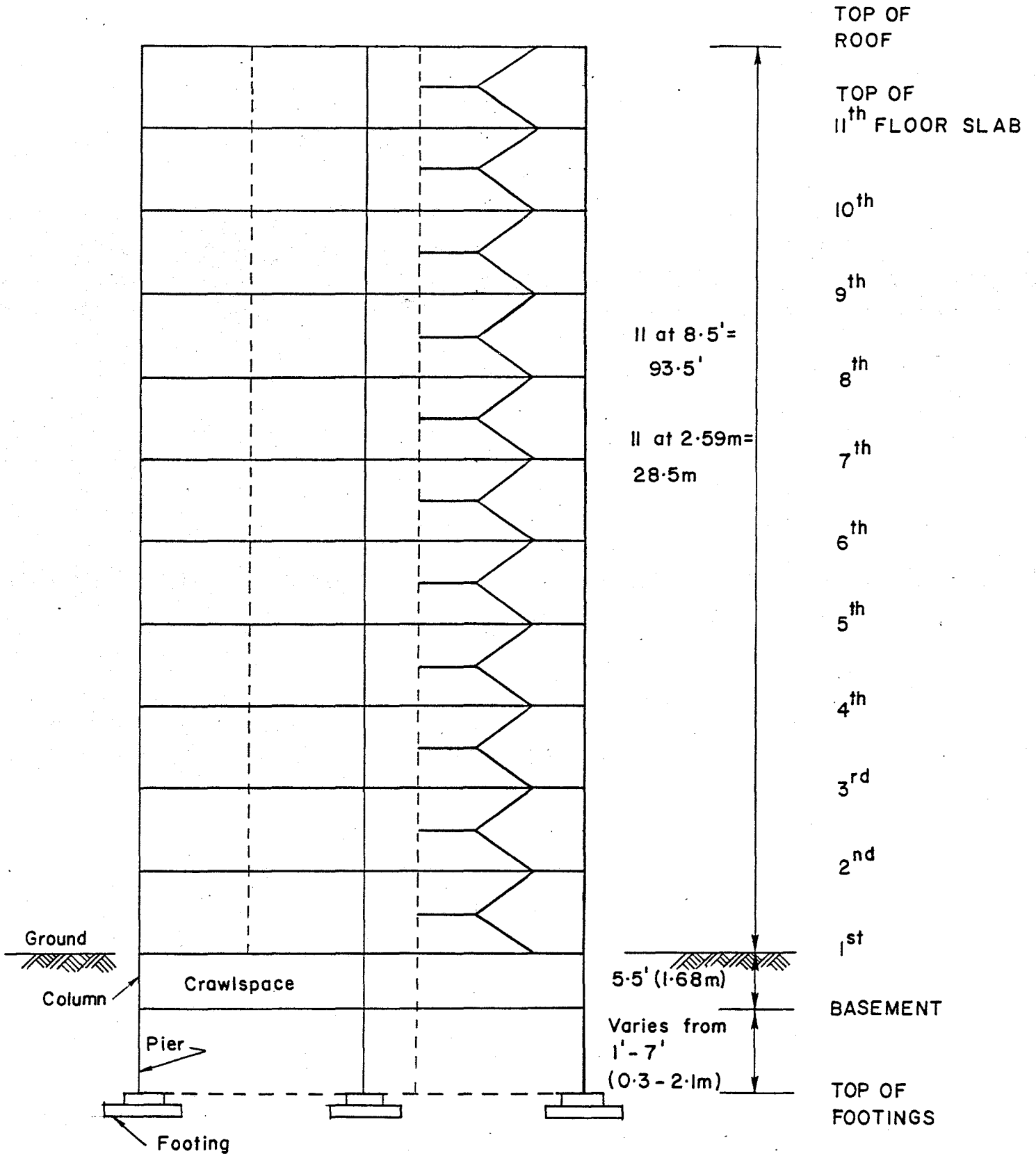


Fig. 39 Building Elevation

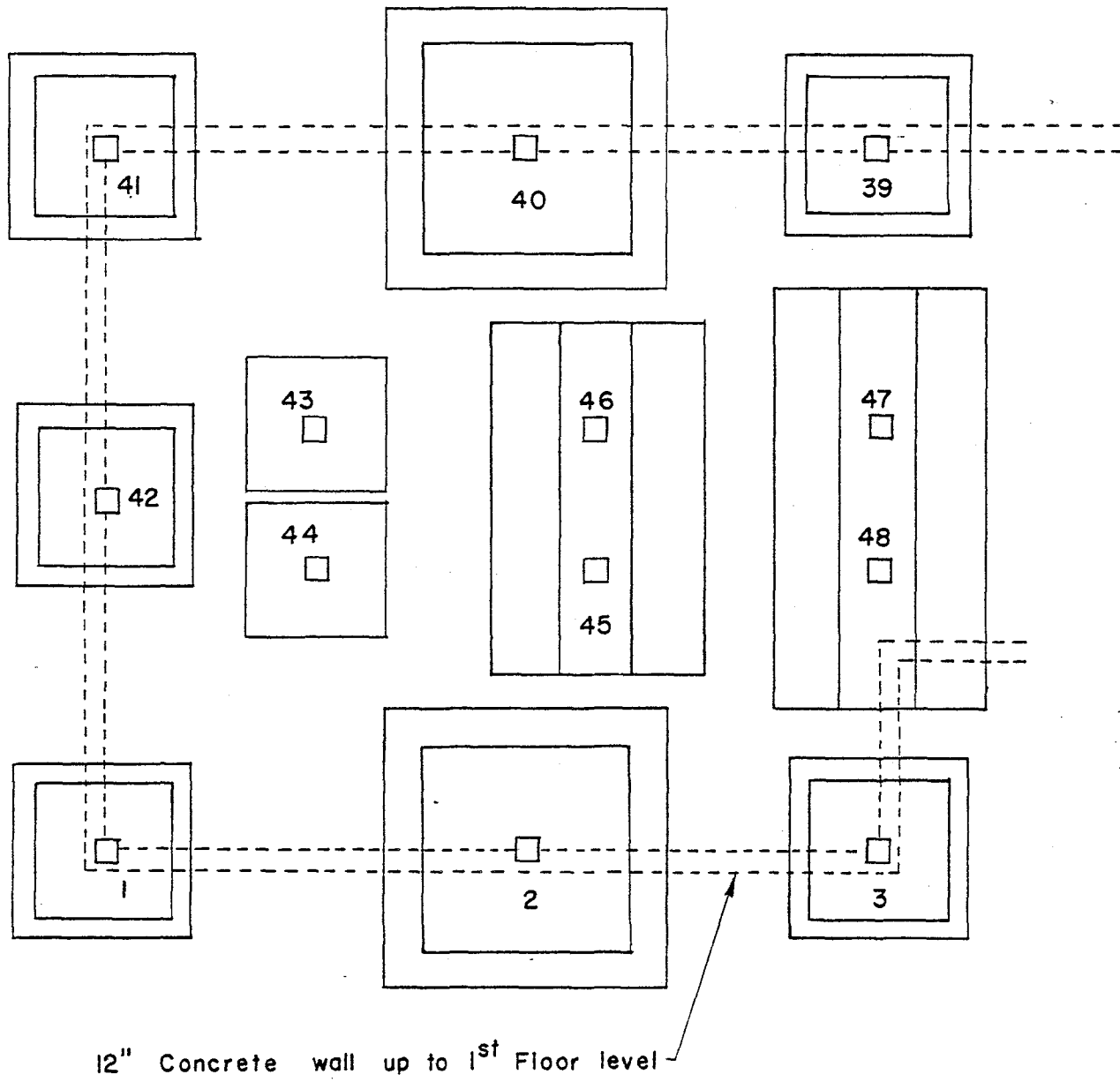


Fig. 40 Footing Plan

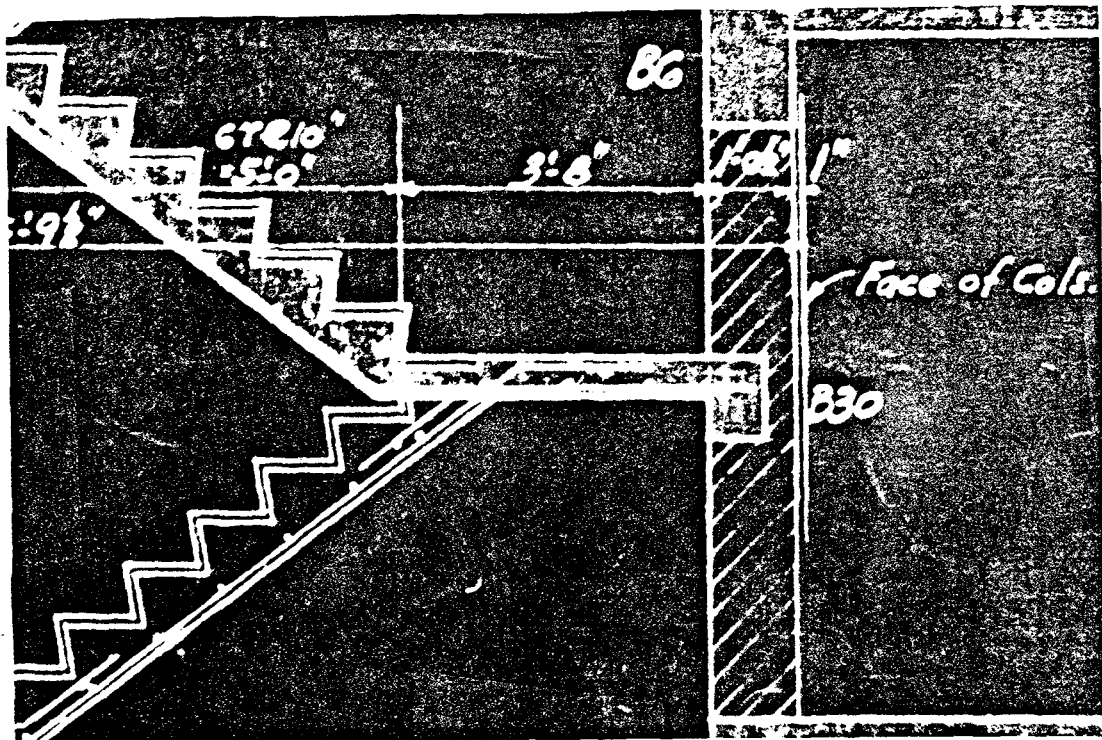


Fig. 42 Stair Details
(from original plans)

Reproduced from
best available copy.



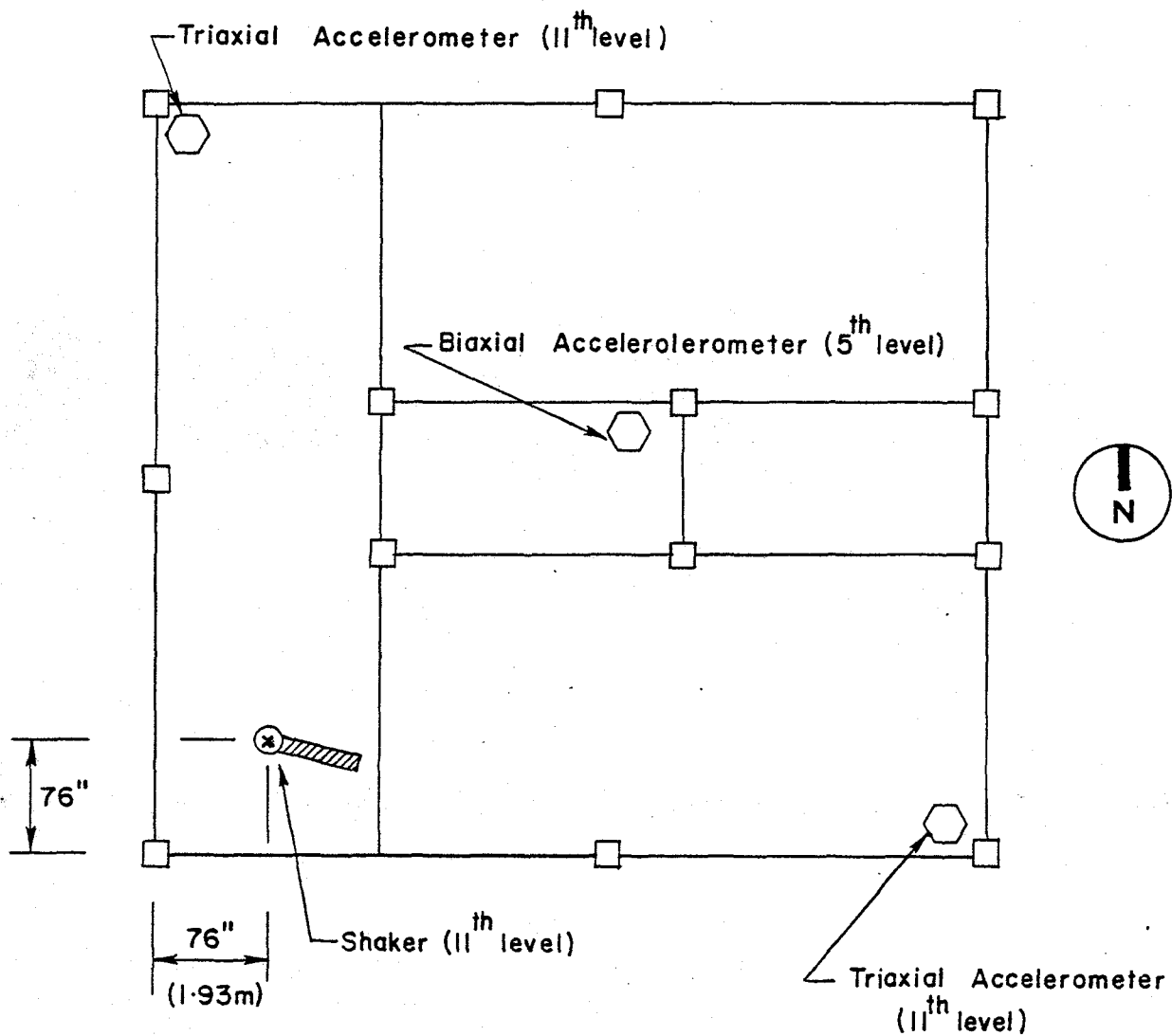


Fig. 43 Location of Applied Nucleonics Shaker and Accelerometers

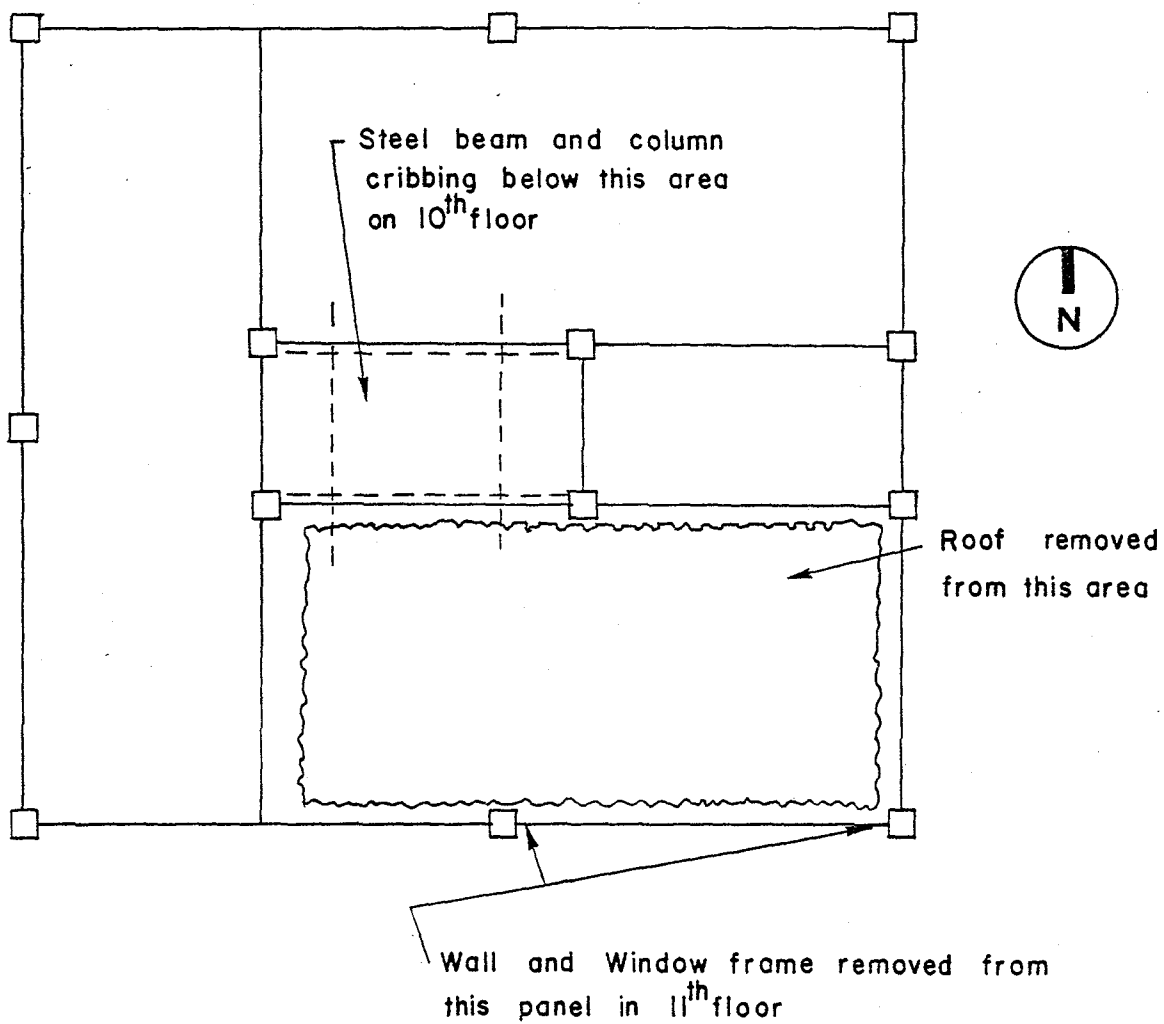
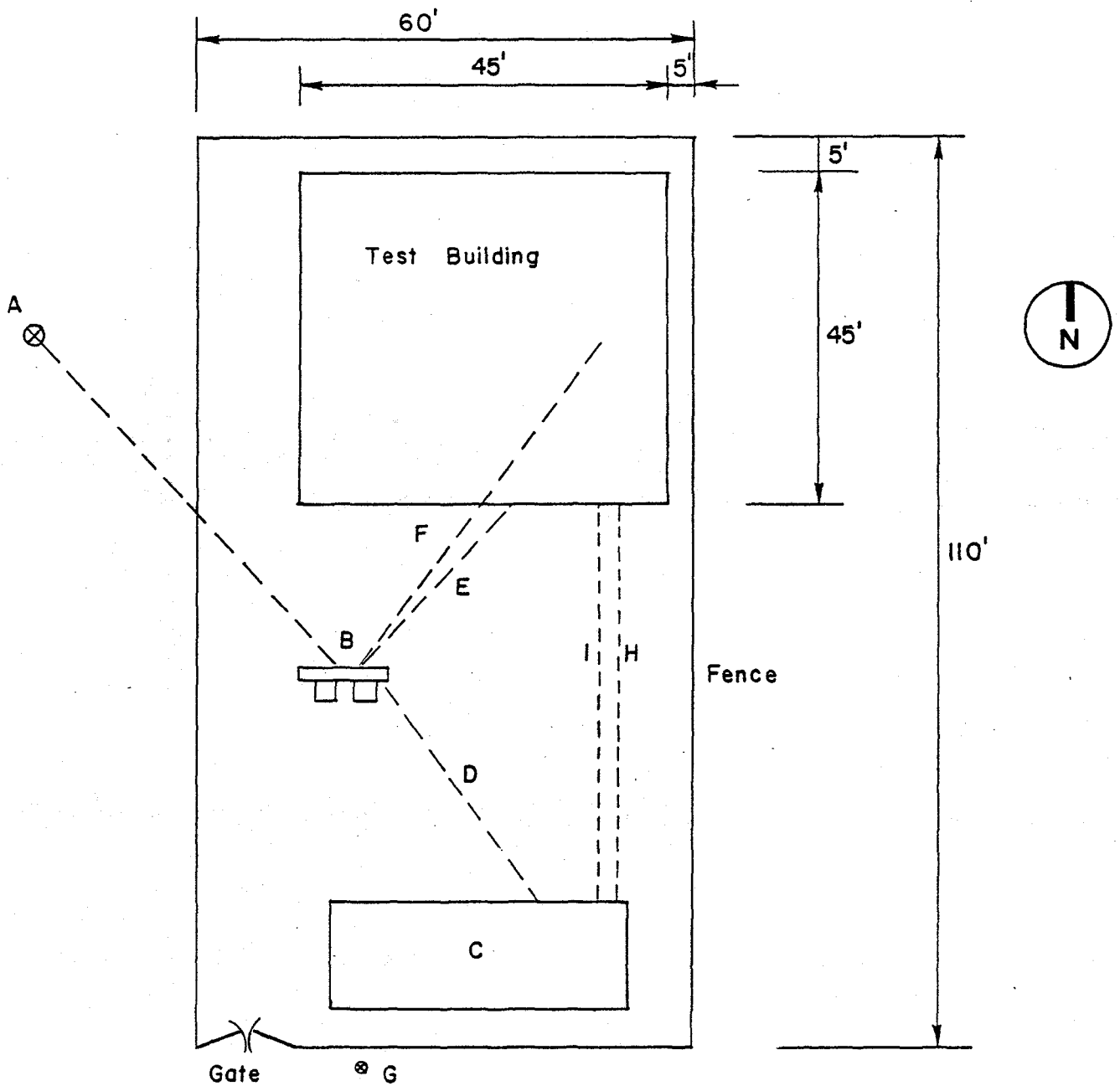
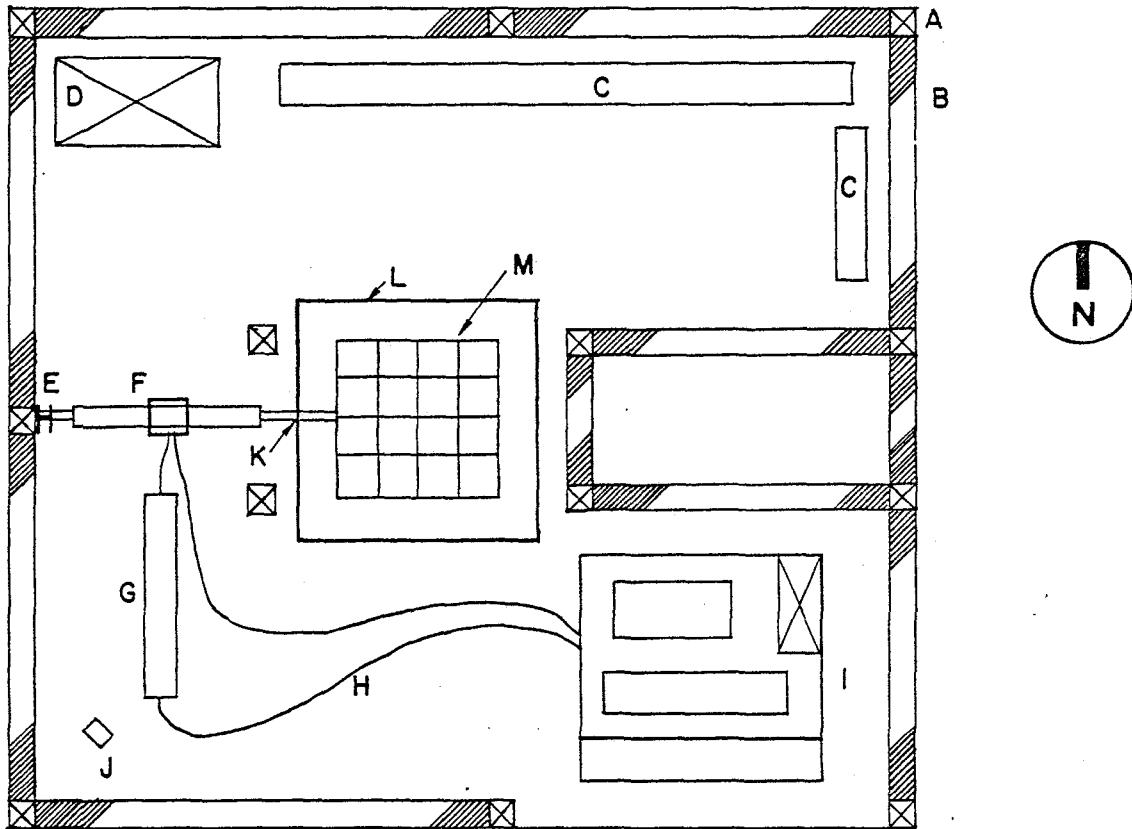


Fig. 44 Building Modifications Prior to Testing With
Large Amplitude Shaker



- A : Union Electric power terminal and transformer
- B : Sachs Electric switch boxes and support on ground level
- C : Instrumentation trailer
- D : 110/220V lines to trailer
- E : 440V line to 11th floor, outside of building
- F : 110/220V lines to building, running up stair-well
- G : Telephone terminal
- I, H : Control, communication and accelerometer connections to building

Fig. 45 The Test Site



- A : Column
- B : Wall
- C : Stored lead ingots
- D : Tool storage
- E : Hydraulic actuator attachment to Building
- F : Hydraulic actuator
- G : Accumulator
- H : Hydraulic lines
- I : Pump-motor assembly
- J : TV Camera
- K : Piston
- L : Stiffened base plate
- M : Moving mass box

Fig. 46 Large Amplitude Shaker Assembly on 11th Floor, E-W Shaking

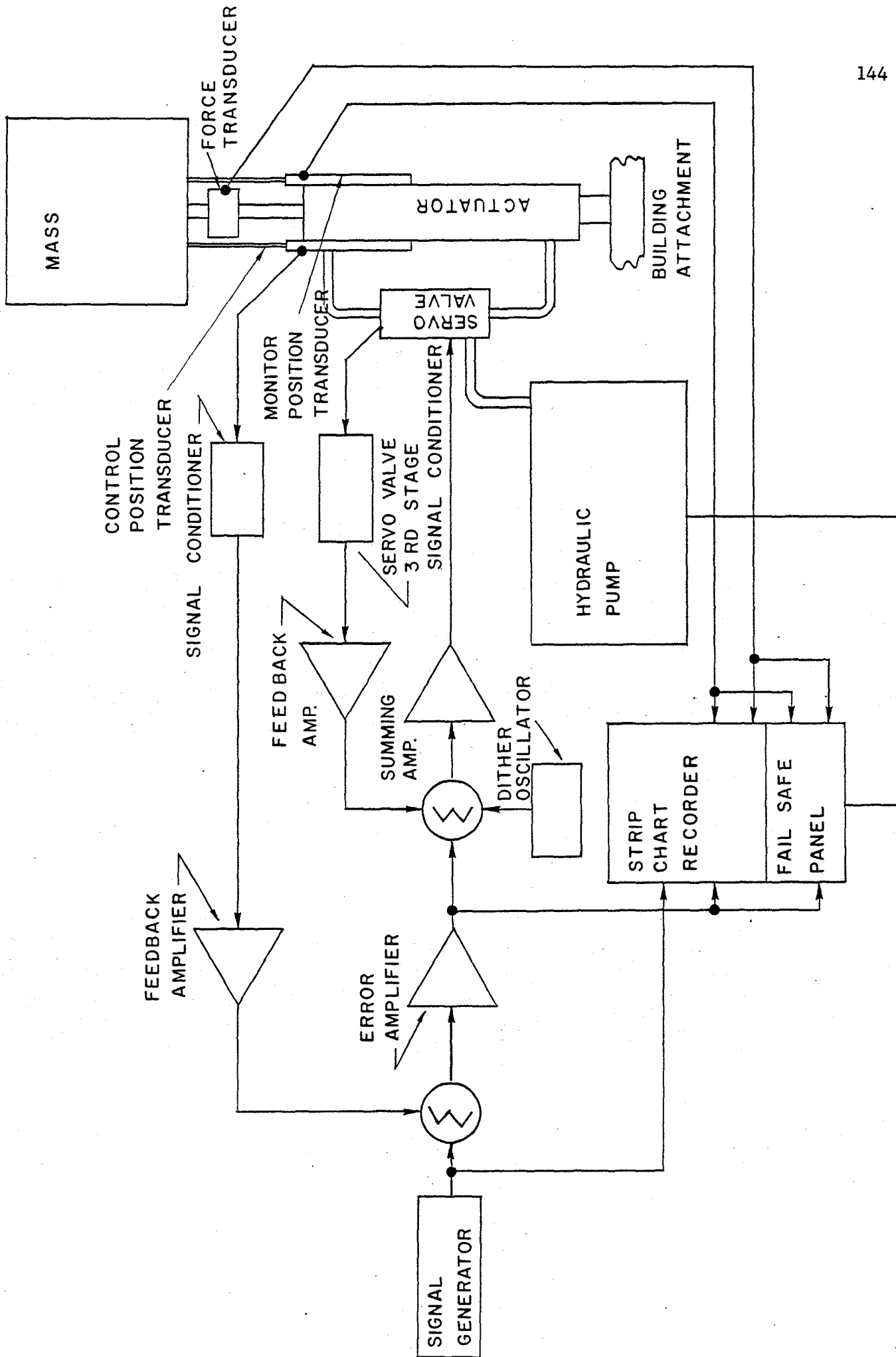


Fig. 47 Block Diagram of Servo-Control System

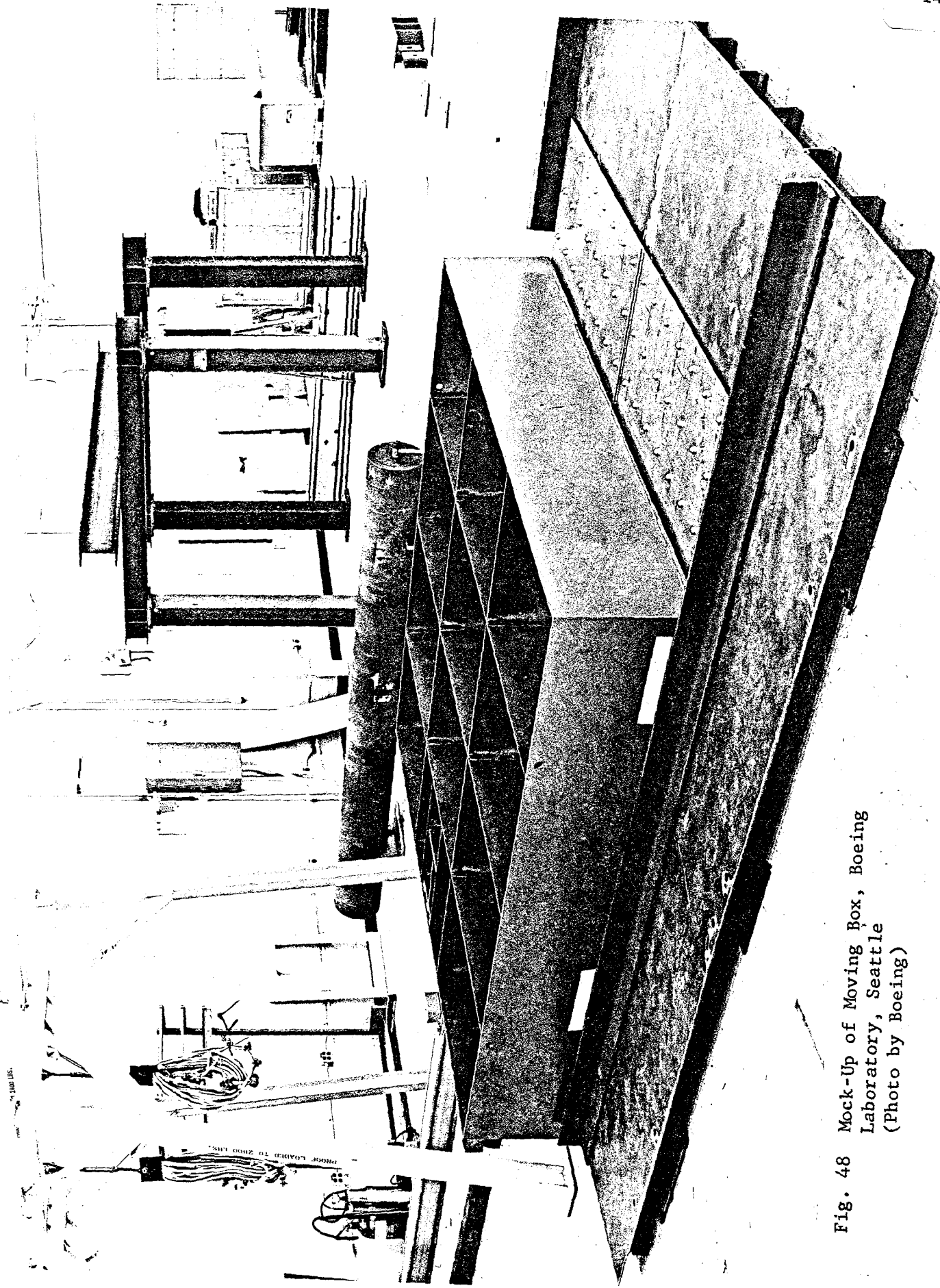


Fig. 48 Mock-Up of Moving Box, Boeing Laboratory, Seattle (Photo by Boeing)

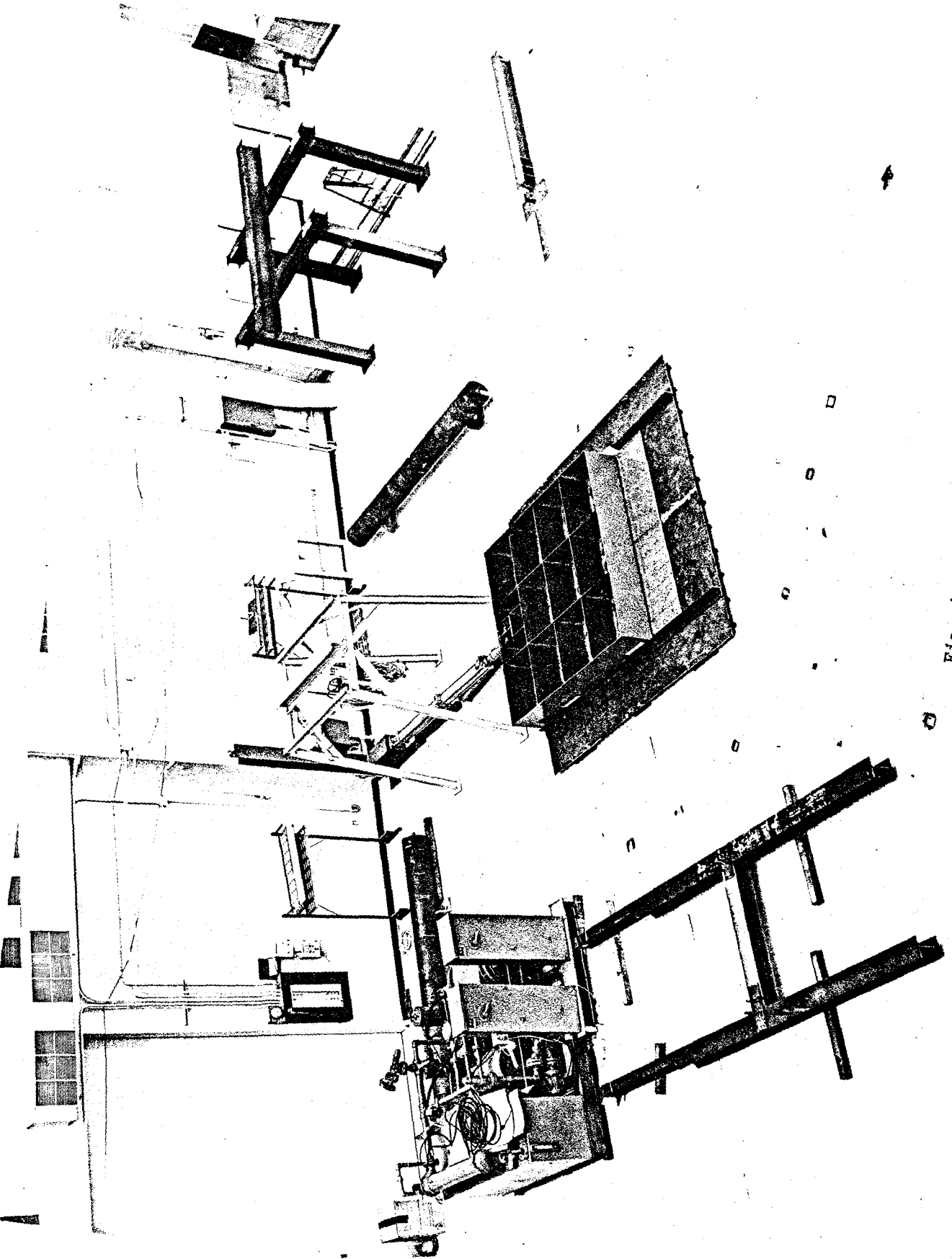


Fig. 49 Mock-Up of Test Set-Up, at Boeing Laboratory in Seattle (Photo by Boeing)

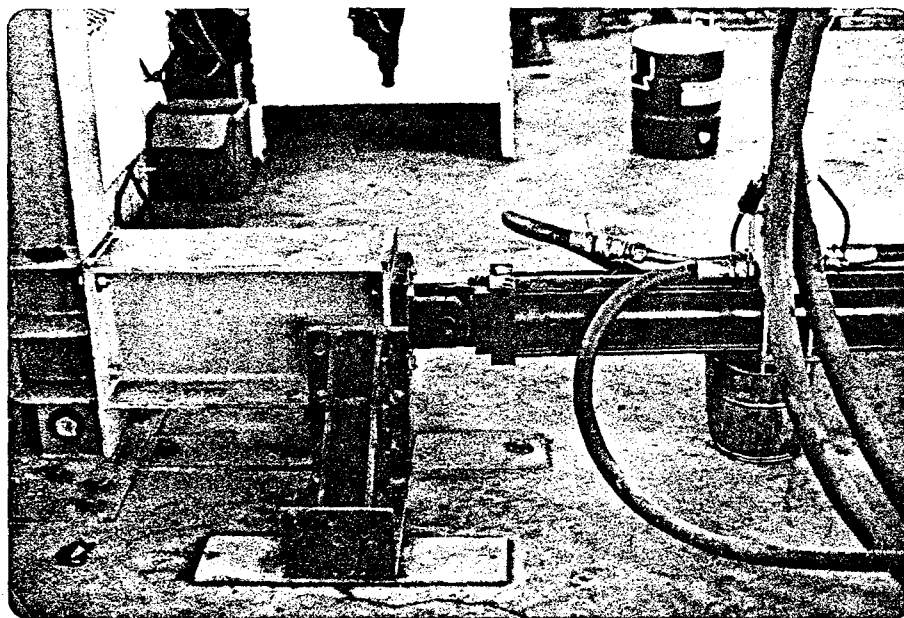


Fig. 50 Connection Between Reaction Column and Actuator

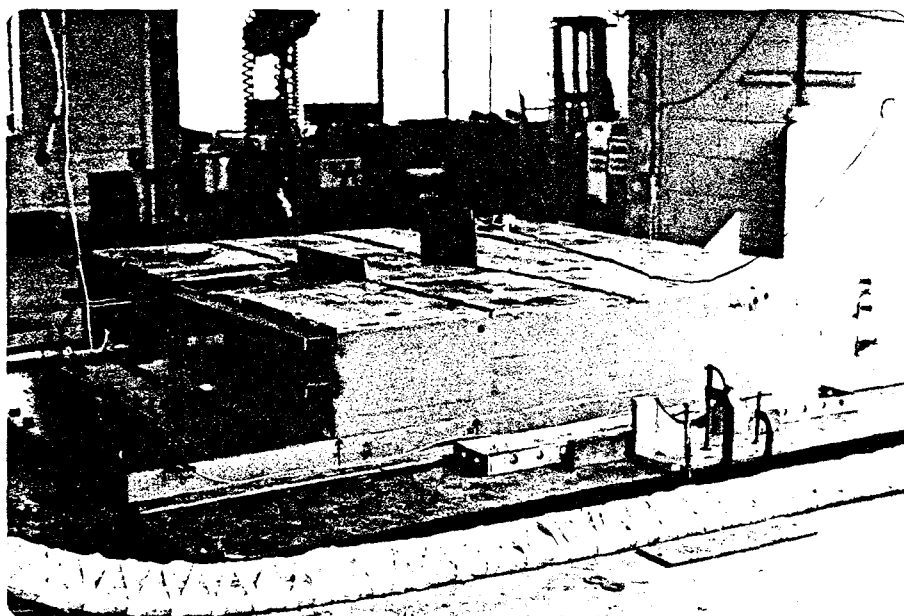


Fig. 51 Moving Mass Box, Fully Loaded with Lead

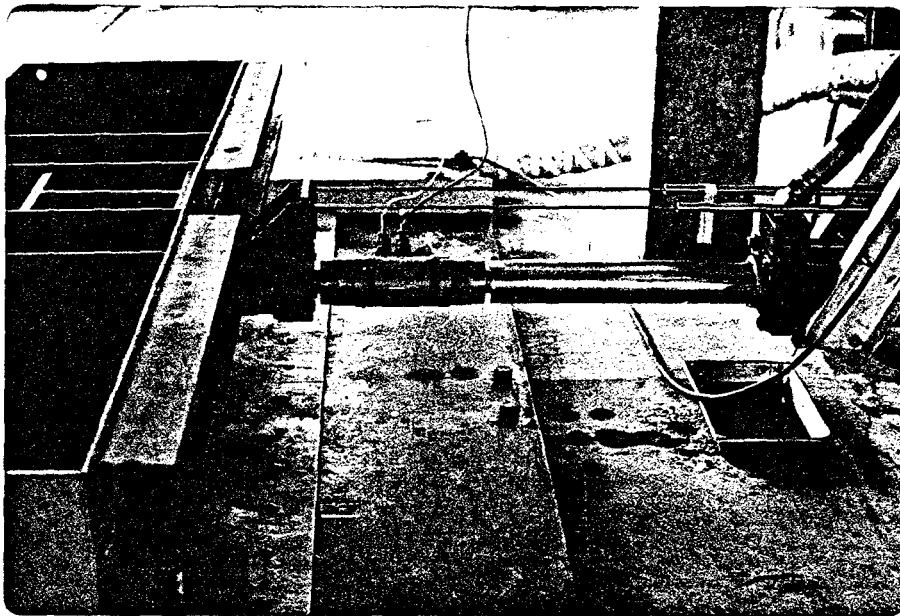


Fig. 52 Force Transducer and Piston

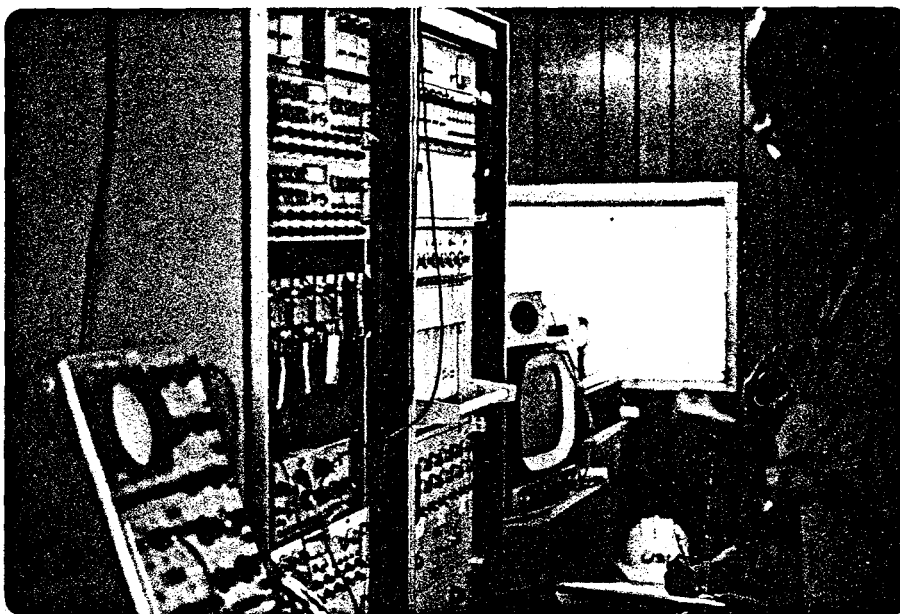


Fig. 53 Instrument Panel

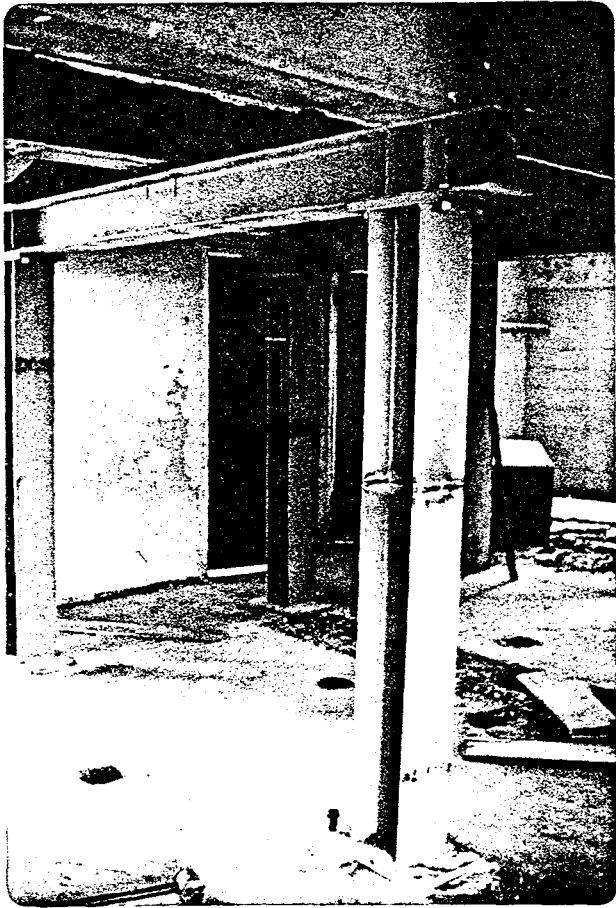


Fig. 54 Cribbing, 10 th
Floor



Fig. 55 Instrument Trailer

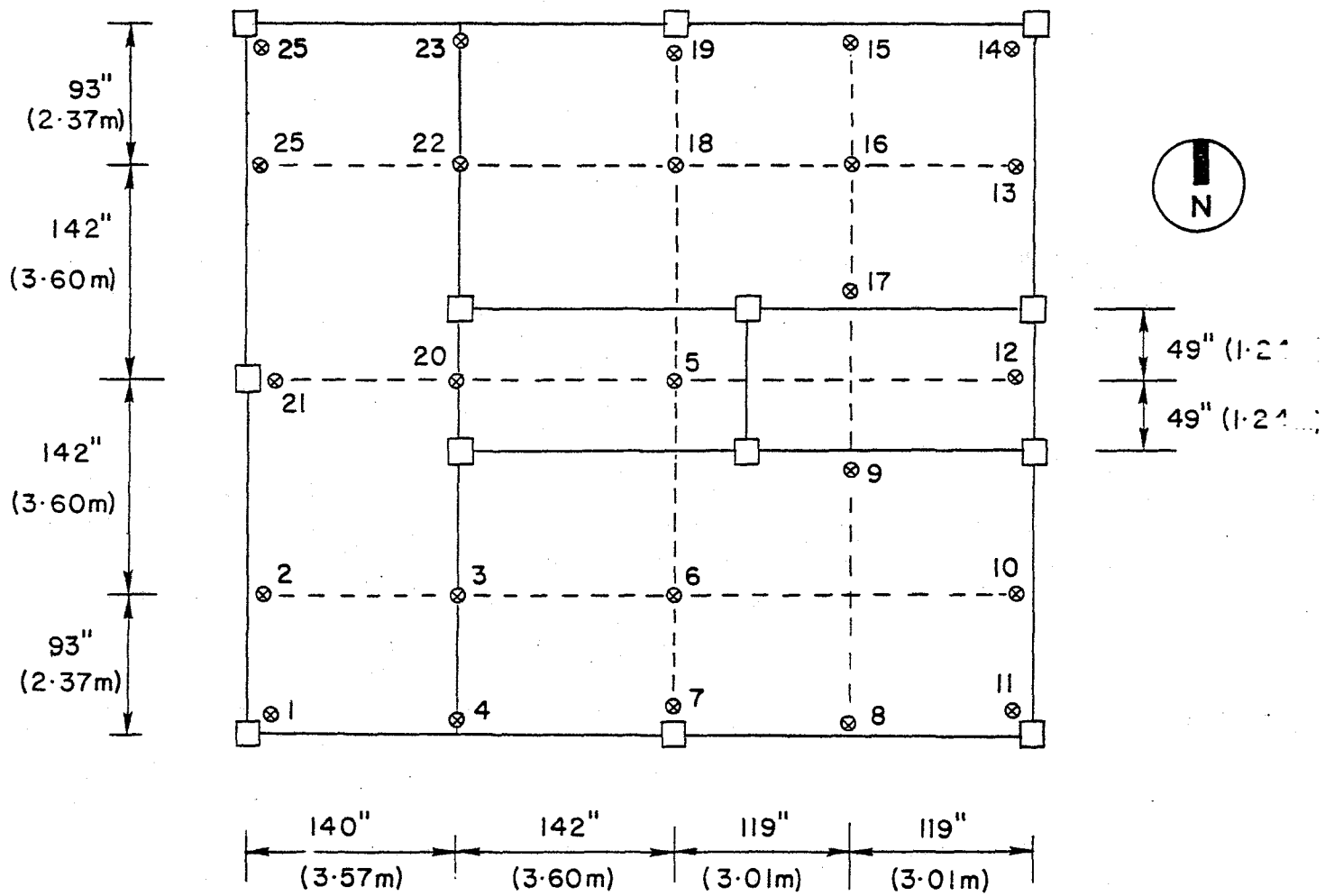


Fig. 56 Accelerometer Location Grid Pattern

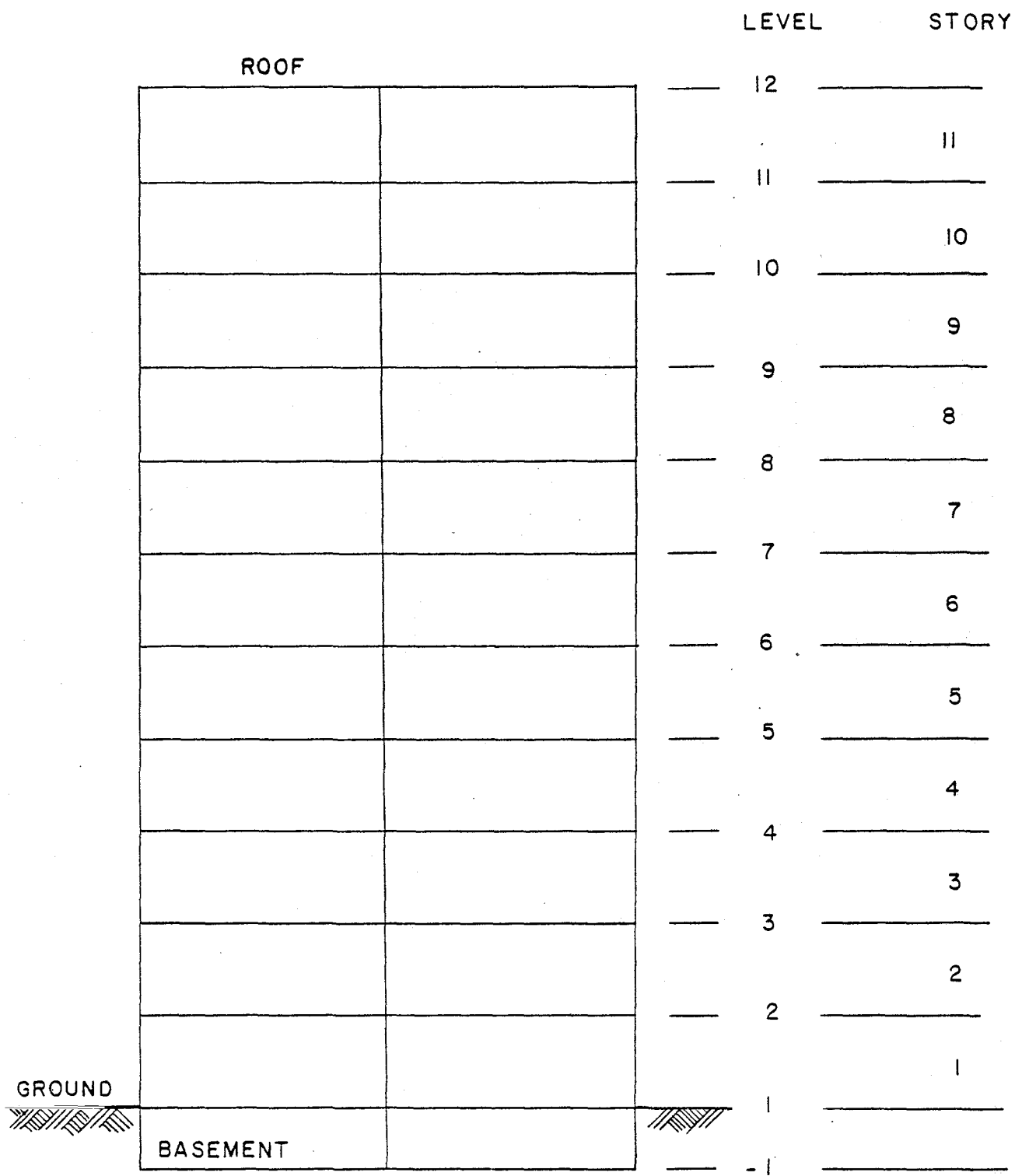


Fig. 57 Designation of Vertical Coordinates

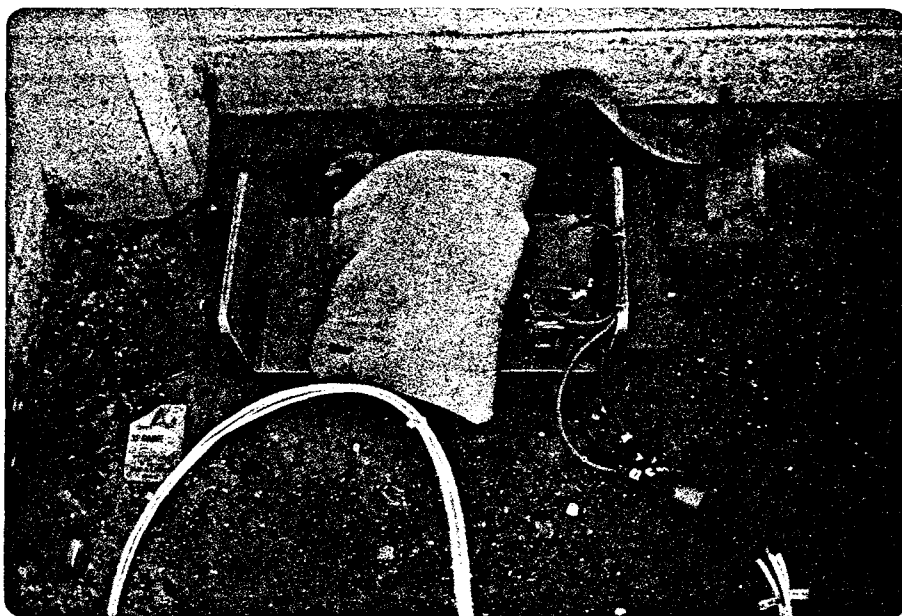
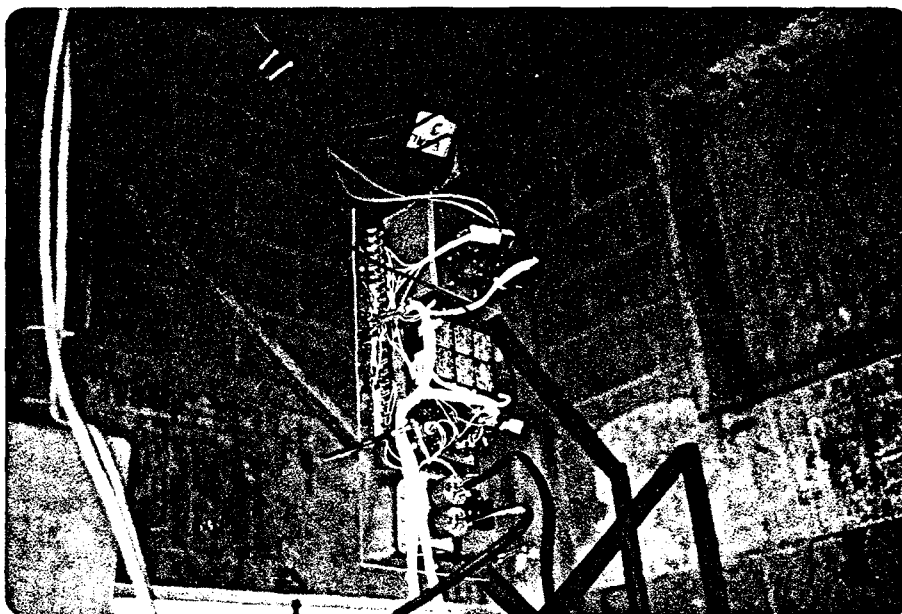


Fig. 58 Accelerometers



Reproduced from
best available copy.



Fig. 59 Multiplex Unit

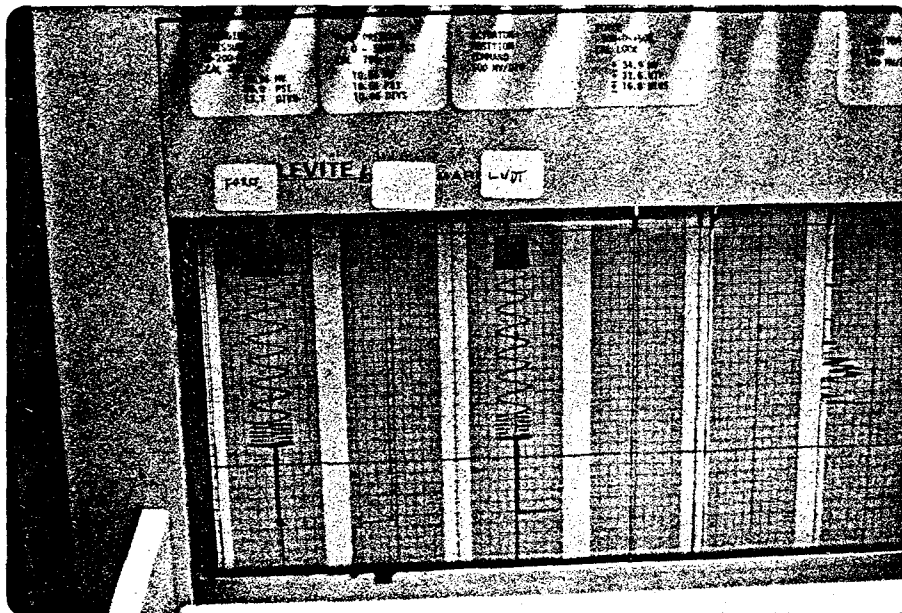


Fig. 60 Strip Chart Showing Force
and Motion of the Moving Mass

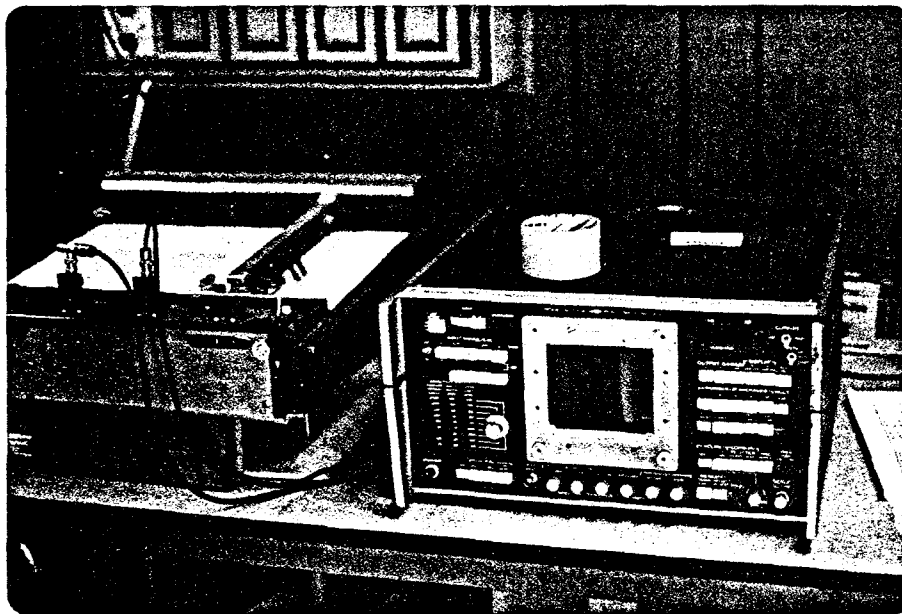


Fig. 61 Spectrum Analyzer

Reproduced from
best available copy.



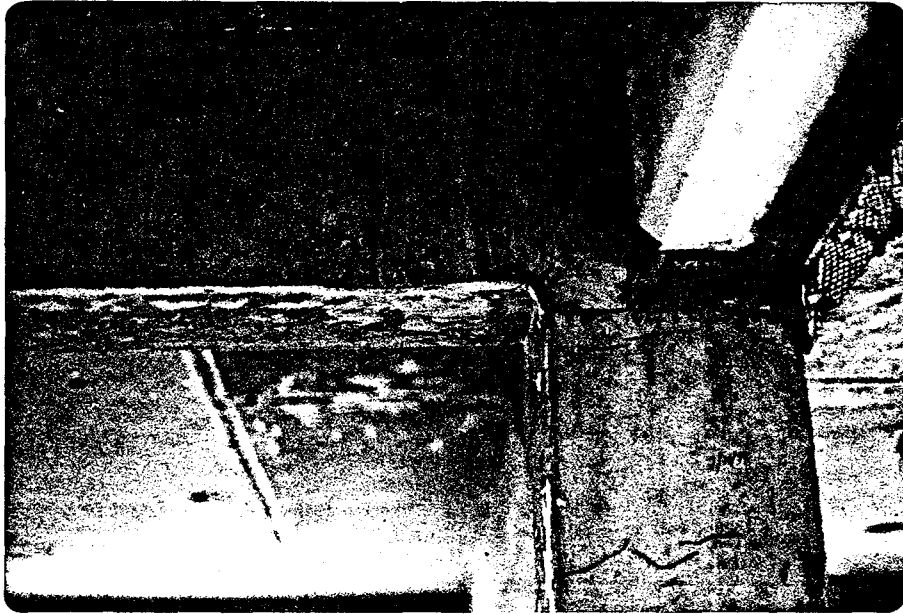
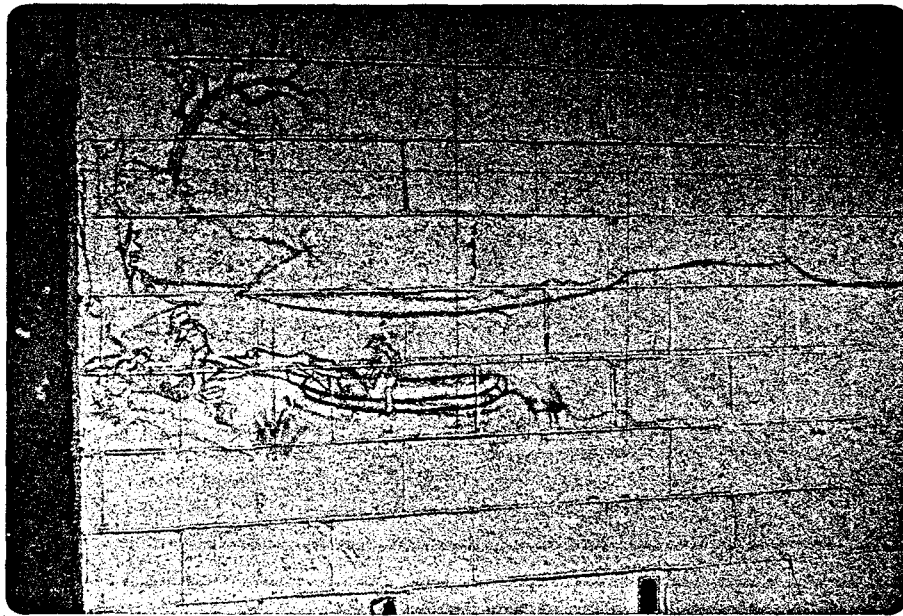


Fig. 62 Minor Cracks in Joint, Level 12, after Small Amplitude Shaking



Reproduced from
best available copy. 

Fig. 63 Damage in E.W. Wall After Small Amplitude Shaking

Reproduced from
best available copy.

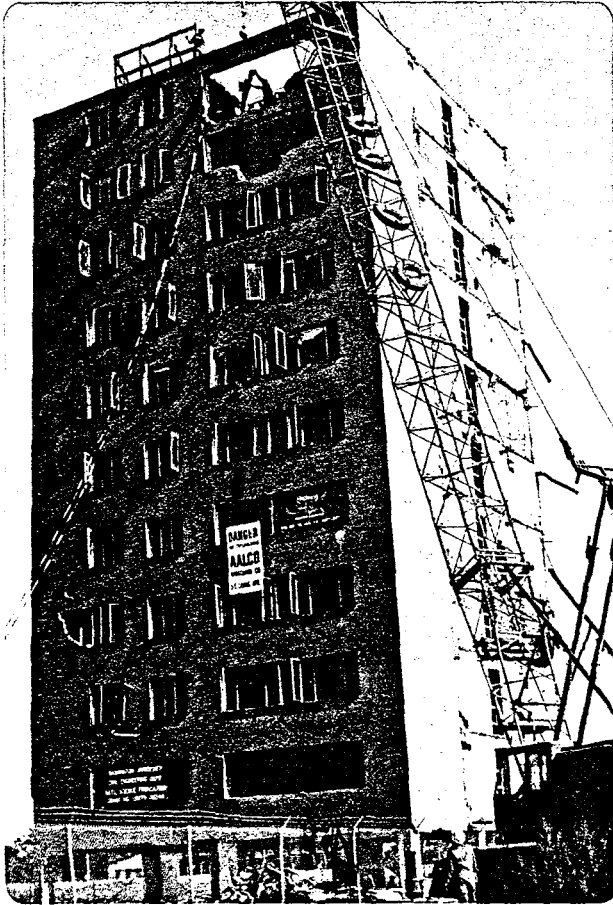


Fig. 64 View of Roof
Opening

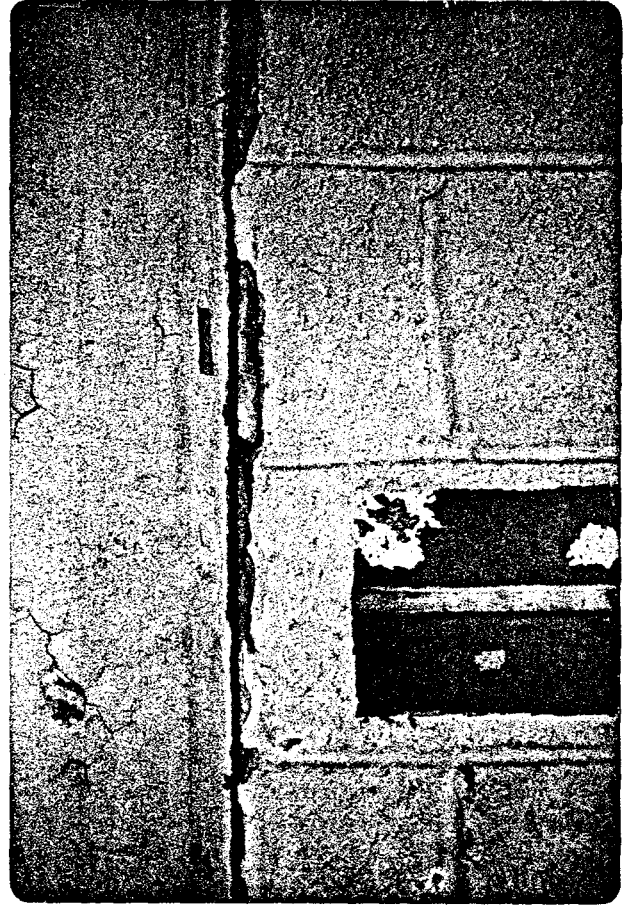
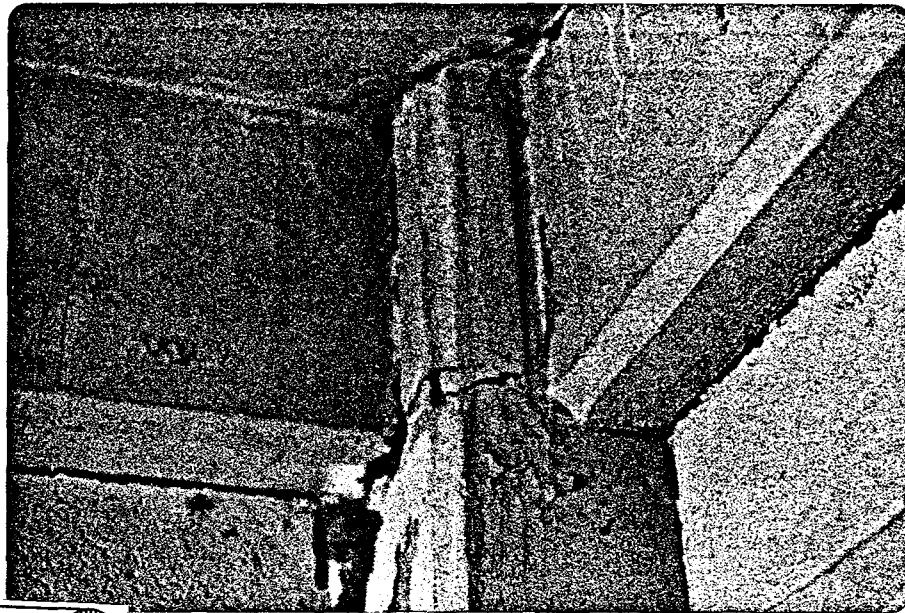


Fig. 65 Column Movement,
EW Stairway Wall,
during E.W. Shaking



Fig. 66 Cracked Joint, Col. 36,
Level 2, During E.W.
Tests



Reproduced from
best available copy. 

Fig. 67 Interior Joint, Col. 11,
Level 3, During E.W.
Tests

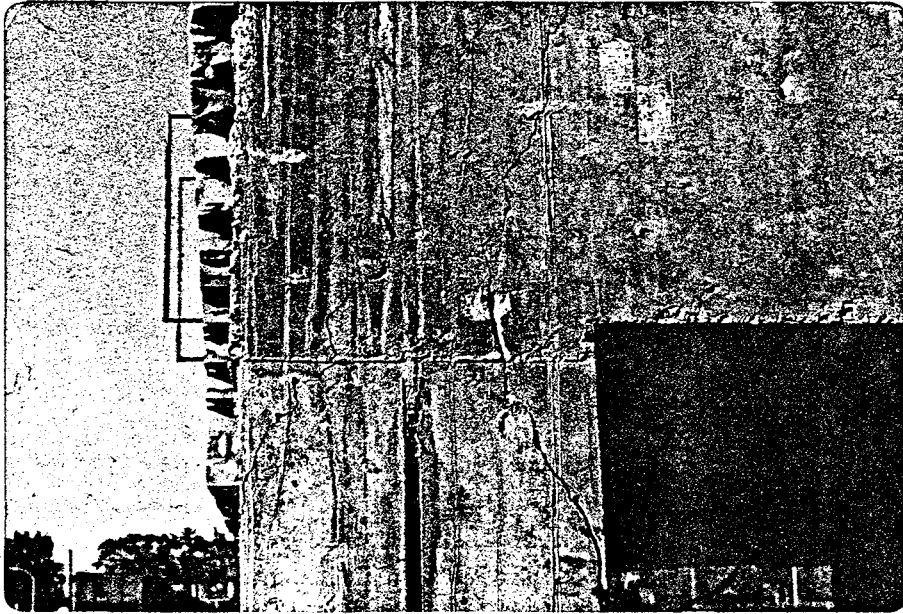


Fig. 68 Cracked Joint, South Face,
Col. 11, Level 2, During
E.W. Shaking



Reproduced from
best available copy.



Fig. 69 Crack at Column Face,
Level 2, Col. 13,
After E.W. Tests



Fig. 70 Top of Col. 37 in the Second
Story, After E.W. Shaking



Fig. 71 Beam-Column Joint Damage,
During E.W. Shaking

Reproduced from
best available copy.



Fig. 72 East End of Beam B-4 Level
2, After E.W. Shaking



Fig. 73 Fractured Reinforcing Bar,
East End of Beam B-4



Fig. 74 Exposed Reinforcing Bar,
After E.W. Shaking



Fig. 75 Stairway Joint Damage,
During E.W. Shaking

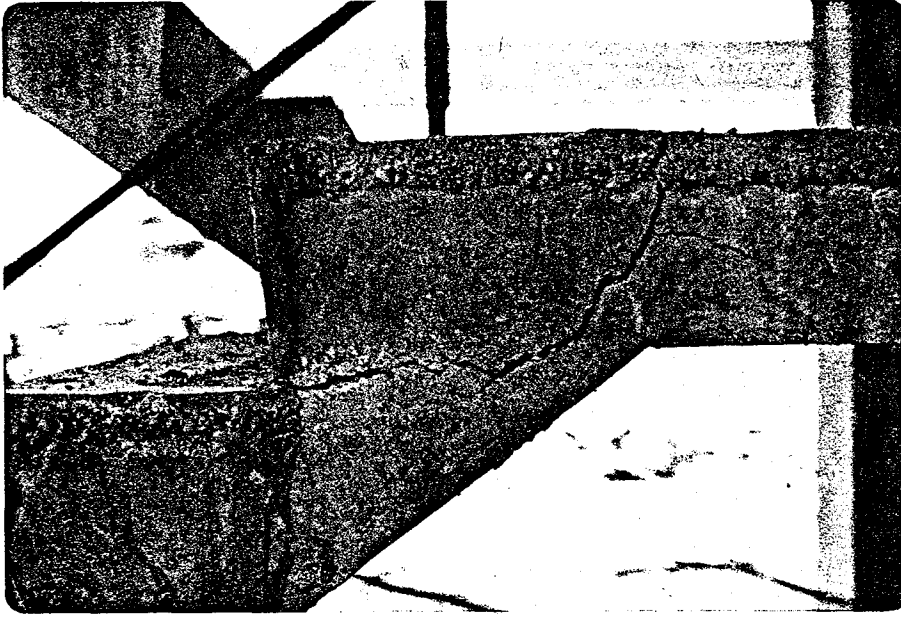


Fig. 76 Stairway Joint Damage,
After E.W. Shaking



Fig. 77 Stairway Joint Damage,
After E.W. Shaking

Reproduced from
best available copy. 



Fig. 78 Top of Stairway Joint,
After E.W. Testing



Fig. 79 Bottom of Stairway Joint,
After E.W. Testing

Reproduced from
best available copy.

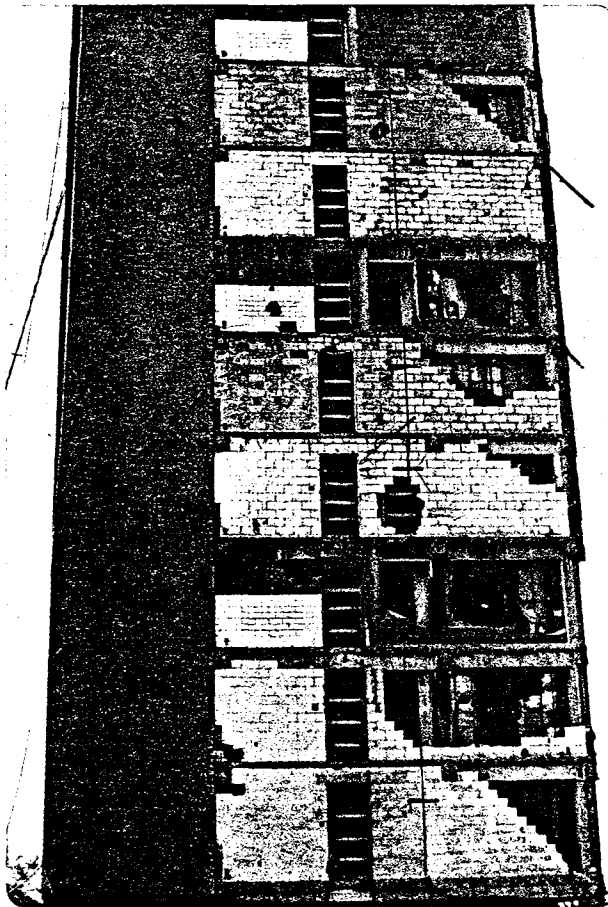


Fig. 80 East Wall, After
E.W. Shaking

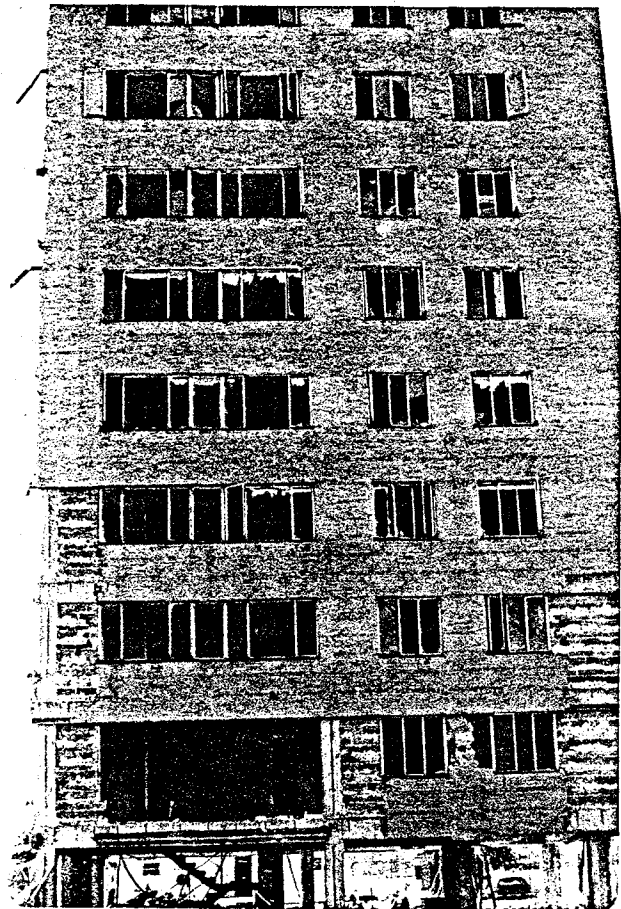


Fig. 81 N. Wall, After
E.W. Shaking

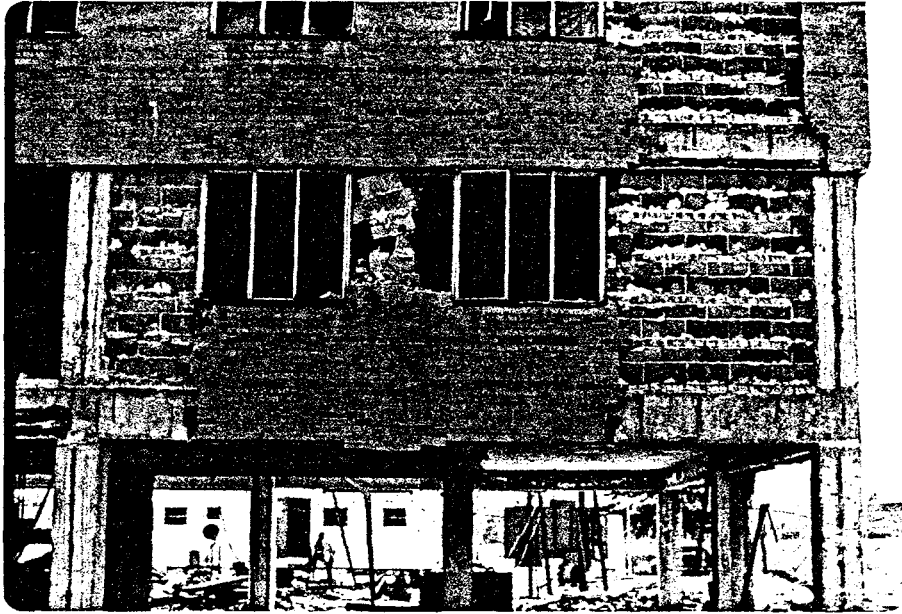


Fig. 82 N. Face After E.W. Shaking

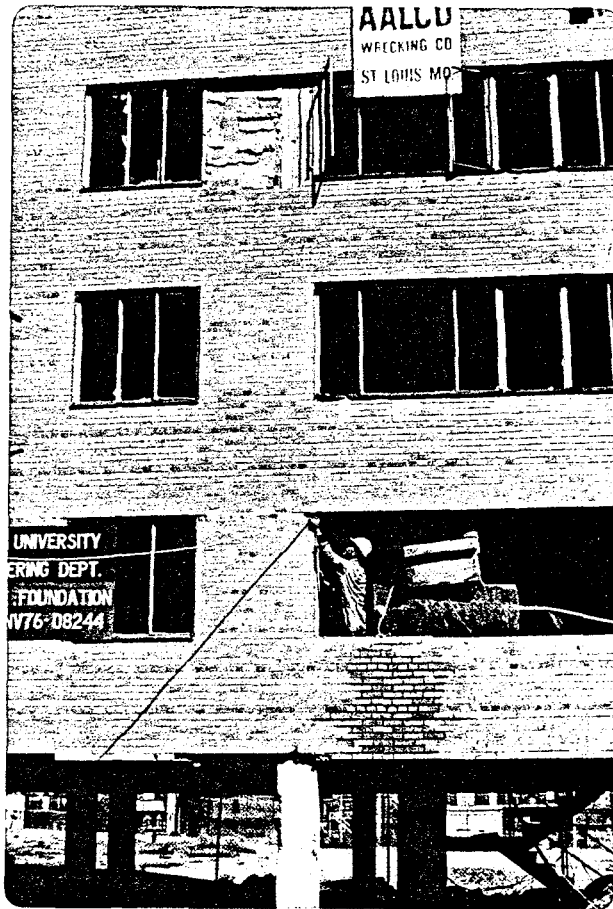


Fig. 83 S. Face, During E.W. Shaking

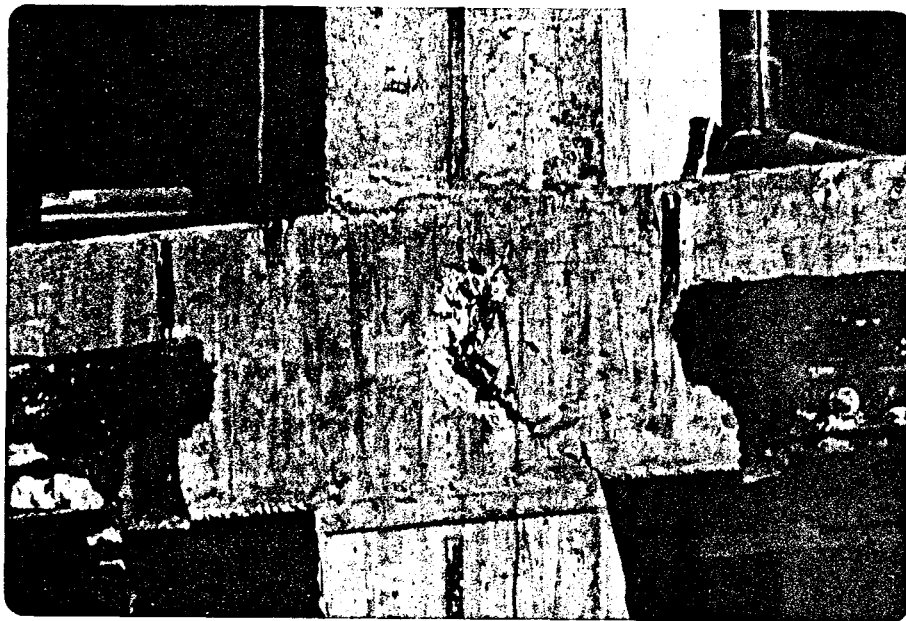


Fig. 84 Damage in Joint, Center
Column, West Face

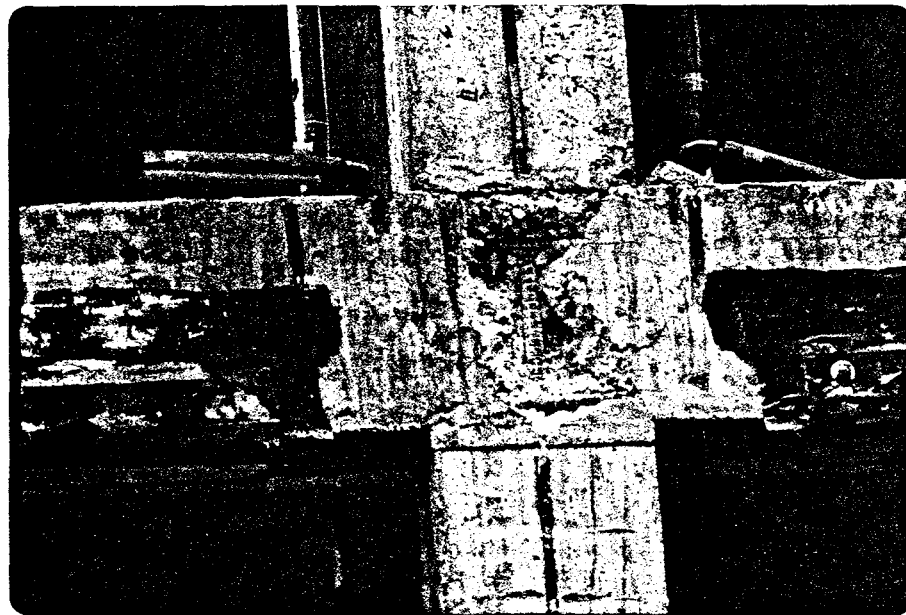


Fig. 85 Damage in Joint, Center
Column, West Face

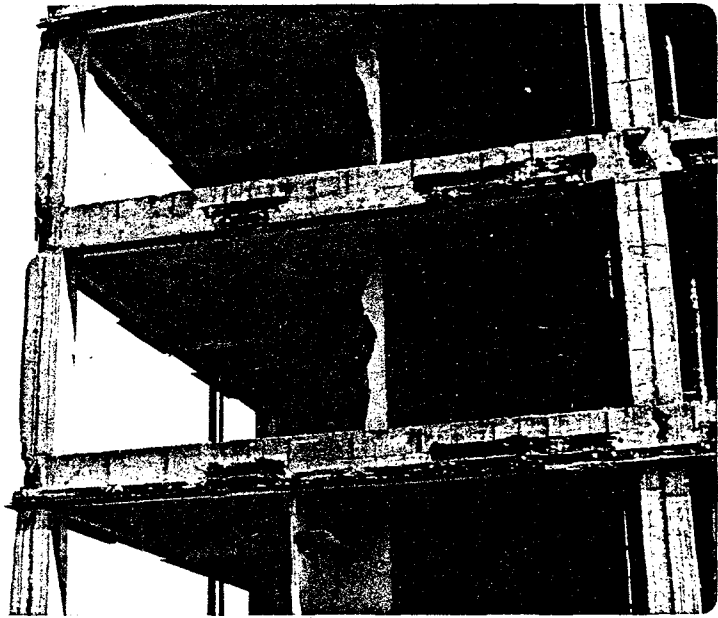


Fig. 86 N.W. Corner Column at
End of Testing

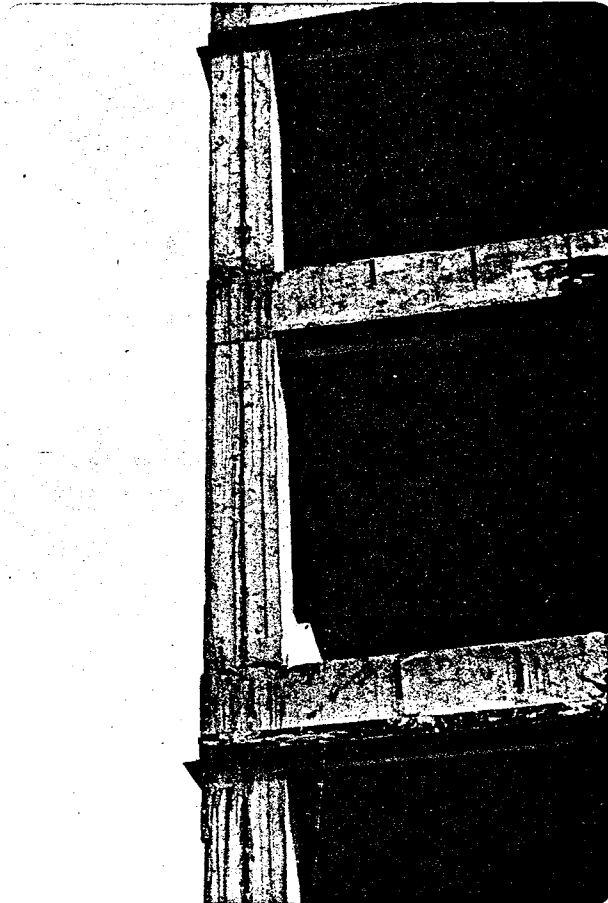


Fig. 87 Col. 9, Level 4,
N.S. Shaking

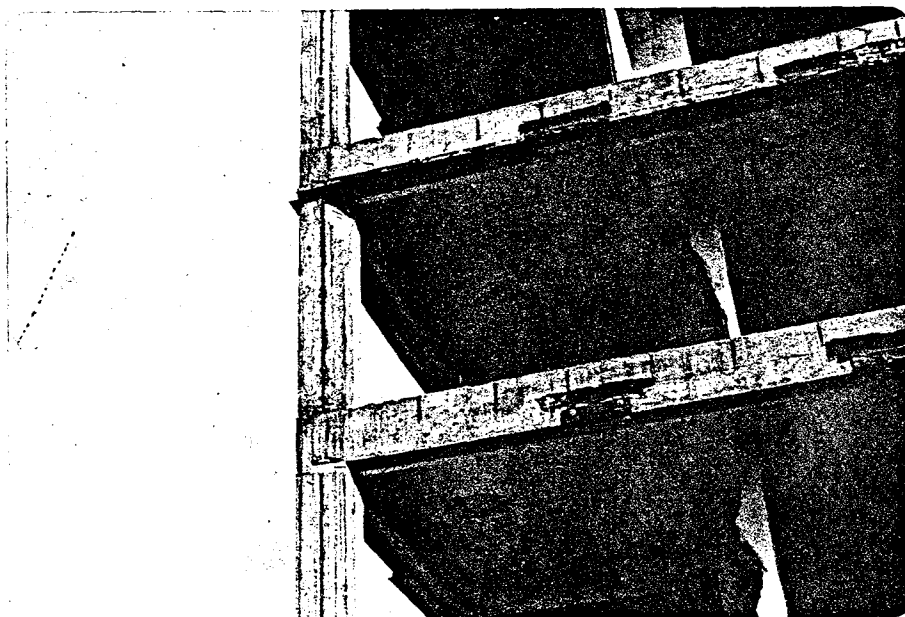


Fig. 88 Col. 9, Level 4

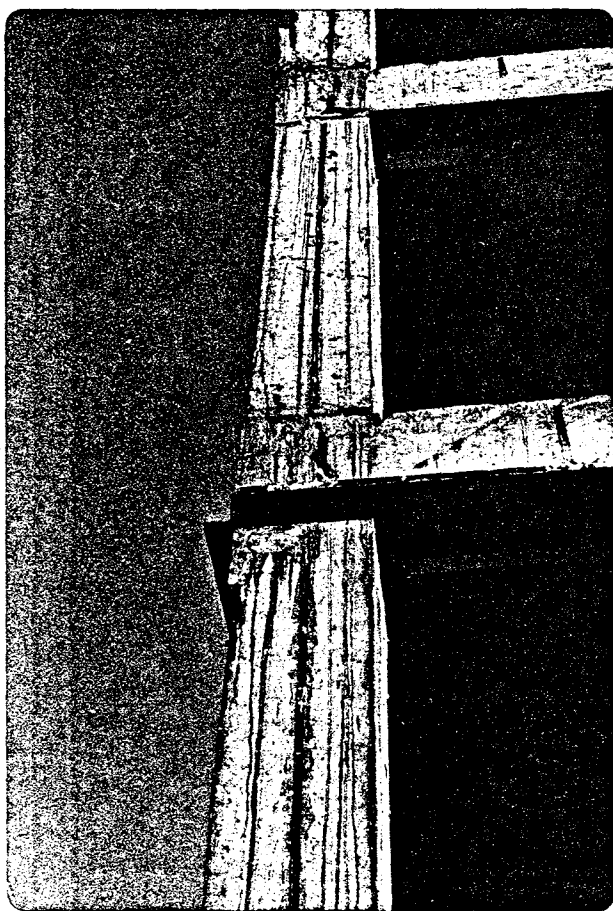


Fig. 89 Col. 9, Level 4

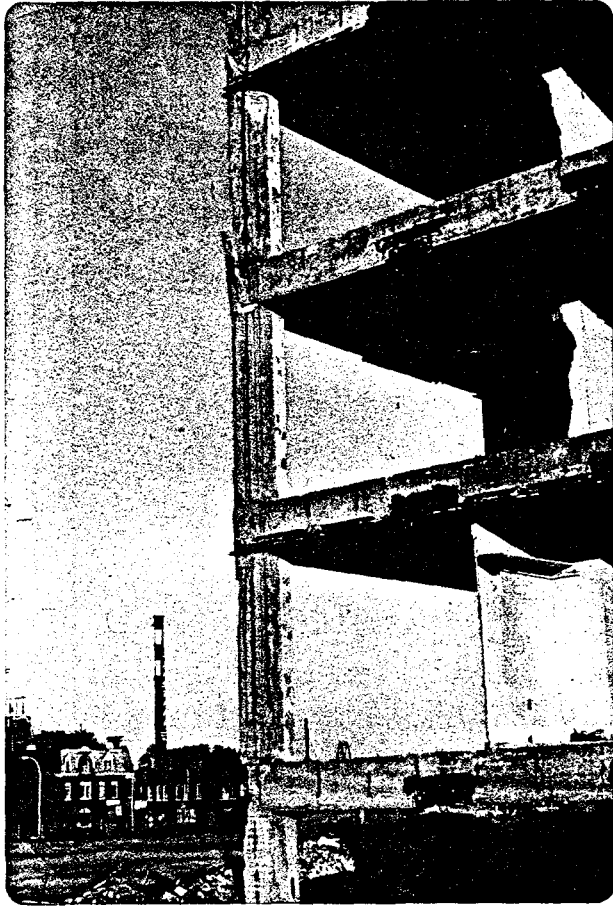


Fig. 90 Col. 9, Level 4

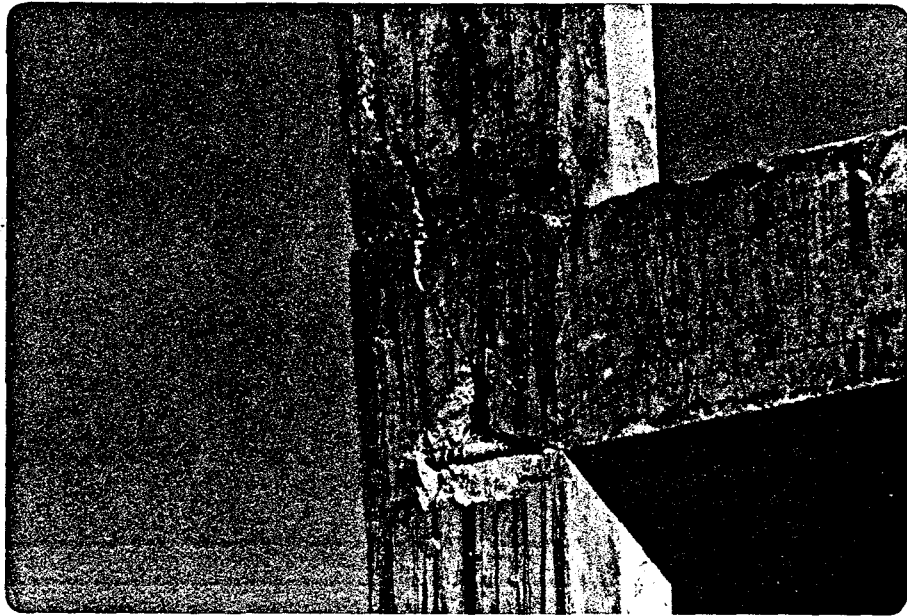


Fig. 91 Col. 9, Level 4

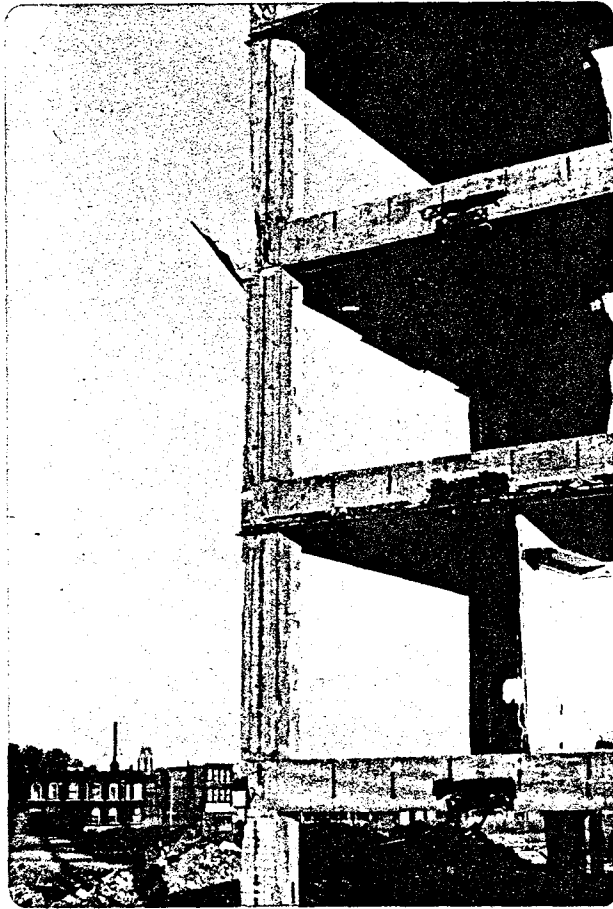


Fig. 92 Col. 9, Level 4

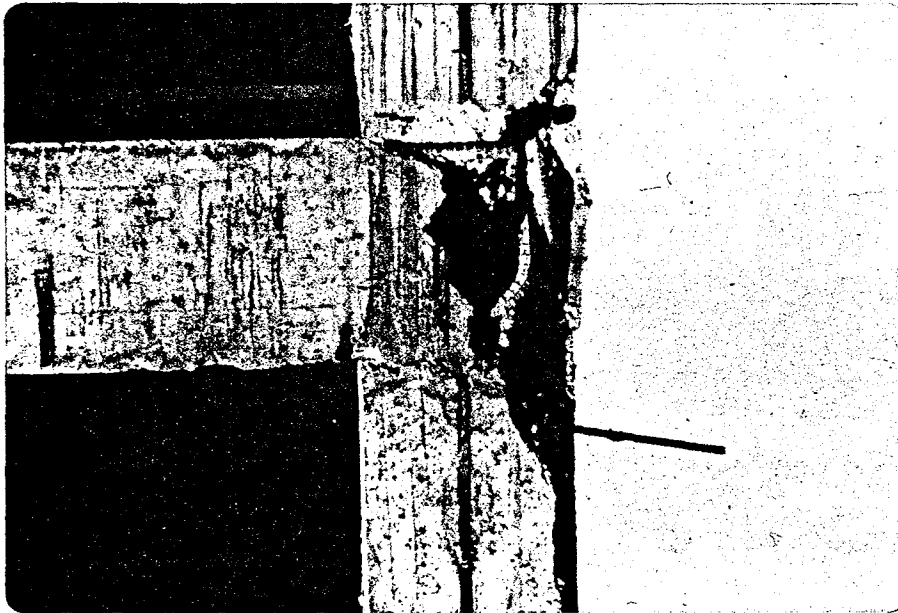


Fig. 93 Col. 9, Level 4

Reproduced from
best available copy.





Fig. 94 Col. 9, Level 4,
Interior Joint

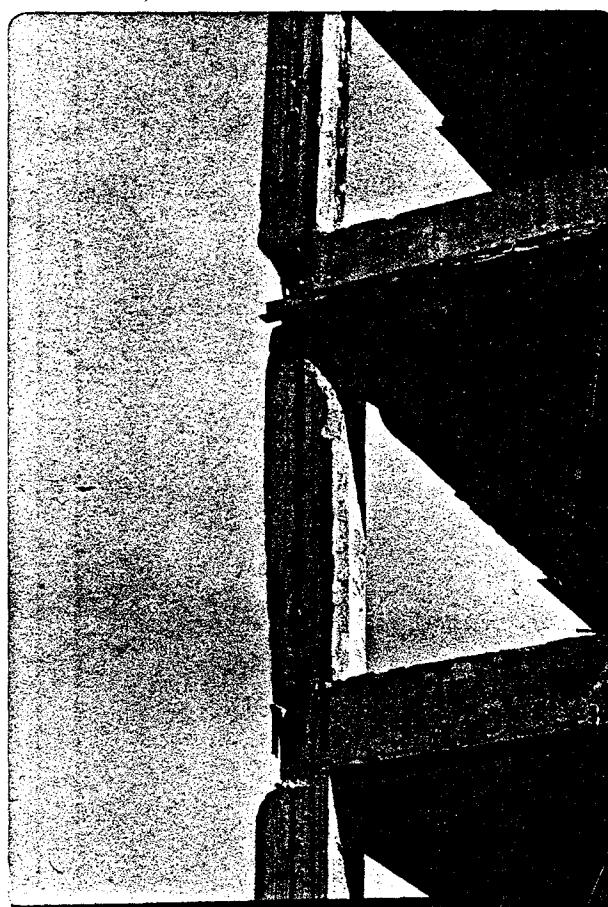


Fig. 95 Col. 9, Level 4



Fig. 96 Col. 38, 4th Floor
Prior to Last Shaking



Fig. 97 Col. 38, 4th Floor
After Completion of
Testing

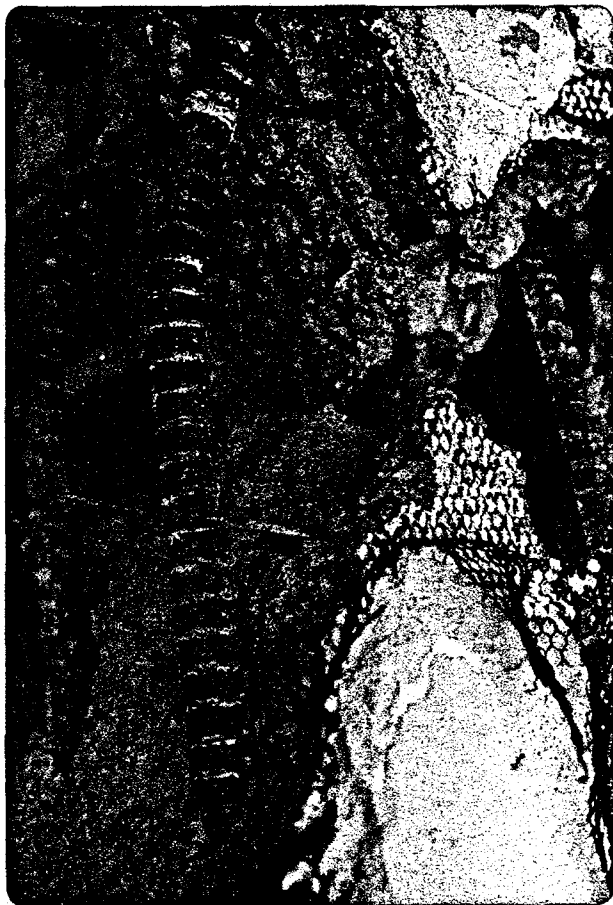


Fig. 98 Col. 38, 4th Floor,
After Testing

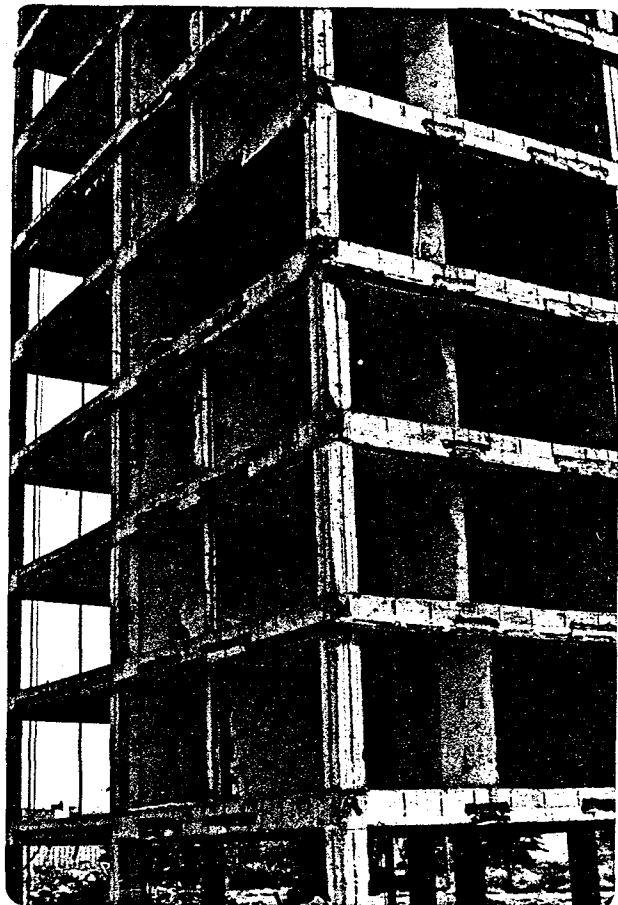


Fig. 99 Building Frame
After Testing

Reproduced from
best available copy. 

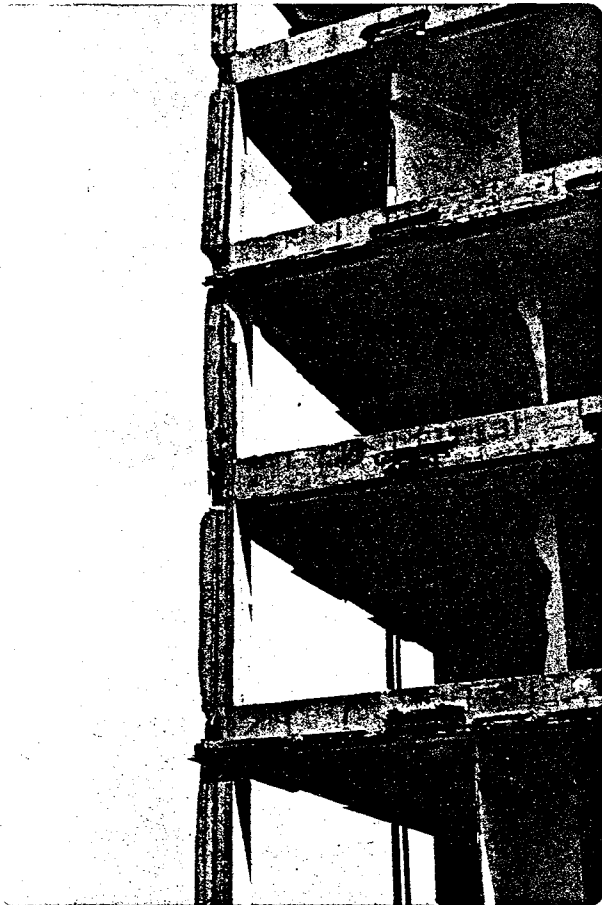


Fig. 100 N.W. Corner
After Testing

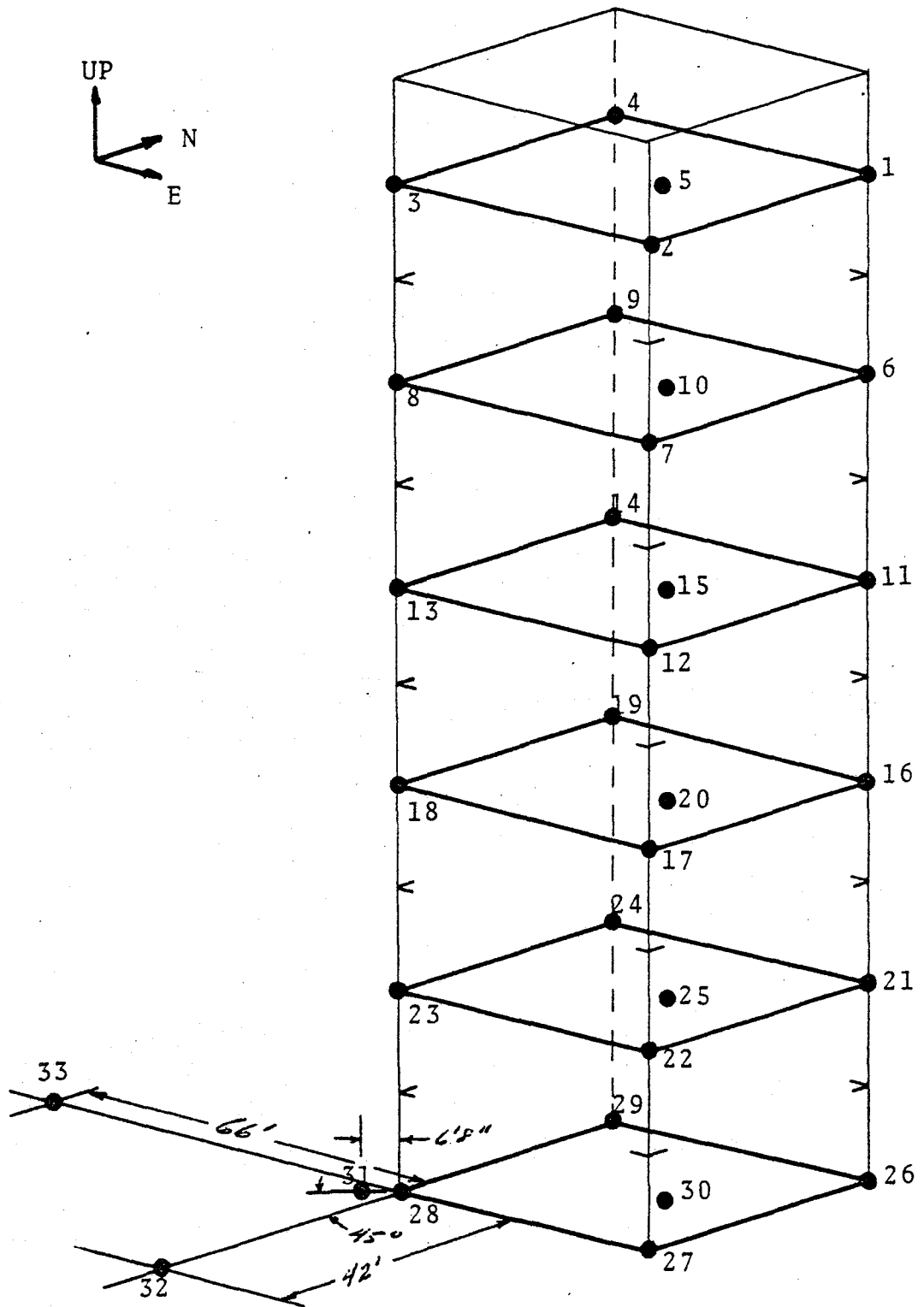
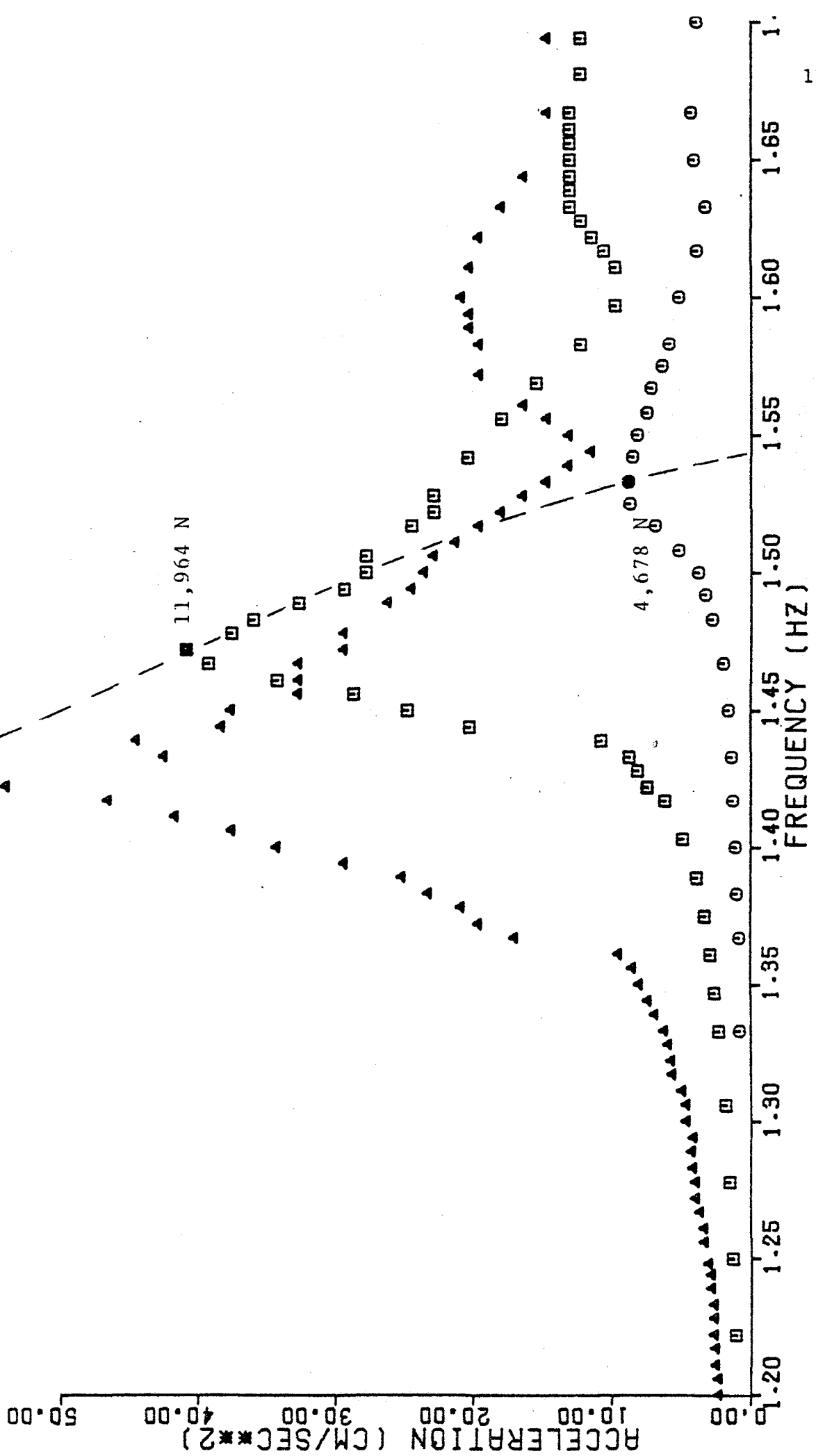


Fig. 101 Nodal Numbering Sequence
for Response Shapes Measured
in Small Amplitude Tests.

- CHANNEL NO. 4. TEST 1. RUN 1
- CHANNEL NO. 4. TEST 1. RUN 2
- ▲ CHANNEL NO. 4. TEST 7. RUN 2

Fig. 102 E-W Resonant Frequency Trends at Various Force Levels (Small Amplitude Shaking).



- CHANNEL NO. 3. TEST 1. RUN 1
- CHANNEL NO. 3. TEST 1. RUN 2
- ▲ CHANNEL NO. 3. TEST 7. RUN 2

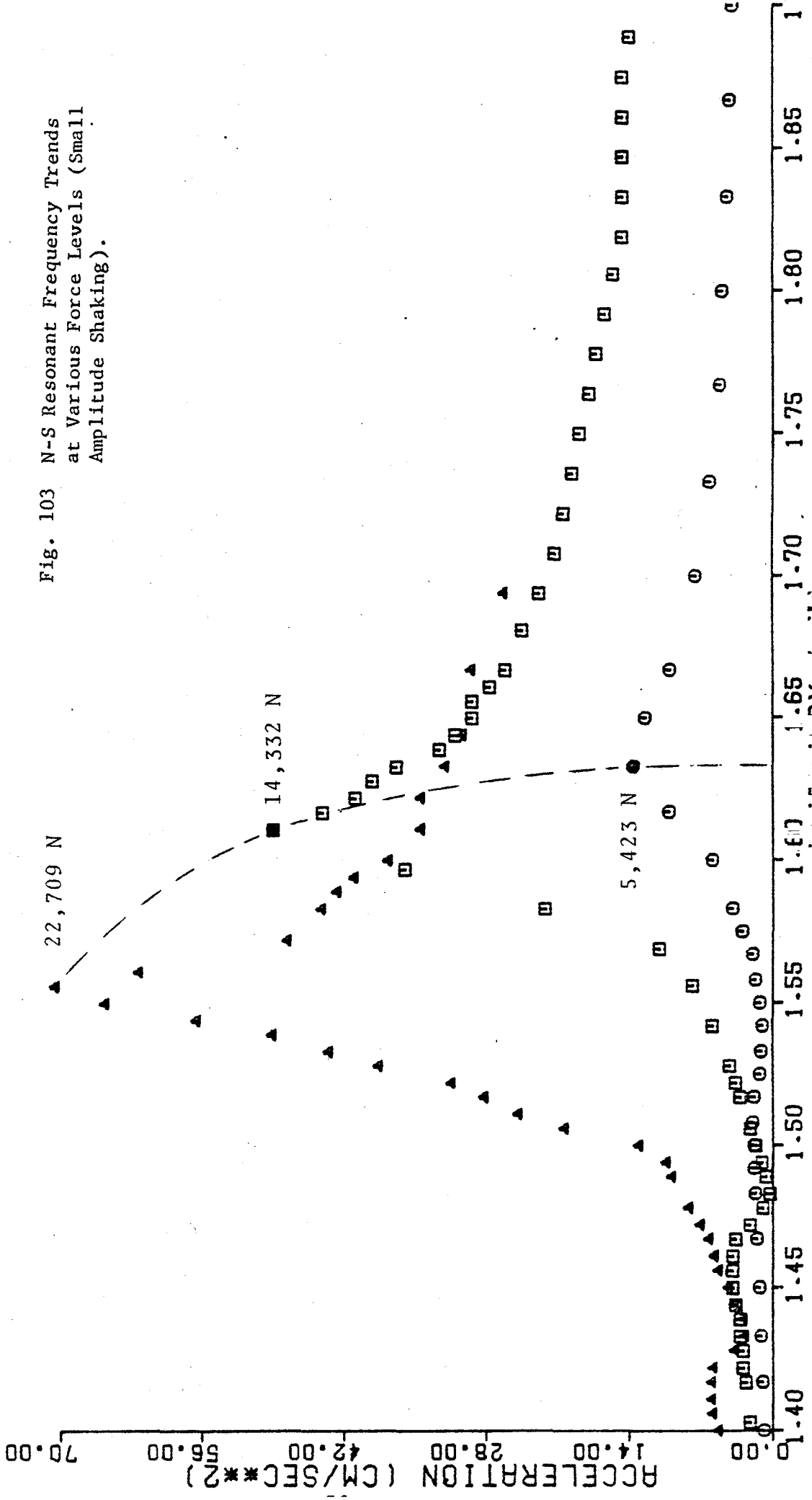
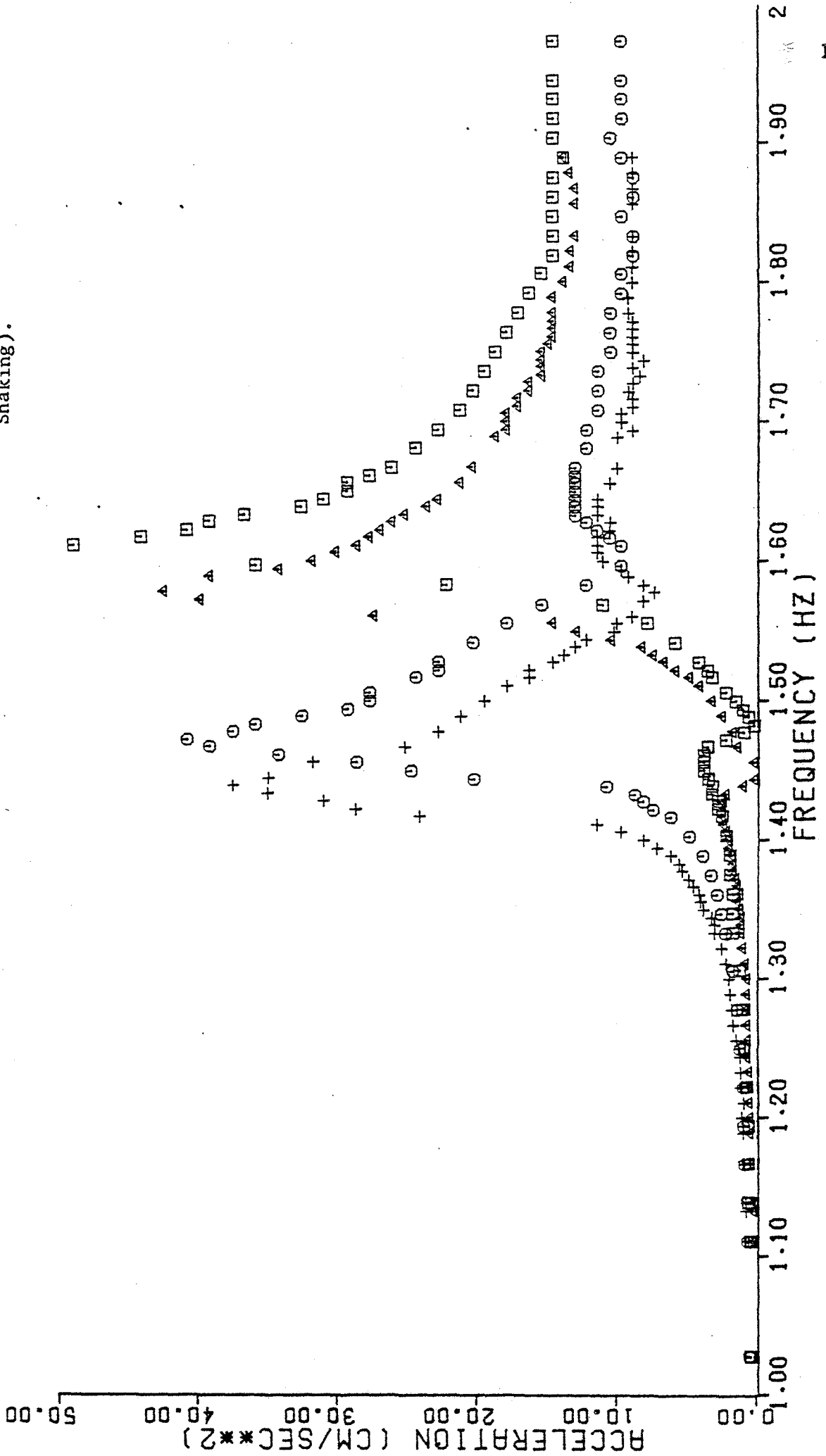


Fig. 103 N-S Resonant Frequency Trends at Various Force Levels (Small Amplitude Shaking).

- CHANNEL NO. 3. TEST 1. RUN 1
- CHANNEL NO. 4. TEST 1. RUN 1
- △ CHANNEL NO. 3. TEST 7. RUN 1
- + CHANNEL NO. 4. TEST 7. RUN 1

Fig. 104 E-W and N-S First Mode
Resonant Frequency Trends
over Time (Small Amplitude
Shaking).



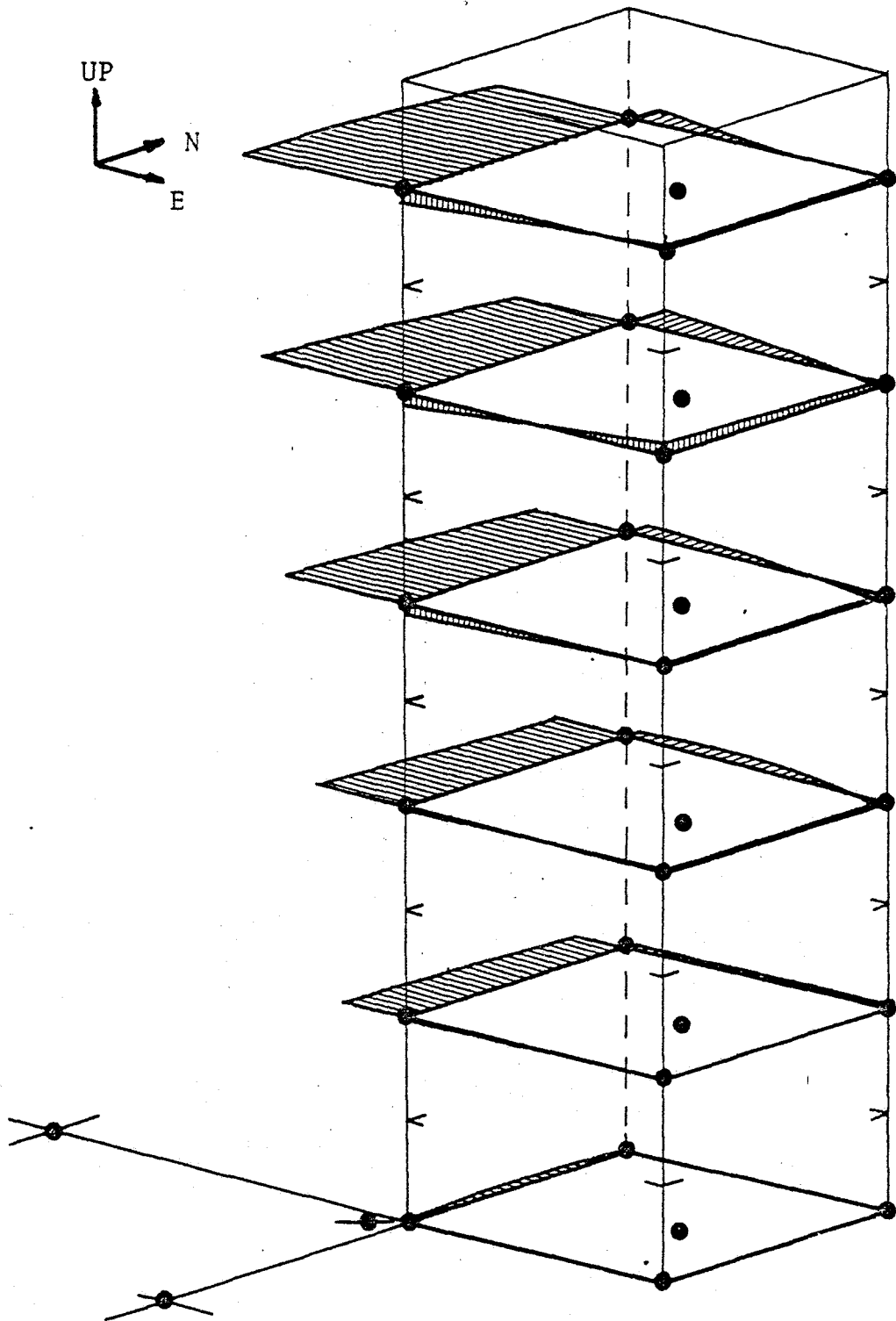


Fig. 105. Response Shape at 1.51 Hz
(Small Amplitude Tests).

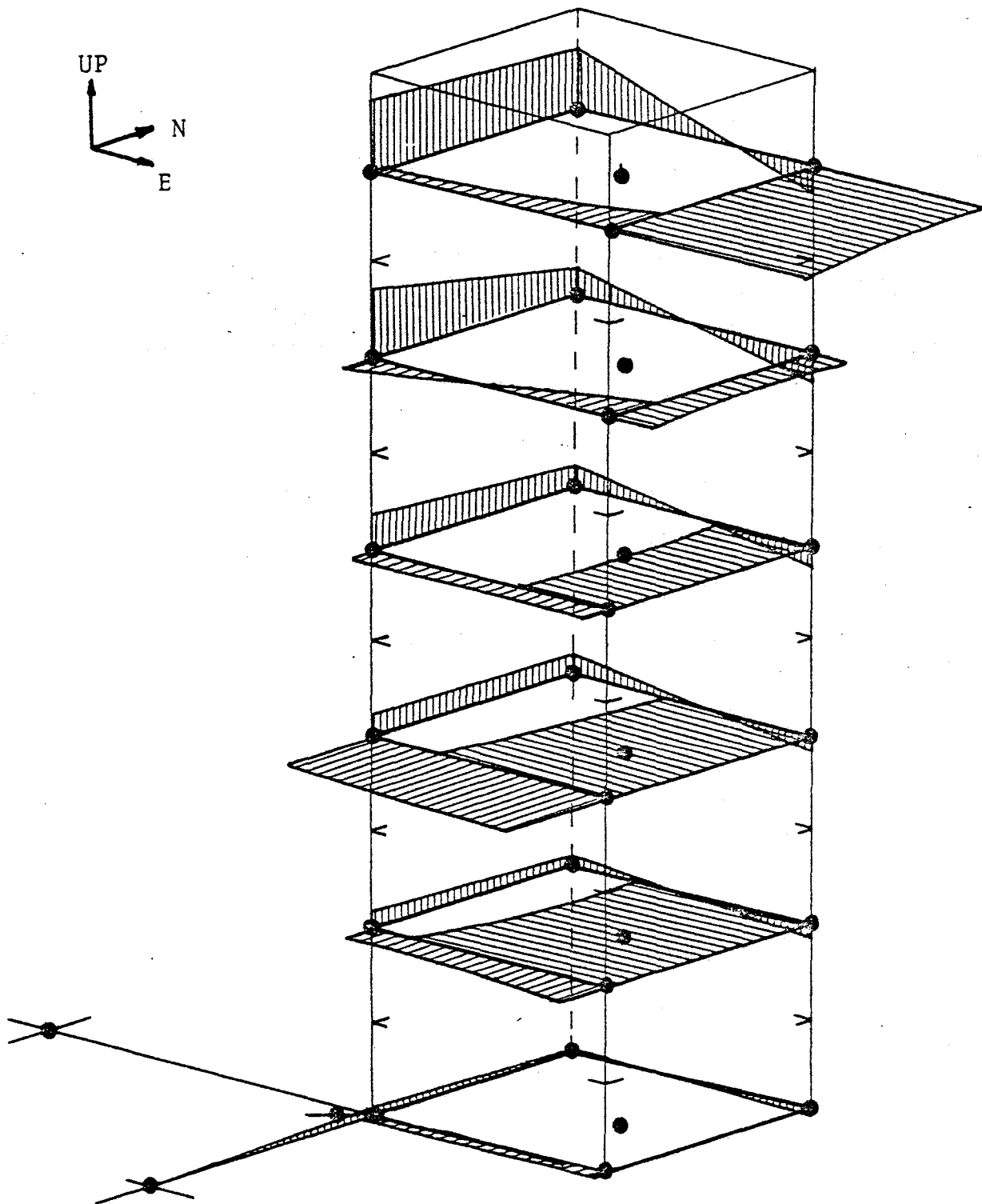


Fig. 106 Response Shape at 4.7 Hz
(Small Amplitude Tests)

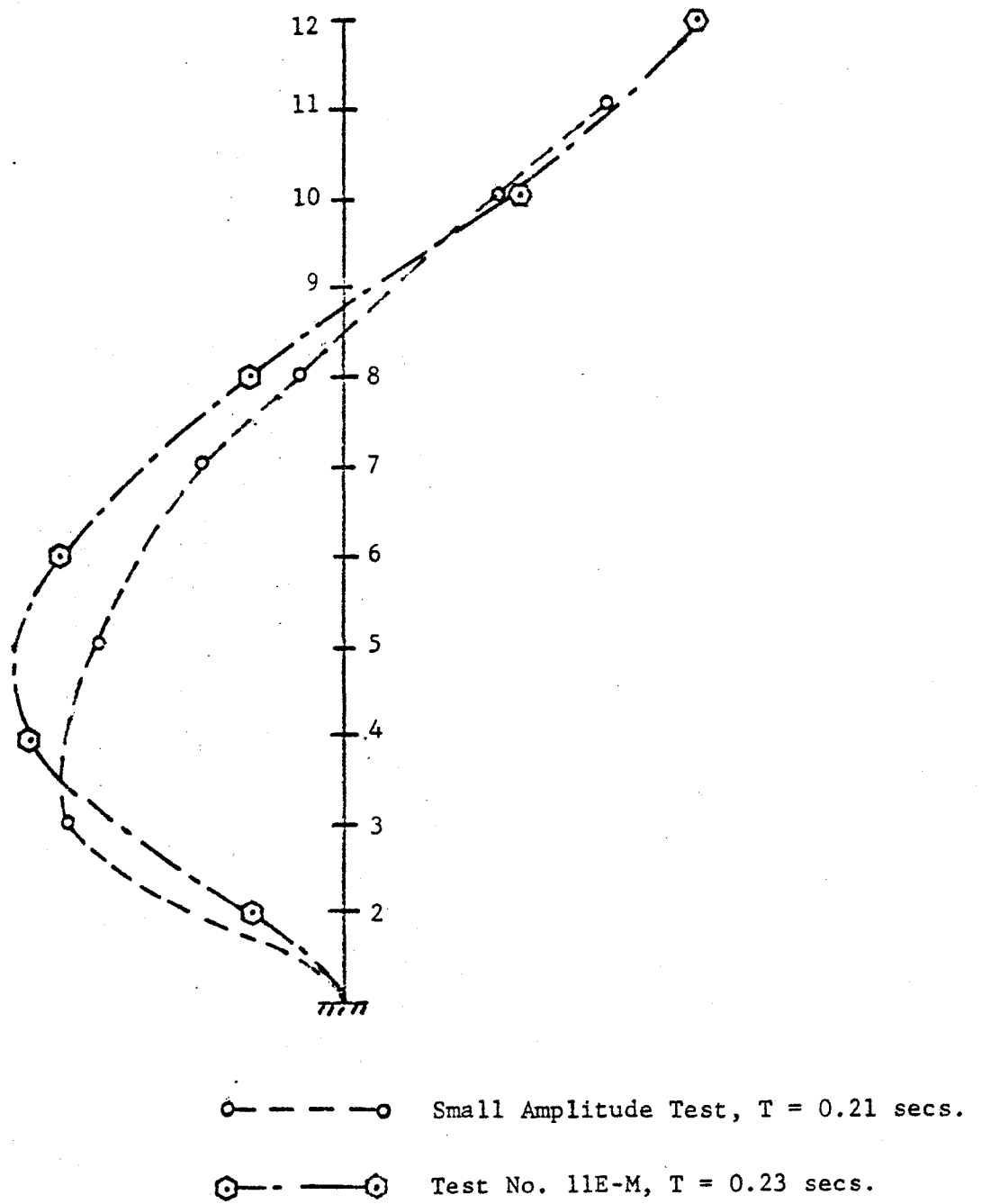


Fig. 107 Comparison of Small and Large Amplitude Mode Shapes - Second EW Translational Mode.

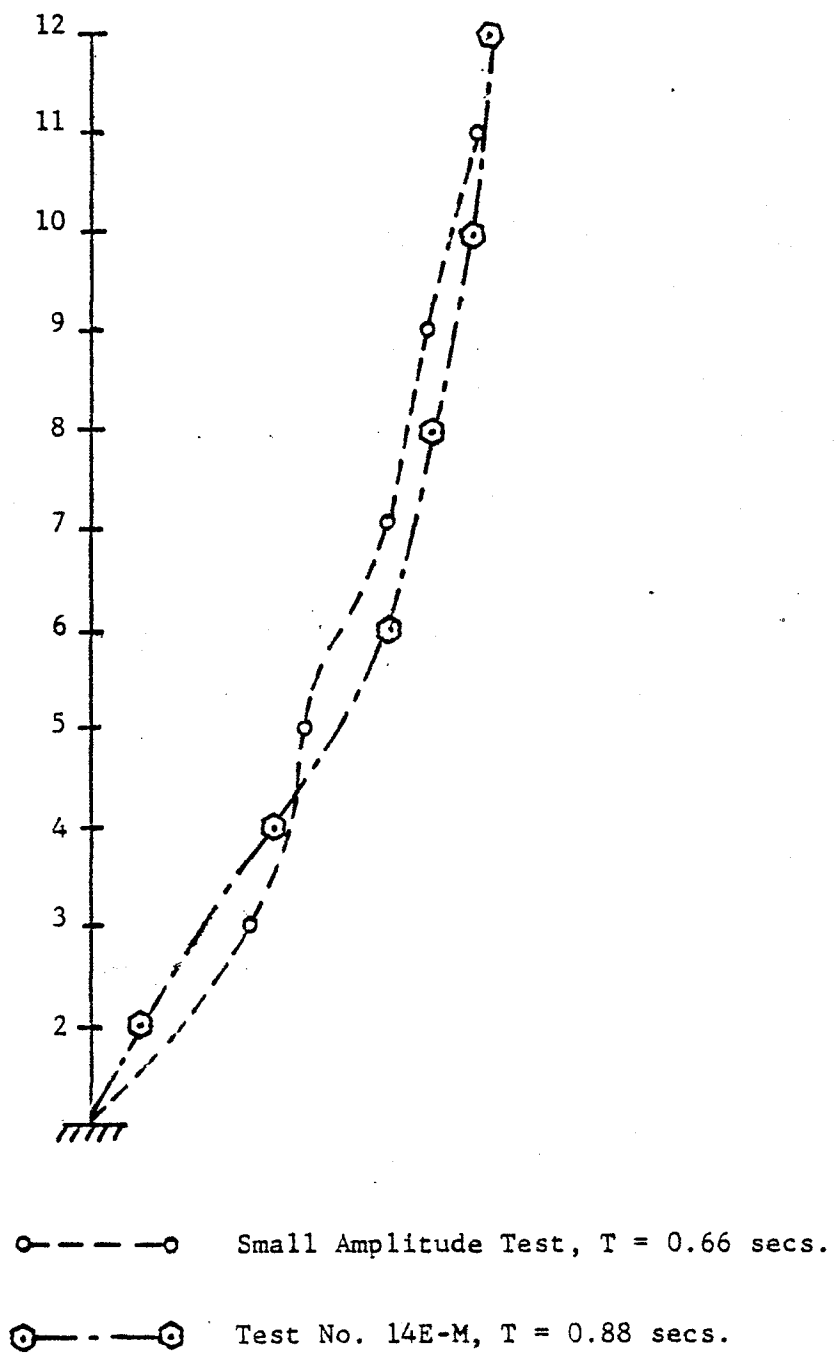
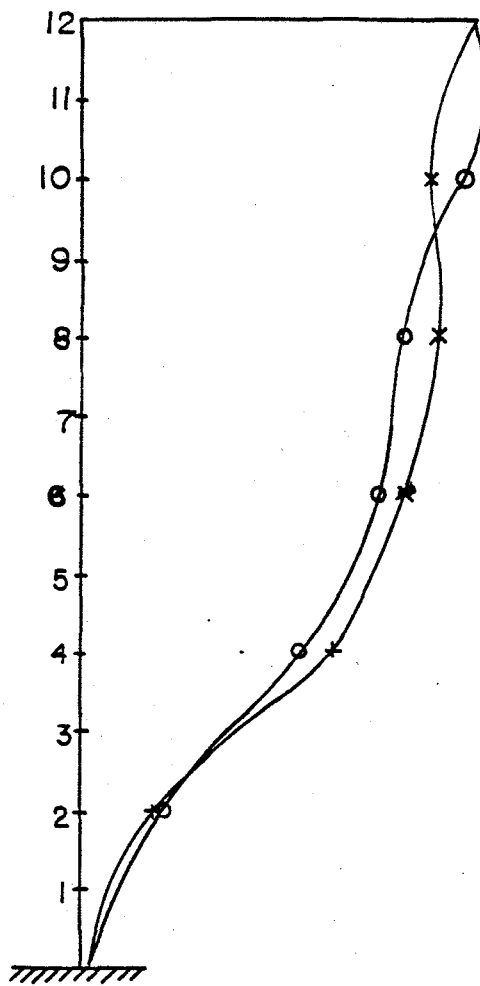


Fig. 108 Comparison of Small and Large Amplitude Mode Shapes - First EW Translational Mode.



—○—○— Experimental, $T=0.88$, Test No. 14 E-M
 —×—×— Experimental, $T=1.85$, Test No. 28 E-M

Fig. 109 Experimental Mode Shapes for the First Translational Mode, EW Tests, Large Amplitude Tests

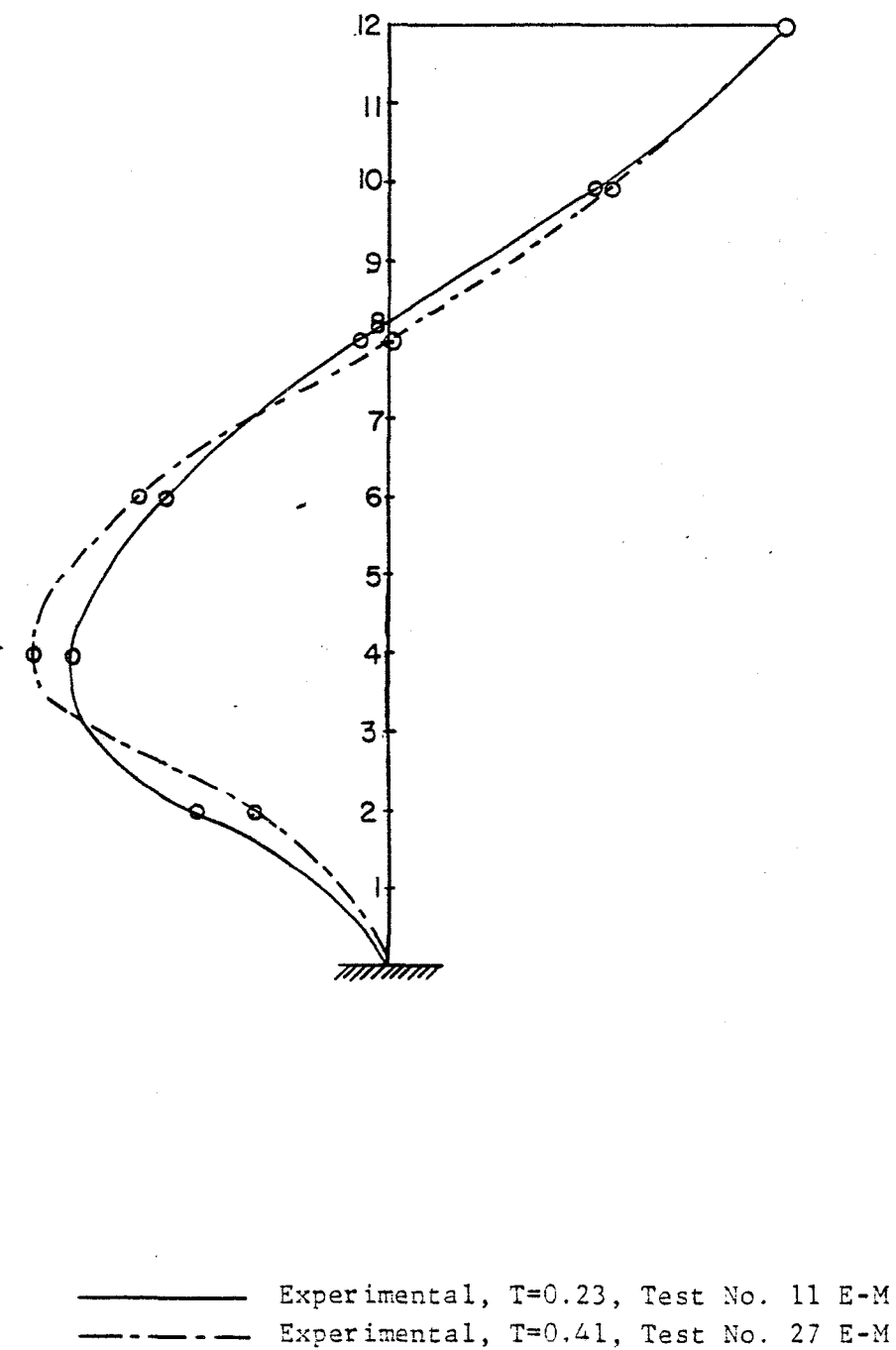


Fig. 110 Experimental Mode Shapes for the Second Translational EW Mode, Large Amplitude Tests

Test 5N-M; T=1.22 sec ————
Test 32N-M; T=2.5 sec - - - - -

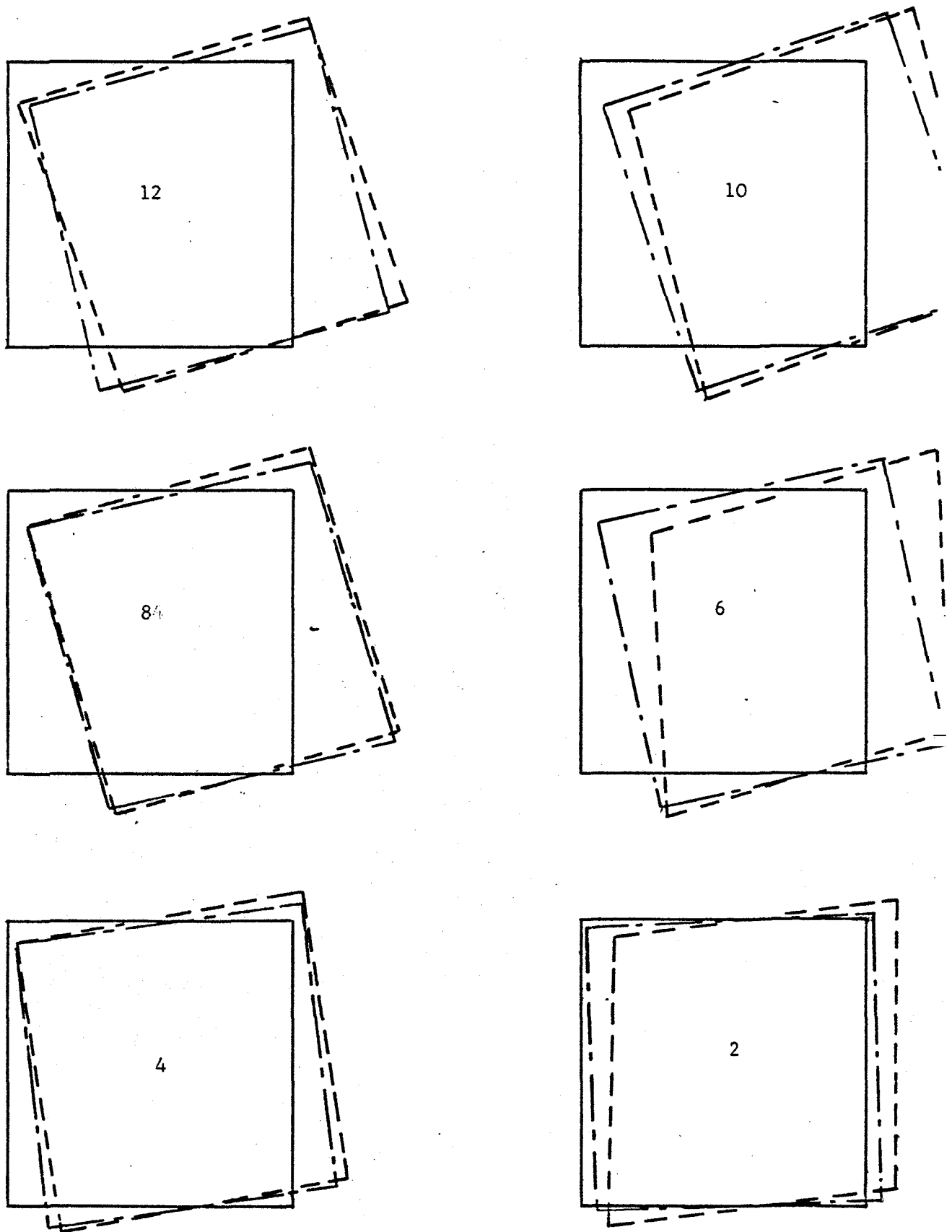


Fig.111(a); Comparison of Experimental Mode Shapes.
First NS Translational Mode -- Floor Components

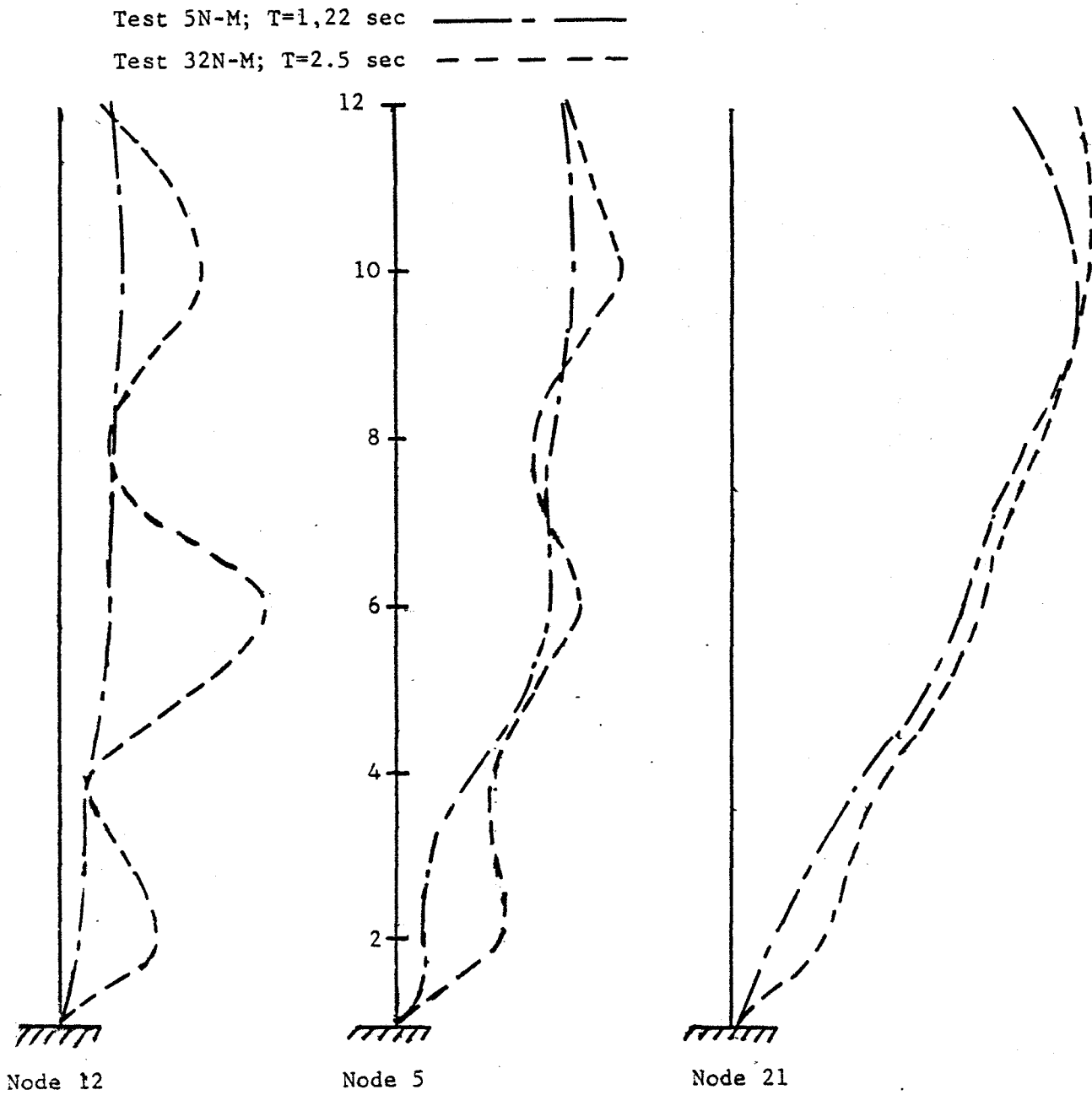


Fig. 111 (b); -- NS Translational Components of Nodes 5, 12, and 21

Test 6N-M; T=1.06 sec ————

Test 33N-M; T=1.33sec - - - - -

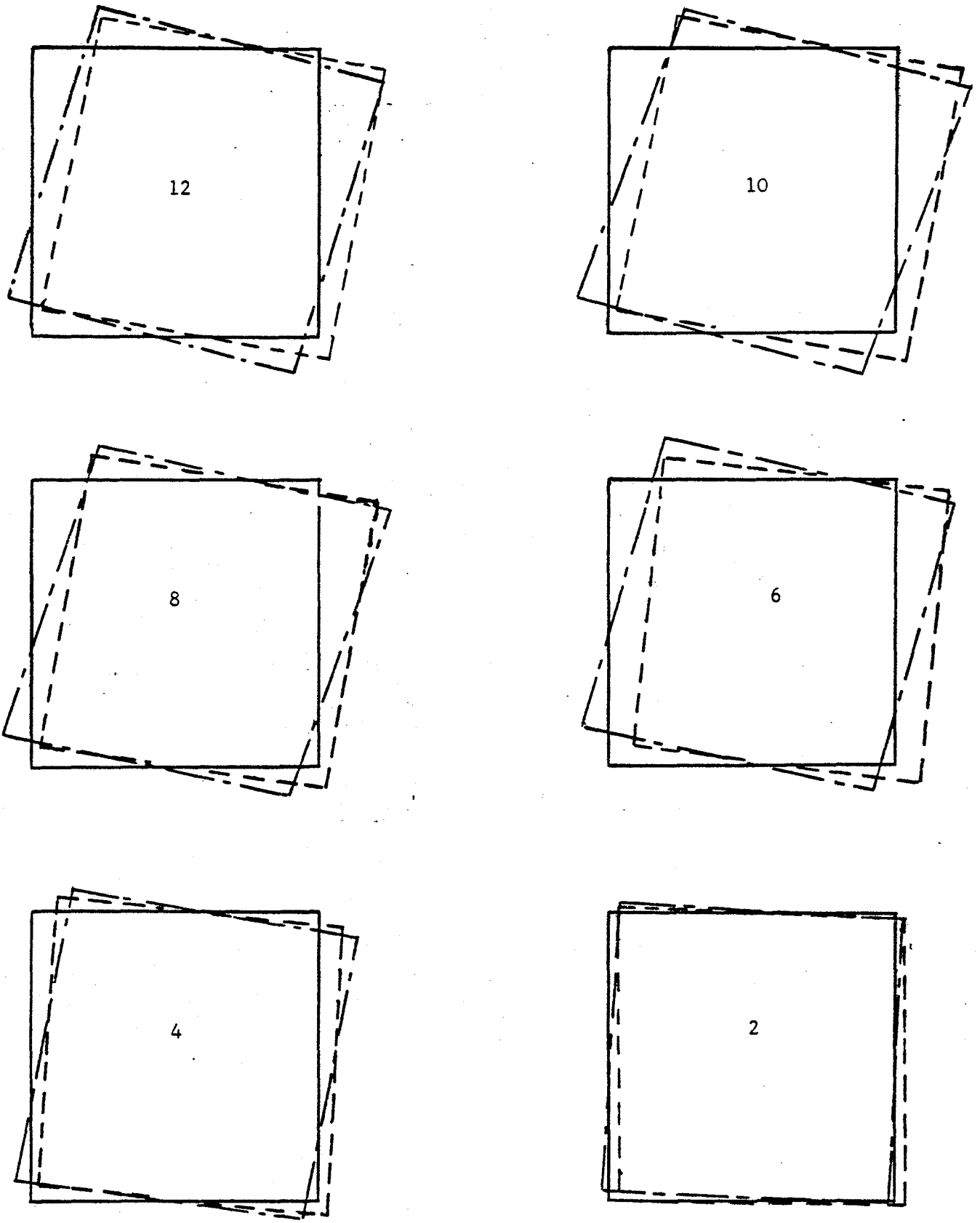


Fig. 112 (a); Comparison of Experimental Mode Shapes.
First NS Torsional Mode --Floor Components

Test 6N-M; T=1.06 sec — — — — —

Test 33N-M; T=1.33 sec - - - - -

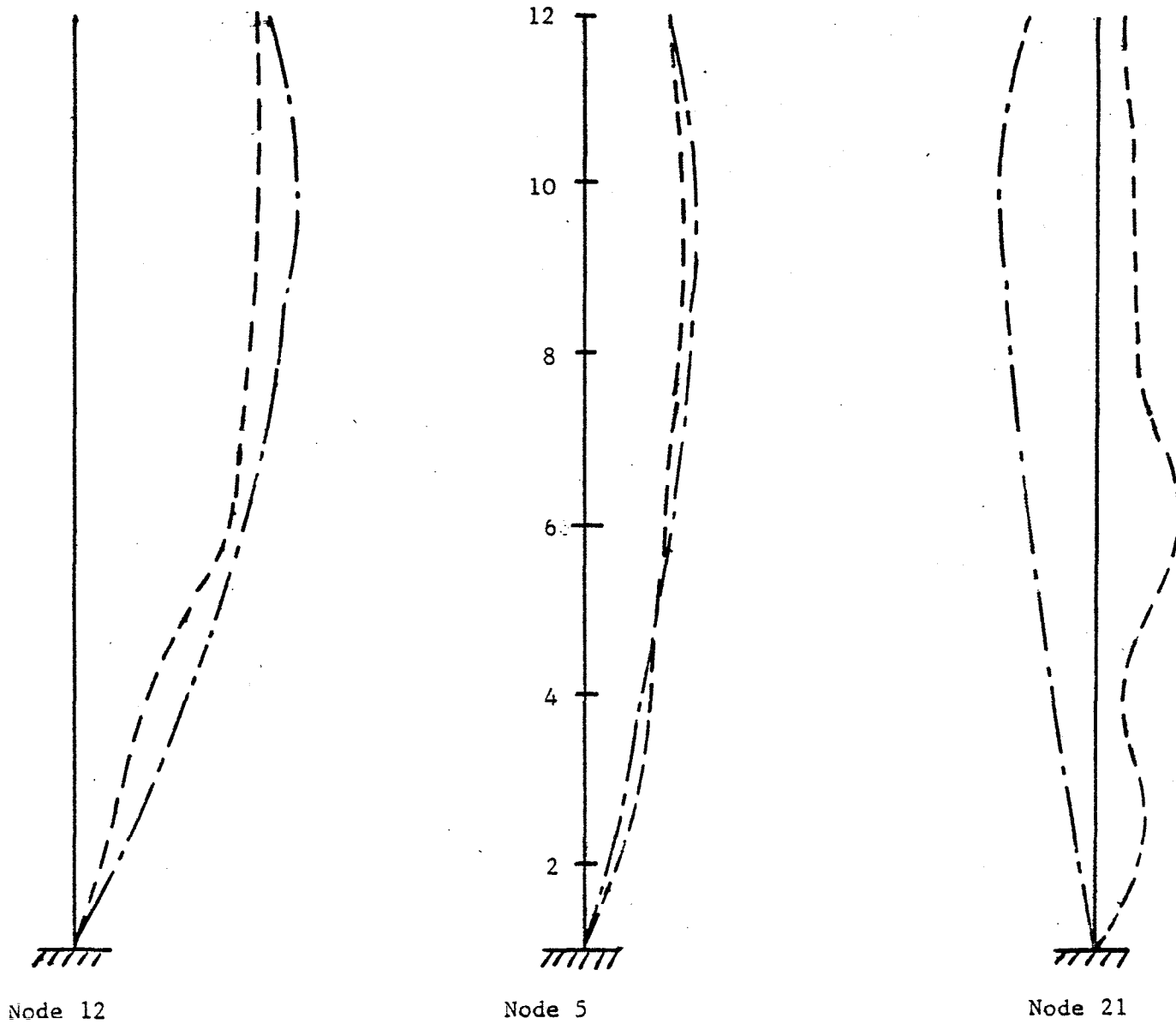


Fig. 112 (b); --NS Translational Components of Nodes 5; 12; 21

Test 7N-M; T=0.32 sec — — — — —

Test 35N-M; T=0.52 sec - - - - -

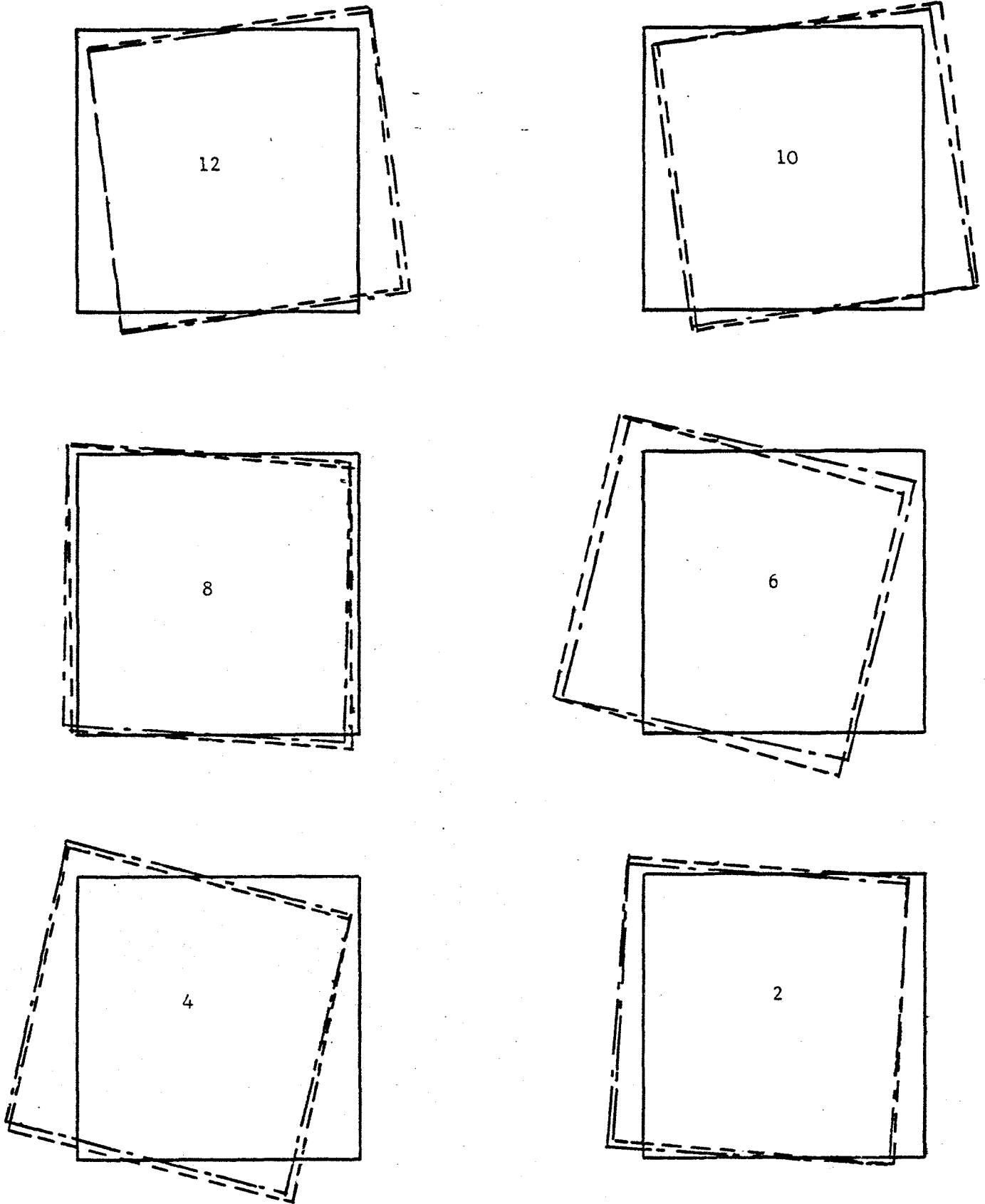


Fig. 113 (a); Comparison of Experimental Mode Shapes.

Second NS Translational Mode -- Floor Components

Test 7N-M; $T=0.32$ sec — — — — —

Test 35N-M; $T=0.52$ sec - - - - -

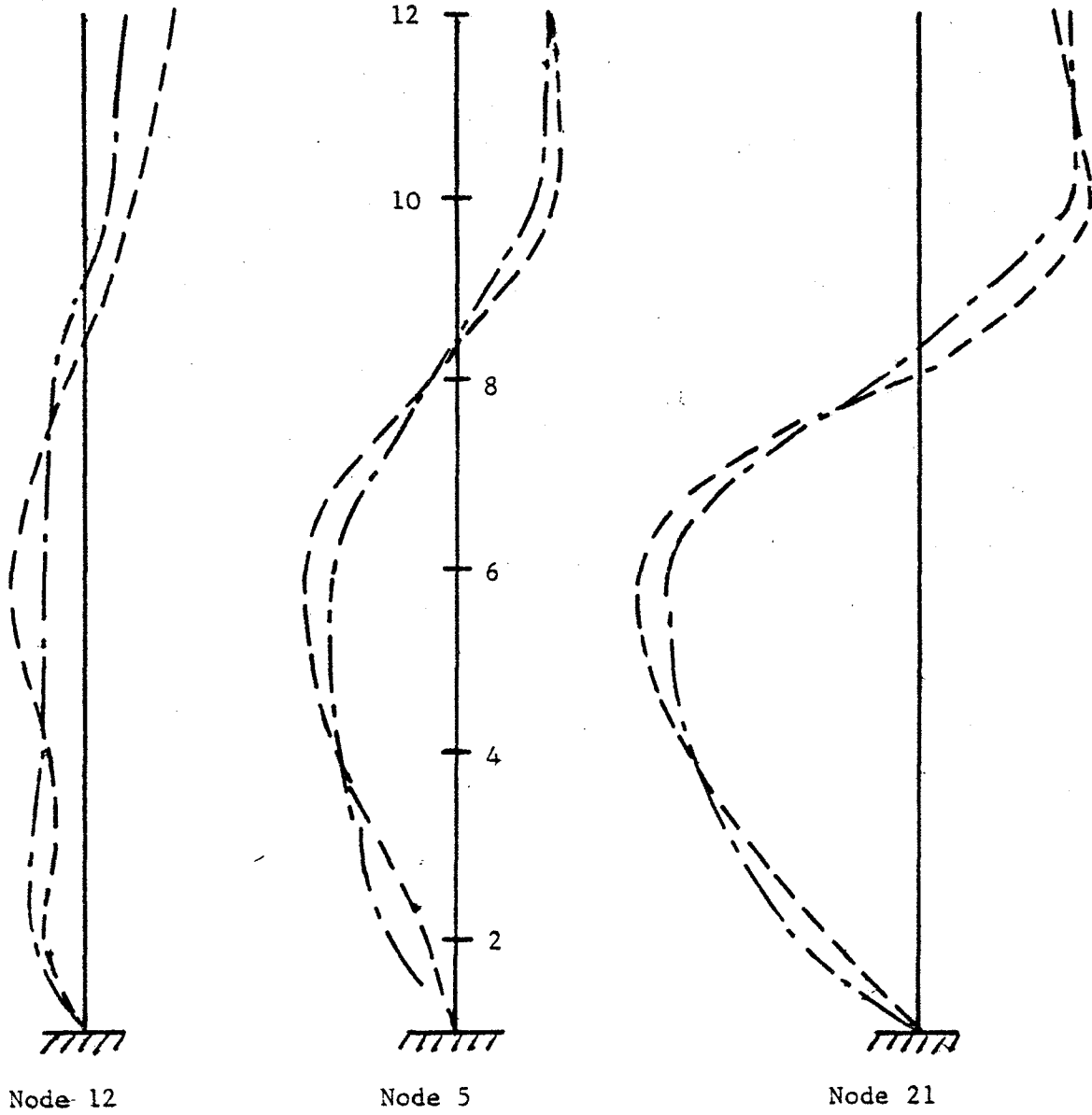


Fig. 113 (b); -- NS Translational Components Of Nodes 5, 12, and 21.

Test 8N-M; T=0.29 sec — — — — —
Test 34N-M; T=0.34 sec - - - - -

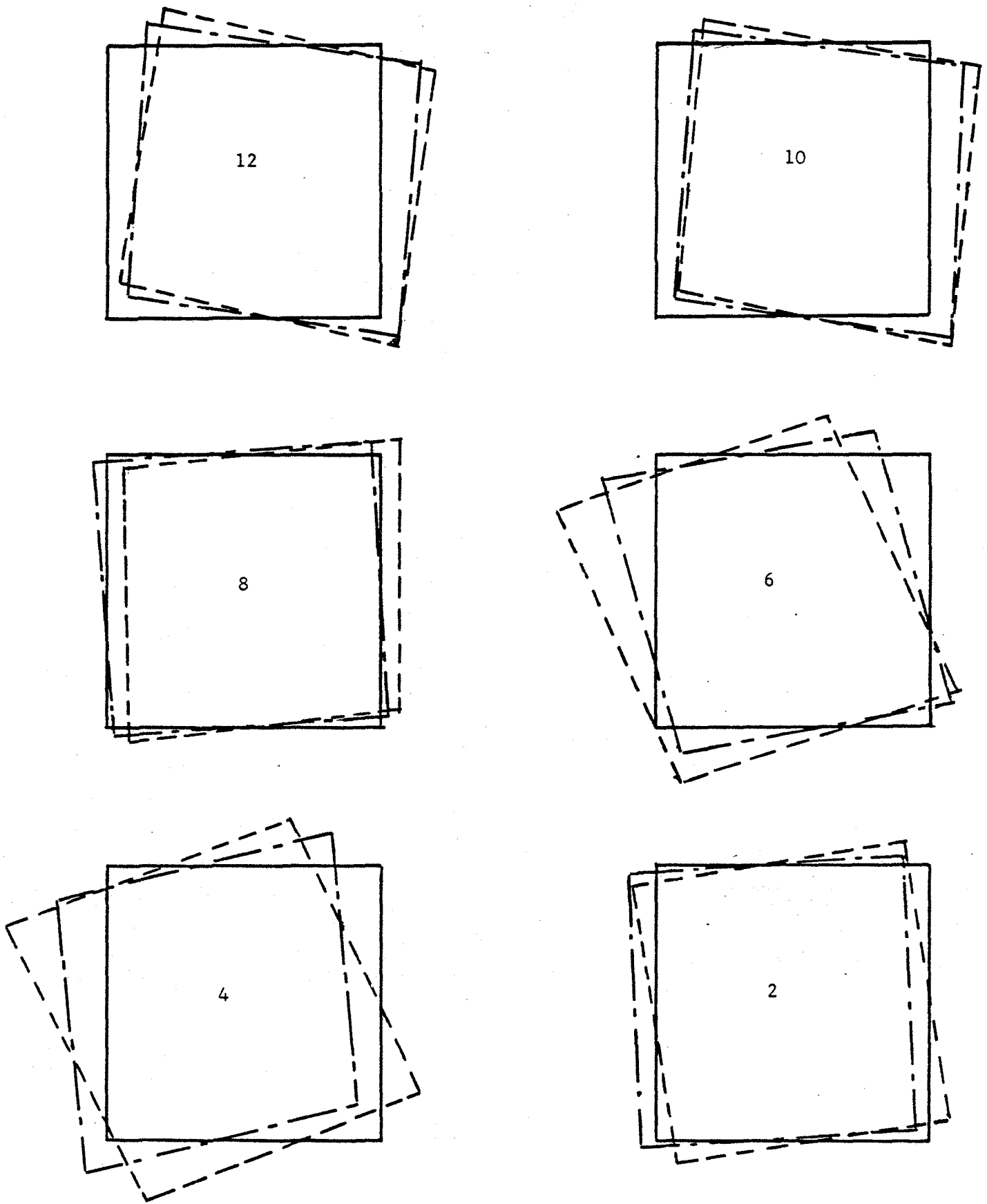


Fig. 114 (a); Comparison of Experimental Mode Shapes.
Second NS Torsional Mode -- Floor Components

Test 8N-M; $T=0.29$ sec — — — — —

Test 34N-M; $T=0.34$ sec - - - - -

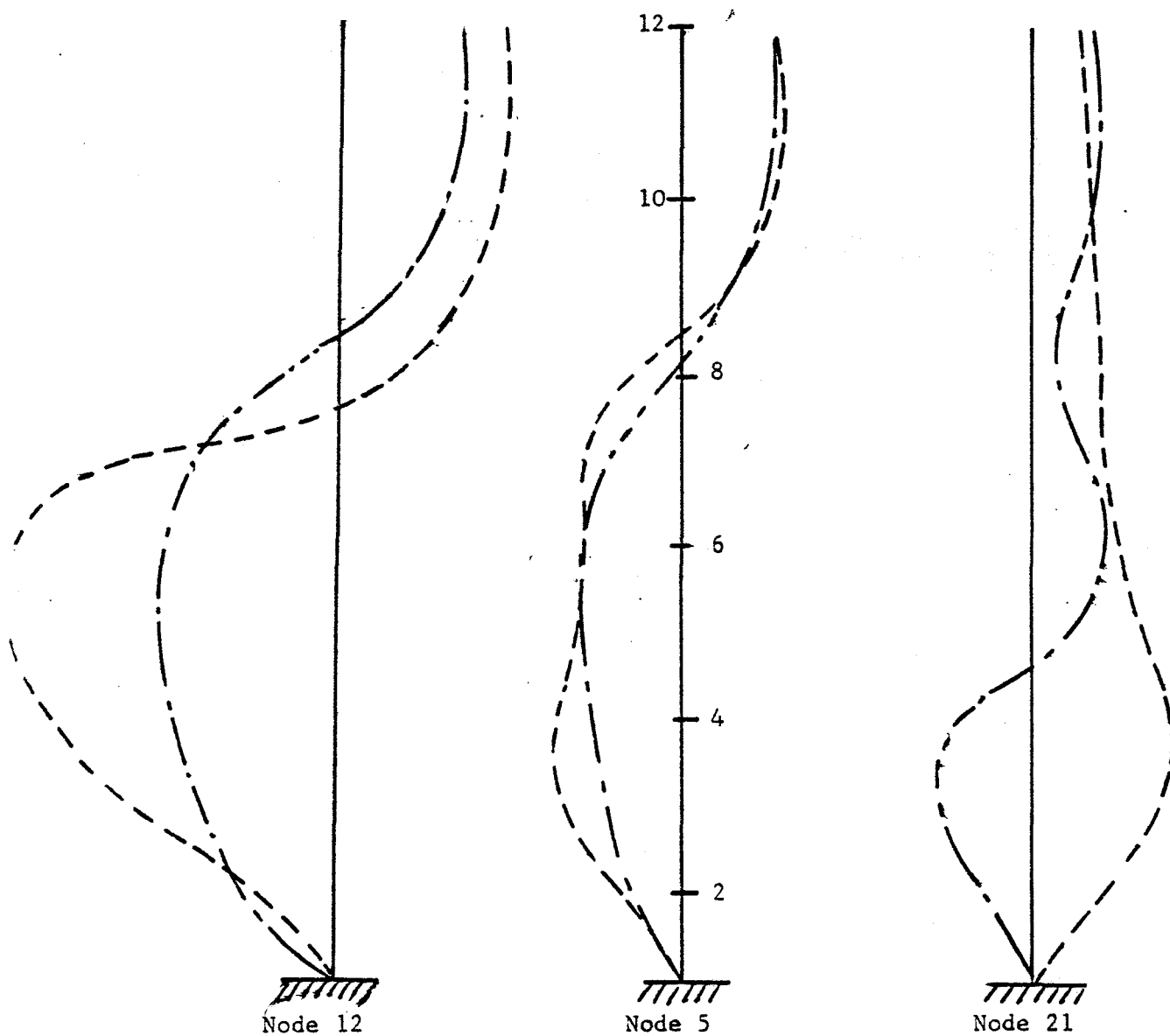
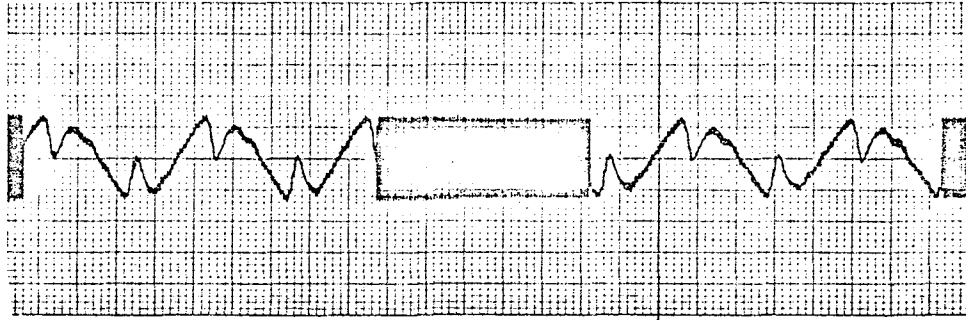
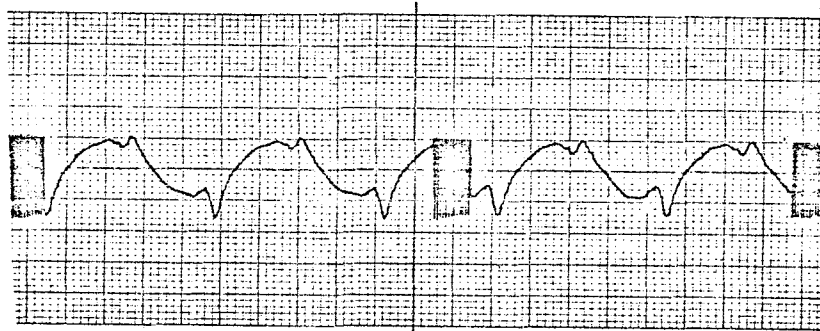


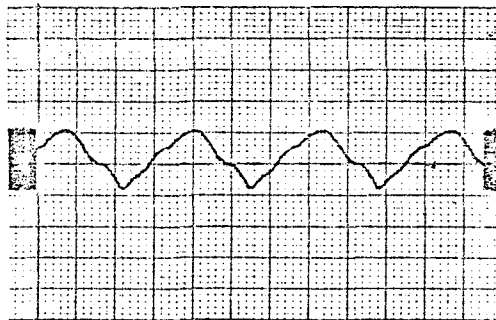
Fig. 114 (b); --NS Translational Components of Nodes 5, 12, and 21



- a) Test 1E-SD, Bucket Weight 5800 lb
(2631 Kg), Actuator Force 5,000 lbf
(22,240 N).

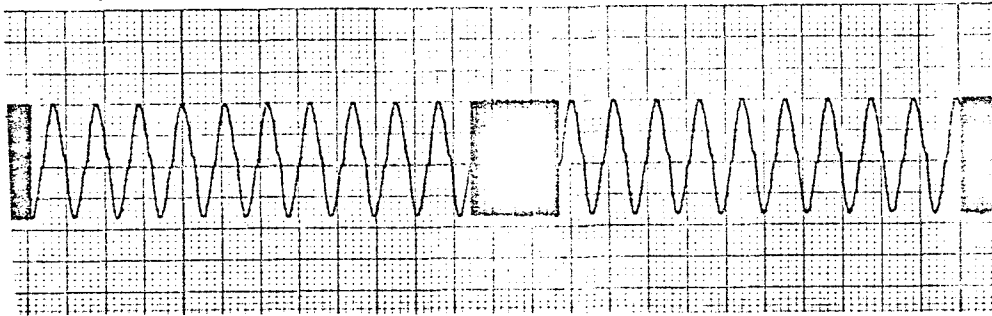


- b) Test 4E-S, Bucket Weight 19,000 lb
(8620 Kg) Actuator Force 10,000 lbf
(44,480 N).

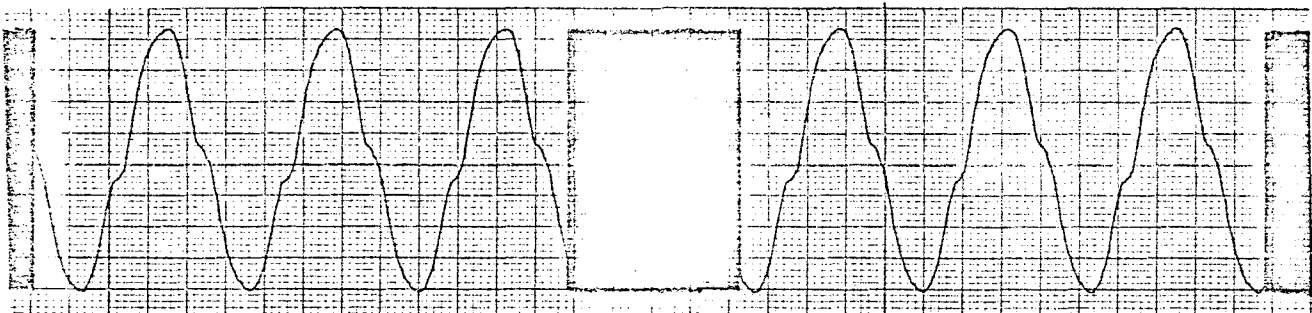


- c) Test SE-SD, Bucket Weight 57,700 lb
(26,170 Kg), Actuator Force 5,000 lbf
(22,240 N)

Fig. 115 Shape of Actuator Force in
First Translational E-W
Modes With Varying Bucket
Weights.

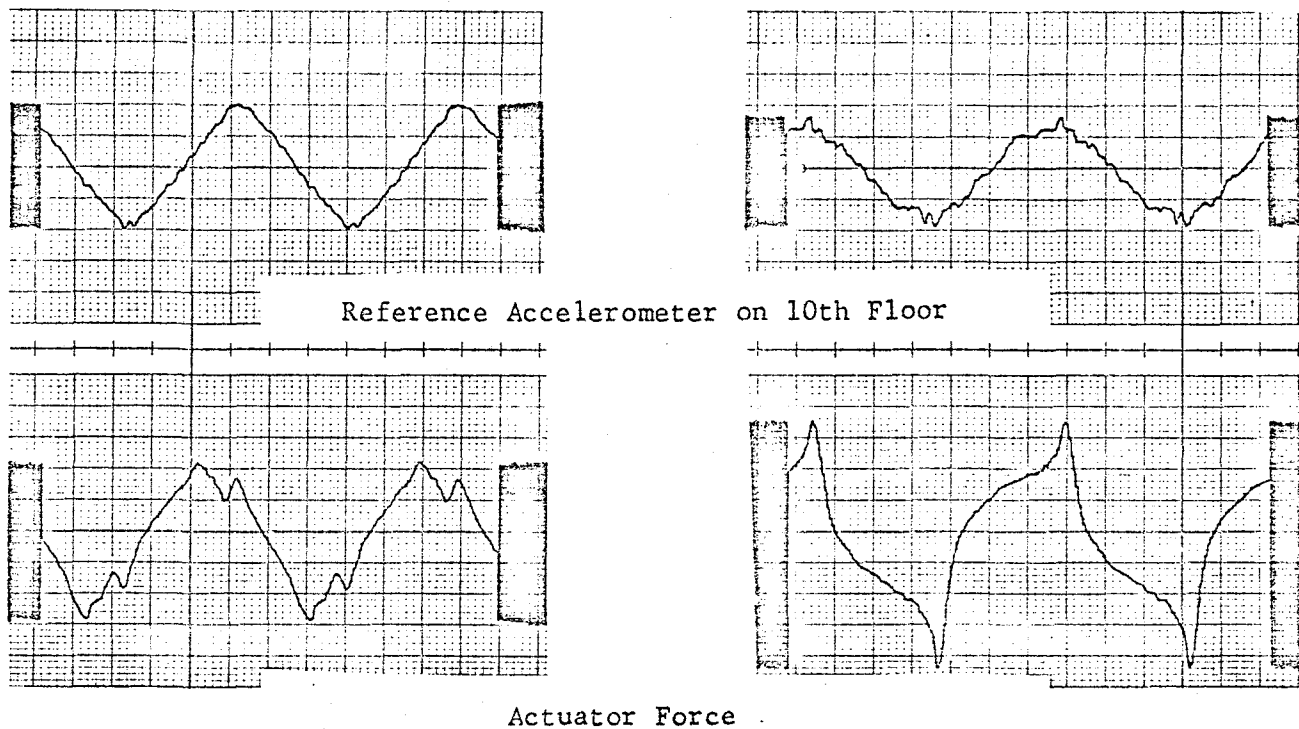


a) Test 18E-D, Actuator Force 18,000 lbf
(80,070 N) at a Frequency of 3.63 Hz.



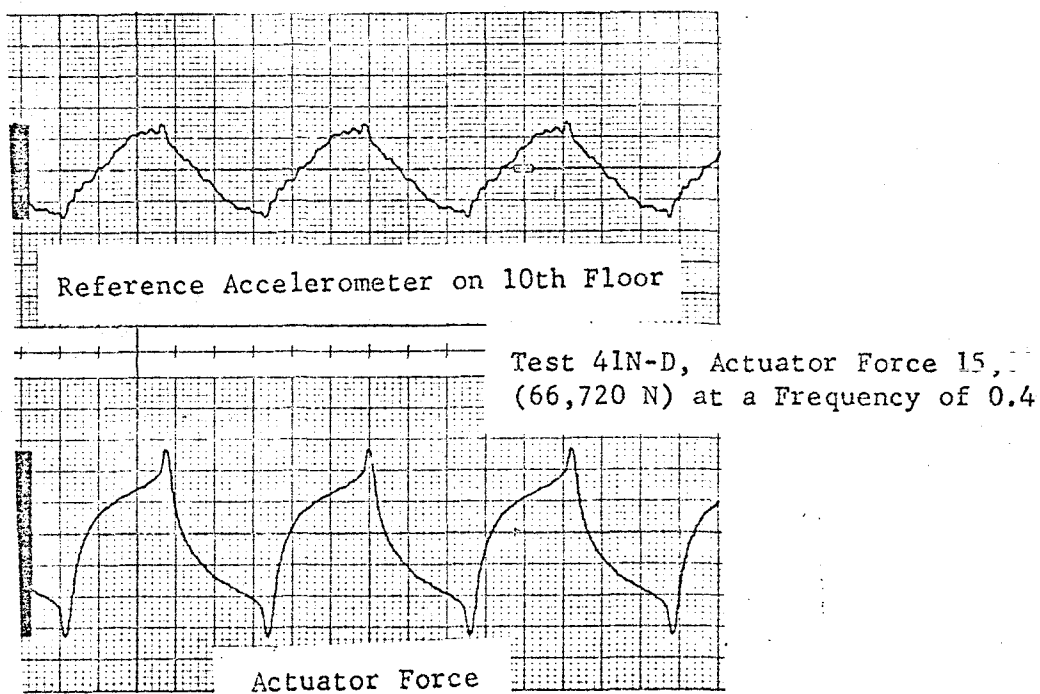
b) Test 23N-D, Actuator Force 22,500 lbf
(100,080 N) at a Frequency of 2.34 Hz.

Fig. 116 Typical Shapes of Actuator Force
for all Second Mode Tests in the
EW and NS Direction.



Test 30N-D, Actuator Force 15,000 lb
(66,720 N) at a Frequency of 0.68 Hz.

Test 24E-D, Actuator Force 25,000 lb
(111,210 N) at a Frequency of 0.52 Hz.



Test 41N-D, Actuator Force 15,000 lb
(66,720 N) at a Frequency of 0.4 Hz.

Fig. 117 Shape of Actuator Force and Measured 10th Floor Acceleration Response for Large Amplitude First Mode Tests.

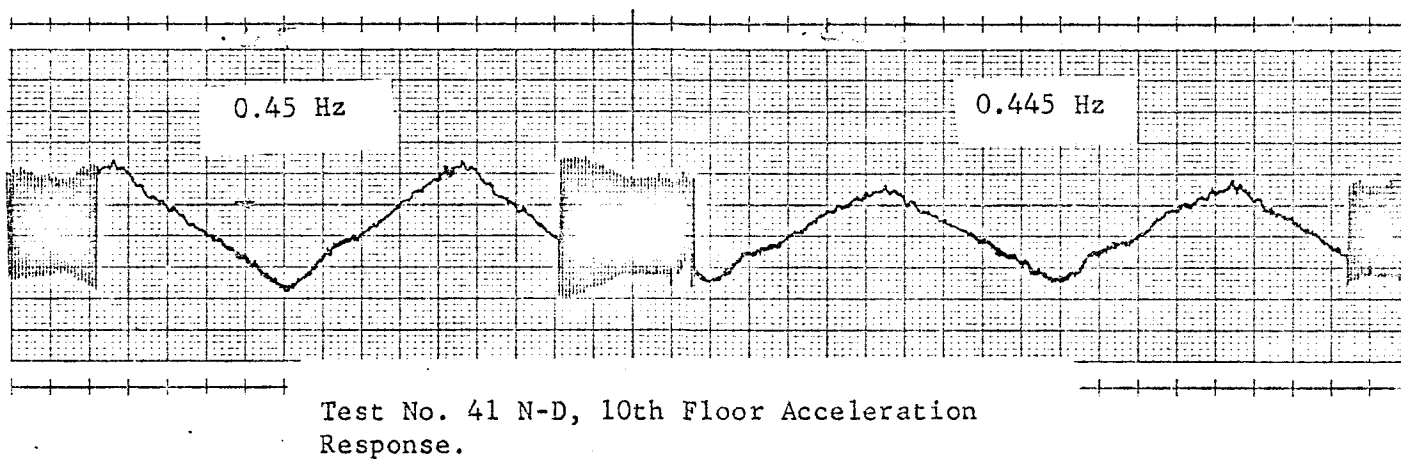
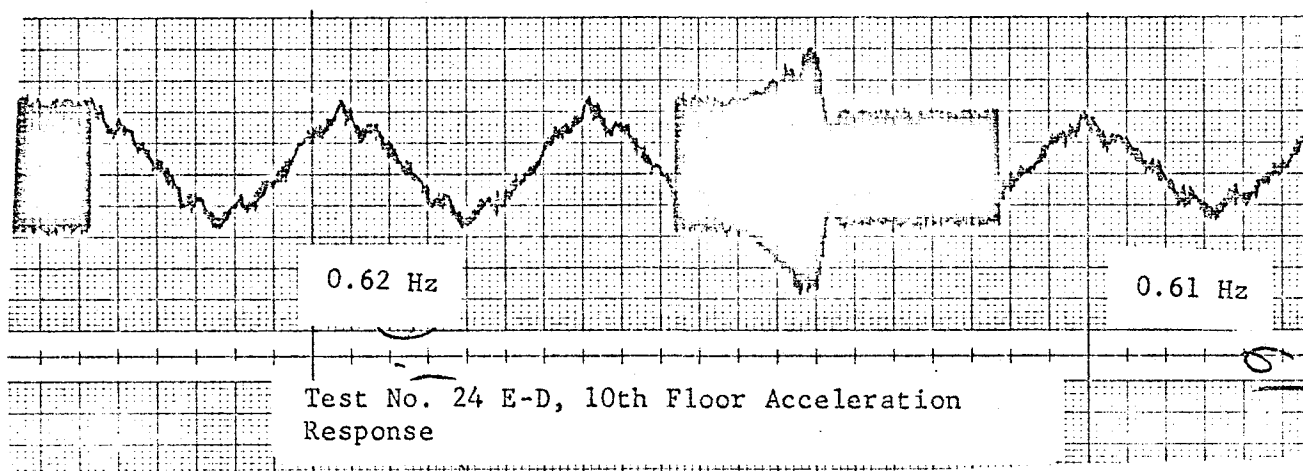


Fig. 118 10th Floor Acceleration Response
During Large Amplitude Tests

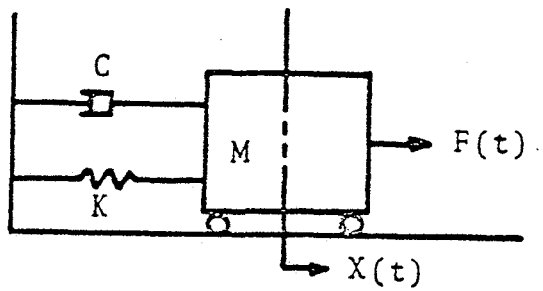


Fig. 119 Single-Degree-of-Freedom Systems

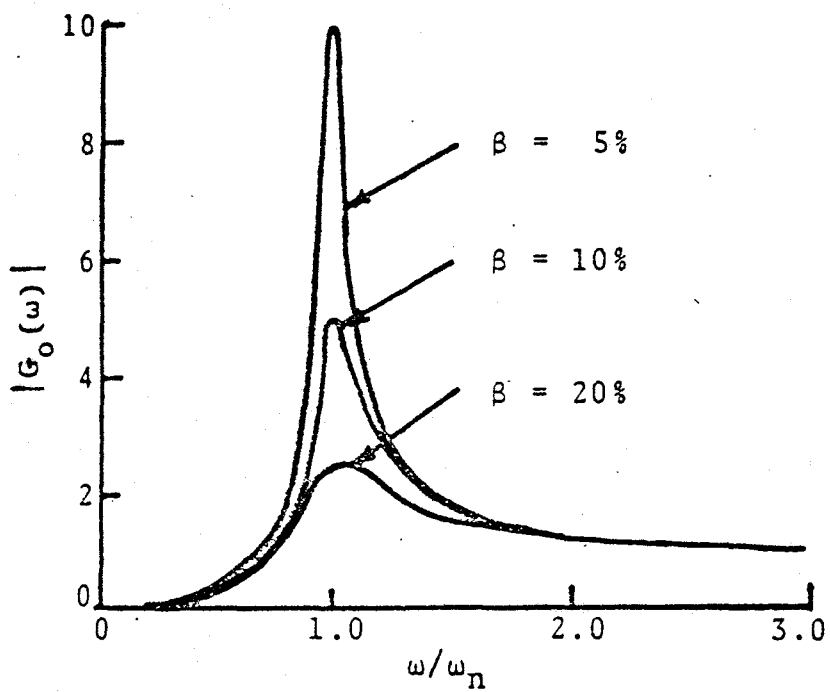


Fig. 120 Transfer Function G_o -versus-Frequency Ratio

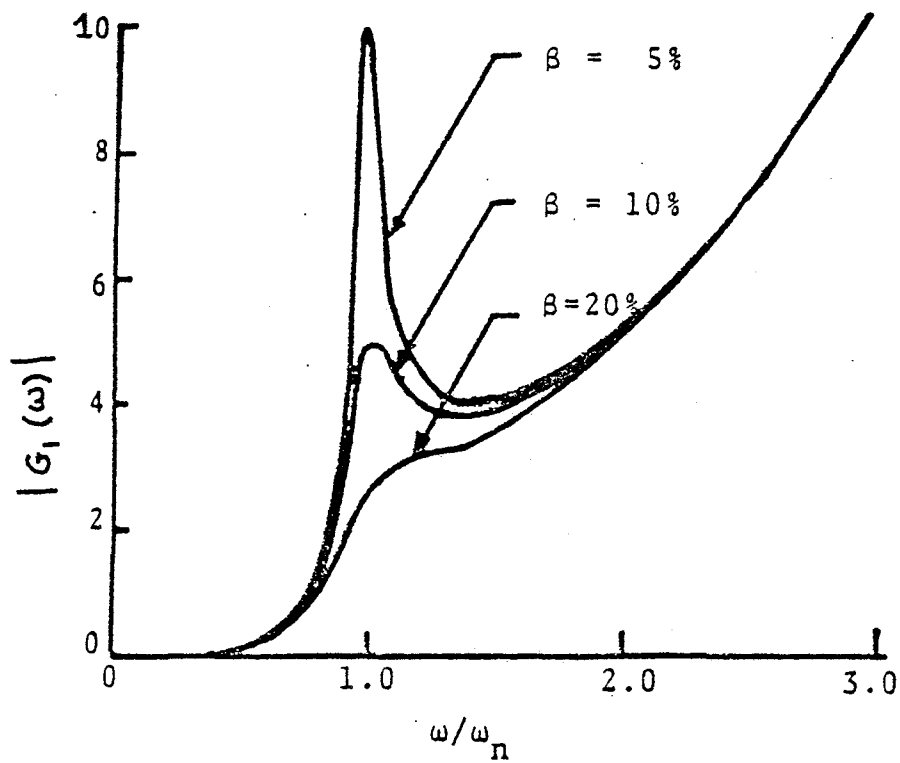
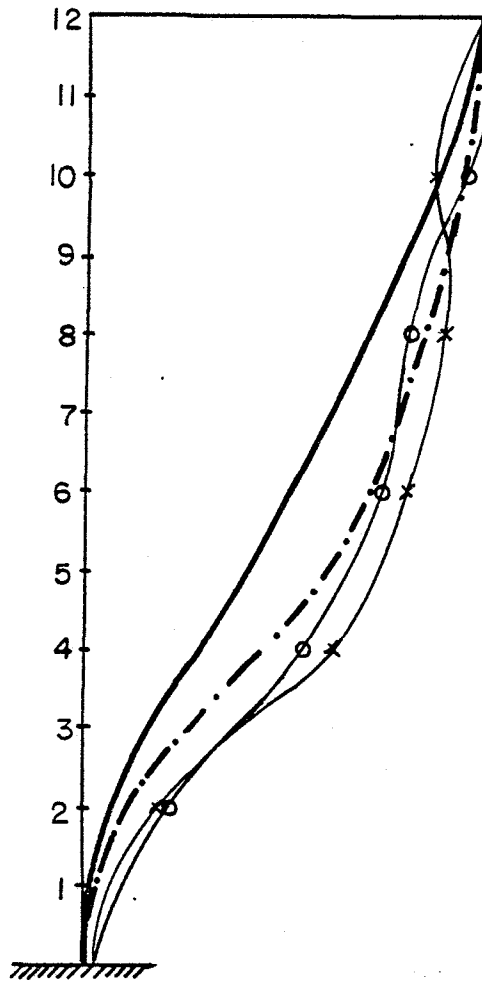


Fig. 121 Transfer Function G_1 -versus-Frequency Ratio



————— Model 1; T=1.00 sec
 - · - · - Model 2; T=1.38 sec
 ○ — ○ Experimental T=0.88 sec 14E-M
 x — x Experimental T=1.85 sec 28E-M

Fig. 122 Comparison of Experimental and Analytical Results. First EW Translational Mode

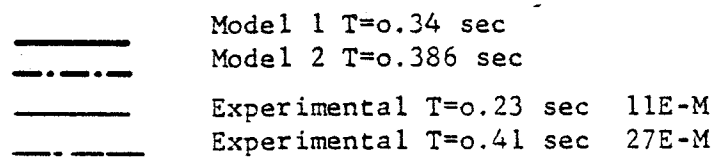
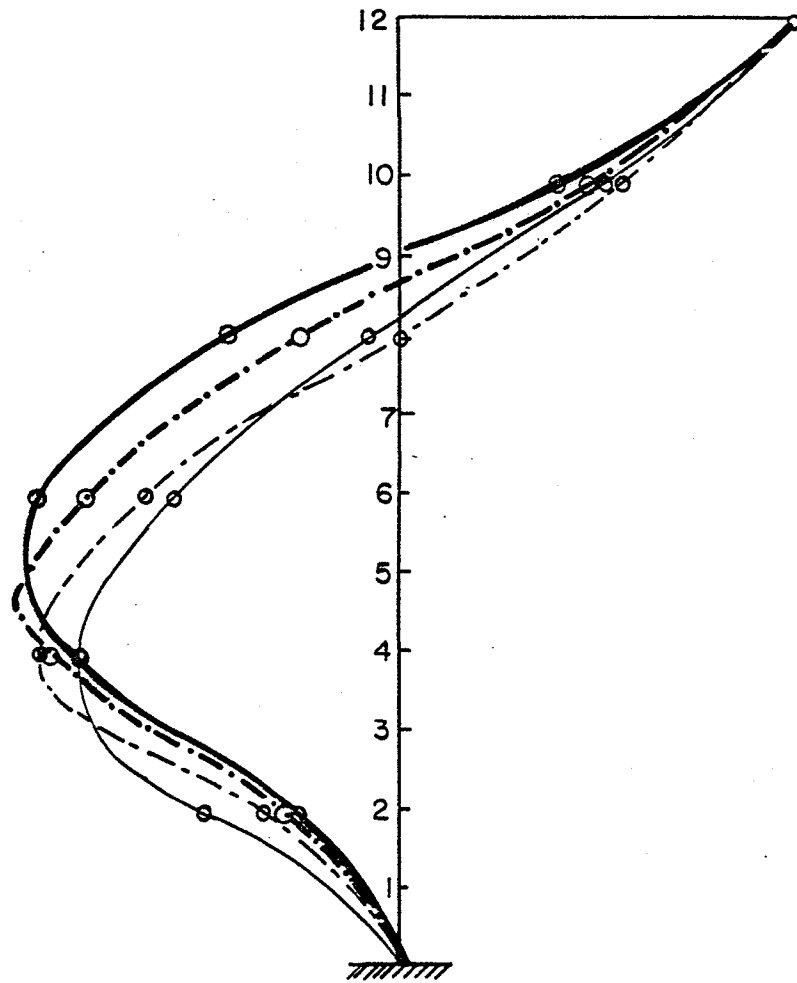


Fig. 123 Comparison of Experimental and Analytical Results. Second EW Translational Mode

Test 5N-M; T=1.22sec ————

Analytical; T=0.93sec - - - - -

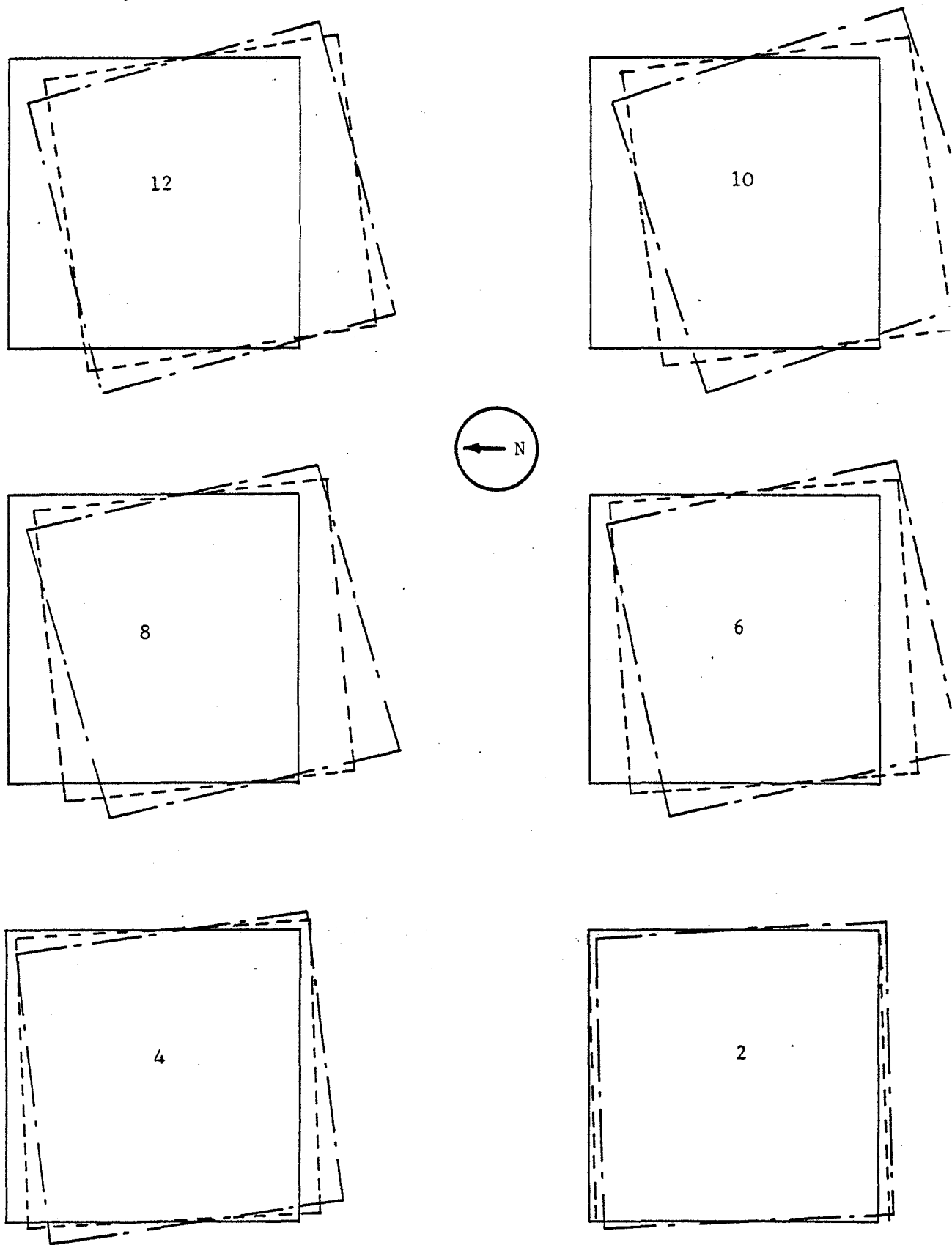


Fig. 124 (a); Comparison of Experimental and Analytical Results.
First NS Translational Mode -- Floor Components.

Test 5N-M; T=1.22 sec — — — — —
Analytical; T=0.93 sec - - - - -

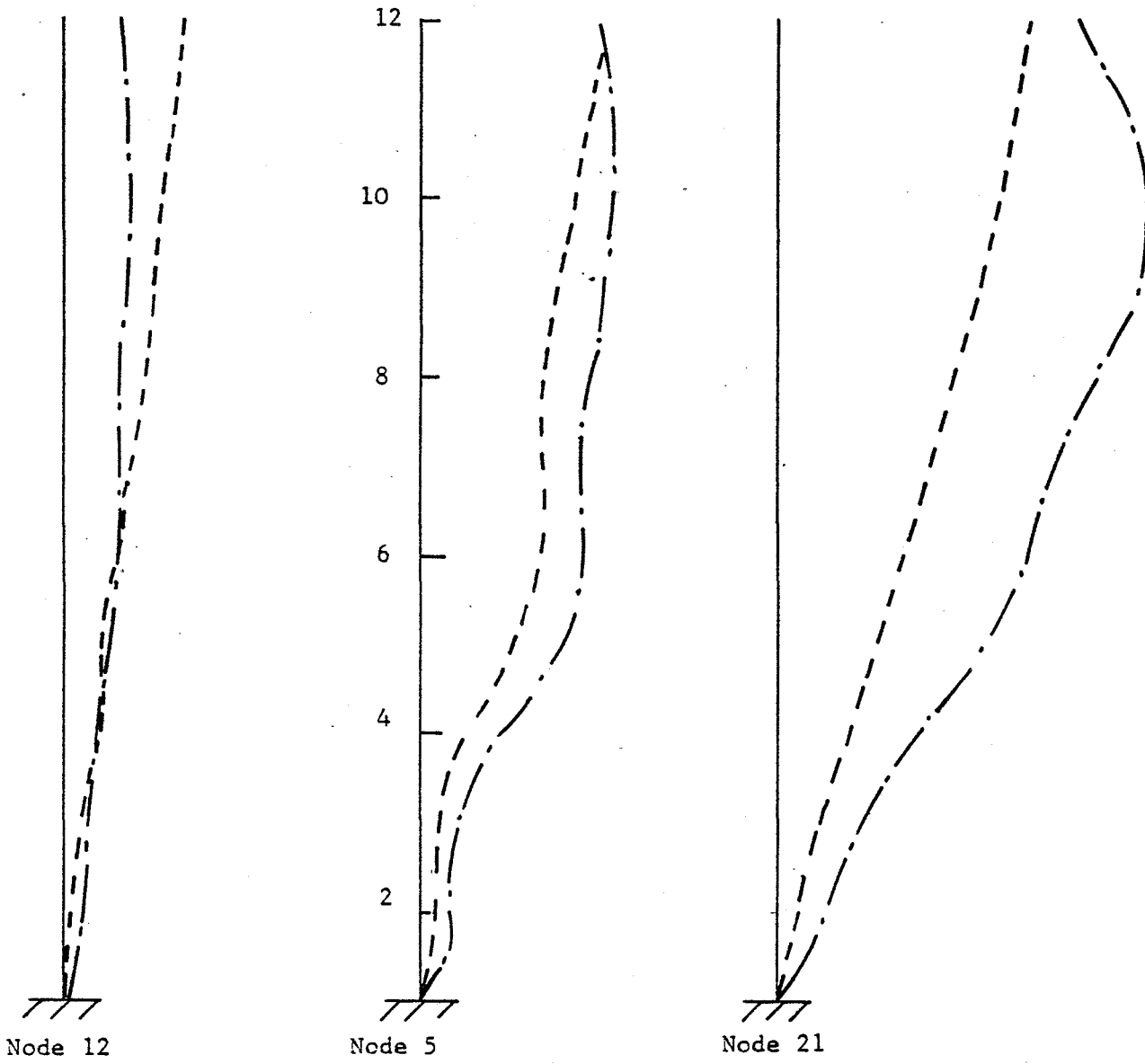


Fig. 124 (b); NS Translational Components of Nodes 5, 12, and 21.

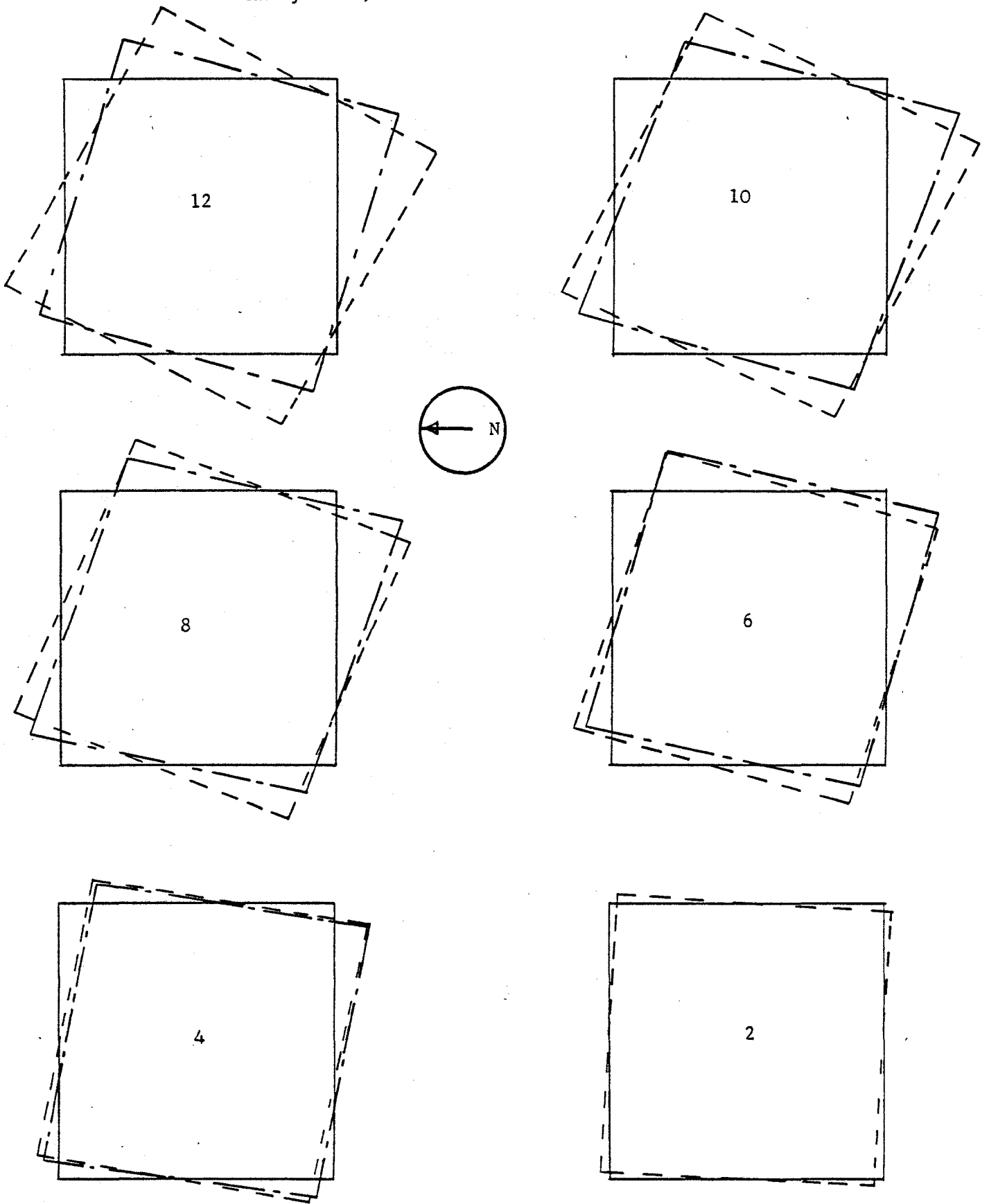


Fig. 125 (a); Comparison of Experimental and Analytical Results.

First NS Torsional Mode -- Floor Components

Test 6N-M; T=1.06 sec 
 Analytical; T=0.68 sec 

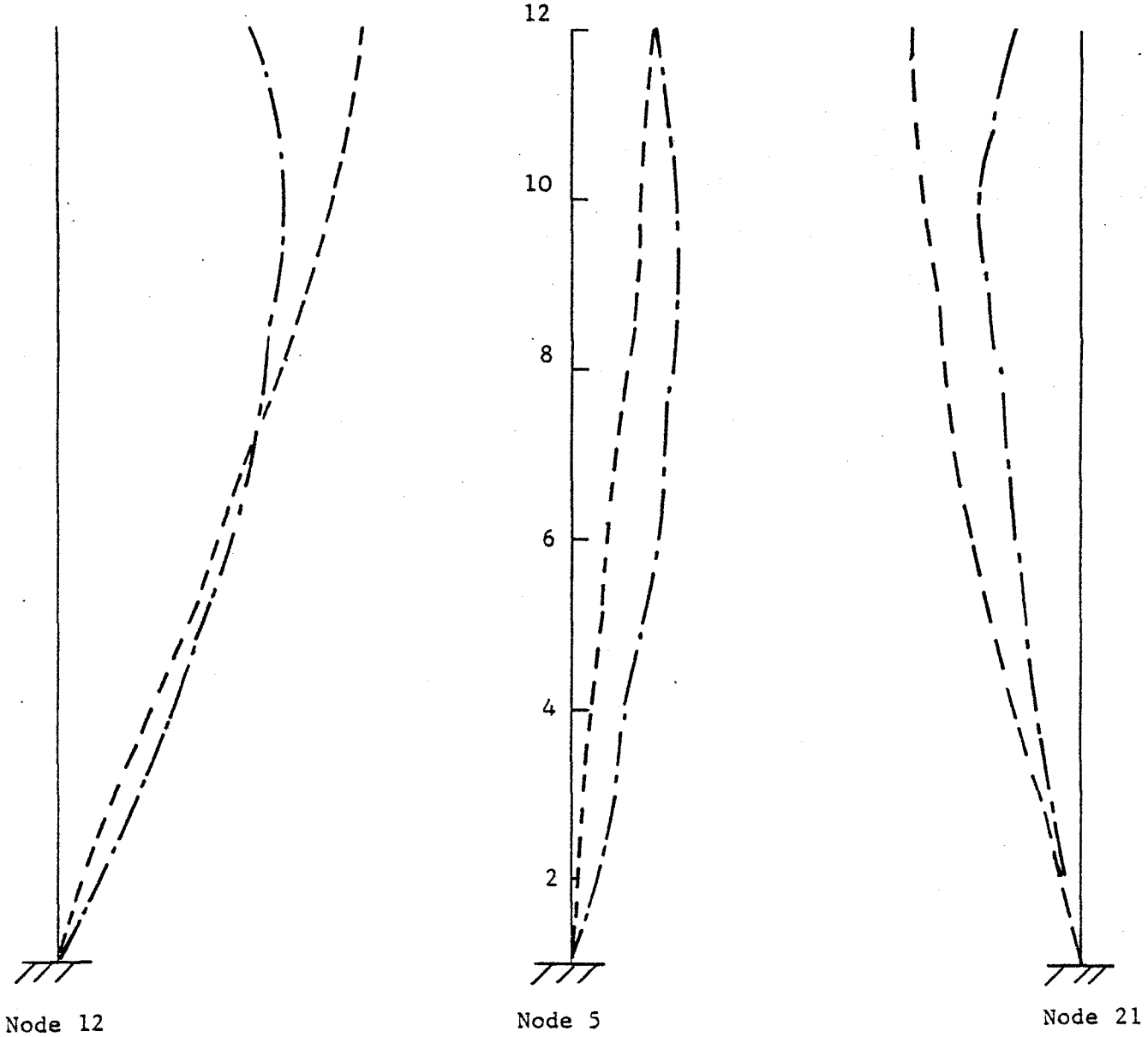


Fig. 125 (b) ; First NS Torsional Mode - NS Translational Components of Nodes 5, 12, and 21.

Test 7N-M; T=0.32 sec — — — — —
Analytical; T=0.29 sec - - - - -

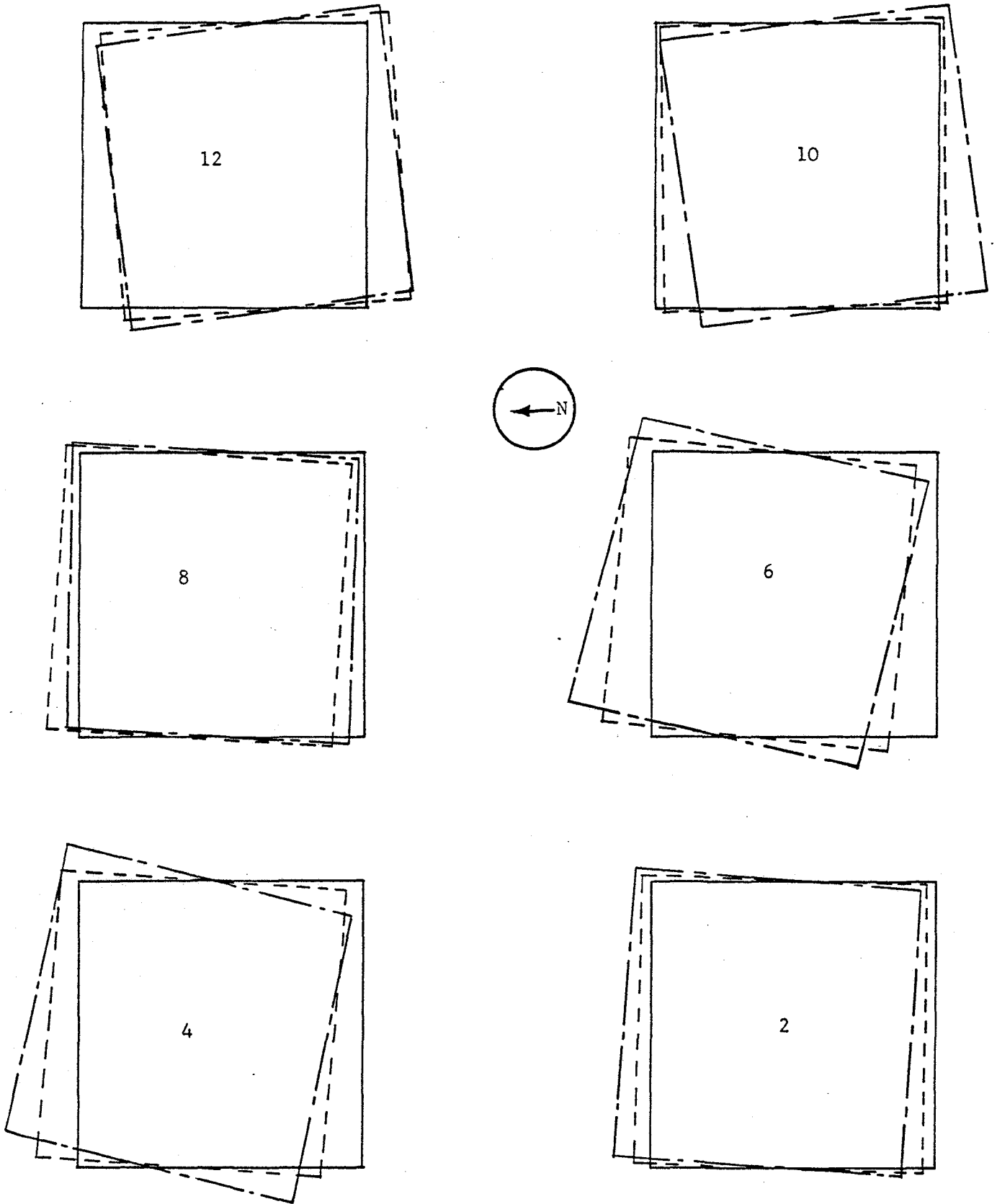


Fig. 126 (a) Comparison of Experimental and Analytical Results.
Second NS Translational Mode -- Floor Components

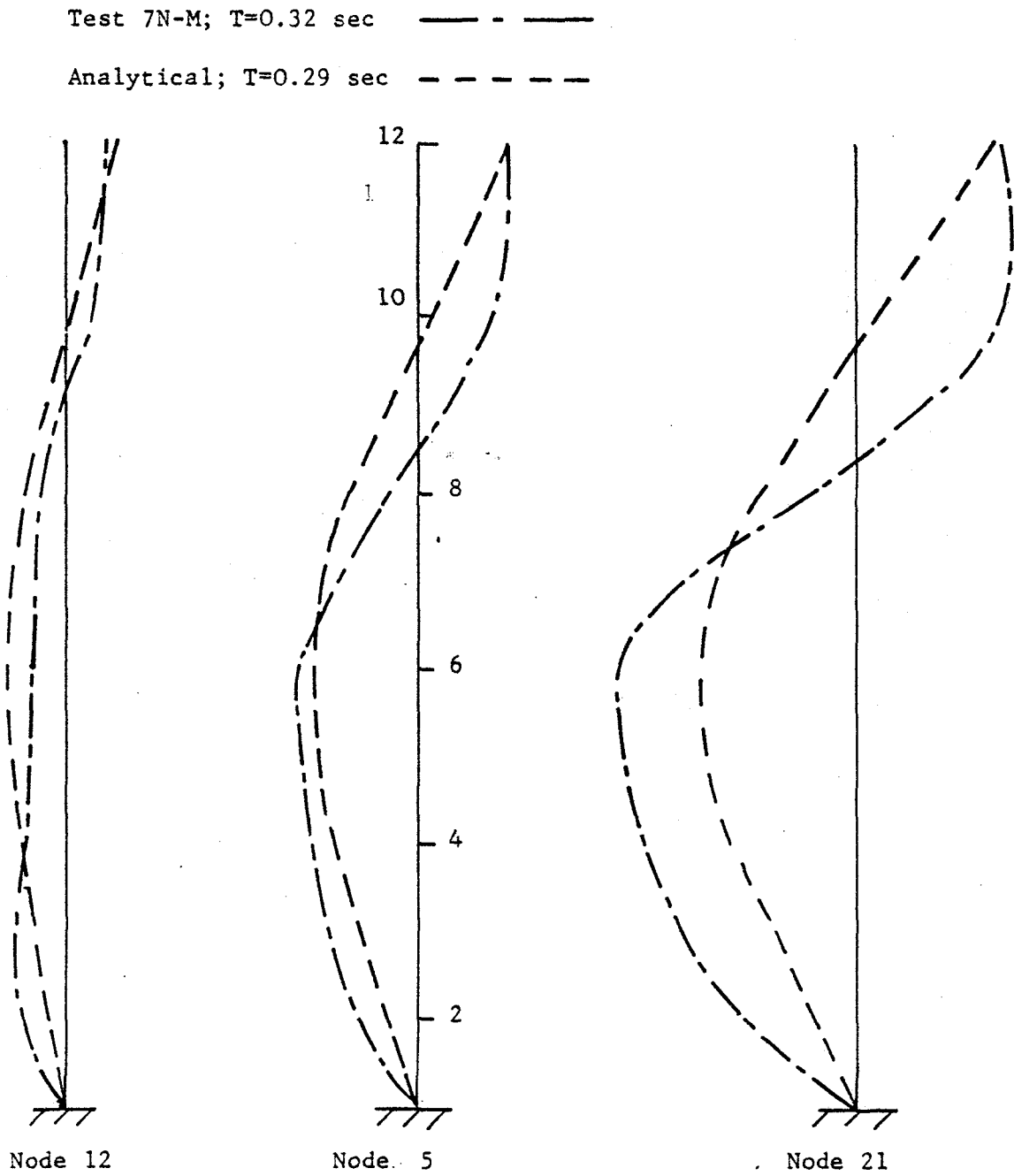


Fig. 126 (b). NS Translational Components of Nodes 5, 12, and 21.

Test 8N-M; T=0.29 sec



Analytical; T=0.21 sec

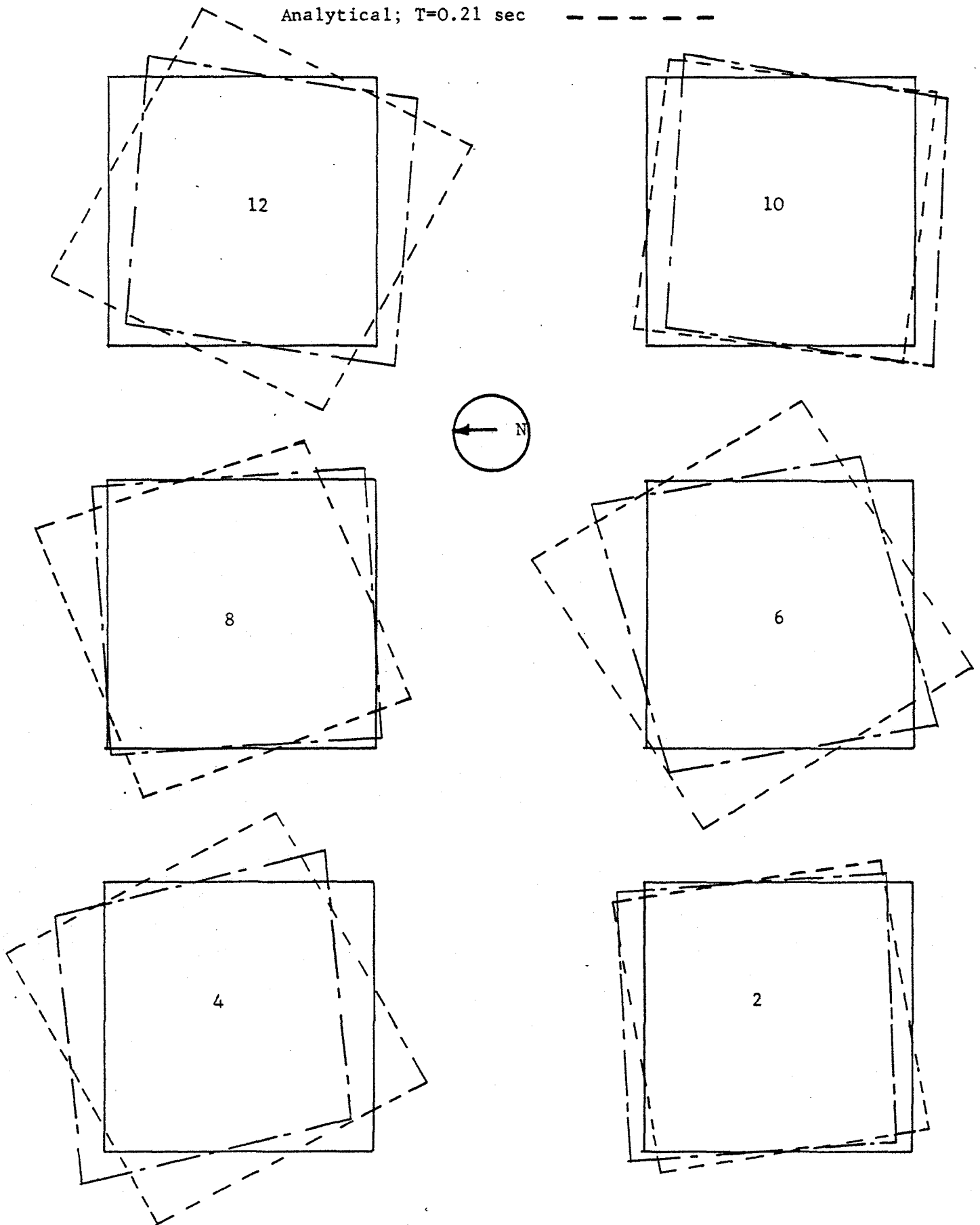


Fig. 127 (a); Comparison of Experimental and Analytical Results.
Second NS Translational Mode -- Floor Components

Test 8N-M; $T=0.29$ sec — — — — —

Analytical; $T=0.21$ sec - - - - -

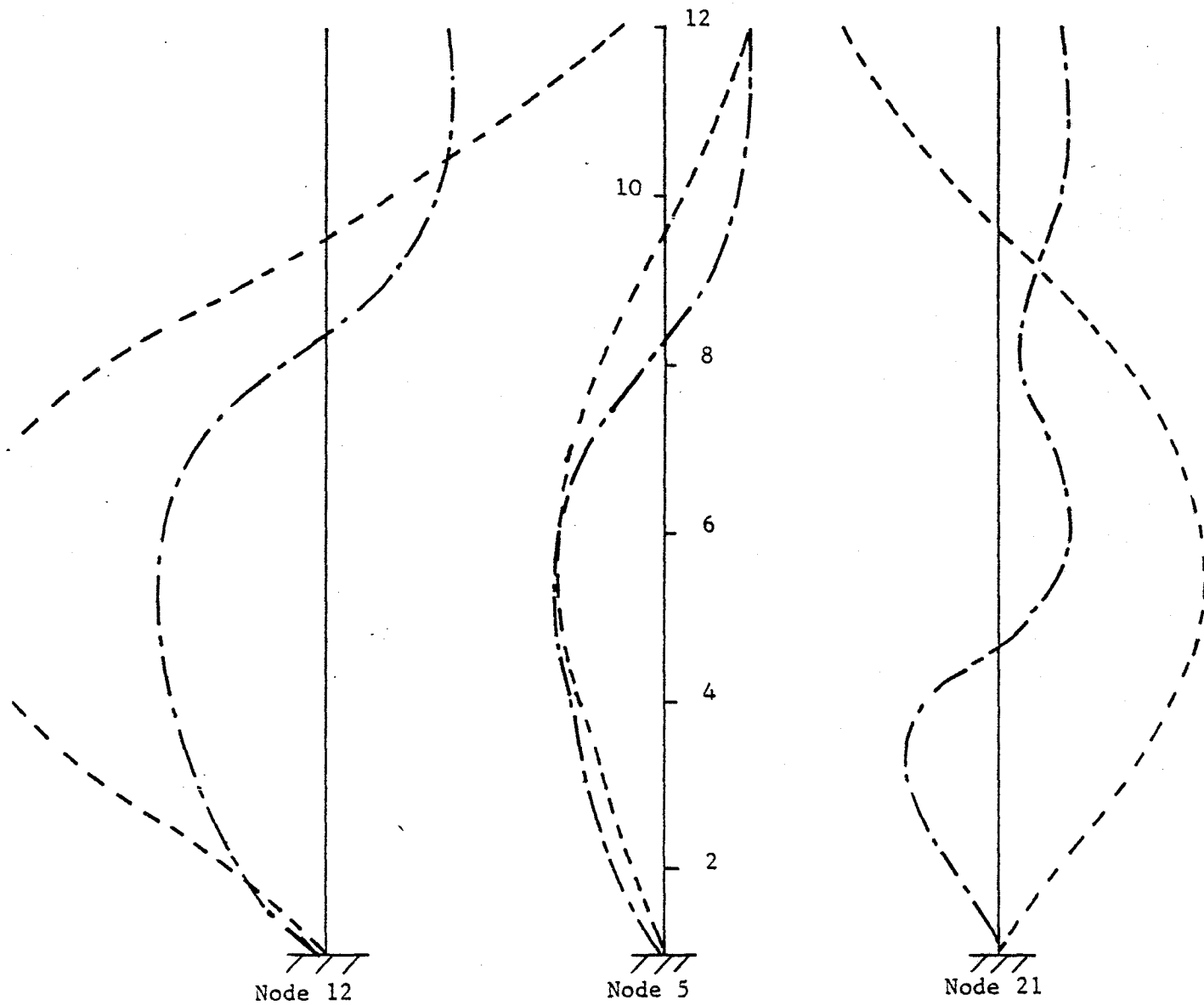


Fig. 127 (b); NS Translational Components of Nodes 5, 12, and 21.

APPENDIX AORGANIZATIONS AND INDIVIDUALS INVOLVED IN THE FRUITT-IGOE DYNAMICTESTING PROJECT

Many individuals and organizations helped make the project possible. Following is a list of the organizations and the people who were involved in one way or another with the work.

The National Science Foundation

The project was funded by the National Science Foundation for the total amount of \$390,500 (\$20,000 for the feasibility study and the remainder for the testing project). The technical direction during the proposal development and during the actual performance of the work was provided by Dr. John Scalzi, Program Manager in the Earthquake Engineering Division of the NSF.

The Principal Research Participants

The project was under the principal supervision of Dr. T. V. Galambos, who was responsible for the overall management and supervision of all phases of the work. Assisting him were his colleague at Washington University, Dr. David S. Hatcher, and Dr. Ronald L. Mayes from Computech, Berkeley. Dr. Hatcher was in charge of the dimensional and material properties survey, and he assisted in the damage assessment during the large amplitude shaking tests. Dr. Mayes brought his considerable experience in dynamic testing to bear on the planning and execution of the small scale and the large scale dynamic tests, and he was responsible for the analysis, interpretation and the presentation of the dynamic data.

Washington University Administration

The responsible officials of Washington University are Dr. William H. Danforth, Chancellor, Mr. Edward L. MacCordy, Associate Vice Chancellor for Research and Dr. James M. McKelvey, Dean of the School of Engineering and Applied Science. During the proposal writing phase Mrs. Blanche W. Jones, Sponsored Projects Associate, and Mrs. Idelle Hirsch, Director of Engineering Accounting, were of great assistance. The most valuable and day-to-day support was provided by Mr. Myron P. Mustaine, Sponsored Projects Administrator, who was particularly helpful in contract negotiations with NSF, Boeing, McDonnell-Douglas and Applied Nucleonics. Dean McKelvey was of great assistance in providing funds to tide the project over the period when the first allotment of the total funds had been used up and the final payment had not yet been received from NSF.

Many individuals in the University's Funds Accounting division were actively helpful in the day-to-day financial operations of the project.

Mr. David R. Armstrong of the Technical Services group of the School of Engineering served the project as photographer and film producer.

In the Civil Engineering Department the typing, phoning and the thousands of administrative and financial details were taken care of by Mrs. Lois R. Brown and Mrs. Alice J. Bletch.

Washington University Students and Staff

Three undergraduate upper level Civil Engineering Students served as overall workers: Ronald A. Gardiner, Elaine M. Gregory and James R. Vosper. These students worked unstintingly in all kinds of weather on jobs ranging from knocking out walls with a sledge hammer to assisting in data taking. Their main effort consisted of the performance of the dimensional and material survey work which was done during July and August. They were

helped from time-to-time as required by other students, especially during the mode-shape surveys.

Mr. Arthur Monsey, affiliate professor of Civil Engineering and a doctoral candidate, was of special value to the project because of his previous experience. At the time of the construction of the Pruitt-Igoe complex in the late 1950's he served as construction engineer for the contractor, the Millstone Construction Company, as supervisor of the work on these buildings. Mr. Monsey's experience with construction, management, planning and labor problems, as well as his intimate knowledge of the St. Louis construction, equipment and labor market, saved the project from countless difficulties.

St. Louis Housing Authority

This agency was the organization responsible for the Pruitt-Igoe Housing Complex, and it was through their cooperation and permission that the test-building was made available. We also received from them copies of the architectural drawings of the buildings. Mr. Thomas Costello is Executive Director of the St. Louis Housing Authority. Mr. Harry Dew, an engineer with the Authority, was of special help to the project in its initial phases.

Applied Nucleonics Company, Inc.

The small-amplitude dynamic tests were performed by this Los Angeles based company specializing in performing analytical and experimental dynamic studies on various types of structures and structural components. The small amplitude tests were performed in the second week of July 1976, only about two weeks after we were permitted to enter the site. The team was supervised and managed by Dr. Paul Ibanez, and the other members of the team were Mr. Robert S. Keowen, Mr. William E. Gundy and Dr. Charles Kircher. These professional engineers, with the aid of the Washington

University workers and the Cleveland Wrecking Company crane, made the set-up, performed the required tests and disassembled the equipment in a record time of about three days. The Applied Nucleonics engineers showed exceptional competence not only in structural dynamics but also in making their intricate electronic equipment work without a hitch. They were extremely hard-working, and they delivered the results of their tests in a final report about two months later. The small-amplitude tests went extremely well, and the Applied Nucleonics engineers, especially Dr. Paul Ibanez, deserve special credit for their work. Credit goes also to Dr. Craig B. Smith and Mr. George B. Howard, administrative officers of the Company.

McDonnell-Douglas Corporation

Engineers from the McDonnell-Douglas Aircraft Corporation were responsible for the data acquisition during the large-amplitude dynamic tests which were performed from mid-September to mid-October of 1976. Mr. Edward L. Smith, senior engineer, was in charge of the planning, installation, operation and disassembly of the instrumentation, and he was also responsible for data taking and data reduction. He was assisted by Mr. Lloyd D. Russell and Ralph T. Jensen. The data taking process worked extremely well and efficiently, thanks to the careful planning and the conscientious hard work of these individuals. They also installed a very efficient internal communications system. Administrative and technical support to the McDonnell-Douglas field crew was provided by many members of this organization, but especially by Messrs. Milton Hieken, Earl C. Stuckman, Jr., J. C. Bass.

The Boeing Airplane Company and the Boeing Engineering and Construction Company

By far the most difficult part of the whole project fell on the engineers of the Boeing Company who were responsible for the equipment which generated the large amplitude vibration. This work had never been done on this scale before, and it seemed doubtful to many that such a large building could be deflected at all with such large amplitudes. The equipment supplied by Boeing consisted of two major components: the mechanical-hydraulic-electrical device which produced the motion, and the auxiliary electronic control devices which kept it on course. Formidable difficulties were overcome in the first three weeks after the arrival of the Boeing team in mid-September, but by early October it was evident that the experiment was going to succeed. The difficulties and problems are described elsewhere in this report. It suffices here to make the statement that the Boeing engineers performed miracles with their equipment under very difficult conditions. No matter how badly things looked, they never gave up or despaired, just as if the word "impossible" was not in their vocabulary.

The Boeing field crew was headed by Mr. Jack Hess. The shaking-machine was designed, operated, assembled and repaired by Mr. Dexter Burlingame who was assisted by Mr. Willard I. Lathrop during the whole period of testing and also by Mr. J. D. King during the first two weeks of assembly. Mr. Burlingame showed unusual resourcefulness and ingenuity in the face of severe difficulties, and it is largely to his credit that the shaking machine performed its intended function. The electronic control system was installed and operated by Mr. David E. Marshall. In addition, Mr. Gene Eilenfeld spent considerable time on the project

during the times when difficulties were encountered. Home-office technical and administrative support was given by Messrs. Thomas E. Miller, Peter D. Schenck, H. Morris Kilborn and P. C. Hill.

The greatest credit for the success of the project must go to the Boeing team; they showed much diligence, good sense, a calm outlook, great resourcefulness and boundless optimism.

The Cleveland Wrecking Company

The Cleveland Wrecking Company is a large Cincinnati-based demolition contractor which obtained the contract to remove the Pruitt-Igoe buildings. To them, as well as to the St. Louis Housing Authority, our research project was essentially a nuisance with people in their way, possibly causing delays or even accidents. However, they did not feel that way about it, and they extended their most open cooperation. Mr. Marvin H. Rose, chairman of the board, visited my office in April 1976, and it was through his whole-hearted cooperation that the legal and insurance difficulties were removed and we could start the project.

The Cleveland Wrecking Company cleared the buildings around the test building away first, leaving an uncluttered open space around it; they repeatedly cleared the ground of rubble, they provided us a number of times with crane service, they removed the walls from the building after the E-W phase of shaking was completed, and they waited patiently for us to get done. The people from this company also helped with advice, they let us use their telephone, and through many courtesies made the work not only pleasant but also less expensive than originally expected.

The following members of the Cleveland Wrecking Company team on the Pruitt-Igoe demolition project were especially helpful: Mr. James B. Crane, Project Manager, Mr. T. B. Laws, project supervisor, and Mr. Morris Mitchell, office manager.

AALCO Wrecking Company of St. Louis

The AALCO Wrecking Company was the St. Louis-based collaborator with the Cleveland Wrecking Company in the Pruitt-Igoe demolition contract. Their officers shared in the help provided to us in the shaking project, especially through the friendly cooperation of the president of the company, Mr. M. Myron Hochman and his son, Mr. Daniel E. Hochman.

Night-Hawk Security Agency

Security on the test project was provided by the guards of the Night-Hawk Security Agency, Col. L. T. Martin, commander. The guards were always prompt, courteous and helpful, and throughout the project no equipment was missing, damaged or stolen. A very excellent job of guarding was done by this group.

Sachs Electric Company of St. Louis

Electrical lines for the motor-pump assembly and the instruments were installed, repaired, maintained and disassembled by the Sachs Electric Company under the supervision of Mr. Myron Hubenschmidt.

Other St. Louis Organizations

Various other organizations provided services for this project, or helped in some way towards its success:

Laclede Steel Company (reinforcing bars, Mr. David B. Neptune)
Collins and Herman, Inc. (fence around project, Mr. James W. Collins)
Pittsburgh Testing Laboratories (concrete cores)
Bell Telephone Company (temporary telephone service)
Union Electric Company (power service, Mr. William L. Waltke)
Wolfert Heavy Hauling and Erecting Co. (riggers, Mr. J. T. Keough)
The Wightman Agency (Insurance)
Millstone Construction Co. (Mr. I. E. Millstone, President)

City of St. Louis, Water Division

Real Estate Research Corporation (Mr. David E. Wuenscher)

Sverdrup and Parcel, Engineers and Architects

Individuals and Organizations Who Provided Advice

Mr. Ben Kacyra, Director, Earthquake Engineering Systems, San Francisco

Mr. Michael N. Salgo, Chairman, ASCE Research Council on Performance
of Structures (RCPS)

Dr. James M. Fisher, advisor to the project, RCPS

Dr. V. Bertero, advisor to the project, University of California at
Berkeley

Dr. Roger Scholl , advisor to the project, Blume Associates of
San Francisco

Dr. Mark Fintel, PCA Laboratory, Chicago

Dr. William J. Hall, advisor to the project, University of Illinois

These individuals, through discussions and site visits, contributed
of their time and their valuable advice.

Many thanks go to all of the above listed individuals in many organiza-
tions. In many different ways they made it possible that in a brief but
intense five month period a large concrete building was made to shake and
weave like a ship tossed on the sea. Grateful acknowledgment is here also
given to Providence for the very favorable weather and for the fact that
no one working on the site was injured.

COMPUTECH

Dr. Mayes was aided in the analysis of the dynamic data by his colleagues at Computech, Dr. Lindsay R. Jones, Dr. Jehlery P. Hollings, Mr. Martin Button and Mr. Mark Skinner. Dr. James L. Beck of the California Institute of Technology was responsible for the development of the computer program that was used to obtain the damping results by the method described in Section 4.2.2. Dr. Jones used the program to obtain the damping results from the EW test data. Dr. Hollings and Mr. Button were responsible for the analytical modelling of the building presented in Chapter . Mr. Button and Mr. Skinner aided in the interpretation of the mode shape data.

APPENDIX BLOG OF ACTIVITIESJune 1 - June 24, 1976

Insurance problems, preliminary planning for testing and equipment; several press interviews; waiting for the final arrival of the funds from NSF and waiting for permission to enter the premises of the project with the crew.

June 25, 1976

First day of work on the project site; clean-up of the first floor and stairs.

June 28 - June 30, 1976

Clear out top-floor; remove partitions; erect barrier on stair openings for safe passage up and down the building; marking locations on floors and on beams for physical measurements of dimensions and material properties; toilet is delivered; clearing passageways by throwing debris and rusty stoves and refrigerators out of the windows.

Note on the condition of the building at start of project:

By June 25, 1976, Cleveland Wrecking Company's demolition operation had progressed to the point where all adjacent buildings to the West Tower of C-3 were demolished completely, the debris was transported away, and the area smoothed out. In fact, all buildings in the general area of the test-building had been removed, leaving a clear area all around the test structure (Fig. 11). The corner of one building (Building A-2) abutted the test structure and during its demolition the lead ball inadvertently damaged the wall of the test structure in the S.W. corner without damaging the structure (Fig. 12). The wall around the first floor of the

tower was removed either during the demolition of the adjacent structure or during the earlier blast-demolition in 1973 of the center of Building C-3. Thus the first floor was completely open, with no walls or other obstructions (Fig. 13). Only the 13 columns and the stair occupied the space of this first floor area.

The interior of the remaining floors was filled with rubble from damaged plaster-board partition and with debris consisting of broken toilet fixtures, rusty refrigerators and stoves, some broken furniture (including a demolished piano), considerable offal and excrement (including the corpse of a dog) and window glass (Fig. 14). Hardly any window was intact and the interior contained nothing of value. The structure had been unoccupied for some few years prior to this, vandals had removed everything of any value, and the weather had an adverse effect on all that remained. Passage throughout the building was difficult because of the debris, and much clearing had to be done. This was made easy by the fact that rubbish could be heaved overboard through the windows, and this junk was then bulldozed away by the Cleveland Wrecking Company.

As clean-up work progressed it became possible to note that the structural elements (columns, beams, slabs) were structurally intact, i.e., no spalling, cracking, exposed steel, etc., and that the outside walls on all but the first floor were intact in the areas where the facing was brick and block (N, W, S and SE faces - see Fig. 15). The block walls encasing the stairwell were also all whole and undamaged. The only wall face which was in poor condition was the NE wall (Fig. 16) where the test tower was originally joined to the center part of the building. This wall consisted of one layer of 8 inch (193 mm) block, essentially held in place by gravity and thin mortar. It was broken in places and the top of

each wall did not fully reach the bottom of the slab above. Many blocks were just sitting loosely on the top row.

July 1 - July 2, 1976

Clearing work and marking of points for data taking continues. The immediate area of the test-building is bulldozed clear of debris and the area is fenced in with an 8 ft (2.4 m) high fence, 60 ft x 110 ft (18 x 34 m) in area and with a 10 ft (3 m) double-swing gate. Room enough is left to position the instruments trailer in this area still far enough away from the building to avoid damage to the trailer from falling debris from the shaking building (Fig. 17). In hind-sight it is evident that all parties would have been more comfortable with a larger fenced-in area so that the trailer could have been located 100 ft (30 m) from the building rather than 50 ft (15 m). As it turned out no damage was done to the trailer, but the people in charge of the equipment in the trailer expressed concern from time-to-time.

The electrical work is started by Sachs Electric Company. At this time this work consists of installing on every second landing in the stair-well an outlet for 110-220 Volts for use with the sonic and magnetic equipment to be used for locating reinforcing bars and measuring the thickness of the slab. Electricity was also needed for coring of concrete samples and for the small amplitude shaking equipment.

July 6 - July 7, 1976

Work is completed on the marking of test points with paint. Dr. Paul Ibanez of Applied Nucleonics arrives on the evening of July 7. Guard service from Night-Hawk Security Agency is initiated (4 PM - 8 AM weekdays, 24 hrs on weekends).

July 8, 1976

Work starts on locating the reinforcing bars with magnetic equipment after a gasoline powered portable generator is installed at the base of the stairs on the first floor level and the electric hook-up is completed.

July 9, 1976

The entire Applied Nucleonics crew arrives with their equipment. This equipment is hoisted into place on the top-floor (11th floor) through an opening in the side of the wall by a crane supplied by the Cleveland Wrecking Company. The Applied Nucleonics crew consists of Dr. Paul Ibanez as director and Messrs. Robert S. Keowen, William E. Gundy and Charles Kircher. The Applied Nucleonics shaker is installed in the S.W. corner of the eleventh floor, the electronic equipment is hooked up and the first frequency sweep is performed.

July 10 - July 12, 1976

Small amplitude shaking tests by Applied Nucleonics crew, aided by the Washington University crew, were completed, and then the equipment was disassembled and removed from the building. The details of the small amplitude shaking tests are described elsewhere in this report. The work progressed rapidly and efficiently thanks to the experienced and hard-working Applied Nucleonics group. Two kinds of rotating shakers were used (Figs. 18 and 19).

July 13 - September 3, 1977

The activities in this one month period consisted of two parts: one activity centered around the measurement of the properties of the building, and the other concerned planning for the large-amplitude dynamic tests. The Washington University student crew measured slab thickness by a sonic apparatus, they located reinforcing bars in the slabs by a magnetic device,

they determined beam and column dimensions by measurement, and they determined concrete strength with a Schmidt hammer. Cores were taken by Pittsburgh Testing Laboratory and these were tested in the Washington University structures laboratory.

The planning for the large-amplitude tests involved visits here in St. Louis with Mr. Edward Smith of McDonnell Douglas, with the co-principal investigator Dr. Ronald Mayes (July 10-14) and with Mr. Dex Burlingame of the Boeing Company (August 3-4). Dr. Mayes also visited the Boeing people in Seattle (July 15). A decision was made during Mr. Burlingame's visit that because of the pressure of time it would not be feasible to completely assemble the large-amplitude shaking machine in the laboratory in Seattle, but that this apparatus would be assembled the first time right on the test-structure. Whether this decision was right or not is difficult to say. Certainly, some of the problems would have been eliminated, and the time of trial and error on the test-site during September would have been shortened. Particularly the problems with the actuator could have been rectified in Seattle. On the other hand, the actual test-environment was quite different from a laboratory so that many parts of the trial and error process would not have been able to be eliminated even with prior laboratory trial.

The planning phase involved coordination with Dr. Mayes, Dr. Hatcher, the Boeing and the McDonnell Douglas people, Mr. Monsey, the University Research Office and the Cleveland Wrecking Company, and it encompassed the following items:

- 1) Design of the shaking machine components, including checking out the Boeing hydraulic pump assembly and the purchase of an actuator.
- 2) Design of the structure connecting the shaking device to the test building, and design of the cribbing under the moving lead mass.

3) Planning, selecting contractors and arranging for electricity (Union Electric), power distribution (Sachs Electric), crane service (Cleveland Wrecking), water permit (City of St. Louis), lead delivery, roof opening, telephone, rigging and drilling, buggy to move equipment on the test floor, plus taking care of many other details.

4) Planning of the placement and location of the accelerometer, data acquisition, and internal communication (McDonnell's Mr. Ed Smith).

During the week of August 23-27 Union Electric came on the site to install power poles, electric lines and a transformer. The last pole with the transformer was located outside of the fence, about 30 ft (9 m) due West of the center of the test-building. This was a poor location because the wires were torn by flying debris while the walls were being removed in October, causing delay and damage to the switching apparatus (Fig. 20).

During the week of August 30 - September 3 a 14' x 14' (4.3 x 4.3 m) hole was cut into the roof slab (Fig. 21) so that equipment could be lowered into the eleventh floor. This operation went smoothly and the placement of the equipment could not have been accomplished conveniently in any other way. The Sachs Electric Company installed switches and lines so that the following electric service was available: 110V - 220V on every second floor on the stairway landing; 440V - 3 phase on the 11th floor for Boeing's motors; and 110V line to the instrument trailer. The wooden frame housing for the switching gear (Fig. 20) was located about 20 ft (6 m) from the South face of the building, and this was too close. The high-voltage wires led diagonally up to the 11th floor outside of the building. This worked out well and this wire was never damaged either through shaking of the building or from flying debris. The wire with the 110V - 220V line

went into the stairwell on the ground and it was cut twice by pieces of masonry. The arrangement of the power supply could have been better and safer (Fig. 20). Fortunately only minor mishaps, and no injury, occurred.

Prior to the arrival of the Boeing equipment the area inside the fence was again smoothed out by a bulldozer, and at the end of the week the instrument trailer was put in its place. Water-line and auxiliary pump were installed and connected to provide cooling water for Boeing's motors and pumps on the 11th floor.

September 6, 1976

The first of two truck-trailers with the Boeing equipment arrives from Seattle. The second truck somehow got lost and it did not arrive until September 9, causing anxiety and some delay.

September 7, 1976

The crew from Boeing arrives (Messrs. Burlingame, Lathrop and King) and arrangements are completed for the start of assembly.

September 8, 1976

A crane is on the site all day, lifting the Boeing equipment to the 11th floor and unloading the 55,000 lb (25,000 kg) of lead ingots. These ingots were all about 750 lb (340 kg) in weight, cast in flat slabs to fit the compartments in the moving box (Fig. 22). The stiffened plate supporting this box is set in place, and the pump-motor assembly is installed (Figs. 23 and 24).

September 9, 1976

Boeing's second truck with the actuator and the electronic control equipment finally arrives. Sachs Electric completes all wiring and connecting of electric lines. Rigging work commences with Boeing crew and two local riggers: drilling holes in concrete, setting steel plates and members,

welding, etc. The pre-cut columns for the cribbing on the 10th floor are discovered to be too long due to faulty original dimensions, so torch and welding rod are put to use (Fig. 25). This day also sees the beginning and the end of labor problems: Business agents of the carpenters and the electrical unions visit the project to check credentials of the union members. After much scowling, headshaking and negotiating, and thanks to the wisdom of our Mr. Monsey, they leave, never to bother us again. Next a shop steward of the operators union appears, demanding that we place a driver from the union on the gasoline powered buggy used on the eleventh floor to lift equipment and lead. Solution: that evening we got a battery powered buggy and are no longer bothered. This minor irritation was the only trouble encountered throughout the project. There was no harrassment or vandalism of any sort. The guard service did a superb and conscientious job throughout, police and local officials were helpful, and the people in the surrounding area were curious and helpful.

September 10 and 11, 1976

Work on rigging, drilling, installing continues. It becomes evident that the Boeing crew, under the supervision of Mr. Burlingame, is expert at solving difficult problems and they simply do not give in until a satisfactory resolution is achieved.

September 13, 1976

Boeing installs electronic gear in the trailer, while the rigging work continues. Mr. David Marshall, the Boeing electronics engineer, arrives and takes over this phase of the work.

September 14, 1976

McDonnell Douglas bring their electronic gear into the trailer and start installing the wiring for the accelerometers and the communications

equipment. Boeing crew works on piping and completes the motor-pump assembly. The motors are turned on and they work. Sachs Electric Company completes all wiring work, and S.W. Bell Telephone Company installs a telephone line.

September 15, 1976

Work on instrumentation installation and on connecting up the actuator to the pumps continues. McDonnell Douglas starts testing their equipment.

September 16, 1976

Dr. Mayes arrives, while instrument testing and work on the shaking machine continues.

September 17, 1976

It is discovered that the water pump and the water hoses used for conveying water for cooling of the Boeing pump-motor assembly from a city water hydrant located 200 ft (60 m) from the test building to the 11th floor do not deliver enough water. This problem is finally solved, after much trial and error, by September 21. As a result we lost four days, having also to install additional power (220V-3 phase) for the water pump.

September 18, 1976

Work on the shaking equipment continues while the accelerometers are being tested. The communications equipment is tested out and ready for use. It consists of a plug-in two-way voice system with wires that can reach every corner on every second floor where accelerometers are placed. At each of these floors there is also a two-way box for speaking (Fig. 26). This communications system worked very well in contrast to two-way walkie-talkies which were tried first. In addition there was also a powerful loudspeaker on the 11th floor which connected to the instrument van. The instrument van also contained a bull horn for emergency.

September 20 - September 22, 1976

Several 6 to 8 ft deep (2-3 m) holes are excavated to undisturbed soil outside the fence for placing ground accelerometers. These holes promptly filled up with water after the next rain and so they were useless. Fortunately they were not needed anyway because the transmission of motion to the ground was negligible.

McDonnell-Douglas completes installation and testing of the data acquisition system on September 20, and their crew is on standby waiting for the shaking system to work until October 3 when testing finally starts. Mr. Jack Hess of Boeing arrives on September 20 to assist in completing the shaking system. The cooling water delivery is finally completed on September 21.

September 22 - October 2, 1976

This is a very trying period because a variety of problems with the shaking system have to be resolved. In hind-sight one can look at these problems as being something that can be normally expected in setting up an untried test system in a difficult environment. The problem with this system was that while the displacement imparted to the moving mass-box was smoothly sinusoidal, the resulting force system was irregular with very high beats. Such an irregular force input was unable to excite resonance of the structure. All components of the shaking system were systematically checked out, many small problems were resolved and finally it was discovered that the actuator piston packing was too stiff, and this was the main cause of the spikes in the force trace. Mr. Gene Eilenfeld of Boeing arrives and assists in the tracing down of the problems. The packing of the actuator is adjusted, and finally on Saturday, October 2, the whole system works satisfactorily and the building responds.

The phases of installation and equipment testing then took a total of six weeks on the site.

Building modifications, electricity, etc.:	2 weeks
Instrumentation and data taking systems:	1 week
Installation of shaking system:	2 weeks
Shakedown of shaking system:	2 weeks

October 4 - October 15, 1976

The details of testing are described elsewhere in this report, and only the general chronology of events is given here. During the period October 4 - October 15 the large-amplitude shaking tests were performed in the E-W direction with the walls in place. After a great many tests, i.e., frequency sweep tests, damping determination runs and mode-shape determinations the building was subjected to a low frequency resonance test with a 30 kip (133 kN) maximum force. During the last run a \pm 8 inch (\pm 200 mm) deflection of the top of the building was achieved. For the brief period of resonance the motion was very dramatic and considerable damage to walls and joints was noted. Unfortunately the 1.5 inch (38 mm) pin connection between the actuator piston and the moving mass-box fractured (the second time that this happened) and testing was halted. The severe shaking also necessitated other repairs (the actuator packing was leaking severely and several control systems were no longer functioning properly), and so it was decided that a halt would be made in the testing while the repairs were made.

At this time (October 15) it became evident that our testing was slowing down Cleveland Wrecking Company's progress: our building was the only one left standing and they were anxious for us to be finished. It also became obvious that as the Fall advanced, rains increased in frequency

and occasional frost occurred, it would be extremely difficult to continue testing. It would have taken much time and effort to have full water proofing and frost proofing of the instrumentation and control systems. Many walls had been severely damaged in the shaking, and it became dangerous to move safely around the building. For these reasons it was decided that while the shaking equipment was being reconditioned it should also be turned 90° for shaking in the NS direction, and at the same time to remove all walls and partitions, leaving only the bare structure: beams, columns, slabs and stairs. In the proposal it was planned that the large amplitude tests would be performed in both the EW and NS direction with and without cladding, i.e., four test sequences with two rearrangements of the shaking apparatus. This was not done because of time shortage and because of the advanced degree of damage both to the walls and to the structure, and so only one move of the equipment and two test sequences were done. In removing the walls it was decided to leave the walls in the upper two floors in place to protect equipment and personnel from wind and rain.

October 16 - October 18, 1976

The top floor is cleaned up; the lead ingots are removed from the box and stored along or near beam lines; clean up of steel balls, repair of base plates and grinding smooth of the surface of the plate on which the box moved. There were grooves up to 1/8 inch (3 mm) deep from the steel balls. The actuator is moved to NS direction and connected to building. All of the instrumentation equipment and wiring is removed from building.

October 19 - October 21, 1976

Walls are removed, using gentle tapping with lead ball suspended from a crane boom, and debris is afterwards pushed off the side of the

building manually (Fig. 27 and 28). This work is done by the Cleveland Wrecking Company. The walls around the stair-well are all removed manually. The wall removal went extremely well and no damage was inflicted to the structure. Only one mishap: the high-tension line between the Union Electric transformer and switching station was broken. The damage was repaired promptly. Prior to the wall removal the fence is disassembled.

October 22 - October 26, 1976

The shaking system is reassembled, repaired and tested, and the accelerometer system is reinstalled and tested.

October 27 - November 4, 1976

Various shaking tests in the NS direction are performed. Low amplitude testing to determine natural frequencies and mode shapes goes very well. High-amplitude testing under high force levels (up to 30 Kip - 133 kN), resulting in amplitudes up to ± 28 inches (± 0.71 in.) at the top of the building, is difficult and is interrupted by various malfunctions (actuator-to-structure support needed to be reinforced, another actuator-to-box pin ruptured and needed to be replaced, a pipe in the pump assembly cracked and needed welding, and various control devices malfunctioned and had to be repaired). These malfunctions are not surprising because of the extreme motion and high acceleration. During the final high-level runs severe damage was inflicted to joints and columns, and I finally decided to stop testing to avoid final collapse of the whole structure.

November 4 - November 7, 1976

Equipment is removed and returned by the various subcontractors. This is done without hitch, injury or mishap. The remaining damaged hulk of the test structure was demolished within one week after we moved our last equipment out of the site.

APPENDIX CSUMMARY OF TESTS OF "FORCID" COMPUTER PROGRAM USING SIMULATED DATA

1. GENERATION OF DATA

To test the forced vibration identification program "FORCID", data was generated in the following way: A uniform shear building model with ten degrees-of-freedom was subjected to a sinusoidal force history of unit amplitude and frequency ω , which was varied. The force was applied at the 9-th floor level, one level down from the top of the 10-floor structure, to simulate the situation of the Pruitt-Igoe test building.

The modal damping factors were each 5 percent, and the modal periods were:

$$\begin{array}{lll} T_1 = 1.000 \text{ sec} & T_5 = 0.120 \text{ sec} & T_8 = 0.083 \text{ sec} \\ T_2 = 0.336 \text{ sec} & T_6 = 0.102 \text{ sec} & T_9 = 0.078 \text{ sec} \\ T_3 = 0.205 \text{ sec} & T_7 = 0.090 \text{ sec} & T_{10} = 0.076 \text{ sec} \\ T_4 = 0.150 \text{ sec} & & \end{array}$$

The participation factors for the first and second modes at floor levels 8, 9 and 10 were:

$$\begin{array}{ll} p_8^{(1)} = 1.73 \times 10^{-3} & p_8^{(2)} = 6.46 \times 10^{-4} \\ p_9^{(1)} = 1.81 \times 10^{-3} & p_9^{(2)} = 1.16 \times 10^{-3} \\ p_{10}^{(1)} = 1.85 \times 10^{-3} & p_{10}^{(2)} = 1.45 \times 10^{-3} \end{array}$$

The mode shapes were

$$\phi_{ir} = \frac{1}{N_r} \sin \frac{(2r-1)\pi i}{21}, \quad \forall i, r = 1, \dots, 10.$$

where

$$N_r = \sqrt{\sum_{i=1}^{10} \sin^2 \frac{(2r-1)\pi i}{21}}$$

selected so that the mode shapes were normalized with

$$\sum_{i=1}^{10} \phi_{ir}^2 = 1, \quad \forall r = 1, \dots, 10$$

The acceleration response histories were generated on a computer at equal digitization intervals of $\Delta t = 0.02$ sec from the analytical steady-state solution for a forcing function $f(t) = \sin \omega t$, that is,

$$\ddot{x}_j(t) = A_j \sin \omega t + B_j \cos \omega t = a_j \sin(\omega t + \phi_j),$$

where

$$a_j = \sqrt{A_j^2 + B_j^2}$$

$$\tan \phi_j = B_j/A_j$$

$$A_j = - \sum_{r=1}^{10} p_j^{(r)} \left\{ \frac{(\omega_r/\omega)^2 - 1}{\left[(\omega_r/\omega)^2 - 1 \right]^2 + \left[2h_r(\omega_r/\omega) \right]^2} \right\}$$

$$B_j = \sum_{r=1}^{10} p_j^{(r)} \left\{ \frac{2h_r(\omega_r/\omega)}{\left[(\omega_r/\omega)^2 - 1 \right]^2 + \left[2h_r(\omega_r/\omega) \right]^2} \right\}$$

A_j is the total in-phase amplitude, that is, the sum of the in-phase modal amplitudes, and B_j is the total 90 degree out-of-phase amplitude, that is, the sum of the out-of-phase modal amplitude. The participation factors are defined by

$$p_j^{(r)} = \phi_{jr} \left[\frac{\phi_{qr}}{M_r} \right]$$

where

$$M_r = \sum_{i=1}^{10} m_i \phi_{ir}^2 = m \sum_{i=1}^{10} \phi_{ir}^2 = m$$

where m is the mass of each floor, selected by assuming that the weight W of each floor was 100 times the shaker force amplitude, and thus

$$m = \frac{W}{g} = \frac{100}{g}$$

The digitized force history and the acceleration response histories at up to three locations ($j = 8, 9$ and 10) were used as input to FORCID for various values of the excitation frequency ω .

2. DISCUSSION OF RESULTS

2.1 Non-uniqueness

To illustrate the ideas about the non-uniqueness of the three parameters T_r , β_r and $p_{jr}^{(r)}$ for the r -th mode, two runs of the program were made to attempt to identify these parameters for the first mode. The time history of the acceleration response at floor 9 of the uniform shear building for an excitation frequency $\omega = \omega_1$ was used. Following are the results of this analysis:

Run No.	Initial Estimate	Final Estimate
1	$\hat{T}_1 = 1.0^*$	$\hat{T}_1 = 0.999$
	$\hat{\beta}_1 = 5\% \text{ (exact)}$	$\hat{\beta}_1 = 4.5\%$
		$\hat{p}_9^{(1)} = 1.63 \times 10^{-3}$
2	$\hat{T}_1 = 0.99$	$\hat{T}_1 = 0.988$
	$\hat{\beta}_1 = 80\%$	$\hat{\beta}_1 = 80.8\%$
		$\hat{p}_9^{(1)} = 2.96 \times 10^{-3}$

* Originally the technique did not require an initial estimate of the participation factors.

The final estimates obviously depend on the assumed initial values, a reflection of non-uniqueness. However, the resulting computer plots of the actual and the theoretical acceleration response gave perfect time-history matching in both cases! What the program did, in effect, was to find a period and damping value close to the initial estimates which gave the correct total phase ϕ_9 , which was equal to 90.7 rather than the 90 degrees of the first mode because of modal interference from the higher modes. The participation factor $p_9^{(1)}$ was then altered to give the correct total amplitude a_9 , which was practically the same as the 90 degree out-of-phase amplitude of $B_9^{(1)}$ of the first mode. Note that the ratio $\hat{p}_9^{(1)}/2\hat{\beta}_1$ for the final estimates has almost the same value of 1.8×10^{-2} for both of the above runs, and that this is equal to $B_9^{(1)}$.

The results of these two runs also illustrate the fact that the requirement of phase-matching for a perfect fit in the time domain constrains the period estimates well, but it does not constrain the damping factor much. A small change in the natural period leads to a large change in the damping to achieve the same phase.

We, therefore, see that a single-degree-of-freedom model can be selected to match exactly the response at one location of the ten-degree-of-freedom uniform shear building, and that there are a range of parameter values which can be used to achieve this.

To illustrate that the situation is not improved by using the response histories at more than one location, the response at floors 8, 9 and 10 were used as input to the "FORCID" program, using again $\omega = \omega_1$. The results were

Initial Estimates

$$\hat{T}_1 = 1.0,$$

$$\hat{\beta}_1 = 5\%$$

Final Estimates

$$\hat{T}_1 = 1,000$$

$$\hat{\beta}_1 = 1.4\%$$

$$\hat{p}_8^{(1)} = 4.94 \times 10^{-4}$$

$$\hat{p}_9^{(1)} = 5.18 \times 10^{-4}$$

$$\hat{p}_{10}^{(1)} = 5.30 \times 10^{-4}$$

The response match at each floor was excellent but not quite exact since modal interference produces a different total phase at each floor and hence the single-degree-of-freedom model is not able to match the total phase at each floor, as it did when only one response history was used. Again, the damping is in error but the correct amplitude was achieved at each floor by the appropriate selection of erroneous values for $\hat{p}_8^{(1)}$, $\hat{p}_9^{(1)}$ and $\hat{p}_{10}^{(1)}$. The ratio of these parameters did give the correct mode shape.

To avoid the non-uniqueness problem, the participation factors can be given a priori estimates and kept constant at these values during the identification process. These a priori values can be estimated from the mode shape and mass distribution by using the expressions

$$p_j^{(r)} = \phi_{jr} (\phi_{ir} / M_r)$$

$$M_r = \sum_{k=1}^N m_k \phi_{kr}^2$$

where the shaker is at location i and m_k is the lumped mass corresponding to coordinate k of an N -degree-of-freedom model of the building being identified.

Ideally, the mode shape should be estimated from the amplitude of the response at each floor during the particular test being used in the identification. However, if this is not possible, the mode shape from a previous test could be used because there is reason to suspect that the mode shape remains reasonably constant, provided the structural changes do not become highly localized. Even then, the local distortion of the mode shape may only produce small changes in the participation factors for points well away from this localized damage.

2.2 A Priori Assignment of Participation Factors

The computer program "FORCID" was modified so that the relevant participation factors are held constant, rather than being "identified" along with the other parameters.

The simulated data for the ten-floor uniform shear building was used as input to the new version of "FORCID", and the participation factors were set at their exact values (see Sec. 1 of Appendix C). The results of applying "FORCID" to data generated by a frequency of 1Hz (which is the first mode resonant frequency) and by a frequency of 1.11 Hz (about 10 percent higher than the resonant frequency) are as follows:

Frequency of Excitation (Hz)	Response Records Used	Estimate	T_1 (sec)	β_1 (%)
1.00	Floor 9	Initial	1.1	2.0
		Final	0.999	4.99
1.00	Floors 8,9,10	Initial	1.1	2.0
		Final	1.000	4.99
1.00	Floors 8,9,10	Initial	0.9	10.0
		Final	1.000	4.99
1.11	Floors 8,9,10	Initial	1.1	2.0
		Final	1.002	5.22

A ten second time was used for the response records in generating this data (i.e., 0 to 10.0 sec.). The exact values of T_1 and β_1 are 1.000 sec and 5.00 percent, respectively.

A similar analysis for the second mode frequency was also performed and the data are given below. The time interval of the record used was from 0 to 5.0 sec, and the exact values of \hat{T}_2 and $\hat{\beta}_2$ are 0.336 sec and 5.00 percent, respectively.

Frequency of Excitation (hz)	Response Records Used	Estimate	\hat{T}_2 (sec)	$\hat{\beta}_2$ (%)
2.98	Floor 10	Initial	0.3	10.0
		Final	0.337	2.15
2.98	Floors 8,9,10	Initial	0.3	10.0
		Final	0.339	4.76
2.98	Floors 8,9,10	Initial	0.4	2.0
		Final	0.339	4.76
3.33	Floors 8,9,10	Initial	0.3	10.0
		Final	0.327	2.93

From these calculations it is evident that the accuracy of the parameter estimates degenerates as the frequency of excitation moves off resonance. This illustrates the importance of using time histories at resonance. The degradation of the accuracy is worse for the second mode because modal interference is more pronounced. For example, the second mode contribution to the total amplitude at floors 8, 9, and 10 is, respectively, 94, 98 and 99 percent at resonance, but only 59, 84 and 79 percent at a frequency of excitation which is 10 percent above resonance.

The first case in the second mode analysis illustrates the importance of using more than one response record to help overcome modal interference. The time match in this case between the "recorded" response and the theoretical response was almost perfect. What happened during the identification process was that the parameters of the single-degree-of-freedom model were altered from their second mode values to compensate for the contributions of the other modes, particularly the first mode. The phase and amplitude contributions of the other modes change from floor-to-floor, and hence, when more records are used, in the subsequent two cases, the technique is better able to identify the second mode contribution.

It should be emphasized that modal interference would be a problem whatever identification procedure is used.